Cover design

Sara Lauwers

Ghent University
Faculty of Pharmaceutical Sciences

Combining the strengths of cytotoxic T cells and nanomedicines for cancer immunotherapy

Laura Wayteck

Pharmacist
Master in Drug Development

Thesis submitted to obtain the degree of
Doctor in Pharmaceutical Sciences

Proefschrift voorgedragen tot het bekomen van de graad van
Doctor in de Farmaceutische Wetenschappen

2016

Dean

Prof. dr. Jan Van Bocxlaer

Promoters

Prof. dr. Stefaan De Smedt

Dr. Koen Raemdonck

Members of the Exam Committee

Prof. dr. **Dieter Deforce** (chairman)	Universiteit Gent
Prof. dr. **Christophe Stove** (secretary)	Universiteit Gent
Prof. dr. **Bart Vandekerckhove**	Universitair Ziekenhuis Gent
Prof. dr. **Karine Breckpot**	Vrije Universiteit Brussel
Prof. dr. **Enrico Mastrobattista**	Universiteit Utrecht

Ghent, June 29th 2016

Promoters

Prof.dr. Stefaan De Smedt

Dr. Koen Raemdonck

Author

Laura Wayteck

Laura Wayteck is a doctoral fellow of the Institute for the Promotion of Innovation through Science and Technology in Flanders, Belgium (IWT-Vlaanderen). Koen Raemdonck is a postdoctoral fellow of the Research Foundation-Flanders, Belgium (FWO-Vlaanderen). Koen Raemdonck received additional financial support via a FWO Research Grant (Krediet aan Navorsers). Kom op Tegen Kanker is acknowledged for their financial support (Beurs Emmanuel van der Schueren).

Table of contents

List of abbreviations

ACT	Adoptive T cell therapy
AGO2	Argonaute 2
APC	Antigen-presenting cell
ATP	Adenosine triphosphate
AuNP	Gold nanoparticle
BCG	Bacillus Calmette-Guérin
Biotin-sulfo-NHS	Biotin 3-sulfo-N-hydroxysuccinimide ester
BM-DC	Bone marrow-derived dendritic cell
BSA	Bovine serum albumin
CAR	Chimeric antigen receptor
CD	Cluster of differentiation
CEA	Carcinoembryonic antigen
CFSE	Carboxyfluoresceinsuccinimidyl ester
CTL	Cytotoxic T lymphocyte/ Cytotoxic T cell
CTLA-4	Cytotoxic T lymphocyte-associated antigen 4
DAMP	Danger-associated molecular pattern
DC	Dendritic cell
Dex-HEMA	Dextran hydroxyethyl methacrylate
DEXS	Dextran sulfate
DiD	1,1'-dioctadecyl-3,3,3',3'-tetramethylindodicarbocyanine
DLS	Dynamic light scattering
DOPC	1,2-dioleoyl-sn-glycero-3-phosphocholine
DOX	Doxorubicin
EDTA	Ethylenediaminetetraacetic acid
Egg PG	Egg phosphatidyl glycerol
ELISA	Enzyme-linked immunosorbent assay
EMA	European Medicines Agency
EPR	Enhanced permeation and retention
FBS	Fetal bovine serum
FD	FITC-dextran
FDA	Food and Drug Administration
FFS	Fluorescence fluctuation spectroscopy
FITC	Fluorescein isothiocyanate
FSC	Forward scatter
fSPT	Fluorescence single particle tracking
GM-CSF	Granulocyte-macrophage colony-stimulating factor
HEPES	4-(2-hydroxyethyl)-1-piperazine ethanesulfonic acid

ICD	Immunogenic cell death
IFN	Interferon
IFNγ	Interferon gamma
IL	Interleukin
IP	Intraperitoneal
IRAE	Immune-related adverse event
IT	Intratumoral
IV	Intravenous
LAG-3	Lymphocyte activation gene-3
LPS	Lipopolysaccharide
MAL	Maleimide
MDSC	Myeloid-derived suppressor cell
MFI	Mean fluorescence intensity
MHC I	Major histocompatibility complex class I
MMP	Matrix metalloproteinase
MPLA	Monophosphoryl lipid A
mRNA	messenger RNA
MSC	Mesenchymal stem cell
NG	Nanogel
NGS	Next-generation sequencing
NK	Natural killer
NP	Nanoparticle
NSC	Neural stem cell
OVA	Ovalbumin
PAMP	Pathogen-associated molecular pattern
PAP	Prostatic acid phosphatase
PBS	Phosphate buffered saline
PD-1	Programmed cell death 1
PD-L1	Programmed cell death ligand 1
PDP	Pyridyldithiopropionate
PE	Phycoerythrin
PEG	Polyethylene glycol
PE-MAL	18:1 1,2-dioleoyl-sn-glycero-3-phosphoethanolamine-N-[4-(p-maleimidophenyl)butyramide]
PE-PDP	18:1 1,2-dioleoyl-sn-glycero-3-phosphoethanolamine-N-[3-(2-pyridyldithio)propionate]
PG	Phosphatidyl glycerol
PRR	Pattern recognition receptor
RBC	Red blood cell
RISC	RNA induced silencing complex

RNAi	RNA interference
SD	Standard deviation
siCD45	siRNA targeted against CD45
siCTRL	Negative control siRNA
siNG	siRNA-loaded nanogel
siRNA	small interfering RNA
STAT3	Signal transducer and activator of transcription 3
STING	Stimulator of interferon genes
TAA	Tumor-associated antigen
TAM	Tumor-associated macrophage
TCR	T cell receptor
TGFβ	Transforming growth factor β
TIL	Tumor-infiltrating lymphocyte
TIM-3	T cell immunoglobulin mucin domain-containing-3
TLR	Toll-like receptor
TMAEMA	[2-(methacryloyloxy)-ethyl]trimethylammonium chloride
TNFα	Tumor necrosis factor alpha
T_{reg}	Regulatory T cell
uPA	Urokinase-type plasminogen activator
uPAS	Urokinase plasminogen activator system

Aim and outline of the thesis

As cancer is one of the leading causes of morbidity and death in the world with every year 14 million new cases with 8 million cancer-related deaths, scientific effort and financial support is of outstanding importance to fight cancer in the coming years. In general, cancer therapy struggles with finding an acceptable balance between potential therapeutic benefit and toxicity of the treatment. Formulating anti-cancer therapeutics such as chemotherapeutics into nanoparticles (nanomedicines) can improve their therapeutic index, enables a tunable drug release, and improves their biodistribution. However, to take full advantage of these benefits, one of the most prominent hurdles remains *in vivo* targeting of the nanoparticles (NPs) to the site of action. Several targeting strategies based on the enhanced permeation and retention (EPR) phenomenon and active targeting by the incorporation of targeting ligands have been clinically investigated. However, the widespread use of these strategies is hampered by several factors such as the heterogeneity in tumor vasculature between patients and tumor types.

An interesting alternative that might overcome targeting limitations is cell-mediated delivery. Certain cell types such as cytotoxic T lymphocytes (CTLs) have the intrinsic ability to migrate to and infiltrate in the tumor tissue, where they can induce specific cytolysis of tumor cells upon tumor antigen recognition. During the last decade, the administration of CTLs has emerged as a highly promising cancer immunotherapy. Although T cell immunotherapy has demonstrated impressive results in metastatic melanoma and hematological malignancies, many patients remain refractory to the therapy. Limitations are related to the immunosuppressive role of the tumor microenvironment, the intratumoral heterogeneity, and loss of antigens to which the T cell immunotherapy was engineered. In recent years, research groups have therefore been investigating in combinatorial strategies to merge the benefits of distinct anti-cancer therapies.

In light of the abovementioned limitations, the first aim of this thesis is to combine nanomedicines with cancer immunotherapy by exploiting the tumor-infiltrating properties of CTLs to guide anti-cancer nanomedicines to the tumor tissue. Moreover, as in many cancers the tumor infiltration and anti-tumor activity of CTLs is blunted by the immunosuppressive tumor microenvironment, it is of interest to evaluate the downregulation of immune-inhibitory pathways in T cells during their *ex vivo* manipulations prior to adoptive transfer. As the standard procedures to transfect primary T cells encounter safety issues and high cell toxicity problems, a second aim of this thesis is to develop an alternative approach based on gold NP-mediated photoporation to deliver small interfering RNA (siRNA) molecules to the cytosol of the cells.

Chapter 1 provides a general introduction to the main topics that were addressed in the thesis. First, an overview of the current problems of targeting nanomedicines to the tumor are highlighted, followed by the potential of cell-mediated drug delivery to overcome these barriers. Secondly, general aspects of cancer immunotherapy are introduced and the major hurdles exerted by the immunosuppressive tumor microenvironment are discussed. Finally, *in vivo* and *ex vivo* transfection methods for T cells are summarized.

In **Chapter 2**, we report on the reversible attachment of lipid-based nanoparticles to the surface of CTLs via a redox-sensitive coupling. For this purpose, we optimized the NP composition and investigated the coupling to both activated and non-activated $CD8^+$ T cells. Next, the influence of the NP-load on the proliferation and cytolytic capacity of T cells was evaluated via *in vitro* assays. As we aim to obtain triggered release of NPs in the tumor, the detachment was evaluated by incubating the NP-loaded cells with the reducing agent glutathione. It has been shown in the literature that glutathione is present in elevated levels in the tumor extracellular fluid. Finally, as a proof-of-concept, we investigated the coupling of siRNA-loaded lipid-based NP to the surface of CTLs.

As the final aim is to exploit the CTL's tumor-migratory capacity to deliver drug-loaded NPs to the tumor, **Chapter 3** provides more information on the *in vivo* evaluation of this T-cell mediated transport. The reversible coupling strategy as described in Chapter 2 was extended by the coupling via a stable thioether bond. We first investigated the tumor infiltration of liposome-loaded CTLs in a mouse melanoma model. Next, the influence of coupling via both strategies on T cell proliferation, viability, and cytokine secretion was investigated. Ultimately, the liposomes were loaded with the immune adjuvant monophosphoryl lipid A (MPLA) to boost the immune responses against the tumor. A preliminary *in vitro* and *in vivo* screening was performed to evaluate the therapeutic potential of T cell-mediated targeting of MPLA to the tumor tissue.

Although a substantial amount of NPs could be released from the cell surface by incubation in glutathione, as shown in Chapter 2, still a considerable amount of NPs remained stably anchored. Therefore, in **Chapter 4,** a coupling system based on an enzyme-sensitive linker was investigated as an alternative to improve the triggered release properties. We developed a peptide linker, containing a cleavable peptide sequence that allows the attachment of liposomes on one side and the binding to the surface of $CD8^+$ T cells on the other side. First, it was assessed whether this peptide construct could be efficiently attached to the cells, followed by the evaluation of the cleavability of this system by the selected proteases matriptase and urokinase-type plasminogen activator.

Besides their ability to migrate to the tumor, CTLs can also directly kill tumor cells. However, a variety of immunosuppressive pathways can inhibit the T cell immune responses. It was anticipated that the knockdown of these immunosuppressive pathways

via siRNA may yield more potent T cells for adoptive transfer. As T cells are known to be hard-to-transfect cells and conventional non-viral transfection methods encounter several limitations, we report in **Chapter 5** on an alternative approach based on vapor nanobubble-mediated photoporation to efficiently deliver siRNA molecules to $CD8^+$ T cells.

In **Chapter 6,** we provide an overview of the recent progress in the field of cancer immunotherapy. We discuss the current challenges and how the combination with nanomedicines, as was evaluated in this work, can improve the efficacy of the treatment.

1

Introduction to nanomedicines and immunotherapy for cancer

Parts of this chapter are published as:

Wayteck Laura[a], Breckpot Karine[b], Demeester Jo[a], De Smedt Stefaan[a], Raemdonck Koen[a], A personalized view on cancer immunotherapy. *Cancer Letters*, 352 (2014) 113-125. (DOI: 10.1016/j.canlet.2013.09.016)

[a]Laboratory of General Biochemistry and Physical Pharmacy, Faculty of Pharmaceutical Sciences, Ghent University, Ottergemsesteenweg 460, 9000 Ghent, Belgium

[b]Laboratory of Molecular and Cellular Therapy, Department of Biomedical Sciences, Vrije Universiteit Brussel, Laarbeeklaan 103/E, 1090 Brussels, Belgium

ABSTRACT

The successful translation of anti-cancer nanomedicines from preclinical research to treatment in patients is still challenged by the low targeting of the nanomedicines to the tumor. As cell-mediated delivery of nanomedicines can tackle this limitation, a brief overview is given about the different cell types and coupling strategies that can be used for this purpose. T lymphocytes, in particular cytotoxic T cells, were suggested as ideal carriers, based on both their tumor migration capacity and their cytolytic effect on tumor cells, the latter one also being the key to the successes of cancer immunotherapy. Therefore, in a second part of this chapter, we provide a general overview of the different cancer immunotherapies and the current challenges they encounter. A final part summarizes the *in vivo* and in particular the *ex vivo* techniques to transfect T lymphocytes, aiming to enhance the anti-tumor responses.

PART I: NANOMEDICINES FOR CANCER

1 ANTI-CANCER NANOMEDICINES

The term nanomedicines can be described as the application of engineered materials with dimensions in the nanoscale (1-1000 nm) for the diagnosis, prevention, and treatment of a disease [1-3]. In the late 19th century, Paul Ehrlich already envisioned the concept of a 'magic bullet' that would target and eradicate the disease-causing pathogens or transformed cells without affecting normal cells [4]. Nowadays, the major advantages of encapsulating anti-cancer drugs in nanoparticles (NPs) still include this enhanced targeted delivery to improve biodistribution and avoid non-specific toxicity to healthy tissues, but can be further extended to (i) the improved bioavailability as nanostructures help to overcome stability and solubility problems, (ii) the protection of a therapeutic from degradation inside the body, and (iii) the controlled drug release at the target site [5, 6]. A widely investigated strategy to improve the circulation time and thus the biodistribution, is the decoration of the NP surface with polyethylene glycol (PEG) chains, also referred to as PEGylation [7].

1.1 Nanocarrier design

In general, an ideal anti-cancer nanocarrier needs to meet the following criteria: it has to be (i) biocompatible and biodegradable, (ii) able to target the drug to the tumor site, (iii) designed to have optimal circulation time and high drug loading, and (iv) amenable for cost-effective commercialization [8]. Numerous types of NPs have been developed and were categorized in the literature in many different ways. Within this dissertation, three main groups were defined, including lipid-based NPs, polymer-based NPs, and inorganic NPs.

From the different types of lipid-based nanocarriers, liposomes and micelles are the most studied [9]. Liposomes are vesicles composed of biocompatible phospholipid bilayers forming one or multiple concentric lipid bilayers around an aqueous core. Liposomes are able to encapsulate both hydrophobic and hydrophilic drugs in their phospholipid shell and aqueous core, respectively [10]. After administration, the drug can be released from the liposomes via distinct strategies, including passive diffusion and triggered release by endogenous and exogenous stimuli, or the nanocarrier can be internalized in the target cells for intracellular drug release [11, 12]. Liposomes are attractive materials based on their low toxicity and immunogenicity, good safety in clinical use, ease of preparation and proven manufacturability at commercial scales [13].

The group of polymeric nanocarriers includes in particular polymeric micelles, dendrimers and polymeric matrix systems [14]. Micelles consist of amphiphilic block copolymers, forming a hydrophilic shell and hydrophobic core, which can encapsulate water-

insoluble drug molecules. Highly branched synthetic polymers, which offers precise control over their architecture, pharmacokinetics and biodistribution can be defined as dendrimers [10]. Polymeric NPs are colloidal systems in which the drugs can be loaded via different strategies, including encapsulation in the polymer matrix, entrapment in the polymeric membrane or covalent attachment to the surface of the NP [14]. In general, polymeric NPs show improved loading capacity compared to liposomes, however, caution is required as several polymeric materials have low biocompatibility. Therefore, research groups have developed hybrid lipid-polymer nanocomposites in which the advantages of both lipid and polymeric NPs were combined [15].

Besides the organic NPs as described above, also inorganic nanomaterials have been investigated for the purpose of cancer therapy, including gold nanoparticles (AuNPs), silica nanotubes, quantum dots, carbon nanotubes, and supra-paramagnetic iron oxide NPs. The inorganic NPs are mainly investigated for imaging and diagnostic purposes. As a therapeutic, the irradiation of AuNPs has been investigated for the induction of hyperthermia-mediated tumor ablation [16, 17].

1.2 Enhancing therapeutic potential of anti-cancer drugs by encapsulation in nanocarriers

The majority of nanomedicines currently on the market encapsulates a chemotherapeutic agent. The first nanomedicine that was approved by the FDA in 1995 is Doxil® (or Caelyx® in Europe), a liposomal formulation containing the anthracycline doxorubicin [18, 19]. Importantly, the liposomal formulation has reduced side effects compared to the free drug, especially with a drastic decrease in cardiotoxicity [20]. Moreover, the encapsulation has demonstrated a substantially higher efficacy compared to the administration of free doxorubicin, due to the longer circulation time of the PEGylated liposomes and passive targeting to the tumor [21]. Another example of a chemotherapeutic with improved performance when encapsulated in NPs is paclitaxel, which is on the market as Abraxane®. Paclitaxel is a hydrophobic drug, which necessitates encapsulation in NPs for systemic delivery. The nanocarrier in this case is albumin which forms a nano-conjugate upon mixing with paclitaxel [22]. An overview of the current nanocarriers on the market that encapsulate chemotherapeutics is illustrated in **Table 1**.

Table 1. Nanomedicines encapsulating chemotherapeutics on the market

Product name	Nanoparticle	Active compound	Indications
Abraxane®	Albumin-conjugate	Paclitaxel	Breast cancer
DaunoXome®	Liposome	Daunorubicin	Advanced HIV-associated Kaposi's sarcoma
DepoCyt®	Liposome	Cytosine Arabinoside (cytarabine)	Neoplastic meningitis
Doxil®/Caelyx®	PEGylated liposome	Doxorubicin	Refractory Kaposi's sarcoma, recurrent breast cancer, ovarian cancer
Genexol-PM®	Polymeric micelle	Paclitaxel	Breast cancer, non-small cell lung cancer, ovarian cancer
Marqibo®	Liposome	Vincristine	Philadelphia chromosome-negative acute lymphoblastic leukemia
Myocet®	Liposome	Doxorubicin	Metastatic breast cancer Ovarian cancer Kaposi's sarcoma
Onivyde®	Liposome	Irinotecan	Metastatic pancreatic cancer
Oncaspar®	Polymeric conjugate	Asparaginase	Acute lymphoblastic leukaemia

Based on Ref. [1, 3, 6, 23].

Besides chemotherapeutics, also small interfering RNA (siRNA) molecules are clinically investigated as anti-cancer therapeutics [8]. siRNA molecules trigger the endogenous RNA interference (RNAi) pathway, active in the cytoplasm of cells, through which the expression of virtually any gene can be silenced [24]. Synthetic siRNA, used for therapeutic application, typically consists of 21-23 base pairs, with 2 nucleotide overhangs at the 3' end of both strands. After entering the cytosol of the target cells, siRNA is incorporated in a protein complex called RNA induced silencing complex (RISC), in which the endonuclease Argonaute 2 (AGO2) unwinds the double stranded RNA and cleaves the sense (or 'passenger') strand [25] (**Figure 1**).

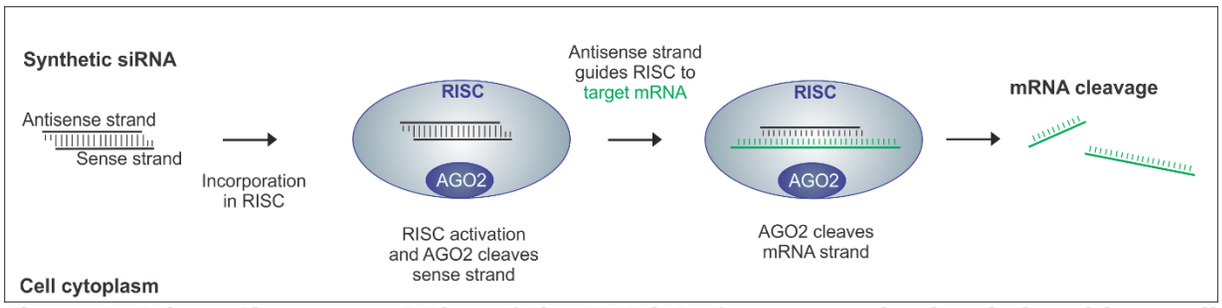

Figure 1. Schematic representation of the RNA interference mechanism induced by small interfering RNA (siRNA) in the cell cytoplasm. RNA induced silencing complex (RISC), Argonaute 2 (AGO2), messenger RNA (mRNA).

Subsequently, the antisense (or 'guide') strand, which is still incorporated in the RISC, directs this RISC to the complementary messenger RNA (mRNA) sequence, followed by the cleavage of the latter one by AGO2. The RISC complex can move to other mRNA strands to further cleave the target mRNAs, inducing potent gene silencing on the post-transcriptional level. Despite the high potential of RNAi to modulate gene expression in a sequence-specific manner, the non-drug like properties of siRNA molecules hinder their effective delivery to the target cell cytoplasm. First, the negative charges on the siRNA molecules impede their spontaneous internalization in target cells. Secondly, siRNA molecules are prone to degradation by nucleases and can be rapidly cleared from the blood via glomerular filtration and renal excretion [26]. As systemic administration of siRNA in cancer is mainly required for targeting both primary and metastatic cancer, also these anti-cancer therapeutics may benefit from the encapsulation in NPs. Although siRNA formulations for cancer are not yet on the market, clinical trials have been initiated, in which genes involved in cell cycle arrest, cell apoptosis, proliferation and tumor angiogenesis were selected as targets for silencing [27].

1.3 Overcoming in vivo barriers for targeting to the tumor

Despite the high amount of studies investigating the use of nanomedicines in cancer, the number of clinical products that are on the market is still very low [5]. One of the major hurdles that contributes to this discrepancy is the low accumulation of nanomedicines in the tumor. A critical barrier remains the vascular endothelium, which controls the extravasation of NPs from the bloodstream into the target tissue [28, 29]. Because NP extravasation is dependent on the size of fenestrae, tumor tissue may favor this delivery route by its leaky blood vasculature, allowing NP extravasation in the size range of 100-780 nm [30]. This increased extravasation in combination with the poor lymphatic drainage found in tumors results in the accumulation of NPs in the tumor tissue and is also known as the enhanced permeation and retention (EPR) phenomenon (**Figure 2**) [31]. Unfortunately, the widespread application of the EPR-based passive targeting to tumors is hampered by the heterogeneity in tumor vasculature both within a single tumor and between different tumor types [32, 33]. Moreover, passive targeting does not avoid the accumulation of NPs

in off-target organs that also have a fenestrated endothelium, such as the liver and spleen [34, 35].

To tackle these limitations, nanomedicines are frequently modified with a targeting ligand that specifically recognizes a receptor that is present on or overexpressed by tumor cells. A wide range of ligands have been investigated for this targeted delivery, including folate, transferrin, aptamers, and antibodies [14]. Several studies have shown that this active targeting strategy enhances the internalization in the target cells, albeit without increasing the accumulation in the tumor tissue after systemic delivery [36-38]. Furthermore, it was observed that active targeting can hinder the diffusion of NPs into the tumor tissue due to the binding-site barrier phenomenon in which particles mainly preferentially bind to perivascular cells, thus impeding deep tumor penetration of the particle and the drug [39].

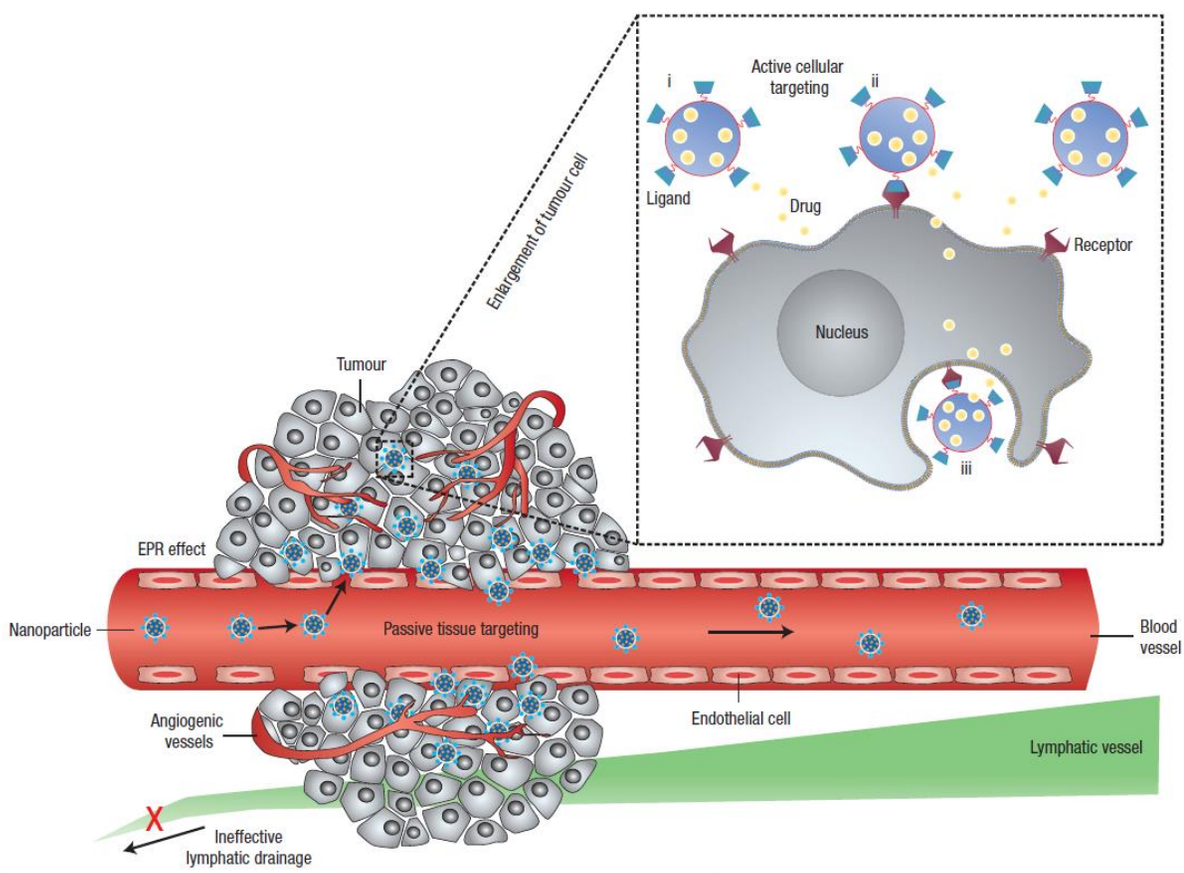

Figure 2. Schematic representation of passive and active targeting of nanoparticles (NPs) to the tumor. Passive targeting by the enhanced permeation and retention (EPR) phenomenon is achieved through a leaky vasculature in combination with an impaired lymphatic drainage. Active targeting (inset) by decorating the surface of NPs with targeting ligands assists the specific binding of NPs to the target cells. NPs can be designed to (i) release their cargo in close contact with the cells, (ii) bind to the cell membrane and function as a sustained-release drug depot or (iii) become internalized in the target cells and deliver their cargo to the cytosol. This figure was adapted with permission from Ref. [40], Nature Nanotechnology, Copyright 2007.

2 HITCHHIKING NANOPARTICLES: CELL-MEDIATED DELIVERY TO THE TUMOR

Despite many efforts to design NPs for efficient passive or active targeting, the tumor infiltration of NPs remains unsatisfactory. Cell-mediated NP delivery can be an interesting alternative to overcome this targeting limitation. The exploitation of cells as drug carriers was inspired by the observation that certain types of pathogens can attach themselves to red blood cells (RBCs) and in this way evade the clearance by the immune system. This discovery paved the way to use this cellular hitchhiking mechanism for the delivery of drugs and drug-loaded NPs. Owing to their long residence time and high abundance in the blood, RBCs have been widely investigated as drug delivery carriers and recently also for nanomedicine hitchhiking approaches. Unfortunately, RBCs do not have the intrinsic capacity to migrate to specific tissues in the body, thus limiting their use to enhancing the circulation time of drug-loaded NPs, which enables sustained drug release in the circulation. To promote the delivery of NPs across biological barriers and stimulate NP accumulation and penetration in diseases tissues (*e.g.* tumors and inflamed tissues), other migratory cells should be selected [41, 42]. Tumors are generally known to continuously produce cytokines and chemokines, which recruits several types of immune cells to the tumor [43]. The general advantages of these cells for NP hitchhiking includes (i) their natural migration to the tumor, (ii) their ability to prevent the NPs from rapid clearance from the blood stream, and (iii) their capacity to cross NP-impermeable barriers and penetrate specific tissues. For example, tumors contain hypoxic and necrotic regions that are generally not easily accessible for NPs, which can lead to incomplete tumor regression [44]. Certain immune cell types may help to overcome these barriers for NPs on their way to the tumor. Mesenchymal stem cells, monocytes, macrophages, and T lymphocytes are the most extensively studied cell types serving this purpose [41]. Of note, important for the cell-mediated drug delivery is that the viability and key functionalities of the tumoritropic cells are not impaired by loading them with NPs.

2.1 Strategies to load tumor-migratory cells with nanoparticles

The loading of tumoritropic cells with NPs can be achieved by either anchoring them to the cell surface or incorporating them inside the cell. The cell surface contains a variety of functional groups (belonging to proteins, lipids or polysaccharides) to which NPs can be covalently or non-covalently coupled. Different coupling strategies have been assessed including passive adsorption, ligand-receptor interactions, or covalent binding (**Figure 3**). The most straightforward coupling strategy is passive adsorption, in which positively charged NPs interact with the negatively charged cell membrane or in which hydrophobic regions of the NPs can insert into the cell membrane [45, 46]. Despite the advantage that cells do not require modification for passive adsorption, an important limitation is that premature drug release after systemic injection may occur due to the uncontrollable strength of this interaction. A strategy that offers higher stability is a ligand-receptor

interaction. Similar to the adsorption strategy, cell surface modifications are not required prior to coupling. Of note, for this approach the NPs have to be modified with a specific ligand at their surface, which requires the inclusion of additional steps in the NP design. Importantly, the ligand-receptor interaction needs to be very specific to avoid undesired interaction of the NPs with other cell types. A ligand-receptor coupling has already been investigated for the coupling of microparticulate patches to the surface of macrophages, T cells, and B cells via their CD44 receptor. For this purpose, the patches were decorated with hyaluronic acid to allow the coupling [47-49]. The most optimal coupling strategy in terms of stability is the covalent binding. Cells contain numerous functional groups at their surface, *e.g.* amine and thiol groups, which can be employed for the covalent attachment of NPs. A first example of this coupling strategy is the incorporation of a maleimide (MAL) or pyridyldithiopropionate (PDP) group on the NP surface that is able to interact with exposed thiol groups at the cell surface and forms a stable thioether and reversible disulfide bond, respectively [50]. Another example is the conjugation of biotin groups to the cell surface via amine groups, which allows the covalent coupling via the interaction with streptavidin/neutravidin-functionalized NPs [51]. Finally, utilizing the phagocytic capacity of cells such as monocytes and macrophages, a fourth strategy is based on the internalization of NPs in carrier cells, acting as a 'Trojan Horse' to deliver the NPs inside the tumor [52]. Although the nanoparticles are thus shielded from off-target interactions with other cells and tissues, this strategy might lead to degradation of the ingested particles and/or the drug and offers limited control over drug release. In addition, dependent on the nature of the drug, such premature drug release can also induce unwanted carrier cell apoptosis.

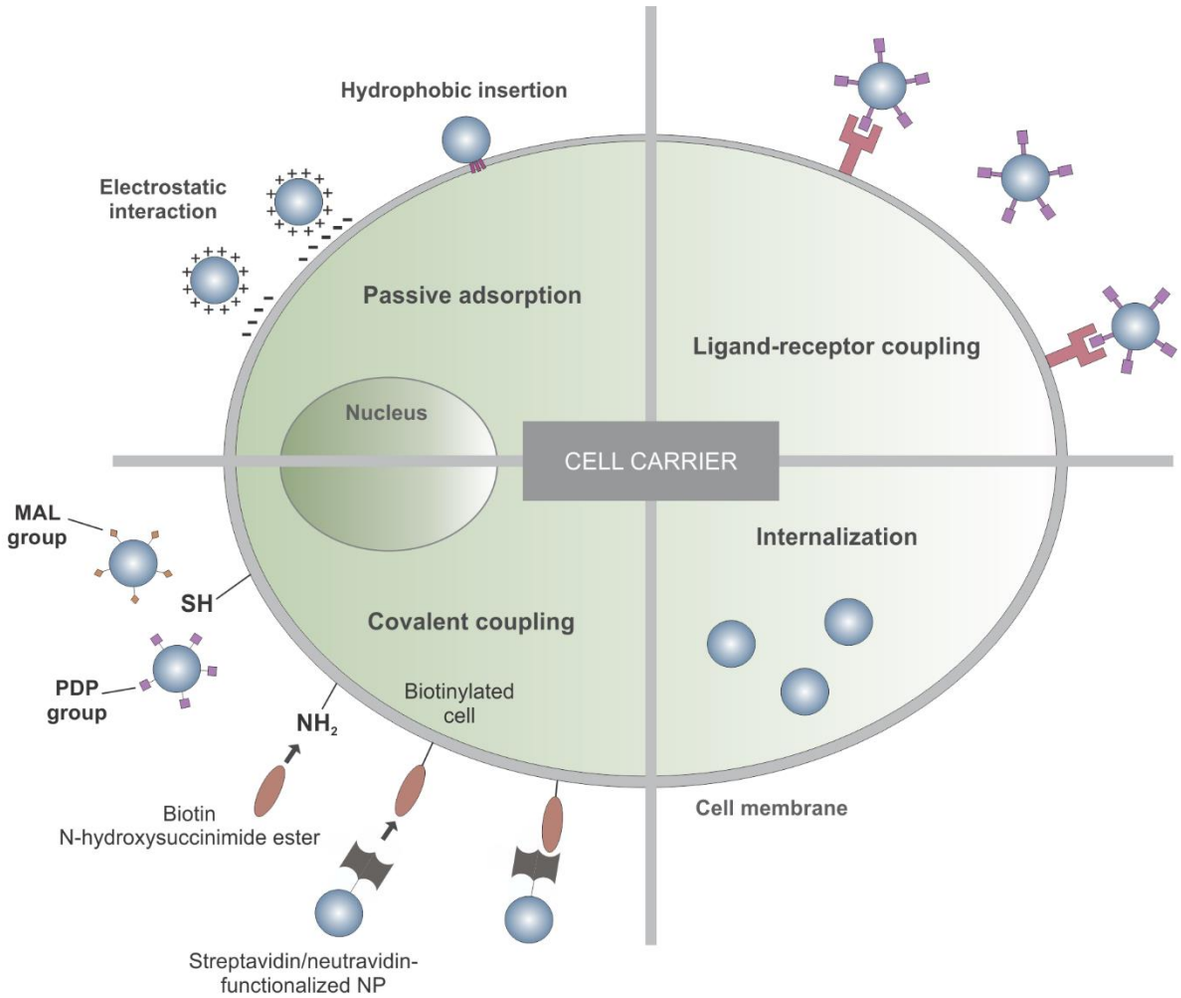

Figure 3. Strategies to load tumoritropic cells with nanomedicines. Nanoparticles (NPs) can be loaded onto the cell surface via passive adsorption, ligand-receptor coupling or covalent coupling. Passive adsorption is achieved via either an electrostatic interaction or hydrophobic insertion of NPs into the cell membrane. NPs can be functionalized with ligands from which the receptors are known to be expressed at the cell surface. Several functional groups present at the cell surface such as thiol groups (SH) and amine groups (NH_2) are used to obtain a covalent coupling. For example, maleimide- (MAL) and pyridyldithiopropionate- (PDP) functionalized NPs can be anchored to the cell surface via a thioether and disulfide bond, respectively. Another covalent binding is mediated by the incorporation of a streptavidin or neutravidin functional group in the NP composition which can bind to biotinylated cells. The carrier cells can be decorated with biotin groups via the interaction of biotin N-hydroxysuccinimide esters with amine groups present at the cell surface. Cells can also be loaded with nanomaterials via the internalization of the NPs.

2.2 Selecting migratory cells for cell-mediated delivery to the tumor

Both mesenchymal (MSCs) and neural stem cells (NSCs) have been exploited for the delivery of NPs to brain tumors such as gliomas. The loading of MSCs and NSCs with NPs has been achieved via either biotin-streptavidin coupling at the cell surface or the internalization of NPs for the delivery of therapeutics or imaging agents [53-57]. An attractive advantage of MSCs and NSCs is that they are able to penetrate hypoxic tumor regions [53, 58]. However, a major limitation of NSCs compared to MSCs is the lower yield of NSCs from a patient. On the other hand, a potential limitation of MSCs for clinical applications is their ability to promote metastasis [59, 60].

Similar to MSCs and NSCs, monocytes and macrophages are well-known to cross the blood brain barrier and migrate to hypoxic areas [61, 62]. In most cases, NPs are loaded into monocytes and macrophages by their phagocytic capability. Due to the internalization of cytotoxic agents such as gold nanoshells and NPs containing chemotherapeutics, the monocytes and macrophages act as 'Trojan Horses', capable of infiltrating the malignant tissue with tumor destructive NPs [63]. Also a few studies reported on the ligand-receptor attachment of microparticles to the cell surface, referred to as cellular backpacks, hence avoiding the phagocytic ingestion of the particles and gaining control over the drug delivery process [64, 65]. On the other hand, the possible negative impact of a surface-bound rigid micron-sized structure on the cell's migratory capacity, should be considered.

T cells play a key role in the immune response against cancer as they are able to induce targeted tumor cell killing. Therefore, they exhibit natural homing to the tumor tissue which makes them attractive carriers for cell-mediated delivery. In contrast to monocytes and macrophages, the internalization of NPs in T cells is limited, which favors the loading of the NPs via plasma membrane anchoring. Several studies have already demonstrated the potential of T cells to deliver NPs to tumor tissues. Irvine and colleagues attached NPs via a thioether bond and demonstrated the successful tumor infiltration of NPs loaded onto T cells, while the injection of free NPs resulted in the rapid clearance via the liver and spleen. This research group investigated the covalent coupling of three different types of therapeutics; (i) cytokines for the autocrine stimulation of T cells, (ii) small molecules that stimulate T cell activity and proliferation, and (iii) chemotherapeutics that kill tumor cells [66-68]. Besides the delivery of NPs, T-cell mediated tumor transport has also been exploited for the successful delivery of oncolytic viruses to the tumor [69, 70].

2.3 T cell-mediated drug delivery: combining migration and effector functions

The cell-mediated delivery of NPs to the tumor via T cells does not only take advantage of their tumor migration capacity, but also of their cytolytic effect on tumor cells. The role of T cells in the fight against cancer is initiated upon the endogenous activation of naive T cells by recognizing antigens present on the major histocompatibility complex I (MHC I) of antigen-presenting cells (APCs) such as dendritic cells (DCs). Both DCs and T cells meet each other in the secondary lymphoid tissues. Upon recognition of the antigen in combination with co-stimulatory signals of the APCs, T cells become activated, which initiates proliferation and homing of the T cells to the inflamed tissue. Activated $CD8^+$ T cells are referred to as cytotoxic T lymphocytes (CTLs). T cell homing is a highly dynamic process, which involves a number of consecutive steps. First, activated T cells lose the expression of CD62L and CCR7, which reduces their capacity to enter the lymph nodes and promotes their circulation in the blood [71]. Secondly, to leave the blood stream at the tumor tissue, T cells express adhesion molecules such as ligands for E- and P-selectin, allowing the T cells to attach to the endothelium of the inflamed tissue (**Figure 4**). However,

the selectin binding is not able to completely arrest the T cells, which results in so-called rolling of the cells over the endothelium. When T cells bind via their chemokine receptors (*e.g.* CXCR3) to chemokines (*e.g.* CXCL9 and CXCL10) that are presented on the endothelial surface or secreted by the inflamed tissues, integrins become activated on the T cell surface. Subsequently, due to binding of these integrins such as lymphocyte function-associated antigen 1 (LFA-1) and very late antigen 4 (VLA-4) to the endothelium via intracellular adhesion molecule 1 (ICAM-1) and vascular cell adhesion molecule 1 (VCAM-1), respectively, T cells are arrested, which makes them amenable for extravasation [72]. Arrested T cells scan the endothelial surface and lumen for chemotactic exit cues, followed by endothelial transmigration. This highlights the importance of the production of chemokines in the tumor tissue to recruit CTLs [73]. Once arrived in the tumor, T cells search their specific tumor antigen presented by MHC I molecules onto the surface of tumor cells. Upon binding of tumor antigen to the T-cell receptor (TCR), they release granules containing the cytotoxic proteins perforin and granzyme, which induces apoptosis of the tumor cell. Most T cell effector cells die when the antigen is cleared, but a few memory T cells remain for long-term immune responses against the tumor antigen [74].

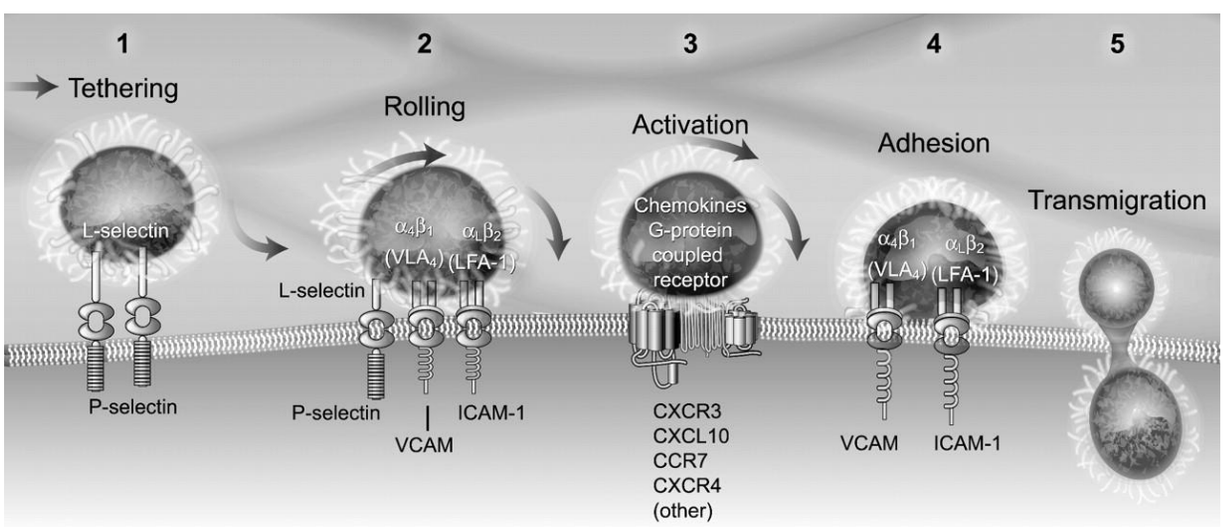

Figure 4: Trafficking of T cells into inflamed tissue. This figure was adapted with permission from Ref. [75], Brain, Copyright 2004.

PART II: CANCER IMMUNOTHERAPY

1 THE PROMISE OF CANCER IMMUNOTHERAPY

Early attempts to detect components or functions unique to cancer cells were made over a century ago, leading to the conviction in the 1950s that 'tumor-specific materials' probably did not exist, since over 50 years of work delivered little to no evidence [76]. However, studies performed by Gross, Foley and Prehn as early as the 1940s and 1950s showed that mice previously cured from a specific tumor, were immune to a rechallenge with the same tumor [77, 78]. These studies together with many others in the 1960s, showing the rejection of transplanted tumors in syngeneic mice, reinstated the idea of 'tumor-specific materials', at that time referred to as 'tumor-specific transplantation antigens' [79, 80]. In this regard, it is important to mention that the first evidence for the existence of such antigens was delivered by Gold and colleagues who demonstrated humoral responses to an antigen specific for colon cancer, in particular for the carcinoembryonic antigen (CEA) [81, 82]. The existence of antigens which can elicit specific humoral immune responses and are expressed by tumor cells, was confirmed in the late 1970s by Steven Rosenberg and colleagues [83]. A decade later, it was shown by Thierry Boon and colleagues that these antigens could also elicit potent T cell responses [84]. These antigens are today known as tumor antigens, i.e. antigens that are uniquely, preferentially or in excess expressed by tumor cells. Importantly, the description of immune responses against these tumor antigens has rationalized the so-called tumor surveillance concept that was formally introduced in the early 1970s by Burnet and Thomas, which confirmed previous observations by Ehrlich [85]. Thus, a model was proposed in which tumor cells are recognized as foreign and subsequently specifically eliminated without damaging healthy cells, much in the same way as for virally-infected cells.

Several immunotherapy strategies have been devised so far, for example strategies aimed at increasing tumor antigen-specific T cells *in vivo* through cancer vaccination or adoptive T cell therapy (ACT). Cancer vaccination aims to activate anti-tumor T cells by stimulating DCs to present tumor-associated antigens (TAA) while in ACT the tumor-specific T cells are directly injected into the patients. Other therapeutic strategies are developed to support tumor antigen-specific T cell responses, including cytokine-based therapy (*e.g.* IL-2) and antibody therapy blocking critical immune checkpoints (*e.g.* cytotoxic T lymphocyte-associated antigen 4 (CTLA-4) and programmed cell death 1 (PD-1)) [86-89]. These strategies interfere with both the innate and adaptive immune system (**Figure 5**). Although immunotherapy in general and its subdomains in particular are complex and challenging fields, there have been major advances in basic and translational research in each of the approaches resulting in clinical trials that are now beginning to deliver on their promise. First, we will give an overview of the different identified tumor antigens, which are of utmost

importance in cancer vaccination and ACT. Next, the immunosuppressive role of the tumor microenvironment will be highlighted and to finally conclude, an in-depth description of the different immunotherapeutics will be provided.

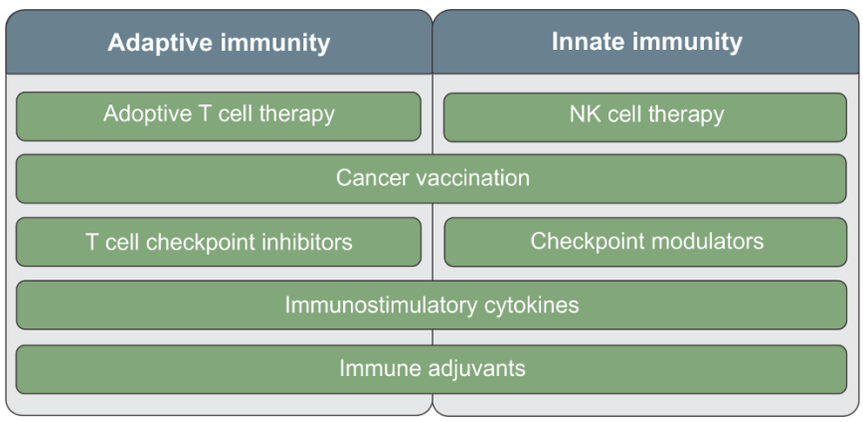

Figure 5. Overview of cancer immunotherapies. (Adapted from [90]).

1.1 Tumor antigens are the key to effective immunotherapy

Generally, tumor antigens are divided into five classes, including tissue-differentiation antigens (*e.g.* Melan-A/MART-1, TRP-2, etc.), antigens that are overexpressed (*e.g.* survivin, telomerase, etc.), antigens derived from epigenetic changes or the so-called cancer-testis antigens (*e.g.* MAGE-A3, NY-ESO-1, etc.), antigens derived from mutated genes (*e.g.* p53, RAS, etc.), and viral antigens (*e.g.* derived from human papillomaviruses, Ebstein-Barr viruses, etc.). Alternatively, these tumor antigens can be subdivided in two main classes: self-antigens and tumor-specific antigens (**Figure 6**).

Self-antigens are present on both tumor cells and normal tissues in contrast to the tumor-specific antigens, of which the expression is restricted to tumor cells. Tumor-specific antigens, also referred to as neoantigens, arise from somatic mutations. In 1991, van der Bruggen and colleagues cloned the first human tumor antigen that is recognized by T cells [91]. This melanoma-associated antigen MAGE-A1 was identified by a genetic approach, which paved the way for the discovery of multiple antigens on a broad range of tumor types [92]. Most of these antigens can be classified in the group of self-antigens. A characteristic of these self-antigens is that they are usually expressed on a wide variety of tumors of different histological origins. Therefore, these antigens can also be classified as so-called shared antigens. Of note, some tumor-specific antigens can also be shared between patients, for example virus-derived antigens and mutRas, mutP53, and mutEGFR [93].

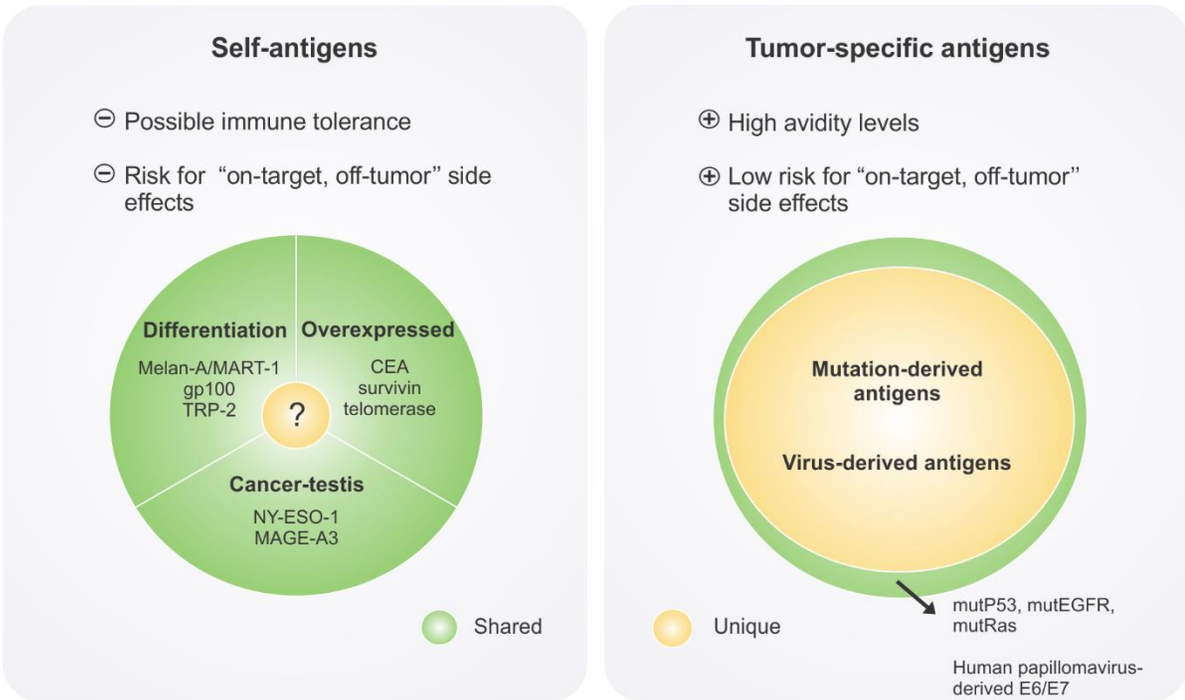

Figure 6. Tumor antigens as targets for cancer immunotherapy. Tumor antigens can be subdivided in two main classes: self-antigens and tumor-specific antigens. The class of self-antigens encompasses differentiation, overexpressed, and cancer-testis antigens. Self-antigens are expressed on both tumor cells and normal tissues. Consequently, cancer immunotherapies that target these antigens can encounter problems due to immune tolerance and 'on-target, off-tumor' side effects. The class of tumor-specific antigens includes mutation-derived and virus-derived antigens. Cancer immunotherapies targeting these antigens have advantages in terms of high avidity levels and low risk for toxic side effects. Generally, self-antigens are shared between patients while the majority of tumor-specific antigens are unique, although virus-derived antigens and some mutation-derived antigens can also be shared between patients. Examples of tumor antigens are illustrated in the figure (adapted from Ref.[94]).

In the past, researchers have focused on the identification of shared antigens for the production of off-the-shelf immunotherapeutics that could be used in a broad range of patients [95]. However, tumor-specific antigens, which are patient-specific, were shown to be the most ideal targets for immunotherapy because of their expression restricted to tumor cells, which limits toxicity towards normal cells. Moreover, as these arise from mutations, there is no tolerance to the presented epitope. In the past, the development of immunotherapies against tumor-specific antigens was hindered by the uniqueness of neoantigens in a patient's tumor together with a lack of techniques able to systematically test T cell responses against neoantigens. The development of the next-generation sequencing (NGS) technology enables the systematic sequencing of whole cancer genomes, providing insights into the mutational landscape of various human cancers [96, 97]. Whole-genome sequencing was already employed to characterize the genome of cancers such as acute myelogenous leukemia, breast cancer and melanoma [98-100]. By comparing the genome of cancer cells with the one of the original healthy cells, cancer-specific mutations can be identified [101].

Table 2. Overview of tumor antigens as potential targets for immunotherapy

Antigen	Characteristics	Examples	Advantages and limitations as target for immunotherapy	References
Tissue-differentiation	Expression on both tumor cells and normal cells of the same tissue Cancers: especially tested for melanoma	Melan-A MART-1 gp100 TRP-2	+ Broad expression range: off-the-shelf immunotherapy - Toxicity towards healthy cells of the same tissue - Immune tolerance	[102, 103]
Overexpressed	Overexpression on tumor cells with low expression on healthy cells Cancers: broad range of epithelial cancers	CEA CAIX Survivin telomerase	+ Broad expression range: off-the-shelf immunotherapy - Toxicity towards healthy cells - Immune tolerance	[104-106]
Cancer-testis	Expression on normal cells is restricted to germline cells in the (immunopriviledged) testis Cancers: melanoma, hematological malignancies, breast, lung, prostate, ovarian, bladder, colorectal, hepatocellular carcinoma	NY-ESO-1 MAGE-A3	+ Broad expression range: off-the-shelf immunotherapy - Several studies reported on toxicity due to low expression on healthy cells, not part of the immunoprivileged site + Considered as foreign-like antigens to which immune tolerance is limited	[91, 107-115]
Virus-derived	Expression arises as a consequence of infection with an oncovirus Cancers: Cervical, penile, anal, head and neck	Human papillomavirus -derived E6/E7	+ Expression only on virus-derived cancers but off-the-shelf possible due to shared antigens between patients infected with the same virus + Expression restricted to tumor cells + No tolerance issues	[116-119]
Mutation-derived = neoantigens	Expression arises from genetic mutations Cancers with high mutation load: *e.g.* melanoma, lung, colorectal		- Highly patient-specific expression: personalized immunotherapy + Expression restricted to tumor cells + No tolerance issues	[93, 94, 120]

Decreasing costs of NGS should facilitate the detection of patient-specific tumor mutations and identification of neoantigens for personalized immune-based cancer therapy. Exceptionally, some neoantigens recognized by autologous T cells are known to be shared between patients such as mutRas, mutP53, and mutEGFR [93]. In addition, a recent study reported on shared frame shift-derived neoantigens that were recognized by antigen-specific T cells in different microsatellite-instable leukemia and lymphoma cell lines [121]. The different types of antigens with their advantages and limitations when used as a target for cancer immunotherapy are summarized in **Table 2**.

1.2 The tumor microenvironment as a major hurdle in cancer immunotherapy

Despite the potential of cancer vaccination and ACT to induce powerful immune responses against cancer, clinical trials have demonstrated that responses were only seen in a subset of patients. This can partially be subscribed to the low infiltration of antigen-specific T cells into the tumor as well as to the dual role of the immune system in cancer. It has been shown that growing tumors can hijack the immune system, causing it to promote tumor progression, rather than suppress tumor outgrowth. The function of the immune system in preventing, controlling and even promoting cancer can be referred to as the process of cancer immunoediting [122, 123].

Patients differ in the immune responses they develop against cancer based on differences that can be related to mutations or polymorphisms in immune regulatory genes or various environmental influences [124]. This can result in tumor heterogeneity between patients with the same type of cancers and can further explain why some tumors show low infiltration by immune cells, while others are highly infiltrated by lymphocytes. In general, immunological classification of cancer types consists of three distinct subtypes, including (i) immunogenic, (ii) inflammatory, and (iii) immune-escaping tumors [125]. Immunogenic tumors are characterized by a high infiltration of CTLs and the secretion of immunostimulatory cytokines such as interferon gamma (IFNγ), resulting in a good prognosis. Although inflammatory tumors show good infiltration by lymphocytes, the microenvironment contains a multitude of angiogenic and immunosuppressive molecules such as transforming growth factor β (TGFβ) and programmed cell death ligand 1 (PD-L1), which results in low immune responses against the cancer and a poor prognosis for the patient. On the other hand, several tumors, referred to as immune-escaping tumors, lack the infiltration of immune cells and do not secrete cytokines, which make them unresponsive to cancer immunotherapy. In this case, therapeutic strategies are required to induce an inflamed tumor microenvironment, for example via innate immune activators such as stimulator of interferon genes (STING) agonists [126].

1.2.1 Trafficking of T cells into the tumor can be blunted

The success of cancer vaccination and ACT largely depends on the capacity to increase the number of effector T cells in the tumor. As several studies demonstrated improved clinical benefit of immunotherapies in patients with a highly T cell-inflamed tumor, it is important to develop strategies to promote T cell infiltration in the tumor site [127-129]. Factors contributing to this low tumor infiltration are the presence of a dense stroma that can sterically impede the infiltration of immune cells as well as low levels of inflammatory chemokines to recruit anti-tumor T cells (**Figure 7**). Indeed, metastatic tumors expressing the chemokines CXCL9 and CXCL10 were shown to be more infiltrated with CTLs [130]. Importantly, T cell migration is not solely regulated by tumor-mediated chemokine secretion; T cells should also exhibit upregulated chemokine receptors to be responsive to the chemotactic recruitment by the chemokines secreted by the tumor.

1.2.2 Immunosuppressive pathways exerted by the tumor and its environment

Tumor-promoting immune cells. The tumor microenvironment consists of a variety of different cell types such as tumor cells and stroma cells, including endothelial cells, fibroblasts, pericytes, and distinct immune cell types [71]. Cancer cells and several immune cells such as myeloid-derived suppressor cells (MDSCs), regulatory T cells (T_{regs}), tumor-polarized or regulatory DCs, and tumor-associated macrophages (TAMs) were shown to induce immunosuppressive pathways (**Figure 7**). MDSCs represent a heterogeneous population of immature myeloid cells that suppresses both innate and adaptive immune responses. They favor tumor progression by a variety of mechanisms including the production of immunosuppressive cytokines which blocks effector T cells, the inhibition of antigen-presenting cells to activate T cells, and the induction of the expansion of T_{regs} [131-133]. Thus, therapeutic strategies to neutralize MDSCs are of interest as adjunct strategy to other immunotherapies [134, 135]. T_{regs} are known to inhibit T cell anti-tumor functions and are therefore eradicated by lymphodepleting regimens prior to adoptive T cell transfer [136]. The clinical benefit of lymphodepletion was demonstrated by various preclinical and clinical trials [137-140]. Mostly, these treatments comprise the lymphoablative chemotherapeutics cyclophosphamide and fludarabine, often in combination with total body irradiation [141].

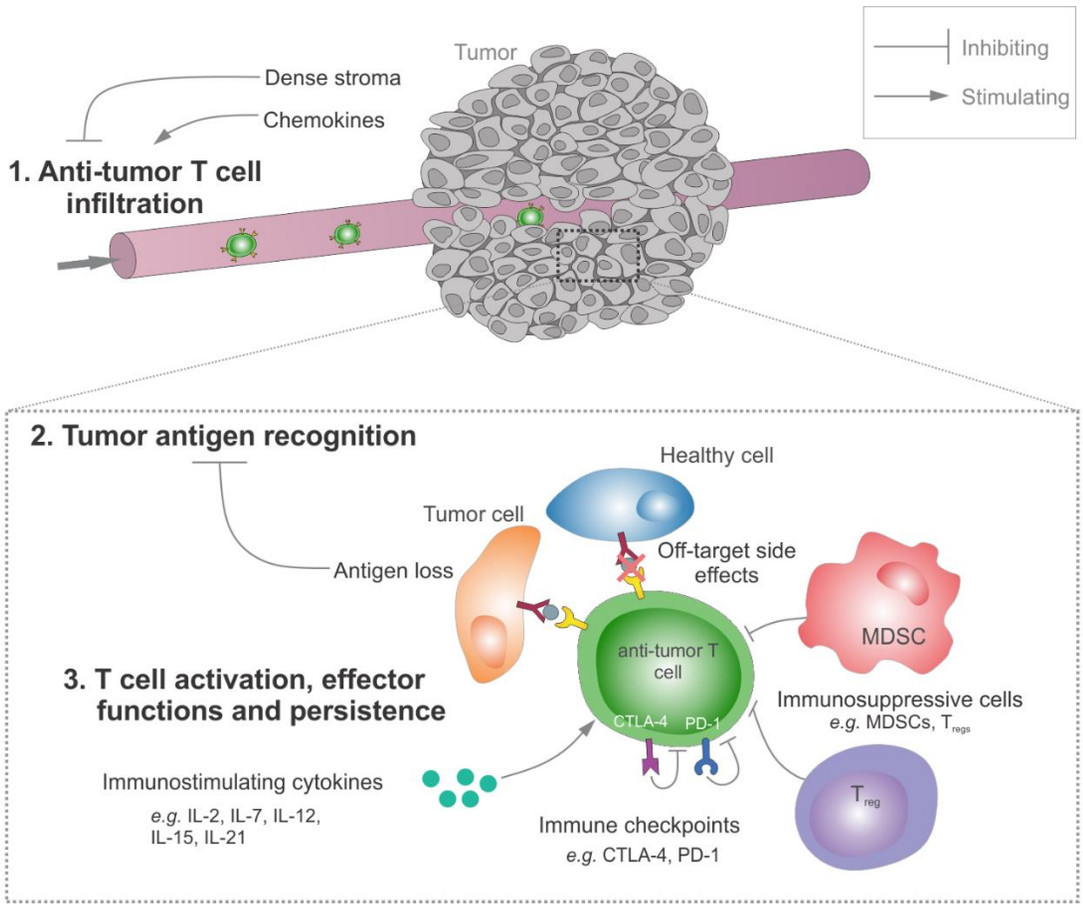

Figure 7. Successful cancer immunotherapy requires infiltration of anti-tumor T cells, tumor antigen recognition, and T cell activation, effector actions and persistence. All of these different steps can be stimulated or inhibited by different molecules or pathways. T cell infiltration can be stimulated by the presence of chemokines in the tumor site or inhibited by a dense stroma. Tumor antigen recognition can encounter problems due to antigen loss or off-target side effects can occur upon interaction of the anti-tumor T cells with healthy cells. T cell activation, effector actions and persistence can be stimulated by cytokines such as interleukins or inhibited by immunosuppressive pathways (immune checkpoints), and cells such as myeloid-derived suppressor cells (MDSCs) and regulatory T cells (T_{regs}). Cytotoxic T lymphocyte-associated antigen 4 (CTLA-4), programmed cell death 1 (PD-1).

In addition to T_{reg} depletion, the destructive effects of total body irradiation and lymphoablative chemotherapy on tumor cells initiate a release of tumor antigens that can be taken up by APCs, resulting in the enhanced activation of T cells [142, 143]. However, the toxicity associated with lymphodepleting preconditioning precludes a number of patients from ACT and warrants the investigation of other strategies that are better tolerated.

Immune checkpoints. One of the best-studied mechanisms of immunosuppressive immune cells to inhibit T cell effector functions is via binding to the so-called immune checkpoints on T cells, *e.g.* CTLA-4 and PD-1. Immune checkpoints are important for the maintenance of self-tolerance and regulate the amplitude and duration of immune responses [144]. However, besides immune cells, tumor cells may also interact with some of these inhibitory pathways to escape immunity. For example, the expression of a PD-L1 ligand on tumor cells indicates an escape strategy of certain tumors by the induction of the PD-1 pathway. Another example is CTLA-4, a CD28 homologue, that is expressed on

activated T cells and downregulates T cell activation upon ligation with CD80 or CD86 on APCs [145].

Tumor heterogeneity. Besides a multitude of immunosuppressive pathways, the clinical success of cancer immunotherapy can also be hindered by tumor heterogeneity, which can be described as the presence of genetically distinct subpopulations within a tumor. Several studies demonstrated different genotypes and phenotypes within separated regions of hematological and solid cancers due to diverse somatic mutational events and DNA copy number aberrations [146]. Consequently, the identification of target neoantigens by a single tumor biopsy sample might often not be representative for the total tumor mass, leading to recurrent disease. Besides somatic mutations and DNA copy number aberrations in neoantigens leading to a decrease in antigen recognition, several studies demonstrated antigen loss or a decrease in antigen expression in tumors as a consequence of the pressure of antigen-specific T cells [140, 147-149].

Based on the issues raised in the previous paragraphs, therapeutic strategies to improve the number of patients that respond to the cancer immunotherapy consist of (i) increasing the number of infiltrated T cells in the tumor, (ii) enhancing the effector function and importantly the persistence of T cells by the delivery of stimulatory cytokines or antibodies and (iii) the inhibition of suppressive immune pathways by checkpoint inhibitors. Some of these strategies are currently used in the clinic as monotherapies. However, it is important to consider that for example stimulatory cytokines and checkpoint inhibitors are only effective when endogenous anti-tumor T cells are initiated. Some tumors, such as melanoma and also small cell lung carcinomas are known to induce endogenous immune responses as they have the highest mutation rates, due to the exposure to respectively ultraviolet radiation and tobacco smoke [150, 151].

1.3 An in-depth overview of the different cancer immunotherapies

1.3.1 Adoptive T cell therapy

The discovery of antigen-specific and tumor-reactive T lymphocytes in the tumors of patients paved the way for ACT, which can be described as the treatment of patients with *ex vivo* selected and expanded tumor-reactive T cells. Both immediate anti-tumor responses by effector T cells and long-term effects by memory T cells can induce complete remission in patients that are incurable by other anti-cancer treatments. Two major sources of T lymphocytes for ACT are the tumor itself and the patient's peripheral blood (**Figure 8**). In case the tumor is infiltrated by anti-tumor T cells, these cells can be isolated from the resected tumor mass. Rosenberg and colleagues reported on a study with 93 metastatic melanoma patients from whom tumor-infiltrating lymphocytes (TILs) were isolated. In these patients, chemotherapy and other immunotherapies such as IL-2 and anti-CTLA-4 treatments had failed. The T cells isolated from the resected tumor were first selected for

anti-tumor reactivity and expanded *ex vivo*. Twenty patients (22%) achieved a complete regression with ongoing complete responses in 19 patients after 3 years [152].

In spite of the successful outcomes in metastatic melanoma patients, a major limitation of TIL therapy is the absence of sufficient numbers of TILs in other types of cancer than melanoma. To extend the treatment of cancers with autologous T cells to a wide variety of cancer types, an alternative approach is the transfer of antigen-specific T cell receptor (TCR) genes into lymphocytes isolated from the patient's peripheral blood [153, 154]. Via transduction of T cells with retroviruses or lentiviruses, T cells can be engineered to recognize tumor antigens and eradicate tumor cells that express these antigens in large numbers of patients [151]. A study by Robbins and colleagues demonstrated objective clinical responses in patients with metastatic synovial cell sarcoma and melanoma treated with TCRs towards NY-ESO-1 antigens. Two melanoma patients out of 11 exhibited complete regression that persisted for more than 1 year [155]. Although most clinical trials show objective responses in melanoma patients, the challenge is now to expand this TCR engineering approach to a broader range of cancers. A recent study by June and coworkers reported on the treatment of multiple myeloma patients with T cells engineered to express a TCR against NY-ESO-1 and LAGE-1. Infusion of the T cells was well-tolerated without inducing the life threatening cytokine-release syndrome. Sixteen out of 20 patients showed a clinical response with a median progression-free survival of 19.1 months [156].

In addition to TCR-engineered T cells, chimeric antigen receptor (CAR)-modified T cells represent a second class of engineered T lymphocytes. In contrast to TCRs that are specific for a certain HLA-peptide complex, CARs can recognize antigens in a non-HLA-dependent way. This can be advantageous for the broad application of CARs in patients with different HLA haplotypes [157].

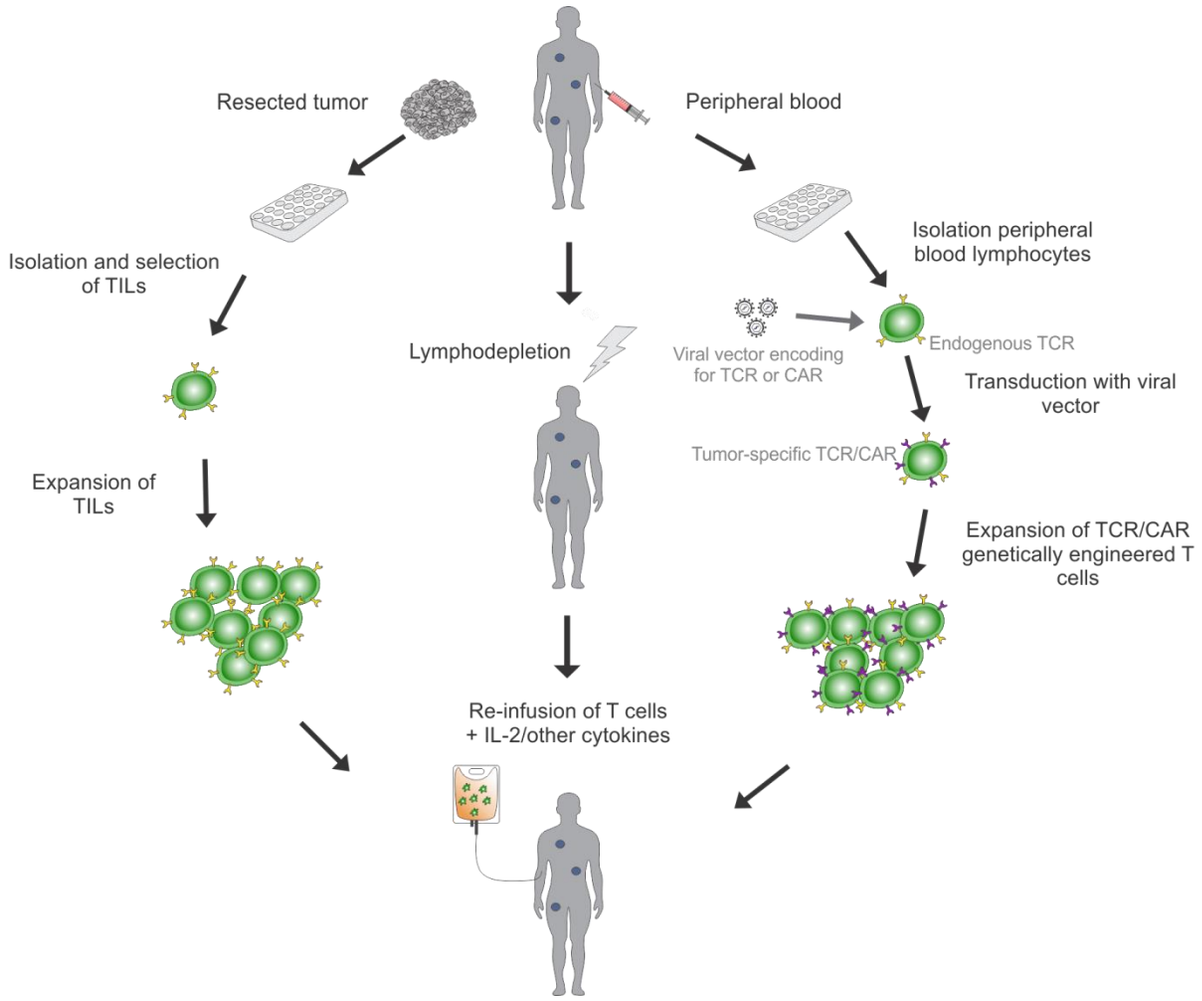

Figure 8. General overview of adoptive T cell therapy (ACT). Two major sources of T lymphocytes for ACT are the tumor itself and the peripheral blood. In case the tumor is infiltrated by anti-tumor T lymphocytes, tumor-infiltrating lymphocytes (TILs) can be isolated and selected for tumor reactivity followed by *ex vivo* expansion. Alternatively, peripheral blood lymphocytes can be isolated from the cancer patient followed by transduction with retroviral or lentiviral vectors encoding for a T cell receptor (TCR) or chimeric antigen receptor (CAR) and *ex vivo* expansion. During the engineering and expansion process of the anti-tumor T lymphocytes, the patient is treated with lymphodepleting chemotherapy, often in combination with total body irradiation. Subsequently, the expanded anti-tumor T cells are re-infused into the patient in combination with interleukins such as IL-2.

Furthermore, CARs increase the number of potential targets due to their recognition of not only proteins but also carbohydrates and glycolipids [158]. Although one of the first successful CAR therapies with complete remissions was reported on a solid neuroblastoma tumor, the most investigated tumors with CARs are hematological malignancies [159]. To date, the most investigated CAR target is CD19, which is expressed on normal B cells as well as on the majority of B cell leukemia's and lymphomas. Several clinical studies on patients with B cell malignancies such as chronic lymphocytic leukemia resulted in partial and complete responses in a subset of patients [160-162]. The clinical success of CAR therapies targeting CD19 was recently shown by complete response rates of almost 90% in both pediatric and adult patients with relapsed or refractory acute lymphoblastic leukemia [163]. However, a specific report on the CD19-targeted CAR treatment of 2 children with relapsed and refractory acute lymphoblastic leukemia clearly indicated one of the important

reasons why patients relapse [164]. The study described the complete regression in both children. One child was reported with an ongoing complete regression while the other child relapsed due to the growth of blast cells that no longer expressed CD19. These observations demonstrated that CD19 CARs are able to kill aggressive leukemia's. Nevertheless, the development of T cells with CARs against other molecules in combination with CD19 CARs is recommended in case the tumor can escape immune responses by downregulation of the CD19 CAR target. Based on the success of CAR therapies in hematological malignancies, the expansion of this therapy to numerous solid tumors is one of the major future goals of ACT. Of note however, the eradication of solid tumors appears to be more challenging by virtue of an immunosuppressive tumor microenvironment that may hinder cell-based immunotherapy. Therefore, combinatorial strategies of ACT with therapeutics that inhibit the immunosuppressive role and stimulate T cells to infiltrate the tumor are gaining much interest in recent years.

1.3.2 Cancer vaccination

Whereas most frequently administered vaccines against microbial infections are aimed at prophylaxis, cancer vaccines are mostly used as a treatment strategy. The immune system can fight against cancer via the presentation of tumor antigens by APCs, notably DCs, to activate tumor-specific $CD4^+$ and $CD8^+$ T lymphocytes. Many different cancer vaccination strategies have been proposed including the immunization with whole tumor cells, tumor lysates, peptides, proteins, recombinant viruses, and nucleic acids, such as DNA and mRNA encoding tumor antigens [165-171]. In the past, the inclusion of immune adjuvants in the vaccines has appeared to be crucial for the induction of an efficacious immune response [172]. Another approach in active immunization is the use of antigen-modified DCs as therapeutic vaccines, for which DCs are loaded *ex vivo* with tumor-derived peptides, proteins, and tumor cell lysates [173]. In 2010, the first cell-based cancer therapy, sipuleucel-T (marketed as Provenge®), was approved by the FDA. Sipuleucel-T is a patient-specific treatment for men with metastatic castration-resistant prostate cancer. In this therapy, peripheral blood mononuclear cells are isolated from the patient and *ex vivo* activated with a recombinant fusion protein consisting of a prostate antigen prostatic acid phosphatase (PAP) that is fused to granulocyte-macrophage colony-stimulating factor (GM-CSF), which is an immune-stimulating growth factor. Subsequently, the cells are re-infused into the patient to activate PAP-specific T cells [174]. In a randomized placebo-controlled clinical trial in 512 patients, an improved survival of 4.1 months was observed [175].

Furthermore, DCs can also be loaded *ex vivo* with tumor-associated antigens (TAAs) by genetic engineering using viral vectors, such as lentiviruses and adenoviruses, or with mRNA encoding TAAs and immune adjuvants [176-178]. The transfer of *ex vivo* mRNA-modified DCs has proven to be an elegant method for cancer vaccination. In 1997, the FDA

approved the first clinical trials with *ex vivo* mRNA-transfected DCs [179, 180]. Over the past decades, clinical trials have shown that vaccines consisting of autologous DCs loaded with tumor antigen mRNA are safe, well-tolerated and capable of inducing T cell-mediated immune responses in a significant number of cancer patients, including patients with colorectal, lung, breast and prostate cancer, as well as melanoma [181-184].

1.3.3 Immunostimulatory cytokines

Interleukins that are currently used in therapy or investigated for the stimulation of anti-tumor T cells are IL-2, IL-7, IL-15, and IL-21. IL-2 is a T cell growth factor that promotes activation, proliferation, survival, and effector functions of anti-tumor T cells. IL-2 (marketed as Proleukin®) is FDA-approved due to its demonstrated complete cancer regression in 8% of the patients with metastatic renal cancer or melanoma [185]. The combination of IL-2 infusion and adoptive T cell transfer after lymphodepletion improved the clinical outcome in melanoma patients [152]. Furthermore, IL-2 is also used to expand anti-tumor T cells *ex vivo*. However, two major disadvantages of this interleukin on the anti-tumor immune responses are the concurrent stimulation of T_{regs} and the strong differentiation of T cells. This differentiation may reduce the generation of an anti-tumor immunological memory [186]. In ACT, not only the direct cytotoxic killing effect by effector $CD8^+$ T cells is important, but also the persistence of T cells which provides an anti-tumor memory. The combination of the homeostatic interleukins IL-7 and IL-15 were suggested to support the survival and proliferation of adoptively transferred T cells while also enhancing their persistence *in vivo* to obtain durable cancer regression [187]. Recent clinical data demonstrated that, compared to IL-2, IL-21 promotes the expansion and function of effector $CD8^+$ T cells with a less-differentiated phenotype and without co-expansion of T_{regs} [188]. These currently investigated T cell-stimulating cytokines can be used to both expand anti-tumor T cells *ex vivo* as well as to provide the transferred T cells with co-stimulatory agents after infusion into the patient [189]. However, the systemic delivery of cytokines, such as the interleukins, is often hampered by toxic side effects. One strategy to overcome this toxicity is the genetic engineering of isolated anti-tumor T cells to produce their own pro-inflammatory or pro-proliferative cytokines [190, 191]. Alternatively, it is possible to chemically conjugate interleukin-loaded NPs onto the cell membrane of adoptively transferred T cells. The sustained release of the interleukins from the stably attached particles provides the cells directly with immunostimulatory agents *in vivo*. A preclinical study by Stephan and coworkers demonstrated the complete tumor regression in mice treated with anti-tumor T cells decorated with cytokine-loaded NPs on their surface, in contrast to only a modest survival improvement in mice treated with anti-tumor T cells with or without systemic infusion of the same doses of cytokines [66]. Another important example of an immune-stimulating cytokine is IL-12, which mediates both innate and adoptive immune responses against tumors. It has been shown to induce the stimulation

and homeostatic expansion of T cells [192]. The local delivery of IL-12 into the tumor was shown to reprogram MDSCs to decrease their immunosuppressive function.

1.3.4 Checkpoint inhibitors and immunostimulatory antibodies

Monoclonal antibodies against the immunosuppressive molecules CTLA-4 and PD-1 block immunoinhibitory pathways, which may enhance endogenous anti-tumor immune responses. Ipilimumab (marketed as Yervoy®) is a human monoclonal antibody that blocks CTLA-4, which results in the enhanced proliferation and effector activity of T cells. The FDA approved this antibody in 2011 for the treatment of patients with metastatic melanoma [193]. Two other important targets for antibody therapy are PD-1 and its ligand PD-L1 [194, 195]. Binding of PD-L1 to its PD-1 receptor on T cells inhibits T cell activation and can induce apoptosis of T cells. PD-L1 expression has been identified on APCs and several solid tumors such as renal cell, colon, breast, ovarian, and hematological cancers [196, 197]. Monoclonal antibodies blocking the PD-1 pathway, pembrolizumab (Keytruda®) and nivolumab (Opdivo®), were approved by the FDA and EMA in 2014 and 2015 while PD-L1 antibodies are currently investigated in clinical trials [90]. In addition, the FDA has also recently approved the combination of ipilimumab and nivolumab for metastatic melanoma [135].

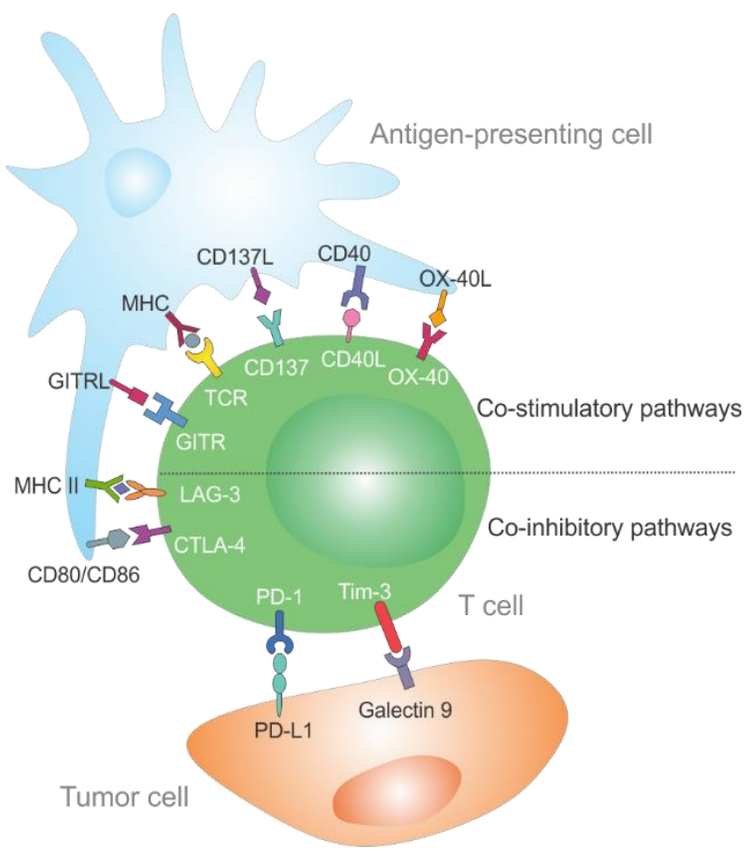

Figure 9. Schematic overview of immune co-stimulatory and co-inhibitory receptor ligand interactions of anti-tumor T cells with antigen-presenting cells and tumor cells. Interfering with these interactions by monoclonal antibodies that either promote immune stimulating pathways or block immunosuppressive pathways enhances the anti-tumor responses and persistence of T cells. Adapted from Ref. [198].

In addition to the well-studied CTLA-4 and PD-1 targets, other co-inhibitory pathways in activated T cells such as T cell immunoglobulin mucin domain-containing-3 (Tim-3) and lymphocyte activation gene-3 (LAG-3) have been identified (**Figure 9**). Studies about monoclonal antibodies against these two pathways reported on the improved expansion and function of antigen-specific $CD8^+$ T cells. Moreover, the combination of antibodies against either Tim-3 or LAG-3 with anti-PD-1 antibodies resulted in synergistic clinical outcomes [199, 200].

Besides antibody treatment against co-inhibitory receptors and ligands, a number of new antibodies against co-stimulatory receptors has been developed such as anti-CD137 (4-1BB), anti-OX-40 (CD134), anti-CD40, and anti-GITR [198, 201]. These agonist antibodies enhance the persistence and anti-tumor activity of the T cells (**Figure 9**). Besides effects on T cells, more recently also monoclonal antibodies stimulating natural killer (NK) cells gained interest. NK cells are part of the innate immune system and are also able to kill tumor cells. However, their killing functions are tightly controlled by a variety of cell surface receptors. In contrast to T cells, they do not require recognition of tumor antigens but act upon cells that lack MHC class I. MHC I is expressed on almost all nucleated cells in the body. Thus, antibodies blocking the receptor that recognizes MHC I, called killer immunoglobulin-like receptor, to activate NK cells against tumor cells are currently in clinical trials [202]. Although safety issues are expected through killing of normal tissues, until now these antibody therapies have shown good safety. The reason behind the specific killing of tumor cells is by their concomitant expression of stress ligands, which bind to NK activating receptors and further induce activation [203].

1.3.5 Immune adjuvants: exploring the role of Toll-like receptor agonists in cancer immunotherapy

Stimulating the innate immune system is the key mechanism in cancer vaccination, as previously described. For this purpose, immune adjuvants were shown to play a very important role [172]. The interaction of immune adjuvants, acting as pathogen-associated molecular patterns (PAMPs) or danger-associated molecular patterns (DAMPs), with pattern recognition receptors (PRRs) on DCs has been shown to induce the upregulation of co-stimulatory molecules (*e.g.* CD40, CD80, CD86), the production of immunostimulatory cytokines (*e.g.* IL-12), and an increase in antigen presentation [204]. The most studied immune adjuvants are agonists of Toll-like receptors (TLRs), which are members of the PRRs [205]. TLRs can be expressed on the cell surface (TLR1, TLR2, TLR4, TLR5, TLR6) as well as within the endosomes (TLR3, TLR4, TLR7, TLR8, TLR9) [204]. Although TLR agonists as monotherapy have disappointed in clinical trials, they still have potential when combined with other anti-cancer therapies. For example, combined with ACT, the T cell-mediated tumor cell death causes the release of tumor antigens that can, together with the stimulation of TLRs, reactivate the innate immune system to induce CTL responses [206].

The best-studied TLR agonists in the context of cancer immunotherapy are poly(I:C), monophosphoryl lipid A (MPLA), imiquimod, and CpG oligodeoxynucleotides for binding to TLR3, TLR4, TLR7/8, and TLR9, respectively [205]. From this set of TLR agonists, only imiquimod is approved for cancer therapy and MPLA is included in Cervarix®, a cancer vaccine against human papillomavirus-16 and -18 [207, 208]. MPLA is a chemically modified derivative of *Salmonella minnesota* endotoxin and is a less toxic version of lipopolysaccharide (LPS), a potent TLR4 agonist. Several preclinical studies have already demonstrated the additional antitumor effects of MPLA when combined with other immunomodulators, such as CD40 agonists and IL-12 [209, 210]. Of note, Bacillus Calmette-Guérin (BCG) which is not a pure TLR agonist, but mainly mediates its immunostimulatory effects via TLR2 and TLR4, is also FDA approved for the treatment of bladder cancer [205]. In addition to the TLR agonists, also STING activators and α-galactosylceramide are under investigation as immune adjuvants [204, 211].

1.4 Non-immune therapies with the power to induce immune responses

1.4.1 Chemotherapy

In addition to their direct killing effect, specific chemotherapeutics have shown to induce immunogenic cell death (ICD), a type of cell death in which dying cells stimulate immune responses against dead-cell antigens [212]. Although the complete underlying mechanisms have not yet been elucidated, four hallmarks for the occurrence of ICD have been identified; (i) the exposure of calreticulin on the outer leaflet of the cell membrane and the release of (ii) ATP, (iii) high mobility group box-1 (HMGB-1), and (iv) type I interferon (IFN) from the dying cells [213]. Besides tumor irradiation and hyperthermia, a few chemotherapeutics such as doxorubicin and cyclophosphamide have been recognized to induce ICD, and are of interest to combine with cancer immunotherapy [213].

1.4.2 Small interfering RNA

Several myeloid-derived immune cells were shown to be key contributors to the suppressive tumor microenvironment such as TAMs, MDSCs, and tumor-polarized DCs. Besides the use of RNAi to directly kill tumor cells, the downregulation of intracellular pathways that regulate the immunosuppressive functions in these immune cells, could be used to re-educate them [214]. In this context, tumor-polarized DCs were already investigated for the downregulation of immunosuppressive modulators such as signal transducer and activator of transcription 3 (STAT3) and PD-L1, a strategy that can also be further extended to the TAMs and MDSCs [215-217]. Due to their endocytic potential, the cells are able to easily internalize siRNA-loaded NPs. In addition, not only an inhibitory effect by the siRNA delivery can be envisioned, but also the siRNA-mediated induction of immunostimulatory signals by the activation of TLRs [218].

2 *IN VIVO* AND *EX VIVO* TRANSFECTION TECHNIQUES FOR TUMOR-SPECIFIC T CELLS

The genetic engineering of T cells has been principally investigated for the introduction of TCR and CAR genes in ACT. The most frequently investigated transfection method for this purpose is through the use of viral vectors, particularly retroviruses and lentiviruses [219]. However, due to the high cost and complexity of clinical-grade production, safety issues, and limited number of genes that can be incorporated, alternative non-viral vectors are gaining interest. For example, DNA plasmid vectors, composed of transposons that contain the gene of interest, and a transposase which helps to integrate the gene in the genome are becoming more popular. The DNA plasmids are delivered to the T cells via physical methods such as electroporation and nucleofection. The electroporation approach uses high-voltage pulses by applying an external electric field that transiently creates small pores in the cell membrane, which allow the delivery of small molecules and nucleic acids through diffusion and electrophoretically-driven transport [220, 221]. Nucleofection is an electroporation-based method that was commercialized by Amaxa® (Lonza) to increase the transfection efficiency of plasmids and siRNA, with particular benefits for hard-to-transfect cells such as primary T lymphocytes [222]. The transfection via DNA plasmid vectors is known to overcome all of the abovementioned issues, since plasmids can incorporate a larger amount of genetic info, are safe and easy to produce, which reduces costs. Currently, clinical trials are investigating the efficiency of CAR T cell therapy after genetically modifying the cells via a transposon/transposase system as an alternative for viral vector gene transfer [223].

Besides engineering T cells to express specific tumor antigen receptors, genetic modifications have also been investigated to enhance migration and infiltration of T cells in the tumor, to enhance their survival and proliferation, and to make them more resistant to immunosuppressive signals from the tumor microenvironment. Indeed, several studies have shown improved anti-tumor responses when the tumor exhibited increased levels of infiltrated CTLs [224, 225]. To enhance infiltration of T cells in the tumor, cells can be engineered to express chemokine receptors that bind chemokines which are secreted in elevated levels in the tumor [226-228]. Improved survival and proliferation of T cells has been demonstrated by the insertion of genes expressing anti-apoptotic molecules or encoding short hairpin RNA to silence apoptosis pathways (*e.g.* FAS) and anti-proliferation regulators (*e.g.* E3 ubiquitin ligase CBLB) [229, 230]. T cells modified to express IL-12 were shown to change myeloid cells in the tumor microenvironment to promote immune-mediated destruction of the tumor [231].

Unfortunately, genetic engineering of T cells has potential safety concerns due to the risk of insertional mutagenesis, resulting in malignant T cells. A non-gene therapy that was described previously and was shown to enhance T cell functionalities is the administration

of monoclonal antibodies for both checkpoint blockade and stimulation of immune-promoting T cell receptors. However, recently several intracellular immunosuppressive pathways have been identified as interesting therapeutic targets [232, 233]. As these targets are not amenable to antibodies, other inhibiting mechanisms such as RNAi, via the delivery of siRNAs, have gained interest. Delivering siRNA to the cytosol of T cells can be mediated by NPs, aptamers, proteins such as penetrating peptides, and physical methods such as electroporation [234].

The non-physical methods have the advantage that they can be used both *in vitro* and *in vivo*. However, *in vivo*, an optimal targeting to the T cells is highly recommended. A recent study by Peer and coworkers demonstrated the targeted delivery of lipid-based siRNA NPs to $CD4^+$ T cells in mice [235]. Although they showed specific silencing in the $CD4^+$ population, the knockdown efficiency was rather low and restricted to a subset of $CD4^+$ T cells. Although the use of physical methods such as electroporation and nucleofection is restricted to *ex vivo* applications, they have the advantage to achieve higher transfection efficiencies. Unfortunately, the major limitation of electroporation-based methods is their high cell toxicity, which stimulated researchers to investigate alternative approaches [234]. For example, a recent study reported on the use of the microfluidic CellSqueeze delivery system, in which suspension cells flow through microfluidic channels and are subjected to a rapid mechanical deformation at a constriction point in the channel, to induce the formation of small pores in the cell membrane and allow the passive diffusion of membrane-impermeable compounds [236].

CONCLUSION

Although many different cancer nanomedicines have been developed over the years, the majority has failed clinical translation due to limited targeting to the tumor. Despite many efforts based on passive and active targeting, the search for novel strategies to increase the number of NPs in the tumor is highly recommended. Cell-mediated NP delivery by using a cell's tumor-migration capacity was suggested as potent alternative. One of the suggested tumoritropic cells are cytotoxic T cells, which have in addition to their capacity to migrate to the tumor also a cytolytic function against tumor cells. This cytolytic effect of T cells has been widely exploited in ACT. Cancer immunotherapy, including ACT, has gained popularity in the last couple of years due to its impressive clinical results for patients refractory to the conventional anti-cancer therapies. However, the immunosuppressive role of the tumor microenvironment remains one of the major hurdles for clinical success in a broad range of cancer patients. Therefore, the search for combinatorial strategies to overcome these challenges is flourishing.

ACKNOWLEDGEMENTS

Laura Wayteck is a doctoral fellow of the Institute for the Promotion of Innovation through Science and Technology in Flanders, Belgium (IWT-Vlaanderen). Koen Raemdonck is a postdoctoral fellow of the Research Foundation-Flanders, Belgium (FWO-Vlaanderen). FWO and 'Stichting tegen Kanker' are acknowledged for their financial support.

Lynn De Backer is acknowledged with gratitude for kindly providing Figure 1.

REFERENCES

1. Wang, R.B., Billone, P.S. & Mullett, W.M. Nanomedicine in Action: An Overview of Cancer Nanomedicine on the Market and in Clinical Trials. *Journal of Nanomaterials*, 1-12 (2013).
2. Ferrari, M. Cancer nanotechnology: opportunities and challenges. *Nat Rev Cancer* **5**, 161-71 (2005).
3. Sanna, V., Pala, N. & Sechi, M. Targeted therapy using nanotechnology: focus on cancer. *Int J Nanomedicine* **9**, 467-83 (2014).
4. Strebhardt, K. & Ullrich, A. Paul Ehrlich's magic bullet concept: 100 years of progress. *Nat Rev Cancer* **8**, 473-80 (2008).
5. Anselmo, A.C. & Mitragotri, S. An overview of clinical and commercial impact of drug delivery systems. *J Control Release* **190**, 15-28 (2014).
6. Wicki, A., Witzigmann, D., Balasubramanian, V. & Huwyler, J. Nanomedicine in cancer therapy: challenges, opportunities, and clinical applications. *J Control Release* **200**, 138-57 (2015).
7. Kamaly, N., Xiao, Z., Valencia, P.M., Radovic-Moreno, A.F. & Farokhzad, O.C. Targeted polymeric therapeutic nanoparticles: design, development and clinical translation. *Chem Soc Rev* **41**, 2971-3010 (2012).
8. Xu, X., Ho, W., Zhang, X., Bertrand, N. & Farokhzad, O. Cancer nanomedicine: from targeted delivery to combination therapy. *Trends Mol Med* **21**, 223-32 (2015).
9. Allen, T.M. & Cullis, P.R. Liposomal drug delivery systems: from concept to clinical applications. *Adv Drug Deliv Rev* **65**, 36-48 (2013).
10. Friberg, S. & Nystrom, A.M. Nanotechnology in the war against cancer: new arms against an old enemy - a clinical view. *Future Oncol* **11**, 1961-75 (2015).
11. Torchilin, V. Multifunctional and stimuli-sensitive pharmaceutical nanocarriers. *Eur J Pharm Biopharm* **71**, 431-44 (2009).
12. Torchilin, V.P. Recent advances with liposomes as pharmaceutical carriers. *Nat Rev Drug Discov* **4**, 145-60 (2005).
13. Moon, J.J. et al. Interbilayer-crosslinked multilamellar vesicles as synthetic vaccines for potent humoral and cellular immune responses. *Nat Mater* **10**, 243-51 (2011).
14. Perez-Herrero, E. & Fernandez-Medarde, A. Advanced targeted therapies in cancer: Drug nanocarriers, the future of chemotherapy. *Eur J Pharm Biopharm* **93**, 52-79 (2015).
15. Raemdonck, K., Braeckmans, K., Demeester, J. & De Smedt, S.C. Merging the best of both worlds: hybrid lipid-enveloped matrix nanocomposites in drug delivery. *Chem Soc Rev* **43**, 444-72 (2014).
16. Jain, S., Hirst, D.G. & O'Sullivan, J.M. Gold nanoparticles as novel agents for cancer therapy. *Br J Radiol* **85**, 101-13 (2012).
17. Almeida, J.P., Figueroa, E.R. & Drezek, R.A. Gold nanoparticle mediated cancer immunotherapy. *Nanomedicine* **10**, 503-14 (2014).
18. Barenholz, Y. Doxil(R)--the first FDA-approved nano-drug: lessons learned. *J Control Release* **160**, 117-34 (2012).
19. Szebeni, J., Fulop, T., Dezsi, L., Metselaar, B. & Storm, G. Liposomal doxorubicin: the good, the bad and the not-so-ugly. *J Drug Target*, 1-7 (2016).

20. Gabizon, A. et al. Prolonged circulation time and enhanced accumulation in malignant exudates of doxorubicin encapsulated in polyethylene-glycol coated liposomes. *Cancer Res* **54**, 987-92 (1994).
21. Gabizon, A., Shmeeda, H. & Barenholz, Y. Pharmacokinetics of pegylated liposomal doxorubicin - Review of animal and human studies. *Clinical Pharmacokinetics* **42**, 419-436 (2003).
22. Kratz, F. Albumin as a drug carrier: design of prodrugs, drug conjugates and nanoparticles. *J Control Release* **132**, 171-83 (2008).
23. Hare, J.I. et al. Challenges and strategies in anti-cancer nanomedicine development: An industry perspective. *Adv Drug Deliv Rev* (2016).
24. Whitehead, K.A., Langer, R. & Anderson, D.G. Knocking down barriers: advances in siRNA delivery. *Nat Rev Drug Discov* **8**, 129-38 (2009).
25. Leuschner, P.J., Ameres, S.L., Kueng, S. & Martinez, J. Cleavage of the siRNA passenger strand during RISC assembly in human cells. *EMBO Rep* **7**, 314-20 (2006).
26. Kanasty, R., Dorkin, J.R., Vegas, A. & Anderson, D. Delivery materials for siRNA therapeutics. *Nat Mater* **12**, 967-77 (2013).
27. Zuckerman, J.E. & Davis, M.E. Clinical experiences with systemically administered siRNA-based therapeutics in cancer. *Nat Rev Drug Discov* **14**, 843-56 (2015).
28. Chrastina, A., Massey, K.A. & Schnitzer, J.E. Overcoming in vivo barriers to targeted nanodelivery. *Wiley Interdiscip Rev Nanomed Nanobiotechnol* **3**, 421-37 (2011).
29. Barua, S. & Mitragotri, S. Challenges associated with Penetration of Nanoparticles across Cell and Tissue Barriers: A Review of Current Status and Future Prospects. *Nano Today* **9**, 223-243 (2014).
30. Hobbs, S.K. et al. Regulation of transport pathways in tumor vessels: role of tumor type and microenvironment. *Proc Natl Acad Sci U S A* **95**, 4607-12 (1998).
31. Maeda, H., Nakamura, H. & Fang, J. The EPR effect for macromolecular drug delivery to solid tumors: Improvement of tumor uptake, lowering of systemic toxicity, and distinct tumor imaging in vivo. *Adv Drug Deliv Rev* **65**, 71-9 (2013).
32. Prabhakar, U. et al. Challenges and key considerations of the enhanced permeability and retention effect for nanomedicine drug delivery in oncology. *Cancer Res* **73**, 2412-7 (2013).
33. Lammers, T., Kiessling, F., Hennink, W.E. & Storm, G. Drug targeting to tumors: principles, pitfalls and (pre-) clinical progress. *J Control Release* **161**, 175-87 (2012).
34. Provenzano, P.P. et al. Enzymatic targeting of the stroma ablates physical barriers to treatment of pancreatic ductal adenocarcinoma. *Cancer Cell* **21**, 418-29 (2012).
35. Gaumet, M., Vargas, A., Gurny, R. & Delie, F. Nanoparticles for drug delivery: the need for precision in reporting particle size parameters. *Eur J Pharm Biopharm* **69**, 1-9 (2008).
36. Bartlett, D.W., Su, H., Hildebrandt, I.J., Weber, W.A. & Davis, M.E. Impact of tumor-specific targeting on the biodistribution and efficacy of siRNA nanoparticles measured by multimodality in vivo imaging. *Proc Natl Acad Sci U S A* **104**, 15549-54 (2007).
37. Kirpotin, D.B. et al. Antibody targeting of long-circulating lipidic nanoparticles does not increase tumor localization but does increase internalization in animal models. *Cancer Res* **66**, 6732-40 (2006).
38. Choi, C.H., Alabi, C.A., Webster, P. & Davis, M.E. Mechanism of active targeting in solid tumors with transferrin-containing gold nanoparticles. *Proc Natl Acad Sci U S A* **107**, 1235-40 (2010).

39. Bertrand, N., Wu, J., Xu, X., Kamaly, N. & Farokhzad, O.C. Cancer nanotechnology: the impact of passive and active targeting in the era of modern cancer biology. *Adv Drug Deliv Rev* **66**, 2-25 (2014).
40. Peer, D. et al. Nanocarriers as an emerging platform for cancer therapy. *Nat Nanotechnol* **2**, 751-60 (2007).
41. Anselmo, A.C. & Mitragotri, S. Cell-mediated delivery of nanoparticles: Taking advantage of circulatory cells to target nanoparticles. *J Control Release* **190**, 531-41 (2014).
42. Tan, S., Wu, T., Zhang, D. & Zhang, Z. Cell or cell membrane-based drug delivery systems. *Theranostics* **5**, 863-81 (2015).
43. Dvorak, H.F. Tumors: wounds that do not heal. Similarities between tumor stroma generation and wound healing. *N Engl J Med* **315**, 1650-9 (1986).
44. Brown, J.M. & Wilson, W.R. Exploiting tumour hypoxia in cancer treatment. *Nat Rev Cancer* **4**, 437-47 (2004).
45. Weiss, L. & Zeigel, R. Cell surface negativity and the binding of positively charged particles. *J Cell Physiol* **77**, 179-86 (1971).
46. Ko, I.K., Kean, T.J. & Dennis, J.E. Targeting mesenchymal stem cells to activated endothelial cells. *Biomaterials* **30**, 3702-10 (2009).
47. Vasconcellos, F.C., Swiston, A.J., Beppu, M.M., Cohen, R.E. & Rubner, M.F. Bioactive polyelectrolyte multilayers: hyaluronic acid mediated B lymphocyte adhesion. *Biomacromolecules* **11**, 2407-14 (2010).
48. Swiston, A.J., Gilbert, J.B., Irvine, D.J., Cohen, R.E. & Rubner, M.F. Freely suspended cellular "backpacks" lead to cell aggregate self-assembly. *Biomacromolecules* **11**, 1826-32 (2010).
49. Swiston, A.J. et al. Surface functionalization of living cells with multilayer patches. *Nano Lett* **8**, 4446-53 (2008).
50. Stephan, M.T., Moon, J.J., Um, S.H., Bershteyn, A. & Irvine, D.J. Therapeutic Cell Engineering Using Surface-Conjugated Synthetic Nanoparticles. *Journal of Immunotherapy* **16**, 1035-41 (2010).
51. Cheng, H. et al. Nanoparticulate cellular patches for cell-mediated tumoritropic delivery. *ACS Nano* **4**, 625-31 (2010).
52. Choi, M.R. et al. A cellular Trojan Horse for delivery of therapeutic nanoparticles into tumors. *Nano Lett* **7**, 3759-65 (2007).
53. Mooney, R. et al. Conjugation of pH-responsive nanoparticles to neural stem cells improves intratumoral therapy. *J Control Release* **191**, 82-9 (2014).
54. Cheng, Y. et al. Nanoparticle-programmed self-destructive neural stem cells for glioblastoma targeting and therapy. *Small* **9**, 4123-9 (2013).
55. Roger, M. et al. Ferrociphenol lipid nanocapsule delivery by mesenchymal stromal cells in brain tumor therapy. *Int J Pharm* **423**, 63-8 (2012).
56. Huang, X. et al. Mesenchymal stem cell-based cell engineering with multifunctional mesoporous silica nanoparticles for tumor delivery. *Biomaterials* **34**, 1772-80 (2013).
57. Dai, T. et al. Preparation and drug release mechanism of CTS-TAX-NP-MSCs drug delivery system. *Int J Pharm* **456**, 186-94 (2013).
58. Aboody, K.S. et al. Neural stem cell-mediated enzyme/prodrug therapy for glioma: preclinical studies. *Sci Transl Med* **5**, 184ra59 (2013).

59. Karnoub, A.E. et al. Mesenchymal stem cells within tumour stroma promote breast cancer metastasis. *Nature* **449**, 557-63 (2007).
60. Xu, W.T., Bian, Z.Y., Fan, Q.M., Li, G. & Tang, T.T. Human mesenchymal stem cells (hMSCs) target osteosarcoma and promote its growth and pulmonary metastasis. *Cancer Lett* **281**, 32-41 (2009).
61. Tripathi, C. et al. Macrophages are recruited to hypoxic tumor areas and acquire a pro-angiogenic M2-polarized phenotype via hypoxic cancer cell derived cytokines Oncostatin M and Eotaxin. *Oncotarget* **5**, 5350-68 (2014).
62. Murdoch, C., Giannoudis, A. & Lewis, C.E. Mechanisms regulating the recruitment of macrophages into hypoxic areas of tumors and other ischemic tissues. *Blood* **104**, 2224-34 (2004).
63. Choi, J. et al. Use of macrophages to deliver therapeutic and imaging contrast agents to tumors. *Biomaterials* **33**, 4195-203 (2012).
64. Anselmo, A.C. et al. Monocyte-mediated delivery of polymeric backpacks to inflamed tissues: a generalized strategy to deliver drugs to treat inflammation. *J Control Release* **199**, 29-36 (2015).
65. Doshi, N. et al. Cell-based drug delivery devices using phagocytosis-resistant backpacks. *Adv Mater* **23**, H105-9 (2011).
66. Stephan, M.T., Moon, J.J., Um, S.H., Bershteyn, A. & Irvine, D.J. Therapeutic cell engineering with surface-conjugated synthetic nanoparticles. *Nat Med* **16**, 1035-41 (2010).
67. Stephan, M.T., Stephan, S.B., Bak, P., Chen, J. & Irvine, D.J. Synapse-directed delivery of immunomodulators using T-cell-conjugated nanoparticles. *Biomaterials* **33**, 5776-87 (2012).
68. Huang, B. et al. Active targeting of chemotherapy to disseminated tumors using nanoparticle-carrying T cells. *Sci Transl Med* **7**, 291ra94 (2015).
69. Cole, C. et al. Tumor-targeted, systemic delivery of therapeutic viral vectors using hitchhiking on antigen-specific T cells. *Nat Med* **11**, 1073-81 (2005).
70. VanSeggelen, H., Tantalo, D.G., Afsahi, A., Hammill, J.A. & Bramson, J.L. Chimeric antigen receptor-engineered T cells as oncolytic virus carriers. *Mol Ther Oncolytics* **2**, 15014 (2015).
71. Slaney, C.Y., Kershaw, M.H. & Darcy, P.K. Trafficking of T cells into tumors. *Cancer Res* **74**, 7168-74 (2014).
72. von Andrian, U.H. & Mackay, C.R. T-cell function and migration. Two sides of the same coin. *N Engl J Med* **343**, 1020-34 (2000).
73. Franciszkiewicz, K., Boissonnas, A., Boutet, M., Combadiere, C. & Mami-Chouaib, F. Role of chemokines and chemokine receptors in shaping the effector phase of the antitumor immune response. *Cancer Res* **72**, 6325-32 (2012).
74. Martinez-Lostao, L., Anel, A. & Pardo, J. How Do Cytotoxic Lymphocytes Kill Cancer Cells? *Clinical Cancer Research* **21**, 5047-5056 (2015).
75. Dalakas, M.C. Inhibiting leukocyte recruitment to the brain by IVIg: is it relevant to the treatment of demyelinating CNS disorders? *Brain* **127**, 2569-71 (2004).
76. Hauschka, T.S. [Immunologic aspects of cancer: a review]. *Cancer Res* **12**, 615-33 (1952).
77. Prehn, R.T. & Main, J.M. Immunity to methylcholanthrene-induced sarcomas. *J Natl Cancer Inst* **18**, 769-78 (1957).
78. Foley, E.J. Antigenic properties of methylcholanthrene-induced tumors in mice of the strain of origin. *Cancer Res* **13**, 835-7 (1953).

79. Southam, C.M. History and prospects of immunotherapy of cancer: an introduction. *Ann N Y Acad Sci* **277**, 1-6 (1976).
80. Klein, G. Tumor-specific transplantation antigens: G. H. A. Clowes memorial lecture. *Cancer Res* **28**, 625-35 (1968).
81. Gold, P., Shuster, J. & Freedman, S.O. Carcinoembryonic antigen (CEA) in clinical medicine: historical perspectives, pitfalls and projections. *Cancer* **42**, 1399-405 (1978).
82. Gold, P. & Freedman, S.O. Demonstration of Tumor-Specific Antigens in Human Colonic Carcinomata by Immunological Tolerance and Absorption Techniques. *J Exp Med* **121**, 439-62 (1965).
83. Parker, G.A. & Rosenberg, S.A. Serologic identification of multiple tumor-associated antigens on murine sarcomas. *J Natl Cancer Inst* **58**, 1303-9 (1977).
84. Knuth, A., Wolfel, T., Klehmann, E., Boon, T. & Meyer zum Buschenfelde, K.H. Cytolytic T-cell clones against an autologous human melanoma: specificity study and definition of three antigens by immunoselection. *Proc Natl Acad Sci U S A* **86**, 2804-8 (1989).
85. Burnet, F.M. The concept of immunological surveillance. *Prog Exp Tumor Res* **13**, 1-27 (1970).
86. Tuyaerts, S. et al. Current approaches in dendritic cell generation and future implications for cancer immunotherapy. *Cancer Immunol Immunother* **56**, 1513-37 (2007).
87. Pedrazzoli, P. et al. Is adoptive T-cell therapy for solid tumors coming of age? *Bone Marrow Transplant* **47**, 1013-9 (2012).
88. Nicholas, C. & Lesinski, G.B. Immunomodulatory cytokines as therapeutic agents for melanoma. *Immunotherapy* **3**, 673-90 (2011).
89. Corsello, S.M. et al. Endocrine side effects induced by immune checkpoint inhibitors. *J Clin Endocrinol Metab* **98**, 1361-75 (2013).
90. Hoos, A. Development of immuno-oncology drugs - from CTLA4 to PD1 to the next generations. *Nat Rev Drug Discov* **15**, 235-47 (2016).
91. Vanderbruggen, P. et al. A Gene Encoding an Antigen Recognized by Cytolytic Lymphocytes-T on a Human-Melanoma. *Science* **254**, 1643-1647 (1991).
92. Jager, E. & Knuth, A. The discovery of cancer/testis antigens by autologous typing with T cell clones and the evolution of cancer vaccines. *Cancer Immun* **12**, 6 (2012).
93. Tureci, O. et al. Targeting the Heterogeneity of Cancer with Individualized Neoepitope Vaccines. *Clin Cancer Res* **22**, 1885-96 (2016).
94. Heemskerk, B., Kvistborg, P. & Schumacher, T.N. The cancer antigenome. *EMBO J* **32**, 194-203 (2013).
95. Kvistborg, P., van Buuren, M.M. & Schumacher, T.N. Human cancer regression antigens. *Curr Opin Immunol* **25**, 284-90 (2013).
96. Ku, C.S., Cooper, D.N. & Roukos, D.H. Clinical relevance of cancer genome sequencing. *World J Gastroenterol* **19**, 2011-8 (2013).
97. Meyerson, M., Gabriel, S. & Getz, G. Advances in understanding cancer genomes through second-generation sequencing. *Nat Rev Genet* **11**, 685-96 (2010).
98. Ding, L. et al. Clonal evolution in relapsed acute myeloid leukaemia revealed by whole-genome sequencing. *Nature* **481**, 506-10 (2012).
99. Nik-Zainal, S. et al. Mutational processes molding the genomes of 21 breast cancers. *Cell* **149**, 979-93 (2012).

100. Berger, M.F. et al. Melanoma genome sequencing reveals frequent PREX2 mutations. *Nature* **485**, 502-6 (2012).
101. Ley, T.J. et al. DNA sequencing of a cytogenetically normal acute myeloid leukaemia genome. *Nature* **456**, 66-72 (2008).
102. Johnson, L.A. et al. Gene therapy with human and mouse T-cell receptors mediates cancer regression and targets normal tissues expressing cognate antigen. *Blood* **114**, 535-46 (2009).
103. Kawakami, Y. et al. Identification of a human melanoma antigen recognized by tumor-infiltrating lymphocytes associated with in vivo tumor rejection. *Proc Natl Acad Sci U S A* **91**, 6458-62 (1994).
104. Lamers, C.H. et al. Treatment of metastatic renal cell carcinoma with autologous T-lymphocytes genetically retargeted against carbonic anhydrase IX: first clinical experience. *J Clin Oncol* **24**, e20-2 (2006).
105. Parkhurst, M.R. et al. T cells targeting carcinoembryonic antigen can mediate regression of metastatic colorectal cancer but induce severe transient colitis. *Mol Ther* **19**, 620-6 (2011).
106. Hammarstrom, S. The carcinoembryonic antigen (CEA) family: structures, suggested functions and expression in normal and malignant tissues. *Semin Cancer Biol* **9**, 67-81 (1999).
107. Simpson, A.J.G., Caballero, O.L., Jungbluth, A., Chen, Y.T. & Old, L.J. Cancer/testis antigens, gametogenesis and cancer. *Nature Reviews Cancer* **5**, 615-625 (2005).
108. Neller, M.A., Lopez, J.A. & Schmidt, C.W. Antigens for cancer immunotherapy. *Seminars in Immunology* **20**, 286-295 (2008).
109. Morgan, R.A. et al. Cancer regression and neurological toxicity following anti-MAGE-A3 TCR gene therapy. *J Immunother* **36**, 133-51 (2013).
110. Hofmann, O. et al. Genome-wide analysis of cancer/testis gene expression. *Proc Natl Acad Sci U S A* **105**, 20422-7 (2008).
111. Scanlan, M.J., Simpson, A.J. & Old, L.J. The cancer/testis genes: review, standardization, and commentary. *Cancer Immun* **4**, 1 (2004).
112. Caballero, O.L. & Chen, Y.T. Cancer/testis (CT) antigens: potential targets for immunotherapy. *Cancer Sci* **100**, 2014-21 (2009).
113. Payne, K.K., Toor, A.A., Wang, X.Y. & Manjili, M.H. Immunotherapy of cancer: reprogramming tumor-immune crosstalk. *Clin Dev Immunol* **2012**, 760965 (2012).
114. Scanlan, M.J., Gure, A.O., Jungbluth, A.A., Old, L.J. & Chen, Y.T. Cancer/testis antigens: an expanding family of targets for cancer immunotherapy. *Immunol Rev* **188**, 22-32 (2002).
115. Meklat, F. et al. Cancer-testis antigens in haematological malignancies. *Br J Haematol* **136**, 769-76 (2007).
116. Scholten, K.B. et al. Generating HPV specific T helper cells for the treatment of HPV induced malignancies using TCR gene transfer. *J Transl Med* **9**, 147 (2011).
117. Ramos, C.A. et al. Human papillomavirus type 16 E6/E7-specific cytotoxic T lymphocytes for adoptive immunotherapy of HPV-associated malignancies. *J Immunother* **36**, 66-76 (2013).
118. Turksma, A.W. et al. Immunotherapy for head and neck cancer patients: shifting the balance. *Immunotherapy* **5**, 49-61 (2013).
119. Morrow, M.P., Yan, J. & Sardesai, N.Y. Human papillomavirus therapeutic vaccines: targeting viral antigens as immunotherapy for precancerous disease and cancer. *Expert Rev Vaccines* **12**, 271-83 (2013).

120. Lennerz, V. et al. The response of autologous T cells to a human melanoma is dominated by mutated neoantigens. *Proc Natl Acad Sci U S A* **102**, 16013-8 (2005).
121. Maletzki, C., Schmidt, F., Dirks, W.G., Schmitt, M. & Linnebacher, M. Frameshift-derived neoantigens constitute immunotherapeutic targets for patients with microsatellite-instable haematological malignancies: frameshift peptides for treating MSI+ blood cancers. *Eur J Cancer* **49**, 2587-95 (2013).
122. Schreiber, R.D., Old, L.J. & Smyth, M.J. Cancer immunoediting: integrating immunity's roles in cancer suppression and promotion. *Science* **331**, 1565-70 (2011).
123. Mittal, D., Gubin, M.M., Schreiber, R.D. & Smyth, M.J. New insights into cancer immunoediting and its three component phases--elimination, equilibrium and escape. *Curr Opin Immunol* **27**, 16-25 (2014).
124. Gajewski, T.F., Schreiber, H. & Fu, Y.X. Innate and adaptive immune cells in the tumor microenvironment. *Nature Immunology* **14**, 1014-1022 (2013).
125. Becht, E., Giraldo, N.A., Dieu-Nosjean, M.C., Sautes-Fridman, C. & Fridman, W.H. Cancer immune contexture and immunotherapy. *Curr Opin Immunol* **39**, 7-13 (2016).
126. Gajewski, T.F. The Next Hurdle in Cancer Immunotherapy: Overcoming the Non-T-Cell-Inflamed Tumor Microenvironment. *Semin Oncol* **42**, 663-71 (2015).
127. Schumacher, K., Haensch, W., Roefzaad, C. & Schlag, P.M. Prognostic significance of activated CD8(+) T cell infiltrations within esophageal carcinomas. *Cancer Res* **61**, 3932-6 (2001).
128. Zhang, L. et al. Intratumoral T cells, recurrence, and survival in epithelial ovarian cancer. *N Engl J Med* **348**, 203-13 (2003).
129. Ji, R.R. et al. An immune-active tumor microenvironment favors clinical response to ipilimumab. *Cancer Immunol Immunother* **61**, 1019-31 (2012).
130. Harlin, H. et al. Chemokine expression in melanoma metastases associated with CD8+ T-cell recruitment. *Cancer Res* **69**, 3077-85 (2009).
131. Vasquez-Dunddel, D. et al. STAT3 regulates arginase-I in myeloid-derived suppressor cells from cancer patients. *J Clin Invest* **123**, 1580-9 (2013).
132. Schiavoni, G., Gabriele, L. & Mattei, F. The tumor microenvironment: a pitch for multiple players. *Front Oncol* **3**, 90 (2013).
133. Parker, K.H., Beury, D.W. & Ostrand-Rosenberg, S. Myeloid-Derived Suppressor Cells: Critical Cells Driving Immune Suppression in the Tumor Microenvironment. *Adv Cancer Res* **128**, 95-139 (2015).
134. Gabrilovich, D.I., Ostrand-Rosenberg, S. & Bronte, V. Coordinated regulation of myeloid cells by tumours. *Nat Rev Immunol* **12**, 253-68 (2012).
135. Whiteside, T.L., Demaria, S., Rodriguez-Ruiz, M.E., Zarour, H.M. & Melero, I. Emerging Opportunities and Challenges in Cancer Immunotherapy. *Clin Cancer Res* **22**, 1845-55 (2016).
136. Yao, X. et al. Levels of peripheral CD4(+)FoxP3(+) regulatory T cells are negatively associated with clinical response to adoptive immunotherapy of human cancer. *Blood* **119**, 5688-96 (2012).
137. Kochenderfer, J.N., Yu, Z., Frasheri, D., Restifo, N.P. & Rosenberg, S.A. Adoptive transfer of syngeneic T cells transduced with a chimeric antigen receptor that recognizes murine CD19 can eradicate lymphoma and normal B cells. *Blood* **116**, 3875-86 (2010).

138. Gattinoni, L. et al. Removal of homeostatic cytokine sinks by lymphodepletion enhances the efficacy of adoptively transferred tumor-specific CD8+ T cells. *J Exp Med* **202**, 907-12 (2005).
139. Dudley, M.E. et al. Adoptive cell therapy for patients with metastatic melanoma: evaluation of intensive myeloablative chemoradiation preparative regimens. *J Clin Oncol* **26**, 5233-9 (2008).
140. Dudley, M.E. et al. Adoptive cell transfer therapy following non-myeloablative but lymphodepleting chemotherapy for the treatment of patients with refractory metastatic melanoma. *J Clin Oncol* **23**, 2346-57 (2005).
141. Baba, J. et al. Depletion of radio-resistant regulatory T cells enhances antitumor immunity during recovery from lymphopenia. *Blood* **120**, 2417-27 (2012).
142. Klebanoff, C.A., Khong, H.T., Antony, P.A., Palmer, D.C. & Restifo, N.P. Sinks, suppressors and antigen presenters: how lymphodepletion enhances T cell-mediated tumor immunotherapy. *Trends Immunol* **26**, 111-7 (2005).
143. Paulos, C.M. et al. Microbial translocation augments the function of adoptively transferred self/tumor-specific CD8+ T cells via TLR4 signaling. *J Clin Invest* **117**, 2197-204 (2007).
144. Pardoll, D.M. The blockade of immune checkpoints in cancer immunotherapy. *Nat Rev Cancer* **12**, 252-64 (2012).
145. Hodi, F.S. et al. Improved survival with ipilimumab in patients with metastatic melanoma. *N Engl J Med* **363**, 711-23 (2010).
146. Yap, T.A., Gerlinger, M., Futreal, P.A., Pusztai, L. & Swanton, C. Intratumor heterogeneity: seeing the wood for the trees. *Sci Transl Med* **4**, 127ps10 (2012).
147. Mackensen, A. et al. Phase I study of adoptive T-cell therapy using antigen-specific CD8+ T cells for the treatment of patients with metastatic melanoma. *J Clin Oncol* **24**, 5060-9 (2006).
148. DuPage, M., Mazumdar, C., Schmidt, L.M., Cheung, A.F. & Jacks, T. Expression of tumour-specific antigens underlies cancer immunoediting. *Nature* **482**, 405-9 (2012).
149. Jensen, S.M. et al. Increased frequency of suppressive regulatory T cells and T cell-mediated antigen loss results in murine melanoma recurrence. *J Immunol* **189**, 767-76 (2012).
150. Greenman, C. et al. Patterns of somatic mutation in human cancer genomes. *Nature* **446**, 153-8 (2007).
151. Rosenberg, S.A. Cell transfer immunotherapy for metastatic solid cancer--what clinicians need to know. *Nat Rev Clin Oncol* **8**, 577-85 (2011).
152. Rosenberg, S.A. et al. Durable complete responses in heavily pretreated patients with metastatic melanoma using T-cell transfer immunotherapy. *Clin Cancer Res* **17**, 4550-7 (2011).
153. Park, T.S., Rosenberg, S.A. & Morgan, R.A. Treating cancer with genetically engineered T cells. *Trends Biotechnol* **29**, 550-7 (2011).
154. Morgan, R.A. et al. Cancer regression in patients after transfer of genetically engineered lymphocytes. *Science* **314**, 126-9 (2006).
155. Robbins, P.F. et al. Tumor regression in patients with metastatic synovial cell sarcoma and melanoma using genetically engineered lymphocytes reactive with NY-ESO-1. *J Clin Oncol* **29**, 917-24 (2011).
156. Rapoport, A.P. et al. NY-ESO-1-specific TCR-engineered T cells mediate sustained antigen-specific antitumor effects in myeloma. *Nat Med* **21**, 914-21 (2015).

157. Shi, H., Liu, L. & Wang, Z. Improving the efficacy and safety of engineered T cell therapy for cancer. *Cancer Lett* **328**, 191-7 (2013).
158. Curran, K.J., Pegram, H.J. & Brentjens, R.J. Chimeric antigen receptors for T cell immunotherapy: current understanding and future directions. *J Gene Med* **14**, 405-15 (2012).
159. Louis, C.U. et al. Antitumor activity and long-term fate of chimeric antigen receptor-positive T cells in patients with neuroblastoma. *Blood* **118**, 6050-6 (2011).
160. Kochenderfer, J.N. et al. Eradication of B-lineage cells and regression of lymphoma in a patient treated with autologous T cells genetically engineered to recognize CD19. *Blood* **116**, 4099-102 (2010).
161. Kalos, M. et al. T cells with chimeric antigen receptors have potent antitumor effects and can establish memory in patients with advanced leukemia. *Sci Transl Med* **3**, 95ra73 (2011).
162. Kochenderfer, J.N. et al. B-cell depletion and remissions of malignancy along with cytokine-associated toxicity in a clinical trial of anti-CD19 chimeric-antigen-receptor-transduced T cells. *Blood* **119**, 2709-20 (2012).
163. Maus, M.V. & June, C.H. Making Better Chimeric Antigen Receptors for Adoptive T-cell Therapy. *Clin Cancer Res* **22**, 1875-84 (2016).
164. Grupp, S.A. et al. Chimeric antigen receptor-modified T cells for acute lymphoid leukemia. *N Engl J Med* **368**, 1509-18 (2013).
165. Hunn, M.K. et al. Vaccination with irradiated tumor cells pulsed with an adjuvant that stimulates NKT cells is an effective treatment for glioma. *Clin Cancer Res* **18**, 6446-59 (2012).
166. Kenter, G.G. et al. Vaccination against HPV-16 oncoproteins for vulvar intraepithelial neoplasia. *N Engl J Med* **361**, 1838-47 (2009).
167. Schuster, S.J. et al. Vaccination with patient-specific tumor-derived antigen in first remission improves disease-free survival in follicular lymphoma. *J Clin Oncol* **29**, 2787-94 (2011).
168. Norell, H. et al. Vaccination with a plasmid DNA encoding HER-2/neu together with low doses of GM-CSF and IL-2 in patients with metastatic breast carcinoma: a pilot clinical trial. *J Transl Med* **8**, 53 (2010).
169. Van Lint, S., Heirman, C., Thielemans, K. & Breckpot, K. mRNA: From a chemical blueprint for protein production to an off-the-shelf therapeutic. *Hum Vaccin Immunother* **9**, 265-74 (2013).
170. Cawood, R. et al. Recombinant viral vaccines for cancer. *Trends Mol Med* **18**, 564-74 (2012).
171. Vacchelli, E. et al. Trial watch: Peptide vaccines in cancer therapy. *Oncoimmunology* **1**, 1557-1576 (2012).
172. Kirkwood, J.M. et al. Immunotherapy of cancer in 2012. *CA Cancer J Clin* **62**, 309-35 (2012).
173. Sabado, R.L. & Bhardwaj, N. Directing dendritic cell immunotherapy towards successful cancer treatment. *Immunotherapy* **2**, 37-56 (2010).
174. Bilusic, M. & Madan, R.A. Therapeutic cancer vaccines: the latest advancement in targeted therapy. *Am J Ther* **19**, e172-81 (2012).
175. Kantoff, P.W. et al. Sipuleucel-T immunotherapy for castration-resistant prostate cancer. *N Engl J Med* **363**, 411-22 (2010).
176. Escors, D. & Breckpot, K. Lentiviral vectors in gene therapy: their current status and future potential. *Arch Immunol Ther Exp (Warsz)* **58**, 107-19 (2010).
177. Galluzzi, L. et al. Trial watch: Dendritic cell-based interventions for cancer therapy. *Oncoimmunology* **1**, 1111-1134 (2012).

178. Liechtenstein, T. et al. Immune modulation by genetic modification of dendritic cells with lentiviral vectors. *Virus Res* **176**, 1-15 (2013).
179. Heiser, A. et al. Autologous dendritic cells transfected with prostate-specific antigen RNA stimulate CTL responses against metastatic prostate tumors. *J Clin Invest* **109**, 409-17 (2002).
180. Morse, M.A. et al. Immunotherapy with autologous, human dendritic cells transfected with carcinoembryonic antigen mRNA. *Cancer Invest* **21**, 341-9 (2003).
181. Van Tendeloo, V.F. et al. Induction of complete and molecular remissions in acute myeloid leukemia by Wilms' tumor 1 antigen-targeted dendritic cell vaccination. *Proc Natl Acad Sci U S A* **107**, 13824-9 (2010).
182. Suso, E.M. et al. hTERT mRNA dendritic cell vaccination: complete response in a pancreatic cancer patient associated with response against several hTERT epitopes. *Cancer Immunol Immunother* **60**, 809-18 (2011).
183. Van Nuffel, A.M. et al. Intravenous and intradermal TriMix-dendritic cell therapy results in a broad T-cell response and durable tumor response in a chemorefractory stage IV-M1c melanoma patient. *Cancer Immunol Immunother* **61**, 1033-43 (2012).
184. Van Nuffel, A.M. et al. Dendritic cells loaded with mRNA encoding full-length tumor antigens prime CD4+ and CD8+ T cells in melanoma patients. *Mol Ther* **20**, 1063-74 (2012).
185. Rosenberg, S.A., Yang, J.C., White, D.E. & Steinberg, S.M. Durability of complete responses in patients with metastatic cancer treated with high-dose interleukin-2: identification of the antigens mediating response. *Ann Surg* **228**, 307-19 (1998).
186. Ahmadzadeh, M. & Rosenberg, S.A. IL-2 administration increases CD4+ CD25(hi) Foxp3+ regulatory T cells in cancer patients. *Blood* **107**, 2409-14 (2006).
187. Cha, E., Graham, L., Manjili, M.H. & Bear, H.D. IL-7 + IL-15 are superior to IL-2 for the ex vivo expansion of 4T1 mammary carcinoma-specific T cells with greater efficacy against tumors in vivo. *Breast Cancer Res Treat* **122**, 359-69 (2010).
188. Santegoets, S.J. et al. IL-21 promotes the expansion of CD27+ CD28+ tumor infiltrating lymphocytes with high cytotoxic potential and low collateral expansion of regulatory T cells. *J Transl Med* **11**, 37 (2013).
189. Yang, S. et al. Modulating the differentiation status of ex vivo-cultured anti-tumor T cells using cytokine cocktails. *Cancer Immunol Immunother* **62**, 727-36 (2013).
190. Zhang, L. et al. Improving adoptive T cell therapy by targeting and controlling IL-12 expression to the tumor environment. *Mol Ther* **19**, 751-9 (2011).
191. Kerkar, S.P. et al. Tumor-specific CD8+ T cells expressing interleukin-12 eradicate established cancers in lymphodepleted hosts. *Cancer Res* **70**, 6725-34 (2010).
192. Chinnasamy, D. et al. Local delivery of interleukin-12 using T cells targeting VEGF receptor-2 eradicates multiple vascularized tumors in mice. *Clin Cancer Res* **18**, 1672-83 (2012).
193. Prieto, P.A. et al. CTLA-4 blockade with ipilimumab: long-term follow-up of 177 patients with metastatic melanoma. *Clin Cancer Res* **18**, 2039-47 (2012).
194. Topalian, S.L. et al. Safety, activity, and immune correlates of anti-PD-1 antibody in cancer. *N Engl J Med* **366**, 2443-54 (2012).
195. Brahmer, J.R. et al. Safety and activity of anti-PD-L1 antibody in patients with advanced cancer. *N Engl J Med* **366**, 2455-65 (2012).

196. Ascierto, P.A., Kalos, M., Schaer, D.A., Callahan, M.K. & Wolchok, J.D. Biomarkers for immunostimulatory monoclonal antibodies in combination strategies for melanoma and other tumor types. *Clin Cancer Res* **19**, 1009-20 (2013).
197. Sznol, M. & Chen, L. Antagonist antibodies to PD-1 and B7-H1 (PD-L1) in the treatment of advanced human cancer. *Clin Cancer Res* **19**, 1021-34 (2013).
198. Melero, I., Grimaldi, A.M., Perez-Gracia, J.L. & Ascierto, P.A. Clinical development of immunostimulatory monoclonal antibodies and opportunities for combination. *Clin Cancer Res* **19**, 997-1008 (2013).
199. Matsuzaki, J. et al. Tumor-infiltrating NY-ESO-1-specific CD8+ T cells are negatively regulated by LAG-3 and PD-1 in human ovarian cancer. *Proc Natl Acad Sci U S A* **107**, 7875-80 (2010).
200. Fourcade, J. et al. Upregulation of Tim-3 and PD-1 expression is associated with tumor antigen-specific CD8+ T cell dysfunction in melanoma patients. *J Exp Med* **207**, 2175-86 (2010).
201. Chacon, J.A. et al. Co-stimulation through 4-1BB/CD137 improves the expansion and function of CD8(+) melanoma tumor-infiltrating lymphocytes for adoptive T-cell therapy. *PLoS One* **8**, e60031 (2013).
202. Garber, K. Natural killer cells blaze into immuno-oncology. *Nat Biotechnol* **34**, 219-20 (2016).
203. Gasser, S., Orsulic, S., Brown, E.J. & Raulet, D.H. The DNA damage pathway regulates innate immune system ligands of the NKG2D receptor. *Nature* **436**, 1186-90 (2005).
204. Dewitte, H., Verbeke, R., Breckpot, K., De Smedt, S.C. & Lentacker, I. Nanoparticle design to induce tumor immunity and challenge the suppressive tumor microenvironment. *Nano Today* **9**, 743-758 (2014).
205. Pradere, J.P., Dapito, D.H. & Schwabe, R.F. The Yin and Yang of Toll-like receptors in cancer. *Oncogene* **33**, 3485-95 (2014).
206. Guha, M. Anticancer TLR agonists on the ropes. *Nat Rev Drug Discov* **11**, 503-5 (2012).
207. Vacchelli, E. et al. Trial watch: FDA-approved Toll-like receptor agonists for cancer therapy. *Oncoimmunology* **1**, 894-907 (2012).
208. Vacchelli, E. et al. Trial Watch: Toll-like receptor agonists for cancer therapy. *Oncoimmunology* **2**, e25238 (2013).
209. Van De Voort, T.J., Felder, M.A., Yang, R.K., Sondel, P.M. & Rakhmilevich, A.L. Intratumoral delivery of low doses of anti-CD40 mAb combined with monophosphoryl lipid a induces local and systemic antitumor effects in immunocompetent and T cell-deficient mice. *J Immunother* **36**, 29-40 (2013).
210. Meraz, I.M. et al. Adjuvant cationic liposomes presenting MPL and IL-12 induce cell death, suppress tumor growth, and alter the cellular phenotype of tumors in a murine model of breast cancer. *Mol Pharm* **11**, 3484-91 (2014).
211. Faveeuw, C. & Trottein, F. Optimization of natural killer T cell-mediated immunotherapy in cancer using cell-based and nanovector vaccines. *Cancer Res* **74**, 1632-8 (2014).
212. Kroemer, G., Galluzzi, L., Kepp, O. & Zitvogel, L. Immunogenic cell death in cancer therapy. *Annu Rev Immunol* **31**, 51-72 (2013).
213. Pol, J. et al. Trial Watch: Immunogenic cell death inducers for anticancer chemotherapy. *Oncoimmunology* **4**, e1008866 (2015).

214. Conde, J., Arnold, C.E., Tian, F.R. & Artzi, N. RNAi nanomaterials targeting immune cells as an anti-tumor therapy: the missing link in cancer treatment? *Materials Today* **19**, 29-43 (2016).
215. Luo, Z. et al. Nanovaccine loaded with poly I:C and STAT3 siRNA robustly elicits anti-tumor immune responses through modulating tumor-associated dendritic cells in vivo. *Biomaterials* **38**, 50-60 (2015).
216. Heo, M.B. & Lim, Y.T. Programmed nanoparticles for combined immunomodulation, antigen presentation and tracking of immunotherapeutic cells. *Biomaterials* **35**, 590-600 (2014).
217. Hobo, W. et al. Improving dendritic cell vaccine immunogenicity by silencing PD-1 ligands using siRNA-lipid nanoparticles combined with antigen mRNA electroporation. *Cancer Immunology Immunotherapy* **62**, 285-297 (2013).
218. Cubillos-Ruiz, J.R. et al. Polyethylenimine-based siRNA nanocomplexes reprogram tumor-associated dendritic cells via TLR5 to elicit therapeutic antitumor immunity. *Journal of Clinical Investigation* **119**, 2231-2244 (2009).
219. Kershaw, M.H., Westwood, J.A. & Darcy, P.K. Gene-engineered T cells for cancer therapy. *Nat Rev Cancer* **13**, 525-41 (2013).
220. Lakshmanan, S. et al. Physical energy for drug delivery; poration, concentration and activation. *Adv Drug Deliv Rev* **71**, 98-114 (2014).
221. Gehl, J. Electroporation: theory and methods, perspectives for drug delivery, gene therapy and research. *Acta Physiol Scand* **177**, 437-47 (2003).
222. Gresch, O. et al. New non-viral method for gene transfer into primary cells. *Methods* **33**, 151-63 (2004).
223. Singh, H., Moyes, J.S., Huls, M.H. & Cooper, L.J. Manufacture of T cells using the Sleeping Beauty system to enforce expression of a CD19-specific chimeric antigen receptor. *Cancer Gene Ther* **22**, 95-100 (2015).
224. Kmiecik, J. et al. Elevated CD3+ and CD8+ tumor-infiltrating immune cells correlate with prolonged survival in glioblastoma patients despite integrated immunosuppressive mechanisms in the tumor microenvironment and at the systemic level. *J Neuroimmunol* **264**, 71-83 (2013).
225. Galon, J. et al. Type, density, and location of immune cells within human colorectal tumors predict clinical outcome. *Science* **313**, 1960-4 (2006).
226. Moon, E.K. et al. Expression of a functional CCR2 receptor enhances tumor localization and tumor eradication by retargeted human T cells expressing a mesothelin-specific chimeric antibody receptor. *Clin Cancer Res* **17**, 4719-30 (2011).
227. Craddock, J.A. et al. Enhanced tumor trafficking of GD2 chimeric antigen receptor T cells by expression of the chemokine receptor CCR2b. *J Immunother* **33**, 780-8 (2010).
228. Di Stasi, A. et al. T lymphocytes coexpressing CCR4 and a chimeric antigen receptor targeting CD30 have improved homing and antitumor activity in a Hodgkin tumor model. *Blood* **113**, 6392-402 (2009).
229. Charo, J. et al. Bcl-2 overexpression enhances tumor-specific T-cell survival. *Cancer Res* **65**, 2001-8 (2005).
230. Stromnes, I.M. et al. Abrogating Cbl-b in effector CD8(+) T cells improves the efficacy of adoptive therapy of leukemia in mice. *J Clin Invest* **120**, 3722-34 (2010).

231. Pegram, H.J. et al. Tumor-targeted T cells modified to secrete IL-12 eradicate systemic tumors without need for prior conditioning. *Blood* **119**, 4133-41 (2012).
232. Zhou, P. et al. In vivo discovery of immunotherapy targets in the tumour microenvironment. *Nature* **506**, 52-7 (2014).
233. Waugh, K.A., Leach, S.M. & Slansky, J.E. Targeting Transcriptional Regulators of CD8+ T Cell Dysfunction to Boost Anti-Tumor Immunity. *Vaccines (Basel)* **3**, 771-802 (2015).
234. Freeley, M. & Long, A. Advances in siRNA delivery to T-cells: potential clinical applications for inflammatory disease, cancer and infection. *Biochem J* **455**, 133-47 (2013).
235. Ramishetti, S. et al. Systemic Gene Silencing in Primary T Lymphocytes Using Targeted Lipid Nanoparticles. *ACS Nano* **9**, 6706-16 (2015).
236. Sharei, A. et al. Ex vivo cytosolic delivery of functional macromolecules to immune cells. *PLoS One* **10**, e0118803 (2015).

2

Hitchhiking nanoparticles: Reversible coupling of lipid-based nanoparticles to cytotoxic T lymphocytes

Parts of this chapter are published as:

Wayteck Laura[a], Dewitte Heleen[a], De Backer Lynn[a], Breckpot Karine[b], Demeester Jo[a], De Smedt Stefaan[a,*], Raemdonck Koen[a,*], Hitchhiking nanoparticles: reversible coupling of lipid-based nanoparticles to cytotoxic T lymphocytes. *Biomaterials*, 77 (2016) 243-254. (DOI: 10.1016/j.biomaterials.2015.11.016)

[*]Both authors contributed equally to this work

[a]Laboratory of General Biochemistry and Physical Pharmacy, Faculty of Pharmaceutical Sciences, Ghent University, Ottergemsesteenweg 460, 9000 Ghent, Belgium

[b]Laboratory of Molecular and Cellular Therapy, Department of Biomedical Sciences, Vrije Universiteit Brussel, Laarbeeklaan 103/E, 1090 Brussels, Belgium

ABSTRACT

Following intravenous injection of anti-cancer nanomedicines, many barriers need to be overcome en route to the tumor. Cell-mediated delivery of nanoparticles (NPs) is promising in terms of overcoming several of these barriers based on the tumoritropic migratory properties of particular cell types. This guided transport aims to enhance the NP accumulation in the tumor and moreover enhance the infiltration of regions that are typically inaccessible for free NPs. Within this study, cytotoxic $CD8^+$ T cells were selected as carriers based on both their ability to migrate to the tumor and their intrinsic cytolytic activity against tumor cells. Many anti-cancer nanomedicines require tumor cell internalization to mediate cytosolic drug delivery and enhance the anti-cancer effect. This proof-of-concept therefore reports on the reversible attachment of liposomes to the surface of cytotoxic T lymphocytes (CTLs) via a reduction-sensitive coupling. The activation status of the T cells and the liposome composition are shown to strongly influence the loading efficiency. Loading the cells with liposomes does not compromise T cell functionalities like proliferation and cytolytic function. Additionally, the triggered liposome release is demonstrated upon the addition of glutathione. Based on this optimization using liposomes as model NP, a small interfering RNA (siRNA)-loaded NP was developed that can be coupled to the surface of CTLs.

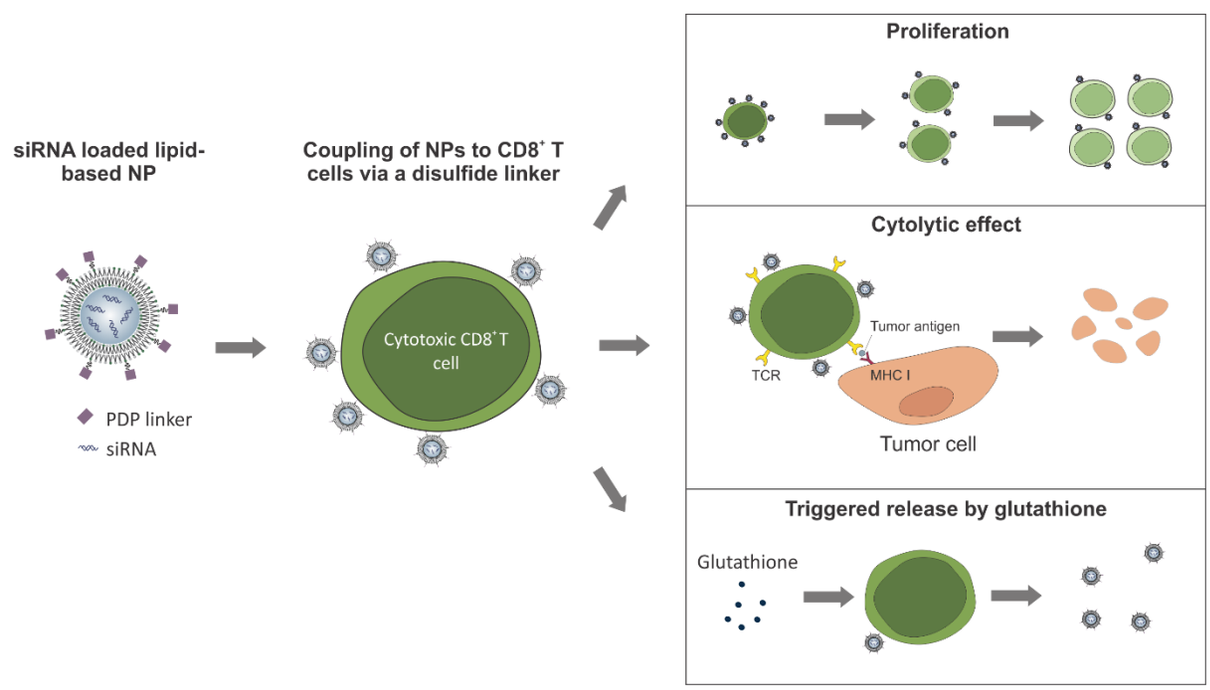

1 INTRODUCTION

In **Chapter 1,** it was introduced that nanoparticles (NPs) have been widely investigated for the delivery of anti-cancer drugs to tumor tissues [1-3]. Although a lot of research has been performed, to date, only few nanomedicines are in clinical use for the treatment of cancer [4, 5]. One of the key challenges is inadequate targeted delivery of drug-loaded NPs to the tumor tissue following systemic administration.

One alternative strategy that might overcome these targeting limitations is cell-mediated delivery [6, 7]. Certain cell types have the intrinsic ability to cross the endothelial barrier and infiltrate the tumor tissue, which makes them attractive carriers for NP delivery [8]. For example, T cells have the capacity to migrate to the tumor tissue. Moreover, cytotoxic $CD8^+$ T lymphocytes (CTLs) have the added advantage of exerting a cytotoxic effect on tumor cells upon their recognition and binding of tumor-associated antigens. By virtue of these specific traits, the adoptive transfer of T cells is a widely investigated cancer immunotherapy. Although adoptive T cell therapy (ACT) already showed impressive clinical outcomes, complete tumor regression was only observed in a restricted number of patients mainly due to the immunosuppressive tumor microenvironment and also the loss of tumor antigens to which the therapy was targeted [9, 10]. Therefore, strategies combining conventional chemotherapies with cancer immunotherapy have gained interest in recent years [11].

The use of T cells as NP carrier cells has been assessed previously by Irvine and colleagues, who irreversibly attached drug-loaded NPs to their surface and also by Vile and coworkers, who exploited T cells for the intratumoral delivery of therapeutic viral vectors [12-14]. Here, we propose a synergistic strategy based on CTLs that serve a dual purpose, i.e. induce a direct killing effect on tumor cells and enhance the delivery of drug-loaded NPs into tumor tissue, which may kill T cell-refractory tumor cells. To this end, we investigated the covalent attachment of NPs to the surface of CTLs. Moreover, we envisioned the triggered release of the cell surface-conjugated NPs in the tumor microenvironment which could allow their subsequent internalization by target tumor cells and hence a more efficient delivery of anti-cancer drugs. This concept is of particular interest for charged macromolecular therapeutics that are membrane-impermeable such as small interfering RNA (siRNA), which require NP-mediated cytosolic delivery in target cells. To date, a reversible coupling strategy of NPs to the surface of CTLs has not yet been investigated.

Given their outstanding promise and versatility as drug delivery systems, we used liposomes as model nanomedicines within this proof-of-concept [15]. First, it was assessed whether liposomes can be attached to the surface of CTLs based on disulfide bond formation between exofacial thiols present on the CTL plasma membrane and thiol-reactive liposomes. Next, we showed the triggered release of liposomes in the presence of glutathione as a

reducing agent. Importantly, *in vitro* data indicated that the NP-load did not affect the T cell functionalities such as proliferation and cytotoxic effector functions.

It has been demonstrated that the adoptive transfer of less-differentiated T cells is associated with superior persistence and anti-tumor responses compared to the more-differentiated effector T cells [16, 17]. On the other hand, the differentiation of naive T cells into $CD8^+$ effector T cells is required for their migratory and cytotoxic function. Since both activated and naive T lymphocytes are investigated for ACT, we therefore evaluated the reversible coupling of liposomes as a function of their activation status [18]. It has also been shown that combining $CD8^+$ and $CD4^+$ T cells can lead to improved anti-cancer effects [19-21]. Therefore, we subsequently investigated the attachment of PDP-functionalized liposomes to other immune cell types, especially $CD4^+$ T cells.

Finally, building further on this optimized reversible coupling strategy, we demonstrated the coupling of lipid-enveloped nanogels, loaded with siRNA, to the surface of activated CTLs. RNA interference has been shown to downregulate distinct pathways in both tumor cells and immune cells [22]. The T cell-mediated delivery of siRNA may help to target tumor cells escaping the ACT and surrounding immune cells that have an immunosuppressive effect onto the cancer immunotherapy, all together enhancing the outcome of the therapy.

2 MATERIALS AND METHODS

2.1 Preparation of liposomes and characterization

The liposomes were composed of 1,2-dioleoyl-sn-glycero-3-phosphocholine (DOPC), egg phosphatidyl glycerol (egg PG) or 18:1 1,2-dioleoyl-sn-glycero-3-phosphoethanolamine-N-[3-(2-pyridyldithio)propionate] (PE-PDP), and the fluorescent 1,1'-dioctadecyl-3,3,3',3'-tetramethylindodicarbocyanine (DiD). DOPC and PE-PDP lipids were purchased from Avanti Polar Lipids (Alabaster, USA), PG lipids from Lipoid (Ludwigshafen, Germany), and DiD from Molecular probes (Invitrogen, Merelbeke, Belgium). The typical liposome composition comprised 50 wt% PE-PDP or PG, 3 wt% DiD, and 47 wt% DOPC. When varying the PE-PDP or PG content, the fraction of DOPC lipids was adjusted accordingly. To form the liposomes, a lipid mixture in chloroform was prepared and pipetted in a round-bottom glass flask, followed by evaporation of the chloroform solvent to form a thin lipid film. The dried lipids were rehydrated in phosphate buffered saline (PBS; Gibco-Invitrogen, Merelbeke, Belgium) at ambient temperature followed by an extrusion of the resultant multilamellar liposomes through a 200 nm polycarbonate filter (Whatman, Diegem, Belgium). Liposome size and surface charge were measured in HEPES buffer (20 mM, pH 7.4) at 25 °C by dynamic light scattering and zeta potential measurements, respectively, using a Zetasizer Nano ZS (Malvern, UK) equipped with Dispersion Technology Software (DTS).

2.2 Cell culture

$CD8^+$ T cells were isolated from the spleen of OT-I mice using a negative isolation $CD8^+$ kit (Stem Cell Technologies, Grenoble, France). Cells were activated with anti-CD3/CD28 Dynabeads® (Gibco-Invitrogen) at a density of 2 x 10^6 cells/well and a bead-to-cell ratio of 1:1 in a 24-well plate. The cells were cultured in complete T cell culture medium containing advanced RPMI medium (Gibco-Invitrogen) supplemented with 10% fetal bovine serum (FBS; Hyclone, Thermo Scientific, MA, USA), 2 mM L-glutamine (Gibco-Invitrogen, Merelbeke, Belgium), 1% penicillin/streptomycin (Gibco-Invitrogen). According to the manufacturer's protocol 30 U ml^{-1} rIL-2 (Miltenyi Biotec, Leiden, The Netherlands) was added to the culture medium and restimulation was performed by adding new beads every 7 days.

The mouse thymoma cell lines EL4 and E.G7-OVA were purchased from the American Type Culture Collection (ATCC). The E.G7-OVA cell line is an EL4 cell line that was stably transfected with the plasmid pAc-neo-OVA, which carries a complete copy of chicken ovalbumine (OVA) mRNA. Both cell lines were cultivated in RPMI 1640 (Gibco-Invitrogen) supplemented with 10% FBS, 2 mM L-glutamine, and 1% penicillin/streptomycin.

2.3 Visualization of exofacial thiol groups

$CD8^+$ T cells were incubated for 15 min with 100 µg ml^{-1} Cy5-labeled maleimide (GE Healthcare Life Sciences, Diegem, Belgium) at room temperature. After washing the cells with PBS, the cells were fixed with 4% paraformaldehyde (Sigma-Aldrich, Bornem, Belgium). Confocal microscopy images were acquired using a Nikon C1si confocal laser scanning microscope (Nikon Benelux, Brussels, Belgium) equipped with a Plan Apo VC 60x 1.4 NA oil immersion objective lens (Nikon). The Cy5 dye was excited with a 636 nm diode laser (CVI Melles Griot, NM, USA).

2.4 Reversible coupling of liposomes to the surface of $CD8^+$ T cells

$CD8^+$ T cells (3 x 10^5 cells per sample) were incubated in serum-free advanced RPMI with the liposomes during 1h at 37 °C with gentle mixing after 30 min. A liposome concentration of 2 mg ml^{-1} lipids was used, if not indicated differently. Subsequently, the cells were washed with PBS (supplemented with 5% FBS) and to discriminate the $CD8^+$ population the cells were stained with a CD8-Alexa Fluor® 488 antibody (BD Pharmingen, Erembodegem, Belgium) for 30 min at room temperature in PBS (supplemented with 5% FBS). The amount of liposomes attached to the $CD8^+$ T cells was quantified via flow cytometry by measuring the DiD (red) fluorescence intensity per cell. In addition, a dead cell stain was performed by incubating the (liposome-loaded) cells with 60 nM SYTOX® green nucleic acid stain (Molecular Probes/Invitrogen, Merelbeke, Belgium) for 15 min at room temperature in PBS (supplemented with 5% FBS). The viable population was identified and selected based on the SYTOX® green stain. The activation status of the T cells was evaluated with a phycoerythrin (PE)-labeled CD25 antibody (BD Pharmingen). In addition, the coupling was also evaluated on the total splenocyte population. To this end, red blood cells were removed by a freeze and thaw cycle and the residual splenocytes were incubated with 5 mg ml^{-1} liposomes, followed by antibody staining with CD3-PE, CD8-Alexa Fluor® 488, and CD19-FITC (all BD Pharmingen).

To evaluate the detachment of the liposomes from the T cell surface, the liposome-loaded cells were incubated with mounting concentrations of glutathione (Sigma-Aldrich) for 30 min at 37 °C. The glutathione dilutions were prepared in PBS (supplemented with 5% FBS) and the pH was adjusted to physiological pH. After incubation, the released liposomes were removed by washing the cells in PBS (supplemented with 5% FBS) and the remaining DiD fluorescence per $CD8^+$ T cell was quantified by flow cytometry. Flow cytometry data were acquired by a FACSCalibur™ (BD Pharmingen) and analyzed using BD CellQuest™ and FlowJo (Treestar Inc, Ashland, USA) software.

2.5 Characterization of detached liposomes by fluorescence single particle tracking (fSPT)

$CD8^+$ T cells were first incubated with PDP-functionalized liposomes that were fluorescently labeled with DiD as described in the previous section, followed by two washing steps with PBS to remove the unbound particles. Subsequently, the cells were incubated with 2 mg ml^{-1} glutathione during 30 min at 37 °C. After centrifugation of the cells, the supernatant was collected and analyzed by fSPT. The latter technique enables the measurement of the size of NPs in biological fluids by recording the movement of the fluorescently labeled particles. The DiD fluorophores in the liposomes were excited by swept-field laser illumination (100 mW Spectra Physics Excelsior 642 nm, CA, USA) on an epi-fluorescent microscope (Eclipse T, Nikon BeLux, Brussels, Belgium) equipped with a Plan Apo VC 100x 1.4 NA oil immersion objective lens (Nikon). The diffusion of individual liposomes was recorded in high-speed movies by a fast and sensitive CCD camera (Ixon Ultra 897, Andor Technology, CT, USA). The motion trajectories of single particles were obtained by in-house developed software. Subsequently, the diffusion coefficient for each trajectory was calculated and transformed in a size distribution using the Stokes-Einstein equation. Data were further refined by the maximal entropy deconvolution method, as described by our group previously [23].

2.6 Visualization of T cell surface-conjugated liposomes by confocal microscopy

DiD-labeled liposomes were conjugated to the cell surface of $CD8^+$ T cells as previously described, followed by a cell nucleus stain with 10 µg ml^{-1} Hoechst 33342 (Molecular Probes) and a CD8-Alexa Fluor® 488 antibody stain (BD Pharmingen). The dyes were respectively excited by a 636 nm diode laser, a 408 nm diode laser, and a 488 nm argon-ion laser (all purchased from CVI Melles Griot). Images were recorded with a Plan Apo VC 60x 1.4 NA oil immersion objective lens (Nikon).

2.7 T cell proliferation assay

$CD8^+$ T cells activated during 9 days were first stained with 7.5 µM CFSE (Life Technologies, Merelbeke, Belgium) and subsequently conjugated with DiD-labeled liposomes as previously described. The proliferation of the T cells was then measured by the dilution of the CFSE stain over the daughter cells with flow cytometry at varying time points (0h, 24h and 48h) after loading. The distribution of the liposomes over the daughter cells was determined by measuring the DiD fluorescence intensity per cell. During the experiment, the activated cells were incubated in cell culture medium supplemented with 30 U ml^{-1} rIL-2.

2.8 In vitro cytotoxic T cell (CTL) assay

EL4 and E.G7-OVA cells were stained with 5 µM and 15 µM CFSE stain, respectively. The OT-I CTLs were activated for 9 days with anti-CD3/CD28 Dynabeads® and incubated with PDP-functionalized liposomes at a concentration of 5 mg ml^{-1} lipids, followed by two washing steps to remove unbound particles. Subsequently, the OT-I T cells were co-cultured with EL4 and E.G7-OVA cells at two different effector-to-target ratios. To increase cell contact between T cells and target cells, the incubation was performed in a U-bottom 96-well plate (Falcon, BD Biosciences) in complete T cell culture medium. After 4h at 37 °C the ratio of EL4 cells compared to E.G7-OVA cells was quantified by flow cytometry, in which the viable population was selected based on forward scatter/side scatter and both cell lines could be distinguished by their different CFSE fluorescence intensity signal.

2.9 Coupling of siRNA-loaded NPs to cytotoxic T cells

Our group has developed biodegradable dextran nanogels *via* an inverse mini-emulsion photopolymerization of dextran hydroxyethyl methacrylate (dex-HEMA) in mineral oil. To incorporate cationic charges in the nanoscopic hydrogel network, cationic methacrylate monomers ([2-(methacryloyloxy)-ethyl]trimethylammonium chloride, TMAEMA) were copolymerized with dex-HEMA [24]. Recently, experimental evidence was provided that these siRNA-loaded NGs (siNGs) can efficiently be coated with a lipid bilayer [25]. Here, the NGs were first loaded with 5 pmol Alexa Fluor® 488-labeled siRNA (Eurogentec, Seraing, Belgium) per µg NGs. Next, the siNGs were layered with a lipid mixture composed of 50 wt% PE-PDP, 3 wt% DiD, and 47 wt% DOPC. Briefly, the siNGs were incubated for 10 min at 4°C with the hydrated lipid mixture, allowing electrostatic interaction, applying 10 mg lipid per mg NGs. After incubation, the lipid coat was formed by high-energy sonication using a probe sonicator (Branson Digital Sonifier®, amplitude 10 %). The lipid-coated siNGs were separated from excess lipids by centrifugation through a 7.5 wt% OptiPrep™ (Sigma-Aldrich) cushion for 30 min at 30000 g (L8-70M Centrifuge with SW55 Ti rotor; Beckman Coulter, Suarlée, Belgium). The supernatant, containing empty lipid vesicles, was discarded. The resulting pellet, containing the purified lipid-coated siNGs, was resuspended in nuclease-free water. Subsequently, equal volumes of the resuspended formulation and double-concentrated PBS were mixed, in order to obtain physiological salt concentrations. Using this protocol, lipid-coated siNGs were obtained with a hydrodynamic diameter around 400 nm as analyzed using fluorescence single particle tracking (fSPT) [26].

The lipid-coated siNGs (0.25 mg ml^{-1} NG) were incubated with 3 x 10^5 $CD8^+$ T cells (9 days-activated) for 45 min at 37°C in serum-free advanced RPMI. Cells were washed with PBS (supplemented with 5% FBS). The amount of lipid-coated siNGs per cell was quantified by flow cytometry and visualized by confocal microscopy, as previously described. Flow

cytometry data were acquired by a CytoFLEX (Beckman Coulter) and analyzed using FlowJo software.

2.10 Quantifying siRNA release via fluorescence fluctuation spectroscopy

Fluorescence fluctuation spectroscopy (FFS) is a microscopy-based technique that monitors fluorescence intensity fluctuations in the excitation volume of a confocal microscope. Fluorescence fluctuations originate from the diffusion of fluorescent molecules in and out the excitation volume. To calculate the percentage free siRNA in the formulation, a fluorescence baseline of free siRNA molecules was recorded and compared with the baseline of the complexed siRNA. Upon encapsulation in NPs, the fluorescence baseline of the siRNA molecules will drop from which the loading efficiency can be calculated as described earlier. As was shown by our group, the complexation of siRNA molecules in NPs can be determined in different media including full human serum [26]. Within this study, the siRNA release from the non-coated versus lipid-coated siNGs was measured in the presence of competing polyanions such as dextran sulfate (DEXS; 10kDa; 2.5 mg ml^{-1}; Sigma-Aldrich) and human serum (obtained from a healthy donor and stored at -20°C). Equal volumes of serum or the competing polyanions in HEPES buffer were mixed with the siNGs and incubated for 10 min at room temperature before transferring to a glass-bottom 96 well-plate for FFS analysis (Greiner Bio-One GmbH, Frickenhausen, Germany). Measurements were performed with a Nikon C1si confocal laser scanning microscope (Nikon Benelux) equipped with a Plan Apo 60x 1.2 NA water immersion objective lens (Nikon), using a 488 nm argon-ion laser (CVI Melles Griot) This setup was combined with the detection channels of a fluorescence correlation spectrometer MicroTime 200 (Picoquant GmbH, Berlin, Germany) equipped with SymPhoTime software. Fluorescence fluctuations were recorded during 1 min.

2.11 Statistical analysis

A two-tailed Student's t-test was performed to determine statistical differences between datasets. All statistical analyses were performed using GraphPad Prism 6 software (La Jolla, CA, USA). p-values <0.05 were regarded significant. Statistical significance is indicated as follows: ** p <0.01; *** p < 0.001; **** p < 0.0001.

3 RESULTS

3.1 Nanoparticles for reversible attachment to cytotoxic T lymphocytes

Within this study liposomes were selected as model nanoparticles (NPs) to optimize reversible coupling to cytotoxic T lymphocytes (CTLs). Varying amounts of thiol-reactive phospholipids, carrying a pyridyldithiopropionate (PDP) head group, were incorporated in the liposome bilayer, next to DOPC lipids. The PDP moiety can form a reducible disulfide bond with the thiol groups exposed at the cell surface (exofacial thiols), allowing the reversible covalent coupling of the liposomes (**Figure 1A**) [27]. Importantly, PDP-functionalized lipids (PE-PDP lipids) contain a negative charge that may interact with cationic regions at the plasma membrane, thereby possibly causing nonspecific binding [28]. To account for these nonspecific interactions, the cellular attachment of control liposomes, in which the PDP-functionalized lipids were replaced by the negatively charged phosphatidylglycerol (PG) lipids, was evaluated in parallel. Both PDP and PG liposomes have a similar hydrodynamic diameter (~150 nm) and zeta potential, of which the latter depends on the liposomal composition. For instance, when 50 wt% PDP or PG lipids were incorporated, a mean zeta potential value around -65 mV was measured. Whenever other compositions were used, their respective zeta potential values are indicated in a table additional to the experimental data.

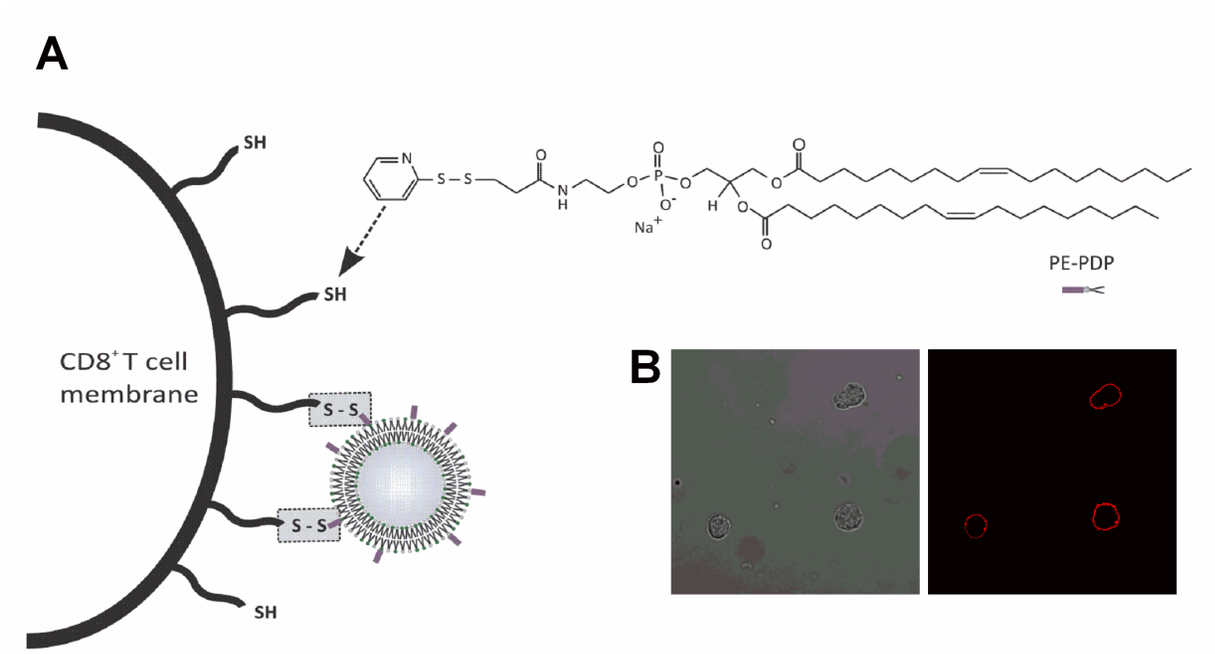

Figure 1. (A) Schematic representation of the formation of a disulfide bond between PDP-functionalized lipids that are incorporated into the liposome bilayer and reduced exofacial thiol groups, present at the cell surface. **(B)** Transmission and confocal fluorescence images of non-activated murine OT-I $CD8^+$ T cells incubated with Cy5-labeled maleimide.

3.2 Reversible coupling of liposomes to the surface of non-activated CD8$^+$ T cells

Murine OT-I CD8$^+$ T cells, which are genetically engineered to express a T cell receptor (TCR) against ovalbumine (OVA), were selected as carriers for the cell-mediated delivery of the liposomes. To allow the formation of a disulfide bond between free thiol groups at the CTL plasma membrane and PDP liposomes, we first assessed the availability of free thiol groups at the CD8$^+$ T cell surface by incubating them with Cy5-labeled maleimide [27]. The maleimide group can interact with thiol groups to form a stable thioether bond. Confocal images clearly demonstrated the presence of thiol groups that appeared to be uniformly distributed over the entire cell surface (**Figure 1B**).

3.2.1 Attachment of liposomes to the surface of non-activated CD8$^+$ T cells

Isolated CD8$^+$ T cells from the spleen of OT-I mice were incubated with fluorescently labeled (DiD) liposomes and the amount of liposomes coupled to the cell surface was quantified by flow cytometry. We first determined the fraction of PDP lipids that needs to be incorporated into the liposomal membrane to achieve efficient binding. To this end, the cells were incubated with liposomes containing increasing amounts of PDP lipids, ranging from 10 to 50 wt%. Cells were incubated with a 2 mg ml^{-1} lipid concentration as we determined that a higher concentration only results in a moderate increase in cellular attachment (**Figure 2A**). To quantify nonspecific interactions, the cellular binding of PG liposomes with PG lipid wt% also ranging from 10 to 50, was determined in parallel. It was verified that both PDP and PG liposomes have equivalent zeta potentials (**Figure 2B**). As displayed in **Figure 2C**, the nonspecific binding was independent of the liposomal composition. Strikingly, only liposomes composed of 50 wt% PDP-modified lipids showed specific binding to the T cells, accompanied by a more than three-fold difference in mean fluorescence intensity per cell between PG and PDP liposomes for this composition. Hence, further experiments were performed with liposomes carrying 50 wt% PDP-functionalized or PG lipids.

The presence of fluorescently labeled liposomes at the surface of the CD8$^+$ T cells was visualized by confocal microscopy. The images depicted in **Figure 2D** show localized bright fluorescent spots at the T cell surface, contrary to the free thiol staining with Cy5-labeled maleimide that showed a more uniform distribution (**Figure 1B**). Of note, from these images it is evident that the liposomes are indeed predominantly anchored to the surface of the cells and not internalized, confirming previous reports [12, 29].

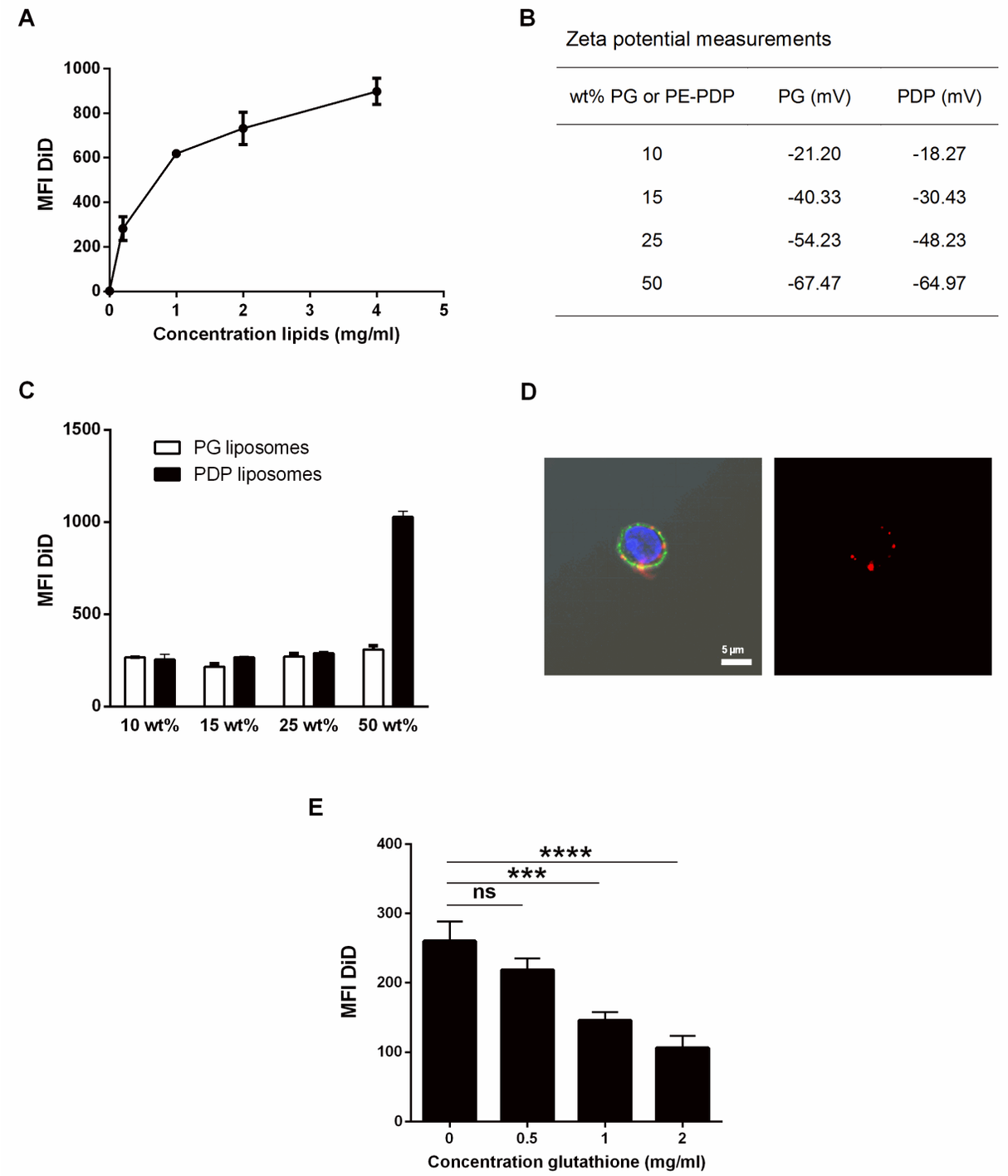

Figure 2. The reversible coupling of DiD fluorescently labeled liposomes to the surface of non-activated OT-I CD8⁺ T cells. (A) Binding of DiD-labeled liposomes with 50 wt% PDP lipids to non-activated CD8⁺ T cells as a function of total lipid concentrations. The liposomes were composed of 50 wt% PE-PDP, 3 wt% DiD and 47 wt% DOPC lipids. Data represent DiD mean fluorescence intensity (MFI) per cell ± SD (*n* = 2). **(B)** Zeta potential measurements of the different liposome compositions. **(C)** CD8⁺ T cells were incubated with PG and PDP liposomes with increasing wt% PG and PDP lipids as indicated in the graph. Data represent DiD mean fluorescence intensity (MFI) per cell ± SD (*n* = 2). **(D)** Confocal overlay image (left) and red channel (right) of T cells incubated with Alexa Fluor® 488-labeled anti-CD8 antibodies (green), Hoechst cell nucleus stain (blue), and DiD-labeled liposomes (red) (Scale bar = 5 µm). **(E)** Decrease in DiD MFI after incubation of the cells with increasing concentrations of glutathione. Data represent MFI ± SD (*n* = 3; ns = not significant; *** *p* <0.001; **** *p* <0.0001).

3.2.2 Triggered detachment of the liposomes from the cell surface of non-activated CD8$^+$ T cells.

Having established the optimal liposome composition, we next sought to evaluate whether the liposomes can be detached again from the cell surface. We anticipated that incubating the liposome-loaded T cells with reducing agents such as glutathione can cause a thiol-disulfide exchange reaction, resulting in the release of the disulfide-bound liposomes from the T cell surface [30]. To explore the latter, the liposome-loaded CD8$^+$ T cells were incubated with mounting concentrations of glutathione. As depicted in **Figure 2E**, an increase in the glutathione concentration was associated with a decrease in the amount of attached DiD-labeled PDP liposomes, indicative of their triggered release. Upon incubation with 2 mg ml^{-1} glutathione, a release of 60% of the attached particles was observed.

3.3 Reversible coupling of liposomes to the surface of activated CD8$^+$ T cells

Given that activated T cells outperform their non-activated counterparts in terms of tumor migratory capacity and cytolytic activity, we next aimed to assess the impact of T cell activation on the covalent coupling of liposomes. For this purpose, murine OT-I T cells were activated using anti-CD3/CD28 Dynabeads®. The activation status was evaluated by the expression of the IL-2 receptor CD25, which is upregulated after stimulation [31].

3.3.1 Attachment of liposomes to the surface of activated CD8$^+$ T cells

Similar to the attachment of liposomes to the surface of non-activated T cells, the coupling of liposomes to activated CD8$^+$ T cells was first quantified as a function of wt% incorporated PDP lipids. The zeta potential data from the different liposome compositions were represented in **Figure 3A**. In accordance with the results on non-activated CD8$^+$ T cells, we again observed a significant specific binding only for the liposomes with 50 wt% PE-PDP lipids incorporated (**Figure 3B**). Thus, also for the activated T cells this composition was selected for further investigation. To evaluate the maximal coupling, the cells were incubated with increasing liposome concentrations. A sharp increase in cell binding was observed from 0.1 to 1 mg ml^{-1} lipids while a further increase up to 10 mg ml^{-1} only resulted in a moderate improvement of the coupling (**Figure 3C**). In analogy with non-activated T cells, liposomes bound to activated T cells also remain localized at the cell surface in distinct foci, as verified with confocal microscopy (**Figure 3D**).

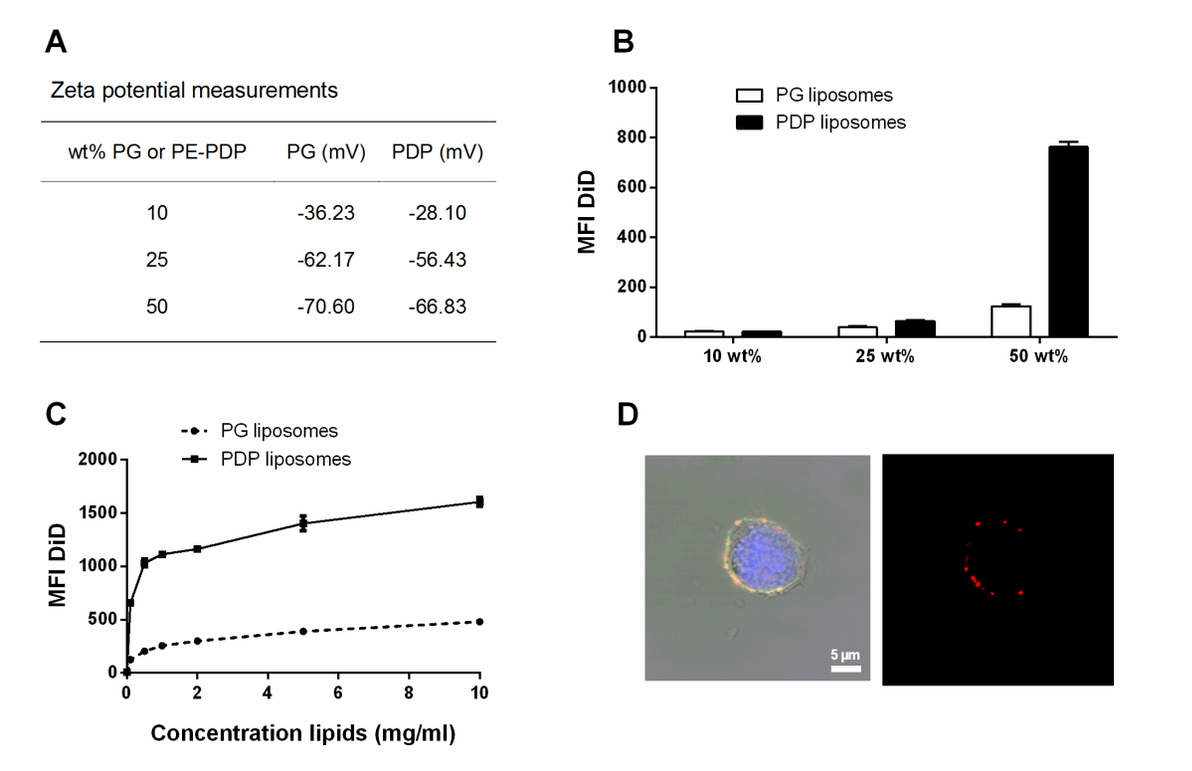

Figure 3. The coupling of DiD fluorescently labeled liposomes to the surface of activated OT-I CD8⁺ T cells, activated with anti-CD3/anti-CD28 Dynabeads® during 10 days. (A) Zeta potential measurements of the different liposomal compositions. **(B)** CD8⁺ T cells were incubated with 2 mg ml^{-1} PG and PDP liposomes with increasing amounts of PG and PDP lipids as indicated. Data represent the mean fluorescence intensity (MFI) of DiD per cell ± SD (*n* = 3). **(C)** Binding of DiD-labeled liposomes to CD8⁺ T cells as a function of lipid concentrations. Data represent DiD mean fluorescence intensity (MFI) per cell ± SD (*n* = 3). **(D)** Confocal images of T cells incubated with Alexa Fluor® 488-labeled anti-CD8 antibodies (green), Hoechst cell nucleus stain (blue), and DiD-labeled liposomes (red) (Scale bar = 5 µm).

3.3.2 Attachment of liposomes as a function of T cell activation status

During the activation process CD8⁺ T cells undergo a marked increase in size (**Figure 4**) and phenotypic changes such as upregulation of multiple surface markers like CD25, as represented in **Figure 5A**. To address whether these changes influence the attachment of particles to the cell surface, CD8⁺ T cells were activated with anti-CD3/CD28 Dynabeads® over a two-week time period and the specific coupling of liposomes was quantified at different activation time points (**Figure 5A**). In accordance with the manufacturer's protocol, the cells were restimulated with new Dynabeads® on day 7 of activation.

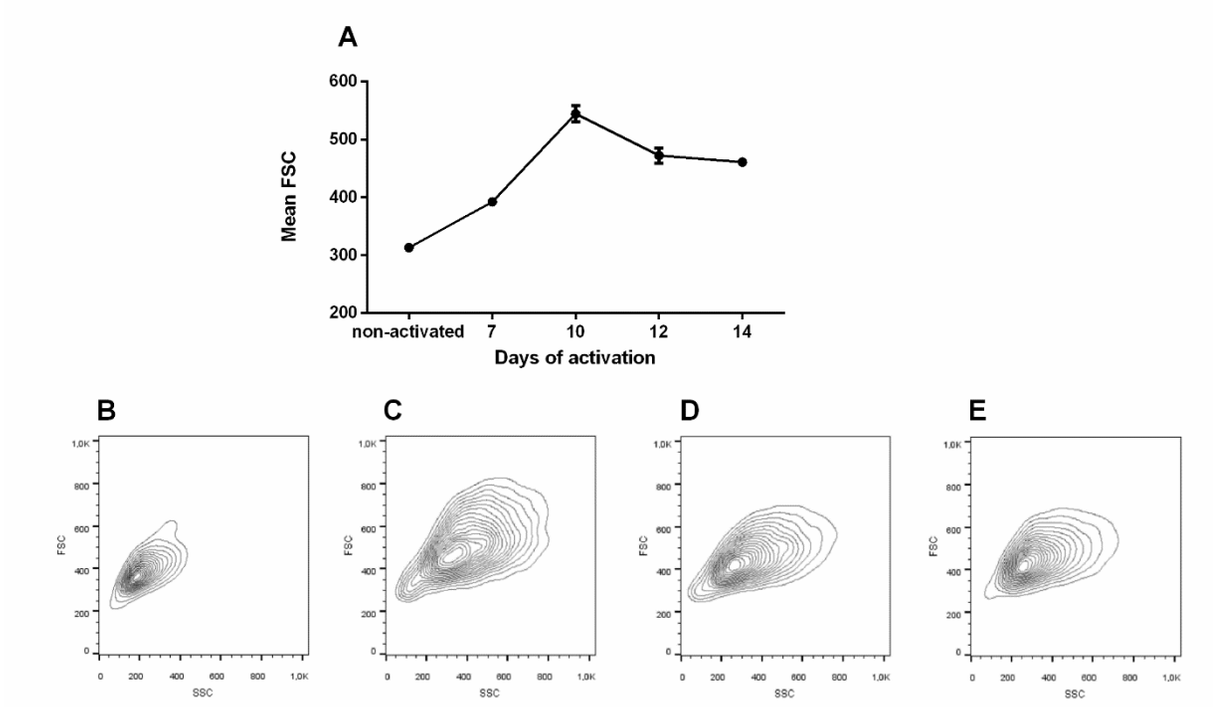

Figure 4. Size of CD8$^+$ T cells as a function of activation time. (A) Mean forward scatter (FSC) ± SD of activated CD8$^+$ T cells as a function of activation time (n = 1 for non-activated cells and n = 3 for activated cells). FSC and SSC plots of cells activated during **(B)** 7, **(C)** 10, **(D)** 12, and **(E)** 14 days. Data represent viable cells that were selected based on a SYTOX® green dead cell stain.

In general, a significantly higher attachment of PDP-functionalized liposomes to activated cells was observed compared to the non-activated T cells. In analogy with previous experiments, PG liposomes were incubated with the T cells as a control for nonspecific binding. Here, a similar trend in T cell binding was detected, albeit with markedly lower fluorescence intensity. Furthermore, the expression of the CD25 surface marker strongly increased from day 7 to day 10 following activation, indicative of an improved T cell activation efficiency upon a second activation step with anti-CD3/CD28 Dynabeads® on day 7. In contrast, when exceeding 10 days of activation again a gradual decrease in CD25 expression was observed. Importantly, the efficiency of liposome coupling to the T cells perfectly correlates with the CD25 expression levels, also reaching optimal specific liposome attachment to the T cell surface at day 10 of activation.

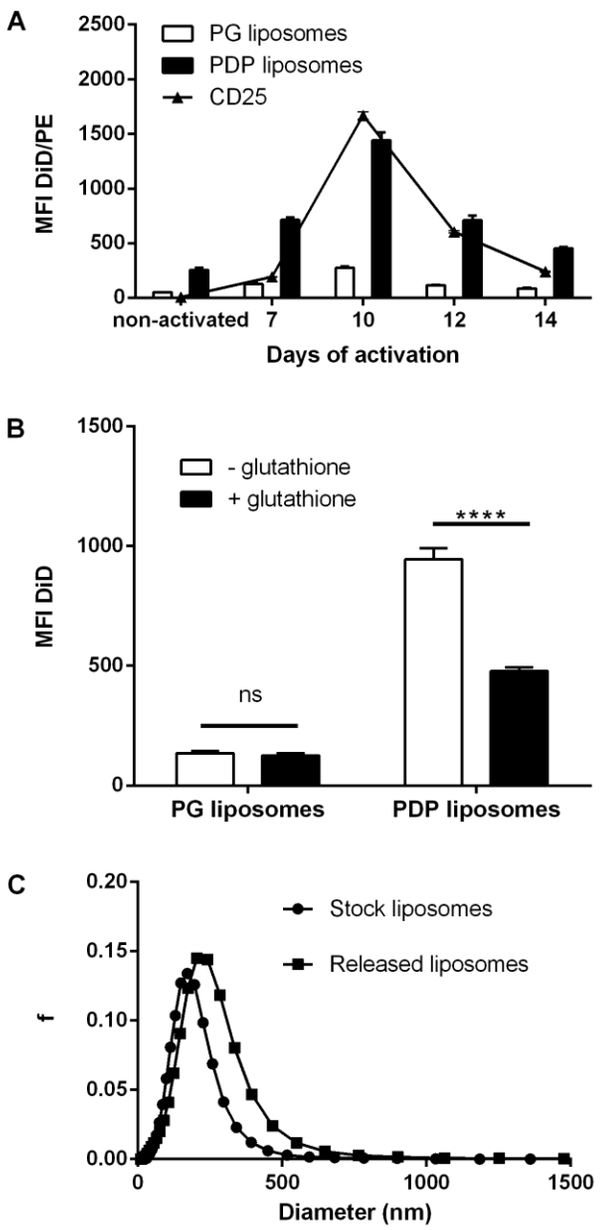

Figure 5. Reversible coupling of liposomes to the surface of OT-I CD8⁺ T cells as a function of their activation status. (A) Attachment of DiD-labeled PG or PDP liposomes (50 wt% PG/PDP – 2 mg ml^{-1}) to the surface of activated $CD8^+$ T cells after the indicated days of activation. CD25 expression was quantified as a marker for T cell activation. Data represent the mean fluorescence intensity (MFI) per cell ± SD from both DiD labeled liposomes (PG and PDP) and PE-labeled CD25 antibody staining (n = 4). **(B)** PG and PDP liposomes were attached to the surface of the cells, followed by an incubation step with or without 2 mg ml^{-1} glutathione. Data represent the DiD mean fluorescence intensity (MFI) per cell ± SD (n = 3; ns = not significant; **** p <0.0001). **(C)** Fluorescence single particle tracking (fSPT) size distribution of PDP liposomes both before T cell coupling and after triggered release from the T cell surface with glutathione.

3.3.3 Triggered detachment of liposomes from the cell surface of activated CD8⁺ T cells

To verify that the coupling of PDP liposomes to the surface of activated T cells was indeed reversible, the release of liposomes from the surface was evaluated by incubating the activated and liposome-loaded $CD8^+$ T cells with glutathione. In accordance with the

data obtained from non-activated T cells, the glutathione concentration was fixed at 2 mg ml^{-1}. Glutathione was able to release ~50% of the PDP liposomes from the $CD8^+$ T cells surface, while the DiD fluorescence per cell for the nonspecifically bound PG liposomes remained unaffected (**Figure 5B**). Confocal images of cells incubated with or without glutathione are represented in **Figure 6**.

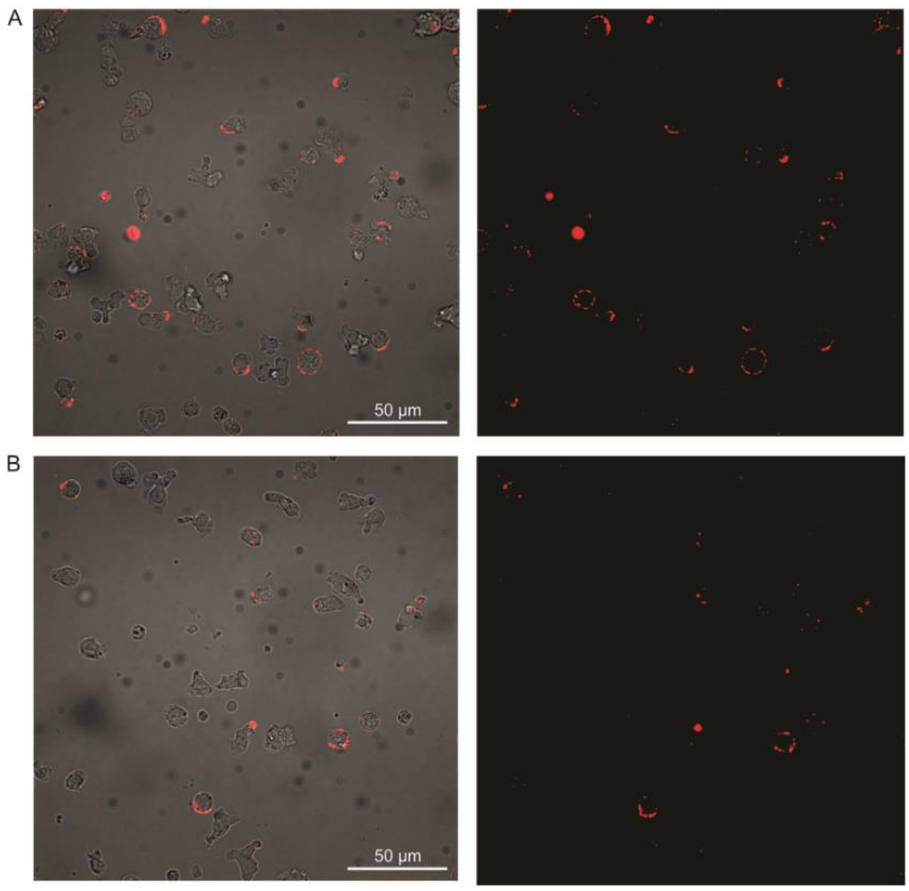

Figure 6. Confocal images of liposomes attached to $CD8^+$ T cells incubated with or without glutathione. Cells were first incubated with DiD-labeled liposomes, followed by the incubation of the cells with phosphate buffered saline (PBS) supplemented with 5% fetal bovine serum (FBS) **(A)**, and with 2 mg ml^{-1} glutathione in PBS supplemented with 5% FBS **(B)**. The left panel shows overlay images and the right panel DiD fluorescence (scale bar = 50 µm).

To determine whether the released liposomes still have the required size to allow subsequent internalization by target cells, we analyzed the size of the detached particles in the extracellular medium by fluorescence single particle tracking (fSPT). This technique is a microscopy-based method in which fluorescently labeled particles are illuminated by laser light and the Brownian motion of the particles is recorded by a fast and sensitive EMCCD camera. Based on the trajectories of single particles, calculated from the recorded movies by specialized algorithms, the diffusion coefficient and hence the hydrodynamic size of the moving particles can be determined, even in complex biological fluids [23]. A comparison was made between the liposomes prior to the T cell coupling and the liposomes collected after detachment from the T cell surface with glutathione. The average initial liposome size of 178 nm, as measured by fSPT, is comparable with a diameter of 150 nm obtained with

DLS. The liposomes that were released from the T cell surface in the presence of glutathione have a slightly increased average diameter (228 nm), which remains within an acceptable size range for subsequent endocytosis by tumor cells (**Figure 5C**).

3.4 Influence of cell surface-attached liposomes on T cell functionalities

3.4.1 *Proliferation of CD8$^+$ T cells after coupling of liposomes*

Proliferation is one of the key cellular functions of T cells upon activation. We therefore sought to evaluate whether the proliferative capacity of the cells could be compromised at the highest achievable liposome-conjugation in this study. The proliferation of T cells was determined by staining the activated T cells with CFSE and following the subsequent dilution of this stain over the daughter cells as a function of cell division. To this end, the cells were first incubated with a high concentration of 50 wt% PDP liposomes (20 mg ml^{-1} lipid concentration) for which a maximal coupling is expected (**Figure 3**). For the untreated T cells, a clear decrease in CFSE fluorescence intensity could be observed over time, reflecting CFSE dilution by T cell division. Importantly, T cells carrying a maximal amount of PDP liposomes on their surface also maintained a normal proliferative behavior (**Figure 7A**). Furthermore, the cell surface-attached liposomes were equally distributed over the daughter cells during cell division as was demonstrated by the simultaneous dilution of the DiD fluorescent signal per cell, albeit with all cells still positive for DiD after 48h (**Figure 7B**).

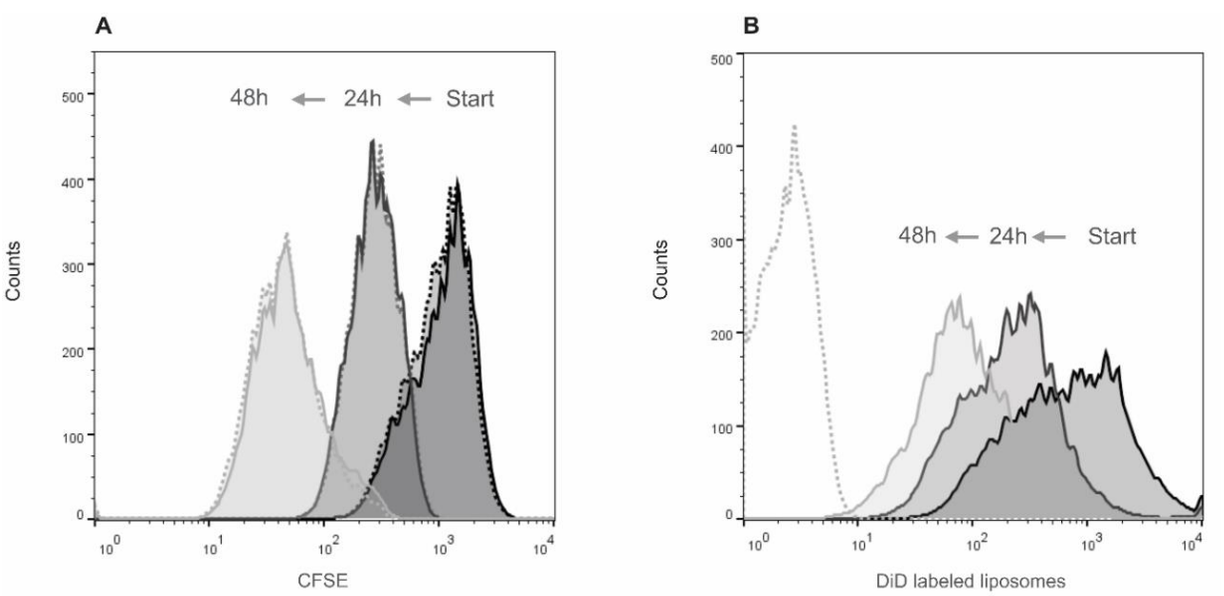

Figure 7. Proliferation of OT-I CD8$^+$ T cells after liposome coupling to the cell surface. CD8$^+$ T cells were first labeled with CFSE and incubated with a high concentration of 50 wt% PDP liposomes labeled with DiD (20 mg ml-1 lipids), followed by the incubation over 24h and 48h within cell culture medium supplemented with 30 U ml-1 rIL-2. **(A)** Flow cytometry histograms representing the CFSE fluorescence intensity and **(B)** liposomal DiD fluorescence intensity per T cell for both liposome-loaded (solid line) and non-loaded cells (dotted line) at the start of incubation (black line), after 24h (dark gray line), and after 48h (light gray line).

3.4.2 *Cytotoxic T cell effector function after coupling of liposomes*

CTLs are designed to specifically kill target tumor cells. To evaluate whether the anchoring of liposomes to the surface of $CD8^+$ T lymphocytes affects their cytotoxic function, OT-I T lymphocytes were used that have a TCR recognizing an ovalbumine (OVA)-derived peptide. Co-culturing of OT-I T cells with E.G7-OVA lymphoma cells that present this OVA-peptide in major histocompatibility complex class I (MHC I), would result in TCR-mediated killing of the E.G7-OVA cells. Isogenic yet OVA negative EL4 cells were included in the co-culture experiment as a control for the specificity of this interaction. To discriminate both cell types, EL4 and E.G7-OVA cells were stained with a low and high concentration of CFSE, respectively (**Figure 8**). The CFSE-labeled EL4 and E.G7-OVA cells were mixed in equal amounts followed by the addition of the OT-I T cells in an effector:target (E:T) ratio of 1:1 and 1:20 as indicated in the **Figures 9A-C**.

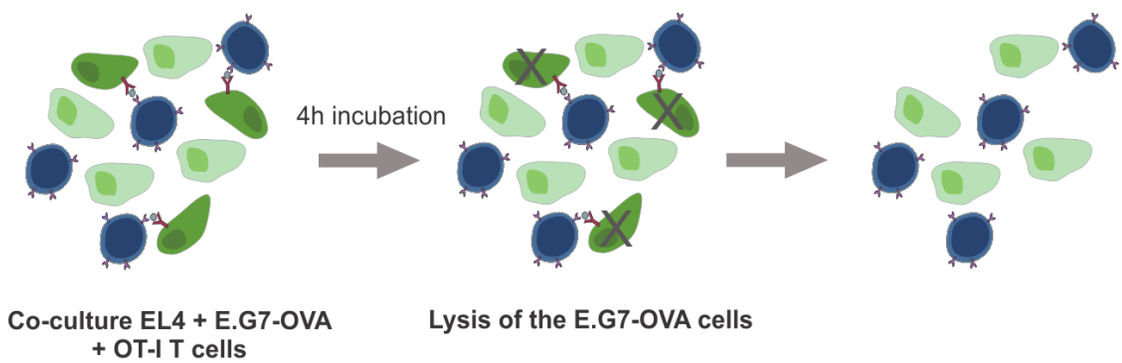

	EL4 cells	Low CFSE label
	E.G7-OVA cells	High CFSE label
		Ovalbumine presentation by MHC-I
	OT-I $CD8^+$ T cell	No CFSE
		Ovalbumine T cell receptor

Figure 8. Schematic overview of co-culturing OT-I $CD8^+$ T cells with E.G7-OVA target cells and EL4 control cells. E.G7-OVA and EL4 cells were labeled with a high and low CFSE concentration, respectively. Both cell types were mixed in equal amounts and incubated for 4h at 37 °C with OT-I $CD8^+$ T cells.

At a 1:1 effector:target ratio the OT-I T cells were able to lyse the majority of the E.G7-OVA population in contrast to the EL4 cells that remained unaffected, reflecting the specificity of the CTL effector function assay. Notably, **Figure 9B** clearly demonstrates that the covalent attachment of liposomes to the T cell surface does not interfere with their cytotoxic function as both liposome-loaded and non-loaded T cells killed 72% of the E.G7-OVA population. To exclude the possibility that this E:T ratio was too high and could therefore obscure the inhibitory effect of the conjugated liposomes, the co-culture experiment was repeated at a suboptimal E:T ratio of 1:20. Although the killing effect of

the E.G7-OVA cells obtained at the 1:20 ratio is strongly reduced with only 6% lysis compared to 72% for the 1:1 ratio, again the attachment of liposomes to the T cell surface did not affect target cell lysis (**Figure 9C**). Quantitative data of this CTL assay are represented in **Figures 9D-E**.

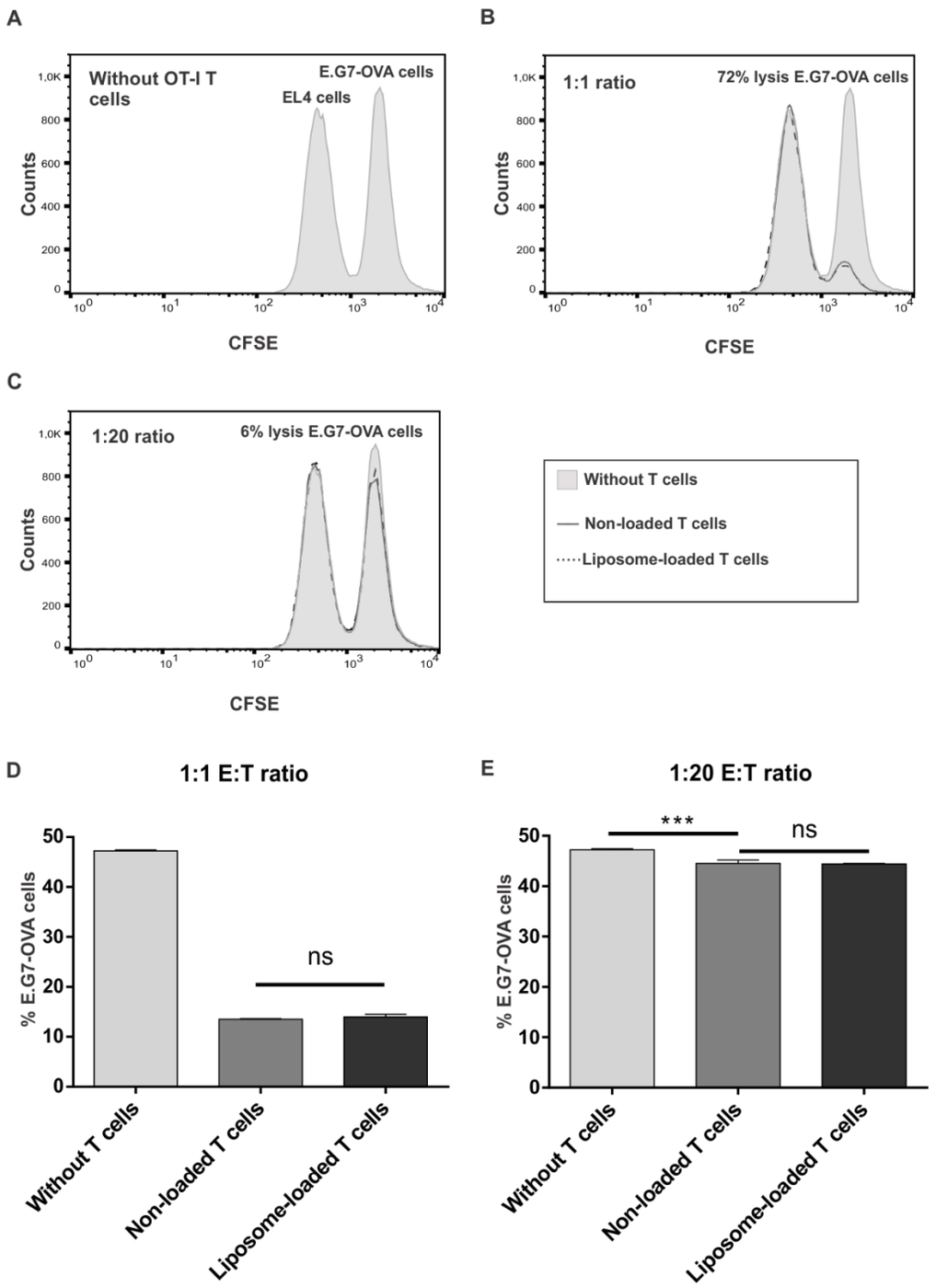

Figure 9. Co-culture of (liposome-loaded) OT-I CD8$^+$ T cells with E.G7-OVA target cells and EL4 control cells. **(A)** Histograms representing a co-culture of EL4 and E.G7-OVA cells without T cells (gray fill), with non-loaded T cells (dotted line), and with liposome-loaded (5 mg ml^{-1} lipids) T cells (solid line). Cells were mixed in both a **(B)** 1:1 effector:target (E:T) ratio and a **(C)** 1:20 E:T ratio. **(D)** Graphs representing the percentage of viable E.G7-OVA cells after the incubation without OT-I T cells, with non-loaded T cells, and with liposome-loaded T cells (5 mg ml^{-1} lipids) in a 1:1 and **(E)** 1:20 effector:target (E:T) ratio. The % E.G7-OVA cells ± SD represented here is the E.G7-OVA cell fraction of the total population of EL4 and E.G7-OVA cells (n = 3, ns = not significant, *** p <0.001).

3.5 Coupling of siRNA-loaded NPs to cytotoxic T cells

Next, a drug-loaded nanoparticle was developed for anchoring to the surface of $CD8^+$ T cells, exploiting our previously optimized coupling protocol. As a therapeutic agent we selected small interfering RNA (siRNA), which needs to be delivered into the cytosol of target cells to activate gene silencing. However, as the PDP liposomes are negatively charged they do not allow loading of siRNA based on electrostatic interaction. To this end, our research group recently developed a hybrid core-shell formulation, in which siRNA is pre-loaded in a biodegradable cationic nanogel (NG) core that is subsequently coated with a negatively charged lipid shell [25]. Here, we modified this nanocomposite formulation using PDP liposomes to construct the outer lipid shell and to enable subsequent coupling of the siRNA-loaded nanogels (siNGs) to the CTL surface.

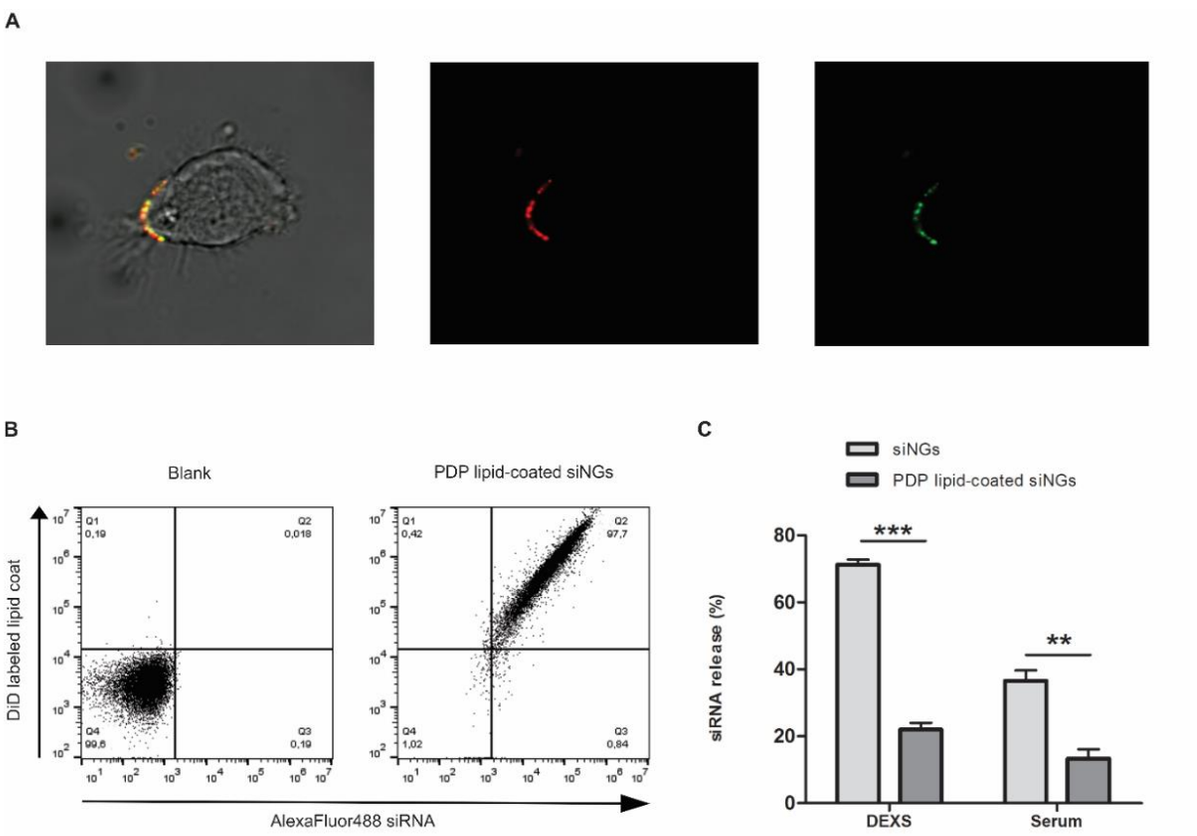

Figure 10. The coupling of siRNA-loaded nanoparticles (NPs) to the surface of cytotoxic T cells. Nanogels (NGs) were first loaded with 5 pmol of Alexa Fluor® 488-labeled siRNA per µg NG (siNGs), followed by coating with a lipid layer composed of 50 wt% PE-PDP, 3 wt% DiD and 47 wt% DOPC. Following purification, the lipid-coated siNGs were incubated with activated $CD8^+$ T cells. **(A)** Confocal images of lipid-coated siNGs coupled to $CD8^+$ T cells via a disulfide binding. siRNA molecules were labeled with Alexa Fluor® 488 (green) and the lipid coat was labeled with DiD (red). **(B)** Flow cytometry plots representing $CD8^+$ T cells incubated with or without lipid-coated siNGs. **(C)** Influence of the lipid coat on the siRNA release in the presence of competing polyanions such as 2.5 mg ml^{-1} dextran sulfate (DEXS) and human serum measured by fluorescence fluctuation spectroscopy. Data represent mean % siRNA release ± SD (n = 3; ** p <0.01; *** p <0.001).

Following incubation of this core-shell formulation with activated CTLs, we could demonstrate their coupling to the CTL cell surface. In **Figure 10A**, confocal images show the coupling of double-labeled PDP lipid-coated siNGs to $CD8^+$ T cells, in which the green-labeled siRNA (Alexa Fluor® 488) perfectly co-localizes with the red-labeled (DiD) lipid coat. In addition, flow cytometry plots indicated that all T cells were loaded with the lipid-coated siNGs as the fluorescent signals of both labeled siRNA and lipids are closely correlated (**Figure 10B**). During the coating procedure of the siNGs with the highly anionic PDP liposomes a small fraction (~10%) of siRNA was released from the NG core. Importantly, **Figure 10C** shows that the lipid coat offers ample protection against siRNA decomplexation in the presence of high concentrations of competing polyanions and in human serum, as was measured through fluorescence fluctuation spectroscopy. This indicates the successful deposition of a protective lipid shell around the siNG core.

3.6 Attachment of liposomes to the surface of splenocytes

To broaden the use of this cell-mediated drug delivery approach, we evaluated the coupling of liposomes to other immune cell types. To this end, a splenocyte population, containing distinct types of immune cells, especially T cells ($CD4^+$ and $CD8^+$ T cells) and B cells, was incubated with the PDP-functionalized liposomes, followed by a staining with CD3 and CD19 antibodies, which distinguish T cells from B cells (**Figure 11**, left panel). **Figures 11B and C** clearly demonstrate the higher attachment of liposomes to the surface of $CD19^+$ B cells compared to the T cell population. $CD4^+$ and $CD8^+$ T cells were distinguished by a CD3 and CD8 antibody stain (**Figure 11**, right panel). The attachment of PDP liposomes was not significantly different between both T cell subtypes, while the coupling was substantially higher for the CD3/CD8-negative population, likely representing B cells (**Figures 11E-F**). Confocal images revealed that CD8-negative cells have the capacity to internalize the PDP liposomes, likely explaining the large difference in liposomal loading between B and T lymphocytes (**Figure 12**).

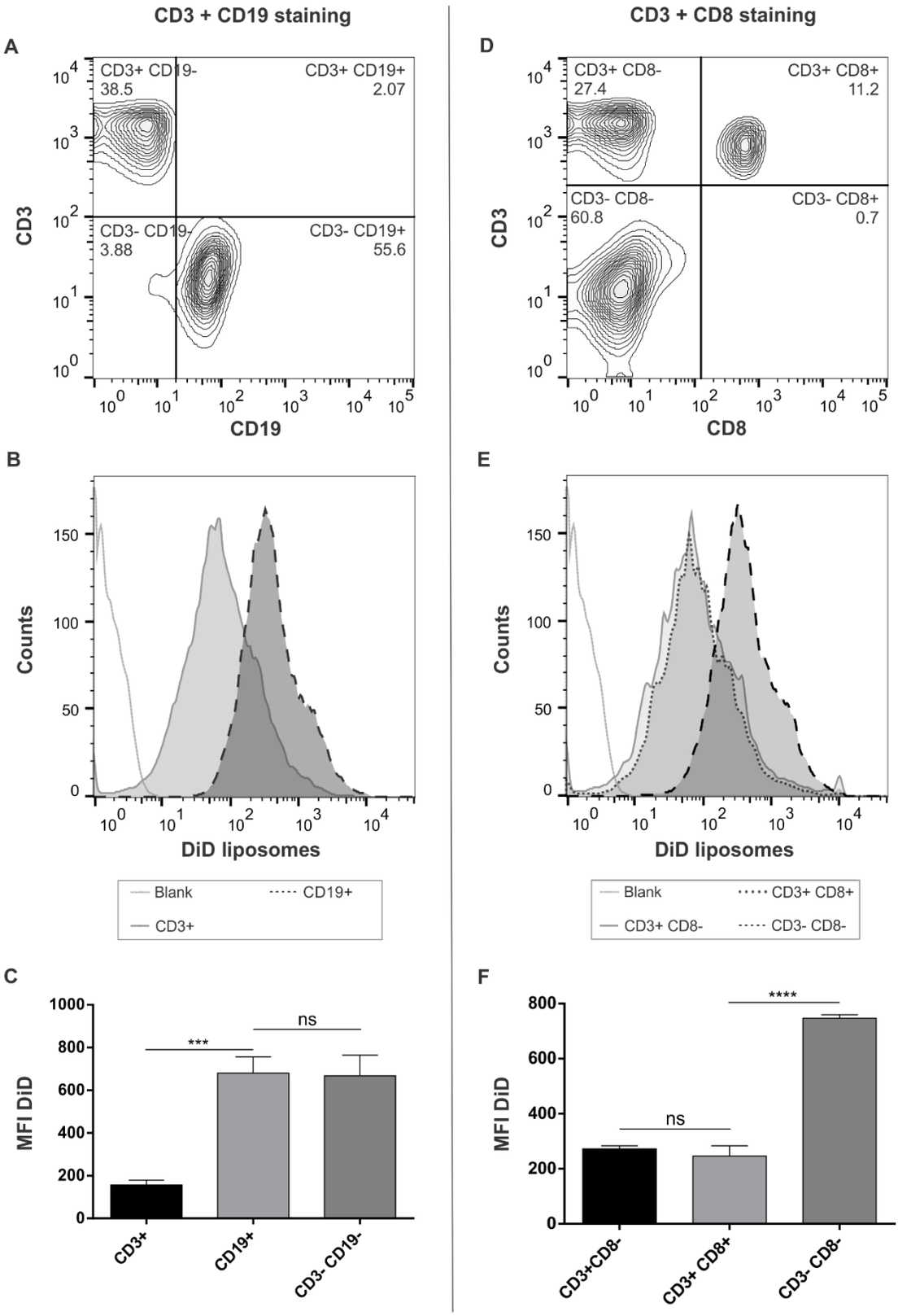

Figure 11. Attachment of PDP-functionalized liposomes to splenocytes. Mouse splenocytes were incubated with DiD-labeled PDP-functionalized liposomes, followed by staining with CD3 either in combination with CD19 or CD8. **(A)** Splenocytes were stained with both CD3 and CD19 antibodies. **(B)** Histograms representing the coupling of DiD labeled liposomes to the surface of $CD3^+$ versus $CD19^+$ cells. **(C)** Graphs showing the DiD mean fluorescence intensity (MFI) per cell ± SD (n = 2). **(D)** Splenocytes were stained with CD3 and CD8 antibodies. **(E)** Histograms representing the coupling of DiD labeled liposomes to $CD3^+$, $CD8^+$ and CD3/CD8-negative splenocytes. **(F)** Graphs showing the DiD mean fluorescence intensity ± SD (n = 2). Statistical significance is indicated as: ns = not significant, *** p <0.001, **** p <0.0001.

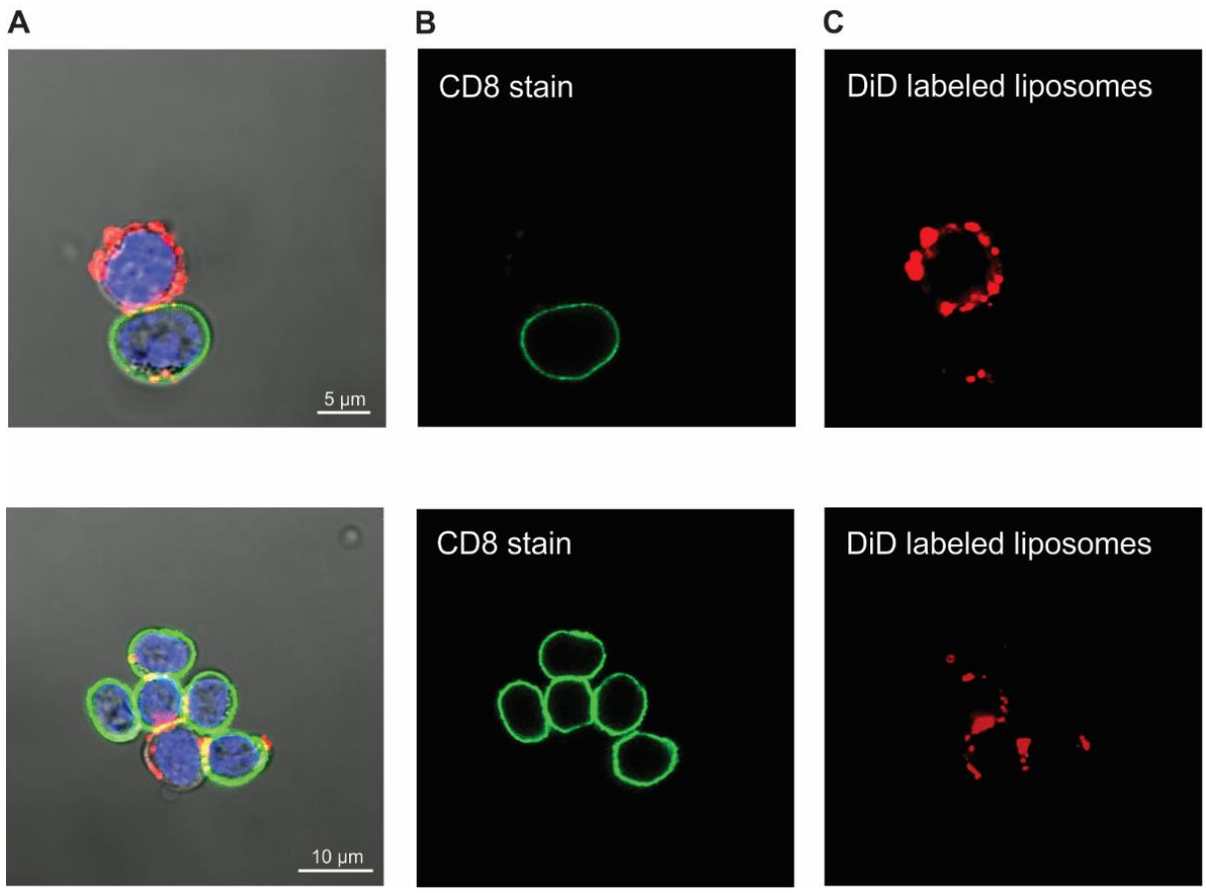

Figure 12. Confocal images of CD8$^+$ T cells contaminated with other types of splenocytes that were incubated with DiD-labeled PDP liposomes. (A) Confocal overlay images of T cells incubated with Hoechst cell nucleus stain (blue), **(B)** Alexa Fluor® 488-labeled anti-CD8 antibodies (green), and **(C)** DiD-labeled liposomes (red) (Scale bar = 5 µm and 10 µm).

4 DISCUSSION

The primary goal of this study was to investigate whether liposomes can be reversibly attached to the surface of cytotoxic T lymphocytes (CTLs). To this end, we exploited the presence of thiol groups naturally present on the surface of cells (exofacial thiols) to covalently couple liposomes that are equipped with thiol-reactive pyridyldithiopropionate (PDP) groups through the formation of a disulfide bond. Our results clearly demonstrate that the surface of the T cells can be conjugated with high amounts of liposomes. Although the exofacial thiol groups appear to be uniformly distributed over the plasma membrane, as evaluated with Cy5-maleimide, confocal microscopy imaging revealed a more speckled distribution profile for the liposomes which is in agreement with previous observations by Irvine and colleagues [29]. It is conceivable that only a fraction of the exposed thiols at the cell surface is accessible for thiol-reactive nanoparticles (NPs) in contrast to small molecules, which are less prone to steric hindrance. Another important observation is the need to incorporate a substantial fraction (50 wt%) of thiol-reactive lipids in the liposomal formulation to achieve a significant and specific cell surface binding, both for activated and non-activated T cells. We hypothesize that the presence of high amounts of thiol-reactive lipids could anchor a single liposome to the T cell surface via multiple disulfide bonds, thereby rendering the coupled liposomes more resistant to the various washing steps and disulfide cleavage possibly occurring at the cell surface by thioredoxins and oxidoreductases, initiating thiol-disulfide exchanges [32, 33]. Our study also revealed the importance of the activation status of the T cells toward liposomal coupling. We could demonstrate a five-fold increase in the attachment of liposomes for T cells activated during 10 days versus non-activated T cells. Further, it was also shown that the attachment of liposomes was strongly correlated with the CD25 receptor expression, as a marker of the T cell activation status. Likely, the enlargement of the cells upon activation is responsible for this higher coupling efficiency, given that the concomitant increase in accessible plasma membrane surface will expose more exofacial thiols per cell. Hence, dramatic differences in cell surface-conjugated liposomes could be observed at different activation time points. Besides the increase in size, also the upregulation of various surface proteins, bearing cysteine-rich extracellular domains, upon activation of the T cells could influence the liposome coupling efficiency. To attain a maximal drug load per T cell, it thus seems more appropriate to employ activated cells instead of naive T cells for the attachment of liposomes. Although it is recommended in adoptive T cell therapy (ACT) to use less-differentiated T cells, naive T cells still require *ex vivo* activation prior to systemic administration to be able to migrate to the tumor site. However, T cell proliferation upon activation results in the rapid division of the surface-conjugated liposomes over the daughter cells as shown in the proliferation assay. Considering the proliferation during the time needed for T cells to migrate and accumulate in the tumor (~24-72h) together with the lower surface liposome-loading, cell-mediated liposome delivery using naive T cells will

likely result in a lower accumulation of drug-loaded liposomes at the tumor site [8, 34]. Importantly, the T cells loaded with the maximum amount of liposomes retain their capacity to proliferate *in vitro* while dividing their liposome cargo over the daughter cells. Furthermore, even when a suboptimal effector-to-target ratio was tested, a similar cytotoxic effect against target tumor cells was observed between liposome-loaded and non-loaded T cells. As was observed by confocal imaging, the liposomes only occupy a limited amount of the cell membrane, likely not influencing the interaction with target cells.

Within this study, the reducing agent glutathione was selected as a tumor-specific trigger for subsequent liposome detachment from the T cell surface. Indeed, glutathione levels are low in the circulation and extracellular fluids while elevated levels can be found inside cells, thus avoiding premature liposome release [35]. On the other hand, the tumor microenvironment typically shows increased thiolytic activity, originating from the release of glutathione by dead cells and the overexpression of thiolytic proteins such as thioredoxin, enabling the uncoupling of disulfide-linked NPs in the direct vicinity of tumor cells [36]. In the presence of glutathione, 50-60% detachment was achieved in both activated and non-activated T cells. The inability to achieve complete release of the coupled liposomes is likely due to both nonspecific interactions and the requirement that multiple disulfide bonds need to be broken up simultaneously. As represented in **Figure 6**, the confocal images show that the partial detachment is not due to internalization of the particles, as it can be observed that the refractory particles are still located at the surface of the T cells. Also previous reports on the internalization of particles in T cells agree that the endocytic uptake of NPs in this cell type is rather exceptional. This observation is in contrast with B cells that tend to internalize nanoparticles and therefore are not suitable for the proposed reversible coupling strategy [37]. In addition, the exact role of B cells in the tumor microenvironment is still unclear, excluding their use in current cancer immunotherapy regimens. In contrast, both $CD4^+$ and $CD8^+$ T cells are of therapeutic interest. For the $CD4^+$ population, it has been demonstrated that they augment proliferation, survival and efficacy of cytolytic $CD8^+$ T cells and further also induce the $CD8^+$ T cell memory functions [20, 38, 39]. Especially the $CD4^+$ T helper type 1 (T_H1) subpopulation has been shown to inhibit tumor growth [40]. $CD4^+$ and $CD8^+$ T cells showed no difference in liposome coupling, which makes the $CD4^+$ T cells also suitable carriers for the reversible coupling of NPs. Similar to $CD8^+$, activation of $CD4^+$ T cells initiates their proliferation and differentiation into effector cells that are able to migrate to the tumor [19].

Importantly, we could show that the liposomes do not aggregate upon release from the cell surface as only a minor increase in the liposome diameter was observed compared to the original liposomes. The latter is of key importance for the envisioned subsequent internalization of the released particles in the target tumor cells.

In general, the use of cells as carriers was inspired by the observation that certain pathogens can evade the immune system by attaching themselves to the surface of red blood cells [41-43]. These observations paved the way for NP cell-mediated delivery, in which the carriers might prevent the clearance of the particles upon intravenous injection and enhance the accumulation of NPs in inaccessible regions [44-46]. Different coupling strategies have been assessed such as passive adsorption and ligand-receptor interactions, however, the covalent linkage of particles to reactive groups that are present at the cellular surface has proven most promising in terms of coupling stability [6, 47].

To our knowledge, this is the first study that demonstrates the reversible coupling of NPs to CTLs. This reversible strategy is of interest to improve the intratumoral delivery of both low molecular weight chemotherapeutic drugs but is of particular interest for membrane-impermeable macromolecular therapeutics, like small interfering RNA (siRNA). While the nanocarriers should prevent siRNA degradation in the systemic circulation and fast renal clearance, the T cell-mediated delivery might actively enhance its accumulation in the tumor site. Triggered detachment of the nanomedicines from the carrier cell surface should enable their subsequent internalization by target cells in the tumor and intracellular delivery of the therapeutic payload. In light of this concept, we developed a lipid-polymer nanocomposite that allows high siRNA loading in the polymer core and is coated with a PDP-modified lipid shell. The latter improves both NP stability and at the same time enables the functionalization of the NP surface with a PDP linker lipid to allow reducible binding to $CD8^+$ T cells. Genetic interference using siRNAs to target genes involved in cancer cell proliferation, survival, angiogenesis, and metastasis has been widely investigated [48, 49]. In the context of cancer immunotherapy, key regulators of the immunosuppressive pathways in immune cells of the tumor microenvironment can also be envisioned. Moreover, applying siRNA as a therapeutic agent to induce sequence-specific silencing of disease-related target genes can avoid off-target toxicity to healthy cells. The latter is also of particular importance to avoid side effects of the released drug onto the CTL carrier. Although the T-cell mediated NP delivery concept can be expanded to lipid-based NPs loaded with chemotherapeutics, within the latter approach it is imperative to also consider the possible toxic effects of the chemotherapeutic agent onto the carrier cells itself.

Although the injection of tumor-specific T cells as a therapy already showed impressive clinical outcomes, the limited number of patients that can be cured with this therapy is often related to the immunosuppressive role of the tumor microenvironment, the intra-tumor heterogeneity and loss of antigens to which the ACT was engineered [50, 51]. These factors jointly underscore the need to investigate combinatorial anti-cancer strategies leading to synergistic effects as was suggested here via the enhancement of the efficacy of the T cell therapy by the concurrent delivery of siRNA-loaded NPs, acting against ACT-refractory tumor cells and/or immunosuppressive cells. Future research will be focused on the *in vivo* evaluation of this novel concept in validated models of ACT.

5 CONCLUSION

A novel technique was developed to reversibly attach lipid-based NPs to the surface of CTLs. This study revealed the importance of both the lipid composition and the cell activation status on the loading efficiency of the $CD8^+$ T cells. Furthermore, it was shown that the presence of NPs on the cell surface does not affect the *in vitro* evaluated cellular functions such as proliferation and cytolytic activity. Cell-mediated delivery of NPs to tumor tissues is promising in terms of overcoming barriers that intravenously injected free NPs encounter on their way to the tumor tissue. Additionally, a reversible coupling strategy is of importance to allow subsequent internalization of the released NPs by tumor target cells, especially for the delivery of membrane-impermeable macromolecular therapeutics that require cytosolic delivery into tumor cells to be functional. To that end, we demonstrated the triggered release of disulfide-coupled liposomes from the T cell surface via glutathione, mimicking the thiolytic tumor microenvironment. Exploiting this optimized coupling strategy, we demonstrated the anchoring of siRNA-loaded lipid-coated nanogels to the surface of activated $CD8^+$ T cells, which can also be expanded to anti-tumor $CD4^+$ T cells.

ACKNOWLEDGEMENTS

Laura Wayteck is a doctoral fellow of the Institute for the Promotion of Innovation through Science and Technology in Flanders, Belgium (IWT-Vlaanderen). Koen Raemdonck, Heleen Dewitte, and Karine Breckpot are postdoctoral fellows of the Research Foundation-Flanders, Belgium (FWO-Vlaanderen). Lynn De Backer is a postdoctoral fellow of the Special Research Fund of Ghent University. FWO is acknowledged for their financial support (Krediet aan Navorsers). The authors would like to thank George Dakwar for kindly providing serum samples.

REFERENCES

1. Bertrand, N., Wu, J., Xu, X., Kamaly, N. & Farokhzad, O.C. Cancer nanotechnology: the impact of passive and active targeting in the era of modern cancer biology. *Adv Drug Deliv Rev* **66**, 2-25 (2014).
2. Peer, D. et al. Nanocarriers as an emerging platform for cancer therapy. *Nat Nanotechnol* **2**, 751-60 (2007).
3. Mitragotri, S. & Lahann, J. Materials for drug delivery: innovative solutions to address complex biological hurdles. *Adv Mater* **24**, 3717-23 (2012).
4. Kamaly, N., Xiao, Z., Valencia, P.M., Radovic-Moreno, A.F. & Farokhzad, O.C. Targeted polymeric therapeutic nanoparticles: design, development and clinical translation. *Chem Soc Rev* **41**, 2971-3010 (2012).
5. Sanna, V., Pala, N. & Sechi, M. Targeted therapy using nanotechnology: focus on cancer. *Int J Nanomedicine* **9**, 467-483 (2014).
6. Stephan, M.T. & Irvine, D.J. Enhancing Cell therapies from the Outside In: Cell Surface Engineering Using Synthetic Nanomaterials. *Nano Today* **6**, 309-325 (2011).
7. Roth, J.C., Curiel, D.T. & Pereboeva, L. Cell vehicle targeting strategies. *Gene Ther* **15**, 716-29 (2008).
8. Boissonnas, A., Fetler, L., Zeelenberg, I.S., Hugues, S. & Amigorena, S. In vivo imaging of cytotoxic T cell infiltration and elimination of a solid tumor. *J Exp Med* **204**, 345-56 (2007).
9. Rosenberg, S.A. et al. Durable complete responses in heavily pretreated patients with metastatic melanoma using T-cell transfer immunotherapy. *Clin Cancer Res* **17**, 4550-7 (2011).
10. Wayteck, L., Breckpot, K., Demeester, J., De Smedt, S.C. & Raemdonck, K. A personalized view on cancer immunotherapy. *Cancer Lett* **352**, 113-25 (2014).
11. Chen, D.S. & Mellman, I. Oncology meets immunology: the cancer-immunity cycle. *Immunity* **39**, 1-10 (2013).
12. Stephan, M.T., Moon, J.J., Um, S.H., Bershteyn, A. & Irvine, D.J. Therapeutic Cell Engineering Using Surface-Conjugated Synthetic Nanoparticles. *Journal of Immunotherapy* **16**, 1035-41 (2010).
13. Cole, C. et al. Tumor-targeted, systemic delivery of therapeutic viral vectors using hitchhiking on antigen-specific T cells. *Nat Med* **11**, 1073-81 (2005).
14. Huang, B. et al. Active targeting of chemotherapy to disseminated tumors using nanoparticle-carrying T cells. *Sci Transl Med* **7**, 291ra94 (2015).
15. Allen, T.M. & Cullis, P.R. Liposomal drug delivery systems: from concept to clinical applications. *Adv Drug Deliv Rev* **65**, 36-48 (2013).
16. Kunert, A. et al. TCR-Engineered T Cells Meet New Challenges to Treat Solid Tumors: Choice of Antigen, T Cell Fitness, and Sensitization of Tumor Milieu. *Front Immunol* **4**, 363 (2013).
17. Klebanoff, C.A., Gattinoni, L. & Restifo, N.P. Sorting through subsets: which T-cell populations mediate highly effective adoptive immunotherapy? *J Immunother* **35**, 651-60 (2012).
18. Snauwaert, S. et al. In vitro generation of mature, naive antigen-specific CD8(+) T cells with a single T-cell receptor by agonist selection. *Leukemia* **28**, 830-41 (2013).
19. Golubovskaya, V. & Wu, L. Different Subsets of T Cells, Memory, Effector Functions, and CAR-T Immunotherapy. *Cancers (Basel)* **8**, 36 (2016).

20. Sommermeyer, D. et al. Chimeric antigen receptor-modified T cells derived from defined CD8(+) and CD4(+) subsets confer superior antitumor reactivity in vivo. *Leukemia* **30**, 492-500 (2016).
21. Liadi, I. et al. Individual Motile CD4(+) T Cells Can Participate in Efficient Multikilling through Conjugation to Multiple Tumor Cells. *Cancer Immunol Res* **3**, 473-82 (2015).
22. Conde, J., Arnold, C.E., Tian, F.R. & Artzi, N. RNAi nanomaterials targeting immune cells as an anti-tumor therapy: the missing link in cancer treatment? *Materials Today* **19**, 29-43 (2016).
23. Braeckmans, K. et al. Sizing nanomatter in biological fluids by fluorescence single particle tracking. *Nano Lett* **10**, 4435-42 (2010).
24. Raemdonck, K. et al. Biodegradable Dextran Nanogels for RNA Interference: Focusing on Endosomal Escape and Intracellular siRNA Delivery. *Advanced Functional Materials* **19**, 1406-1415 (2009).
25. De Backer, L. et al. Bio-inspired pulmonary surfactant-modified nanogels: A promising siRNA delivery system. *J Control Release* **206**, 177-86 (2015).
26. Buyens, K. et al. A fast and sensitive method for measuring the integrity of siRNA-carrier complexes in full human serum. *J Control Release* **126**, 67-76 (2008).
27. Sahaf, B., Heydari, K., Herzenberg, L.A. & Herzenberg, L.A. Lymphocyte surface thiol levels. *Proc Natl Acad Sci U S A* **100**, 4001-5 (2003).
28. Verma, A. & Stellacci, F. Effect of surface properties on nanoparticle-cell interactions. *Small* **6**, 12-21 (2010).
29. Stephan, M.T., Stephan, S.B., Bak, P., Chen, J. & Irvine, D.J. Synapse-directed delivery of immunomodulators using T-cell-conjugated nanoparticles. *Biomaterials* **33**, 5776-87 (2012).
30. Gilbert, H.F. Molecular and cellular aspects of thiol-disulfide exchange. *Adv Enzymol Relat Areas Mol Biol* **63**, 69-172 (1990).
31. Shipkova, M. & Wieland, E. Surface markers of lymphocyte activation and markers of cell proliferation. *Clin Chim Acta* **413**, 1338-49 (2012).
32. Torres, A.G. & Gait, M.J. Exploiting cell surface thiols to enhance cellular uptake. *Trends Biotechnol* **30**, 185-90 (2012).
33. Hogg, P.J. Disulfide bonds as switches for protein function. *Trends Biochem Sci* **28**, 210-4 (2003).
34. Kennedy, L.C. et al. T cells enhance gold nanoparticle delivery to tumors in vivo. *Nanoscale Res Lett* **6**, 283 (2011).
35. Meng, F., Hennink, W.E. & Zhong, Z. Reduction-sensitive polymers and bioconjugates for biomedical applications. *Biomaterials* **30**, 2180-98 (2009).
36. Kaasgaard, T. & Andresen, T.L. Liposomal cancer therapy: exploiting tumor characteristics. *Expert Opin Drug Deliv* **7**, 225-43 (2010).
37. Balkwill, F.R., Capasso, M. & Hagemann, T. The tumor microenvironment at a glance. *J Cell Sci* **125**, 5591-6 (2012).
38. Moeller, M. et al. Sustained antigen-specific antitumor recall response mediated by gene-modified CD4+ T helper-1 and CD8+ T cells. *Cancer Res* **67**, 11428-37 (2007).
39. Shedlock, D.J. & Shen, H. Requirement for CD4 T cell help in generating functional CD8 T cell memory. *Science* **300**, 337-9 (2003).

40. Kayser, S. et al. Rapid generation of NY-ESO-1-specific CD4 T1 cells for adoptive T-cell therapy. *Oncoimmunology* **4**, e1002723 (2015).
41. Chambers, E. & Mitragotri, S. Long circulating nanoparticles via adhesion on red blood cells: mechanism and extended circulation. *Exp Biol Med (Maywood)* **232**, 958-66 (2007).
42. Hamidi, M., Zarrin, A., Foroozesh, M. & Mohammadi-Samani, S. Applications of carrier erythrocytes in delivery of biopharmaceuticals. *J Control Release* **118**, 145-60 (2007).
43. Rossi, L. et al. Erythrocyte-based drug delivery. *Expert Opin Drug Deliv* **2**, 311-22 (2005).
44. Doshi, N. et al. Cell-based drug delivery devices using phagocytosis-resistant backpacks. *Adv Mater* **23**, H105-9 (2011).
45. Choi, M.R. et al. Delivery of nanoparticles to brain metastases of breast cancer using a cellular Trojan horse. *Cancer Nanotechnol* **3**, 47-54 (2012).
46. Cheng, H. et al. Nanoparticulate cellular patches for cell-mediated tumoritropic delivery. *ACS Nano* **4**, 625-31 (2010).
47. Anselmo, A.C. & Mitragotri, S. Cell-mediated delivery of nanoparticles: Taking advantage of circulatory cells to target nanoparticles. *J Control Release* **190**, 531-41 (2014).
48. Miele, E. et al. Nanoparticle-based delivery of small interfering RNA: challenges for cancer therapy. *Int J Nanomedicine* **7**, 3637-57 (2012).
49. Tabernero, J. et al. First-in-humans trial of an RNA interference therapeutic targeting VEGF and KSP in cancer patients with liver involvement. *Cancer Discov* **3**, 406-17 (2013).
50. Motz, G.T. & Coukos, G. Deciphering and reversing tumor immune suppression. *Immunity* **39**, 61-73 (2013).
51. Jensen, S.M. et al. Increased frequency of suppressive regulatory T cells and T cell-mediated antigen loss results in murine melanoma recurrence. *J Immunol* **189**, 767-76 (2012).

3

In vivo evaluation of T cell-mediated delivery of liposome-encapsulated therapeutics to the tumor

This chapter contains unpublished data:

Wayteck Laura[a], Breckpot Karine[b], Dewitte Heleen[a,b], Renmans Dries[b], Verbeke Rein[a], De Smedt Stefaan[a], Raemdonck Koen[a]

[a]Laboratory of General Biochemistry and Physical Pharmacy, Faculty of Pharmaceutical Sciences, Ghent University, Ottergemsesteenweg 460, 9000 Ghent, Belgium

[b]Laboratory of Molecular and Cellular Therapy, Department of Biomedical Sciences, Vrije Universiteit Brussel, Laarbeeklaan 103/E, 1090 Brussels, Belgium

ABSTRACT

In **Chapter 2**, we have developed a novel technique to reversibly attach liposomes to the surface of cytotoxic T lymphocytes (CTLs) without interfering with their proliferation or cytolytic function, as evaluated by *in vitro* assays. However, the final aim is to exploit the CTL's capacity to migrate to and deliver their nanoparticle-load in the tumor tissue. Therefore, we investigated the influence of the liposome-load onto the tumor infiltration of CTLs in a melanoma mouse model. We extended the reversible coupling strategy with a stably attached liposomal formulation and compared both approaches *in vitro* and *in vivo*. Although CTLs loaded with liposomes showed a lower infiltration in the tumor 48h after transfer, this did not result in a negative impact on the tumor growth. On the contrary, a higher control over the tumor growth was observed for the liposome-loaded T cells. Subsequently, *in vitro* data revealed a substantially higher secretion of immunostimulatory cytokines when CTLs were loaded with liposomes, which might explain the enhanced anti-tumor effect. Because the success of adoptive T cell therapy is highly affected by the immunosuppressive tumor microenvironment, we aimed to additionally boost the immune system by concomitant delivery of immune adjuvants. Therefore, the immune adjuvant monophosphoryl lipid A (MPLA) was selected and incorporated into the T cell-anchored liposomes. *In vitro* co-culturing of dendritic cells (DCs) and CTLs loaded with MPLA liposomes demonstrated upregulation of CD40 and CD80 co-stimulatory molecules and higher secretion of the pro-inflammatory cytokine IL-12 by DCs, indicating successful maturation of DCs. Further *in vivo* evaluation by intratumoral injection of CTLs reversibly coupled with MPLA liposomes showed improved survival in the melanoma model.

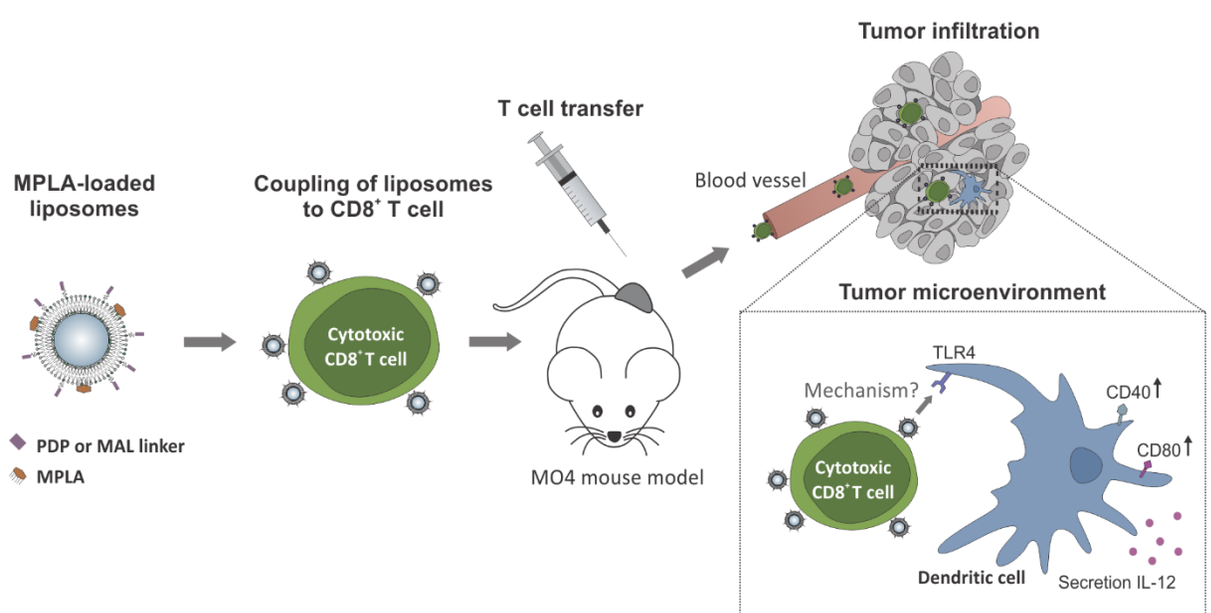

1 INTRODUCTION

As introduced in **Chapter 1**, cancer therapy struggles with finding an acceptable balance between potential therapeutic benefit and toxicity of the treatment. Formulating anti-cancer drugs into nanoparticles (nanomedicines) can improve their therapeutic index, enables a tunable drug release, and improves their biodistribution [1]. However, to take full advantage of these benefits, one of the most prominent hurdles remains *in vivo* targeting of the nanoparticles (NPs) to the site of action. Both passive tumor targeting based on the enhanced permeation and retention (EPR) phenomenon and active targeting by functionalizing the NPs with targeting ligands have been clinically investigated. However, the widespread use of these strategies is hampered by several factors such as heterogeneity in tumor vasculature between patients and tumor types [2].

In **Chapter 2**, we described cytotoxic T cell (CTL)-mediated delivery of NPs as an interesting alternative that might overcome these targeting limitations, by making use of the chemotaxis-driven tumor infiltration of T lymphocytes. We already demonstrated that the reversible coupling of NPs on the CTL surface did not affect the proliferation and cytolytic function of the activated $CD8^+$ T cells. In a next step, we sought to further investigate whether the decoration with NPs would affect the CTL's ability to migrate to the tumor. Migration of activated T cells, as introduced in **Chapter 1**, is a highly dynamic process that involves many consecutive steps, including tethering to the endothelium, rolling, firm adhesion, and finally extravasation into the tumor tissue [3, 4]. Within this chapter, we investigated the *in vivo* tumor migration of CTLs carrying both pyridyldithiopropionate (PDP)-functionalized liposomes (**Chapter 2**) as well as maleimide (MAL)-functionalized liposomes on their plasma membrane. Both liposomes interact with free thiol groups on the cell surface, forming a reducible disulfide-bond or a more stable thioether bond, respectively. Although reversible coupling is beneficial for triggered liposome release (*e.g.* for intratumoral delivery of siRNA), it is important to consider that premature release may occur due to reduction reactions in biological fluids, *e.g.* blood [5]. To account for this, a comparison was made *in vivo* between both coupling strategies.

Next to investigating the impact of liposome coupling on *in vivo* CTL migration, we also aimed to assess the therapeutic value of our approach. As introduced in **Chapter 1**, besides tumor cells also several types of immune cells have an immunosuppressive role in the tumor microenvironment [6]. To this end, liposomes can be loaded with siRNA designed to downregulate such immunosuppressive pathways or chemotherapeutics that specifically trigger immunogenic cell death (ICD), like the anthracycline doxorubicin [7, 8]. In contrast, in this chapter we focused on a different therapeutic approach based on the delivery of immunostimulatory compounds that further potentiate the immune system to eradicate the tumor. For example tumor-infiltrated dendritic cells (DCs) can be altered by the tumor microenvironment to induce T cell anergy and apoptosis, referred to as regulatory DCs [9].

Shifting the phenotypes of these cells from immunosuppressive towards immune-activating by Toll-like receptor (TLR) triggering via TLR-agonists, such as CpG and monophosphoryl lipid A (MPLA), has been shown to improve the therapeutic efficacy [10, 11]. A recent study by Van Lint *et al*. showed that upon intratumoral (IT) delivery of mRNA encoding a constitutively activated TLR4 together with the co-stimulatory molecule CD70 and CD40 ligand, tumor-infiltrated DCs can be reactivated to migrate to the tumor draining lymph nodes and stimulate CTLs [12]. Moreover, it has been shown that also T cells in the tumor microenvironment itself can be reactivated and that this approach also induced CTL responses against neo-epitopes, which shows the potential of the reactivated DCs to present a variety of antigens engulfed in the tumor tissue.

Considering that IT delivery is not suitable for all cancer types and that systemic delivery of adjuvants has been shown to induce severe side effects, we proposed here the targeted tumor delivery of the potent TLR4-agonist MPLA via T-cell mediated transport [11]. TLR4 is predominantly expressed on the surface of monocytes, mature macrophages and DCs [13]. Although other TLRs such as TLR9 (stimulated by CpGs) have been demonstrated to be very potent targets, we preferred to interact with TLR4 as this receptor is accessible at the cell surface, hence bypasses the need for adjuvant internalization, and enables us to compare the therapeutic effect of both stable and reversible coupling strategies. Recently, our group showed the encapsulation of MPLA in liposomes for the maturation of DCs (Verbeke *et al.*, manuscript submitted). Based on this knowledge, we encapsulated the MPLA molecules into our previously optimized liposome composition for coupling to CTLs.

By combining the adoptive T cell therapy with the tumor-targeted delivery of an immune-stimulating adjuvant, we envision a chain of events leading to a more potent anti-cancer immune response. First, we anticipate that adoptively transferred T cells migrate to the tumor and kill cancer cells expressing the antigens to which the therapy was targeted. Simultaneously, the CTLs deliver MPLA-loaded liposomes to the tumor. The interaction of MPLA with tumor-infiltrated DCs can convert these cells into immune-activators, through which also CTLs can be reactivated to induce potent immune responses. Subsequently, as killed tumor cells and their associated antigens can be internalized and cross-presented by tumor-infiltrated DCs, new specific tumor antigens can be presented to CTLs.

In this chapter, we first investigated the infiltration of liposome-loaded tumor-specific CTLs into MO4 tumors in mice and additionally evaluated the impact of liposome coupling on T cell activation in more detail. As the final aim is to achieve a synergistic effect of adoptive T cell therapy with drug-loaded nanoparticle delivery, we further investigated the incorporation of MPLA into our liposome formulation. A co-culture of DCs and CTLs was initiated to assess whether MPLA incorporated in liposomes and anchored to CTLs is still able to interact with the TLR4 of DCs. Finally, we investigated the *in vivo* therapeutic effect of this T cell-mediated delivery of MPLA-loaded liposomes in a MO4 tumor mouse model.

Upon IT delivery of liposome-loaded CTLs, preliminary data showed an improved survival for mice injected with MPLA-loaded liposomes anchored via a reducible bond to CTLs.

2 MATERIALS AND METHODS

2.1 CD8$^+$ and OT-I T cell culture

CD8$^+$ T cells were isolated from the spleen of C57BL/6 or OT-I mice using a negative isolation CD8$^+$ kit (stem cell technologies, Grenoble, France). Cells were activated with anti-CD3/CD28 Dynabeads® (Gibco-Invitrogen, Merelbeke, Belgium) at a density of 2 x 10^6 cells/well and a bead-to-cell ratio of 1:1 in a 24-well plate. The cells were cultured in complete T cell culture medium containing advanced RPMI medium (Gibco-Invitrogen, Merelbeke, Belgium) supplemented with 10% fetal bovine serum (FBS; Hyclone, Thermo Scientific, MA, USA), 2 mM L-glutamine (Gibco-Invitrogen), 1% penicillin/streptomycin (Gibco-Invitrogen). According to the manufacturer's protocol 30 U ml^{-1} rIL-2 (Miltenyi Biotec, Leiden, The Netherlands) was added to the culture medium and restimulation was performed by adding new beads every 7 days.

2.2 MO4 cell culture

The mouse melanoma cell line MO4 was kindly provided by K. Rock, University of Massachusetts Medical Center. The cells were cultured in RPMI 1640 medium (Sigma-Aldrich, Diegem, Belgium) supplemented with 5% FetalClone™ I (FCI; Hyclone™), 100 U ml^{-1} penicillin, 100 µg ml^{-1} streptomycin, 2 mM L-glutamine, 1 mM sodium pyruvate and non-essential amino acids (Sigma-Aldrich).

2.3 Dendritic cell culture

Primary murine bone marrow-derived DC (BM-DC) cultures were generated from C57BL/6 mice. To this end, mice were euthanized and bone marrow was flushed from the hind limbs. The collected bone marrow was cryopreserved in FetalClone™ I serum (FCI, Batch n°AXD36551) with 2% glucose (Sigma-Aldrich, Bornem, Belgium) and 10% DMSO (Sigma-Aldrich). To start a culture of BM-DCs, bone marrow of one mice leg was thawed and collected cells were seeded in a 100 mm Not TC-Treated polystyrene Culture Dish (Corning®, Amsterdam, The Netherlands). Cells were cultured in RPMI 1640 medium (Gibco-Invitrogen, Merelbeke, Belgium) supplemented with penicillin/streptomycin/L-glutamine (1%, Gibco-Invitrogen), β-mercaptoethanol (50 µM, Gibco-Invitrogen) and 5% FCI serum. Granulocyte-macrophage colony-stimulating factor (GM-CSF; 20 ng ml^{-1}, Peprotech, Rock Hill, NJ, USA) was used to promote differentiation of the monocytes into BM-DCs. On day 3 of the culture, an additional 15 ml culture medium containing GM-CSF (40 ng ml^{-1}) was added. After two more days, cells were collected by centrifugation (5 min at 300 g), resuspended in culture medium at 10^6 cells ml^{-1} and seeded in 24 well plates for experiments (5x10^5 cells per well).

2.4 Mice culture

CD45.2$^+$ C57BL/6 and OT-I mice for *in vivo* experiments were ordered from Charles River (L'arbresle, France) and CD45.1$^+$ C57BL/6 mice were obtained from Prof. J. Van Ginderachter (Vrije Universiteit Brussel, Belgium). C57BL/6 mice for *in vitro* experiments were purchased from Harlan (Gannat, France). All mice were housed in specific pathogen free (SPF) facilities according to the regulations of the Belgian law and the local Ethical Committee.

2.5 Liposome formulation and characterization

The liposomes were composed of 1,2-dioleoyl-sn-glycero-3-phosphocholine (DOPC), 18:1 1,2-dioleoyl-sn-glycero-3-phosphoethanolamine-N-[3-(2-pyridyldithio)propionate] (PE-PDP) or 18:1 1,2-dioleoyl-sn-glycero-3-phosphoethanolamine-N-[4-(p-maleimidophenyl)butyramide] (PE-MAL), and the fluorescent dyes 1,1'-dioctadecyl-3,3,3',3'-tetramethylindodicarbocyanine (DiD) or CholEsteryl 4,4-Difluoro-5,7-Dimethyl-4-Bora-3a,4a-Diaza-s-Indacene-3-Dodecanoate (cholesteryl BODIPY® FL C_{12}). DOPC, PE-PDP and PE-MAL lipids were purchased from Avanti Polar Lipids (Alabaster, USA). DiD and cholesteryl BODIPY® FL C_{12} were purchased from Molecular probes (Invitrogen™, Merelbeke, Belgium). The liposome composition comprised 50 wt% PE-PDP or PE-MAL, 3 wt% DiD or 1 wt% cholesteryl BODIPY® FL C_{12}, and 47 or 49 wt% DOPC, respectively. For liposome compositions containing the Toll-like receptor 4 (TLR4) agonist monophosphoryl lipid A (MPLA, Sigma-Aldrich), 0.6 or 3 wt% of the DOPC fraction was replaced by MPLA. To form all the liposomes, a lipid mixture in chloroform was prepared and pipetted in a round-bottom glass flask, followed by evaporation of the chloroform solvent to form a thin lipid film. The dried lipids were rehydrated in phosphate buffered saline (PBS; Gibco-Invitrogen) at ambient temperature followed by an extrusion of the resultant multilamellar liposomes through a 200 nm polycarbonate filter (Whatman, Diegem, Belgium) or the liposomes were sonicated for 2 times 25 s in a bath sonicator (Branson Ultrasonics, Dansbury, USA).

2.6 Coupling of liposomes to the T cell surface

CD8$^+$ T cells that were activated during 9-11 days, were separated from the activation beads and incubated in serum-free advanced RPMI with 5 mg ml^{-1} maleimide or PDP-functionalized liposomes during 45 min at 37°C. Subsequently, the cells were washed with T cell culture medium to remove the unbound liposomes. The amount of liposomes attached to the CD8$^+$ T cells was quantified via flow cytometry by measuring the DiD (red) or cholesteryl BODIPY® FL C_{12} (green) fluorescence intensity per cell using a FACSCalibur™ (BD Pharmingen, Erembodegem, Belgium) or a CytoFLEX (Beckman Coulter, Suarlée Belgium) and analyzed by FlowJo (Treestar Inc, Ashland, USA) software.

2.7 In vitro evaluation of proliferation and T cell viability after coupling of liposomes

$CD8^+$ T cells activated during 9 days, were first stained with 5 µM CFSE (Life Technologies, Merelbeke, Belgium) and subsequently conjugated with DiD-labeled liposomes as previously described. The proliferation of the T cells was then measured by the dilution of the CFSE stain over the daughter cells with flow cytometry 24h after loading. The distribution of the liposomes over the daughter cells was determined by measuring the DiD fluorescence intensity per cell. During the experiment, the activated cells (3×10^5/well) were incubated in cell culture medium supplemented with 30 U ml-1 rIL-2 in a U-bottom 96-well plate (Falcon, BD Biosciences, Erembodegem, Belgium). The viability of the cells was determined via either a WST-1 Cell Proliferation Assay (Cayman Chemical, MI, USA) or a CellTiter-Glo® luminescent Cell Viability Assay (Promega, Leiden, The Netherlands). For the WST-1 assay, the cells were resuspended in T cell culture medium supplemented with 30 U ml^{-1} rIL-2 and 25×10^4 cells/100 µl/well were transferred to a 96-well plate. After 24h of incubation, the cells were treated with 10 µl of the WST-1 mixture, according to the manufacturer's instructions. The cells were shaken for 1 min and incubated for 4h at 37°C. The absorbance for each sample was measured at 450 nm and 690 nm background via an EnVision® Multilabel plate reader (Perkin Elmer, Zaventem, Belgium). For the CellTiter-Glo® assay, T cells were resuspended in T cell culture medium supplemented with 30 U ml^{-1} rIL-2 and 5×10^4 cells/100 µl/well were transferred to an opaque 96-well plate. After 24h of incubation, the cells were treated with a CellTiter-Glo® reagent, according to the manufacturer's instructions. In brief, the cells were first incubated for 30 min at room temperature, followed by the addition of 100 µl of the CellTiter-Glo® reagent. After 10 min incubation, the luminescence signal was recorded by a GloMax™ 96 Luminometer (Promega).

2.8 Migration of OT-I T cells to the MO4 tumors

For the induction of subcutaneous tumors, CD45.1 mice were anesthetized by inhalation of isoflurane (Abbvie) and inoculated with 3×10^5 MO4 tumor cells, suspended in PBS, by subcutaneous injection in the lower back. 14 to 17 days after tumor inoculation, when tumors were present, the mice were randomly divided in different treatment groups. The mice were injected with 1 to 5×10^6 OT-I T cells via different delivery routes (intraperitoneally, intravenously, intratumorally), as indicated in the results section. OT-I T cells were activated during 9 to 11 days as described previously. Depending on the performed experiment, mice were intraperitoneally (IP) injected with cyclophosphamide (2 mg in 100 µl PBS, Endoxan, Baxter S.A., Lessines, Belgium), 1 or 2 days prior to OT-I T cell transfer.

24 to 72h after OT-I transfer, mice were euthanized and the tumors were harvested and collected in gentleMACS™ C tubes (Miltenyi Biotec) in RPMI 1640 medium (Sigma-Aldrich). Single-cell suspensions of the tumor tissue were prepared using the GentleMACS Dissociater (Miltenyi Biotec), followed by incubating the tumor tissue with collagenase I (10 000 U ml^{-1}, Sigma-Aldrich, cat.no. C0130) and dispase II (32 mg ml^{-1}, Roche, Vilvoorde, Belgium) for 40 min at 37 °C while rotating on a MACSmix™ Tube Rotator (Miltenyi Biotec). Next, DNase I (5 mU ml^{-1}, Sigma-Aldrich) was added and an additional mechanical dissociation step was performed on the GentleMACS Dissociater. The digested tumor was filtered over a 70 µm nylon filter (Falcon, BD Biosciences, Erembodegem, Belgium) and a red blood cell lysis buffer was added. Spleens were also harvested, crushed through a 70 µm nylon filter, and treated with red blood cell lysis buffer. The tumor cell suspension and splenocytes were finally stained with CD3-PE-Cy7 (Biolegend, Antwerp, Belgium), CD8-PerCP-Cy5.5 (eBioscience, Vienna, Austria), and CD45.2-biotin (BD Biosciences) in combination with FITC-avidin (BD Biosciences). The amount of infiltrated OT-I T cells in the tumor was determined by flow cytometry using a LSR Fortessa flow cytometer (BD Biosciences) and analyzed by FACSDiva software (BD Biosciences) in combination with FlowJo software (Treestar Inc, Ashland, USA).

2.9 Migration of liposome-loaded OT-I cells to the MO4 tumor and spleen

C57BL/6 mice were inoculated with MO4 tumor cells as previously described. Two days before OT-I transfer, the mice were IP injected with cyclophosphamide. Prior to T cell transfer, the OT-I $CD8^+$ T cells were activated during 9 days and stained with 5 µM CFSE in PBS supplemented with 0.1% bovine serum albumin (BSA, Sigma-Aldrich) for 20 min at 37°C. Subsequently, liposomes were coupled to T cells as previously described and resuspended in PBS for IP injection. For these experiments, the mice received 1.5×10^6 OT-I T cells. Two days after OT-I transfer, the tumors were isolated and investigated for OT-I T cell infiltration as previously described. Additionally, tumor growth was measured before and after OT-I injection using a caliper. The tumor volume was determined by measuring the greatest longitudinal diameter (length) and the greatest transverse diameter (width), followed by the calculation of the tumor volume via the next formula: tumor volume = ½ (length x width²).

2.10 Dendritic cell co-culture

75×10^3 BM-DCs in 100 µl DC cell culture medium were transferred to a U-bottom 96-well plate (Falcon). Activated $CD8^+$ T cells that were loaded with BODIPY® FL-labeled PDP- and MAL-functionalized liposomes (with or without MPLA) as previously described were mixed at a T cell:DC ratio of 1:1 or 1:5 during 24 h at 37°C. As a positive control for maturation, the DCs were incubated with 1 µg ml^{-1} of E. *Coli*-derived lipopolysaccharide (LPS, Sigma-Aldrich) or MPLA in soluble form. After incubation, the cells were stained with

CD11c-APC, CD40-PE, and CD80-PE-Cy7 antibodies (all eBioscience) during 30 min at 4°C in FACS buffer (PBS supplemented with 5% BSA) for evaluation via flow cytometry using a CytoFLEX (Beckman Coulter, Suarlée Belgium) and FlowJo software.

For confocal imaging, BODIPY® FL-labeled liposomes were conjugated to the cell surface of $CD8^+$ T cells as previously described and co-cultured with DCs. The nucleus of the cells was stained with 10 µg ml^{-1} Hoechst 33342 (Molecular Probes). The dyes were respectively excited by a 488 nm argon-ion laser and a 408 nm diode laser (both purchased from CVI Melles Griot). Images were recorded with a Plan Apo VC 60x 1.4 NA oil immersion objective lens (Nikon).

2.11 In vivo therapeutic adoptive T cell transfer with MPLA-loaded liposomes

C57BL/6 female mice were inoculated with MO4 tumor cells as previously described. In a first experiment, 14 days after tumor inoculation, the mice were randomly divided in different treatment groups based on tumor volume and housed per condition in the same cage. The mice were intratumorally injected with 1.5 x 10^6 OT-I T cells (activated during 10 days) that were loaded with PDP- or MAL-functionalized liposomes with or without 0.6 wt% MPLA. Every two days, the tumor size was measured using a caliper (non-blinded). When the tumor volume exceeded 1500 mm^3, the mice were euthanized via cervical dislocation.

2.12 ELISA

Supernatants of $CD8^+$ T cells that were loaded with PDP and MAL liposomes and cultured *in vitro* were screened for the presence of IFNγ and TNFα. Supernatants of DCs that were co-cultured with T cells were screened for IL-12p70. Cytokine measurements were all performed via Ready-SET-Go!® ELISA assays (Affymetrix, eBioscience), according to the manufacturer's instructions.

2.13 Statistical analysis

A two-tailed Student's t-test was performed to determine statistical differences between datasets. All statistical analyses were performed using GraphPad Prism 6 software (La Jolla, CA, USA). p-values <0.05 were regarded significant. Statistical significance is indicated as follows: * $p < 0.05$; ** $p < 0.01$; *** $p < 0.001$; **** $p < 0.0001$. Survival was visualized in Kaplan-Meier plots.

3 RESULTS

3.1 In vivo migration of OT-I T cells to MO4 tumors

In **Chapter 2**, we showed the loading of $CD8^+$ T cells with liposomes without compromising their *in vitro* proliferation and cytolytic functions. Because the final aim is to use T cells as vehicles to deliver nanomedicines to the tumor, we next investigated whether liposome-loaded T cells are able to migrate to the tumor by using a mouse MO4 tumor model. MO4 melanoma cells, expressing ovalbumin, were injected subcutaneously in the lower back of the mice. Subsequently, they were injected intraperitoneally (IP) with $CD8^+$ T cells derived from the spleen of OT-I mice, which express a T cell receptor that specifically recognizes the ovalbumin-derived epitope SIINFEKL in the context of MHC class I. In a first set of experiments, we sought to optimize the protocol to test the tumor-infiltration of liposome-loaded T cells by flow cytometry analysis of the isolated tumor. This stepwise optimization process consists of evaluating (1) the time point of tumor isolation, (2) the number of injected OT-I T cells, and (3) the use of cyclophosphamide as a pretreatment for adoptive T cell transfer. **Figure 1A** represents a schematic overview of the generally used protocol.

Within this set of experiments, CD45.1 congenic C57BL/6 mice were used for tumor inoculation. These mice only express the CD45.1 receptor on their hematopoietic cells. After reaching visible tumors, the CD45.1 mice were IP injected with $CD45.2^+CD8^+$ OT-I T cells that were activated during 9-11 days *in vitro* with CD3/CD28 Dynabeads®. As the injected OT-I cells only express CD45.2, the tumor-infiltrated OT-I cells can be distinguished from the endogenous immune cells by a CD45.2 antibody staining. As shown in **Figure 1B**, the percentage of $CD3^+CD8^+CD45.2^+$ cells in the tumor population is the highest 48h after OT-I transfer, which was consequently selected as the time point for further evaluation. Moreover, also the infiltration into the spleen was assessed, which demonstrated virtually no infiltration (**Figure 1C**).

As in different studies mice were injected with varying amounts of tumor-specific T cells, ranging from $\sim 10^6$ to 10^8 cells, we verified whether the number of injected T cells has an impact on the amount of T cells that are able to infiltrate the tumor and on the tumor growth. For this purpose, we compared the injection of $1x10^6$ versus $5x10^6$ OT-I $CD8^+$ T cells, which resulted in no significant differences, neither in the percentage of infiltrated OT-I T cells (**Figure 1D**) nor in the relative tumor growth assessed 48h after transfer (**Figure 1E**). The benefits of a lymphodepleting strategy before adoptive transfer were already discussed in **Chapter 1**. Both total body irradiation and lymphoablative chemotherapy are used in the clinic [14]. We selected the lymphodepleting chemotherapeutic agent cyclophosphamide to IP inject in mice one day prior to OT-I transfer.

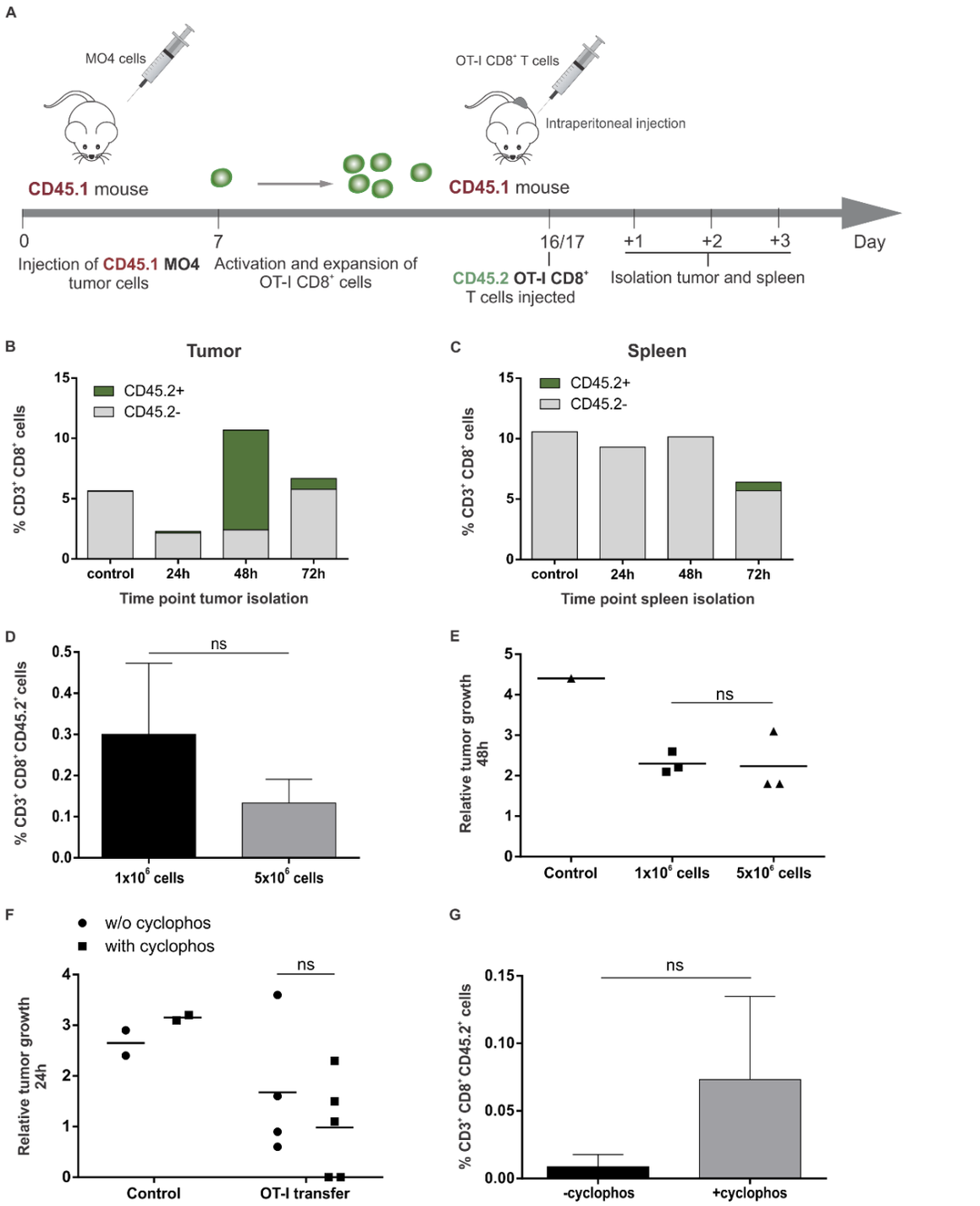

Figure 1. Migration of injected OT-I CD8⁺ T cells to MO4 tumors. (A) Schematic overview of the procedure to evaluate the migration of OT-I CD8⁺ transferred T cells to MO4 tumors. First, CD45.1⁺ C57BL/6 mice were subcutaneously injected with MO4 tumors in the lower back. During the growth of the tumor, OT-I CD8⁺ T cells were isolated from the spleen of OT-I CD45.2⁺ mice, followed by their activation and expansion *ex vivo*. On day 16, the mice were intraperitoneally injected with 1 or 5 x 10^6 CD45.2⁺ OT-I CD8⁺ T cells, followed by isolation of the tumor and spleen after 24, 48, and 72h. **(B)** Graph representing the percentage of CD45.2⁺ cells in the CD3⁺CD8⁺ population at different type points after OT-I transfer in the isolated tumor or **(C)** spleen (Control: *n* = 1, 24-48h: *n* = 3, 72h: *n* = 2). **(D)** The percentage of CD3⁺CD8⁺CD45.2⁺ cells in the total isolated tumor population ± SD for mice injected with 1 versus 5 x 10^6 CD45.2⁺CD8⁺OT-I T cells (*n* = 3). **(E)** Tumor growth 48h after transfer of 1 x 10^6 compared to 5 x 10^6 CD45.2⁺CD8⁺ OT-I T cells versus mice not treated with OT-I cells. **(F)** Mice were treated with 2 mg/mouse of cyclophosphamide (abbreviated as cyclophos) 24h prior to CD45.2⁺CD8⁺ OT-I transfer. The relative tumor growth was determined 24h after OT-I transfer. **(G)** The percentage of CD3⁺CD8⁺CD45.2⁺ cells in the tumor was determined 24h after OT-I transfer (-cyclophos: *n* = 4, +cyclophos: *n* = 3). Statistics are indicated as ns = not significant.

In agreement with earlier studies, the mice were treated with a dose of 2 mg/mouse of cyclophosphamide [15-17]. Remarkably, already 24h after OT-I transfer two mice with an initial tumor size of 40 and 80 mm^3 showed a complete regression of their tumor. However, the average relative tumor growth determined 24h after OT-I transfer showed no significant differences for cyclophosphamide treated and untreated mice (**Figure 1F**). Although at this early time point the percentage of $CD3^+CD8^+CD45.2^+$ cells in the tumor was very low, a trend to a higher amount of OT-I T cells that infiltrated the tumor after cyclophosphamide treatment was observed (**Figure 1G**). In summary, the optimized protocol was decided to include the IP injection of 2 mg of cyclophosphamide two days prior to IP transfer of 1 x 10^6 OT-I cells and followed by tumor isolation 48h after transfer.

3.2 In vivo migration of liposome-loaded OT-I $CD8^+$ T cells to MO4 tumors

Having optimized the protocol to evaluate the migration of OT-I T cells to MO4 tumors, we next sought to investigate whether liposome-loaded T cells are still able to infiltrate the tumor and induce a tumor killing effect. To this end, the cells were first loaded with PDP- or MAL-functionalized liposomes followed by IP injection. Here, the $CD8^+$ OT-I T cells were stained with CFSE prior to transfer to detect infiltrated cells. As depicted in **Figure 2A**, cells loaded with either PDP- or MAL-functionalized liposomes showed lower infiltration in the tumor when analyzed 48h after transfer. Surprisingly, compared to the unloaded T cells, the liposome loaded T cells showed an enhanced therapeutic effect with stabilization or even regression of the tumor, which was most pronounced for the MAL-loaded T cells (**Figure 2B**). In addition, although the liposomes were fluorescently labeled with DiD, no significant differences in DiD label between liposome-loaded cells and non-loaded cells could be observed 48 h after transfer (**Figure 2C**).

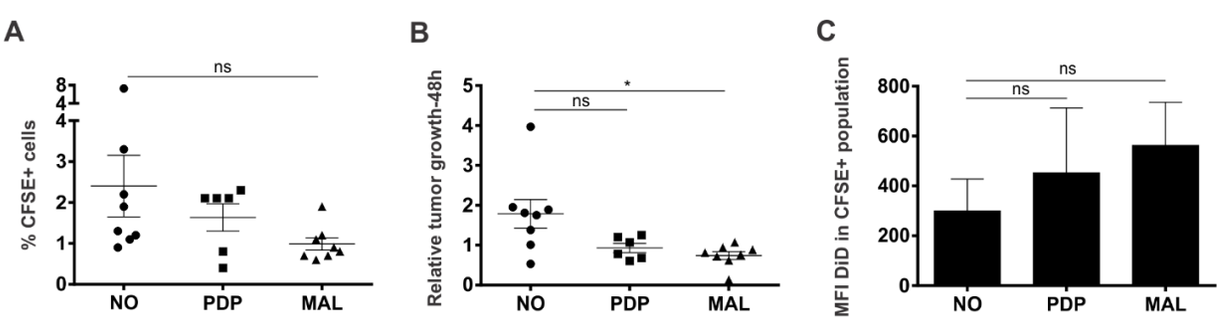

Figure 2. Migration of PDP and MAL liposome-loaded OT-I T cells to MO4 tumors. Mice were subcutaneously inoculated with MO4 tumor cells in the lower back, followed by the intraperitoneal (IP) injection of 2 mg/mouse cyclophosphamide. Two days later the mice were IP injected with 1.5 x 10^6 CFSE-stained $CD8^+$ OT-I T cells. The infiltration of OT-I T cells was compared between cells without liposome-load (NO) and PDP/MAL liposome-loaded OT-I T cells. **(A)** Two days after OT-I transfer, the mice were sacrificed and their tumors were isolated. The percentage of CFSE-positive cells in the tumor tissue was quantified by flow cytometry. **(B)** The relative tumor growth 48h after OT-I transfer was compared between mice injected with OT-I T cells without liposome-load and PDP/MAL liposome-loaded OT-I T cells. **(C)** The mean fluorescence intensity per cell (MFI) ± SD of the DiD-labeled liposomes was quantified by flow cytometry (NO and MAL: n = 8, PDP: n = 6). Statistics are indicated as ns = not significant, * p <0.05.

3.3 Influence of liposome coupling on the in vitro T cell viability, proliferation and cytokine secretion

In an attempt to elucidate the rather remarkable observation that liposome-loaded T cells elicited improved acute anti-tumor responses compared to non-loaded OT-I T cells, *in vitro* assays were initiated investigating the impact of the liposome-load on the T cells. First, we evaluated T cell viability as a function of liposome coupling (0.5 and 5 mg ml^{-1} of total lipids). The loading efficiency of the particles onto the cells is represented in **Figure 3A**. Increasing the lipid concentration ten-fold only slightly increased the attachment of the liposomes to the cells. Importantly, we could show that the viability of the cells, as quantified by a WST-1 assay, was not compromised by the loading with liposomes. In contrast, we could detect a significantly higher amount of cells after liposome loading (**Figure 3B**). Although we already showed in **Chapter 2** that the coupling via a PDP linker did not influence T cell proliferation, we wanted to verify this for the MAL-functionalized liposomes as well. T cells were first incubated with different concentrations of both PDP and MAL liposomes, ranging from 0.1 to 5 mg ml^{-1} of total lipids, demonstrating the saturation of liposome coupling with increasing lipid concentrations (**Figures 4A-B**).

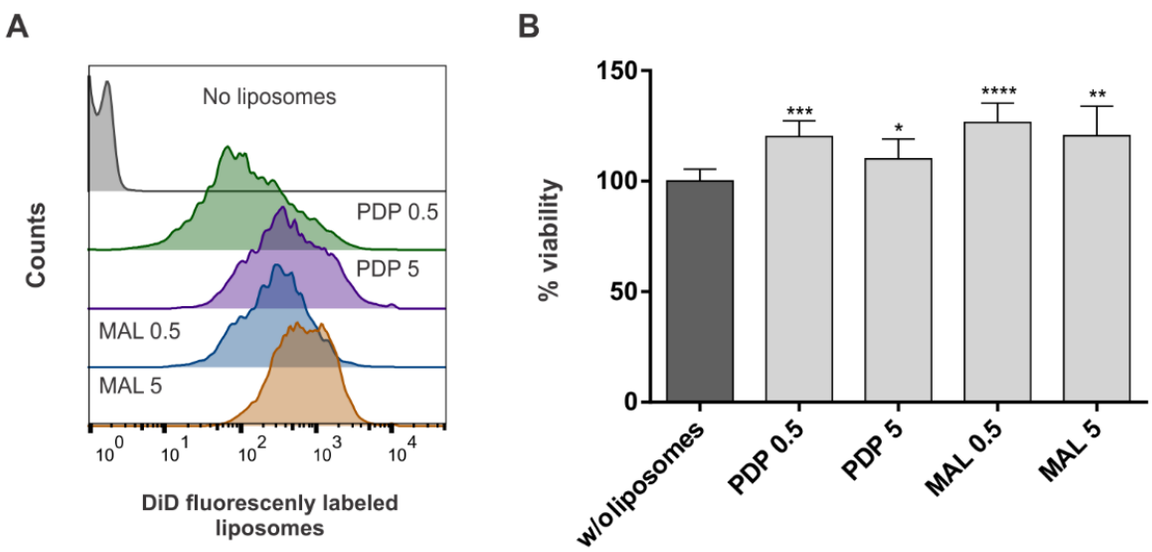

Figure 3: Viability of $CD8^+$ T cells as a function of the liposome-load. Activated $CD8^+$ T cells were first coupled with PDP- and MAL-functionalized liposomes in 2 different concentrations (0.5 versus 5 mg ml^{-1}). **(A)** Histograms representing the liposome-load per T cell as was measured by flow cytometry. **(B)** 24h after incubation, the cell viability was quantified via a WST-1 assay. Data represent the percentage viability ± SD of 2 independent experiments with $n = 3$ (ns = not significant; * p <0.05; ** p <0.01; *** p <0.001; **** p <0.0001).

T cell proliferation, as determined by the dilution of CFSE stain over the daughter cells, remained unaffected by both PDP and MAL liposomes over 24h of incubation (**Figures 4C-D**). Another important feature of activated T cells is the secretion of immune-promoting cytokines, including interferon gamma (IFNγ), tumor necrosis factor alpha (TNFα), and IL-2, which are important mediators of cytotoxic T cell anti-tumor responses.

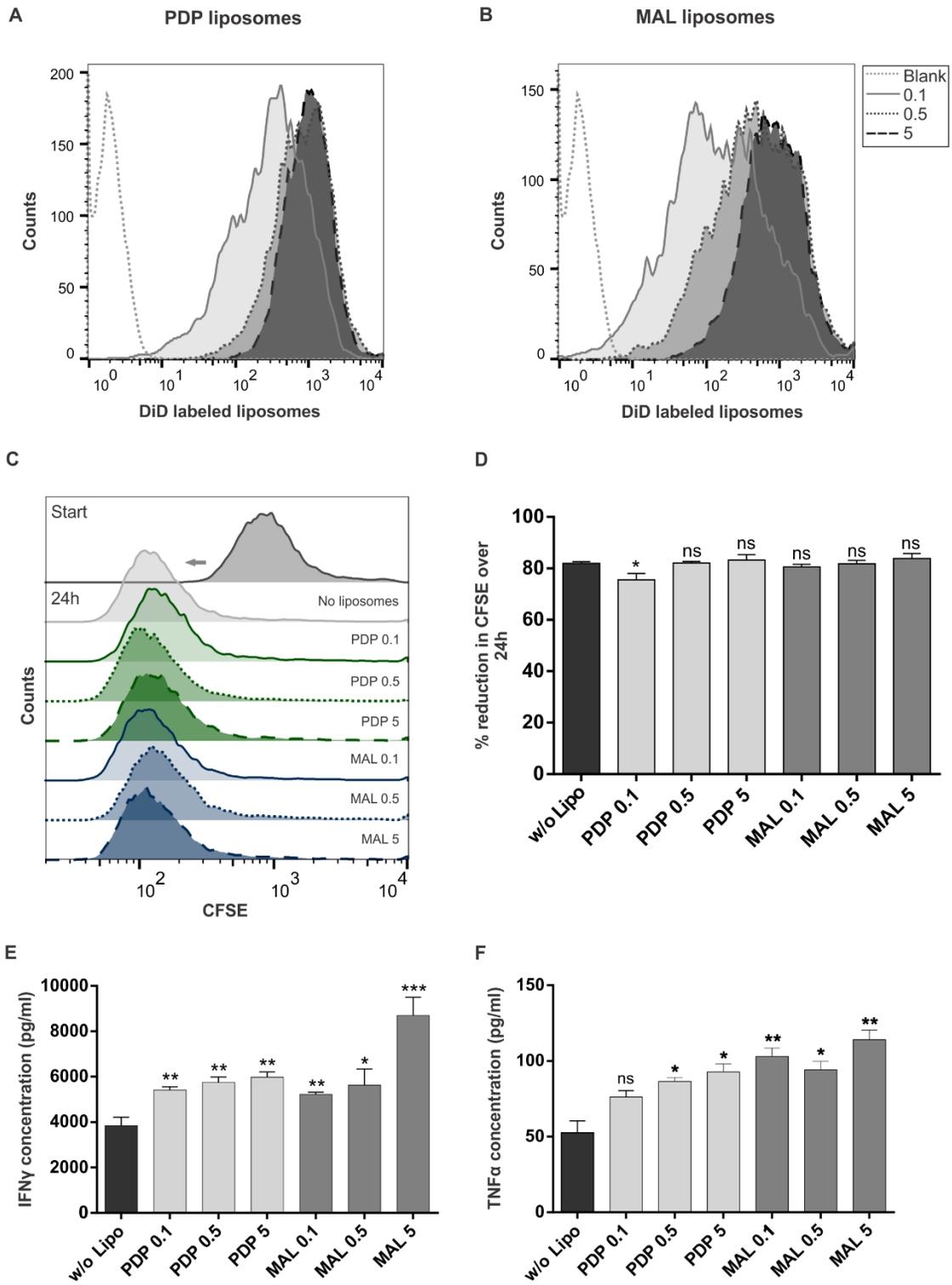

Figure 4. Proliferation and cytokine secretion after loading CD8⁺ T cells with PDP- and MAL-functionalized liposomes. Activated CD8⁺ T cells were first coupled with **(A)** PDP- and **(B)** MAL-functionalized DiD-labeled liposomes in 3 different concentrations (0.1 - 0.5 - 5 mg ml^{-1}). **(C)** Histograms representing the CFSE fluorescence intensity per cell as was measured by flow cytometry at time point 0h and 24h, indicated in the graph. **(D)** Upon proliferation, the CFSE stain is diluted over the daughter cells which is indicated in the graph as the percentage of reduction in CFSE fluorescence intensity per T cell ± SD over 24h of incubation (n = 1 experiment with 3 independent samples; ns = not significant; * p <0.01). Supernatants of CD8⁺ T cells loaded with PDP and MAL liposomes were assessed for the presence of **(E)** IFNγ and **(F)** TNFα (experiment was performed 3 times from which 1 experiment with n = 3 was selected for representation; ns = not significant; * p <0.05; ** p <0.01; *** p <0.001).

Of note, we observed a significant increase in both IFNγ and TNFα secretion by T cells carrying liposomes on their cell surface, independent from the coupling strategy or the amount of attached liposomes (**Figures 4E-F**). We were not able to determine the amount of IL-2 as this was supplemented to the growth medium to support the survival of the activated T cells.

3.4 Intratumoral, intraperitoneal and intravenous injection of liposome-loaded CD8$^+$ T cells

Independent of the coupling chemistry, liposomes remained undetectable in the tumor 48h after IP injection of liposome-loaded T cells (**Figure 2C**). To investigate this in more detail, we also aimed to determine the presence of DiD-labeled MAL liposomes after direct intratumoral (IT) injection of liposome-loaded and CFSE stained CD8$^+$ OT-I T cells in the MO4 tumors. Prior to transfer, more than 99% of the transferred cells had both a CFSE and DiD label (**Figures 5A-B**). In contrast, already one day after IT injection, only a very low percentage of cells is still positive for both CFSE and DiD (**Figures 5C-D**). Interestingly, a high percentage of DiD-positive cells without CFSE label could be isolated from the tumor. Taken together, these data suggest both a fast proliferation rate of the IT injected T cells as well as the transfer of DiD particles to endogenous cells in the tumor microenvironment.

Finally, the T cell-mediated delivery of liposomes via IP injections was compared with intravenous (IV) delivery. Judging from the low infiltration of transferred CFSE-labeled OT-I T cells in MO4 tumors 48h after injection, IV administration has no advantage over the IP route (**Figures 5E-G**). In addition, it was verified whether fluorescently-labeled liposomes coupled to OT-I cells could be observed in the tumor after IV injection. Unfortunately, IV injection did not improve the presence of DiD-labeled liposomes in the tumor (**Figure 5H**). Moreover, the percentage of infiltrated cells is very low for all conditions and no significant differences were observed for both delivery routes (**Figure 6A**). As IP injection of OT-I cells compared to IV achieved better control over tumor growth, the IP delivery route was maintained for the next *in vivo* experiments (**Figure 6B**).

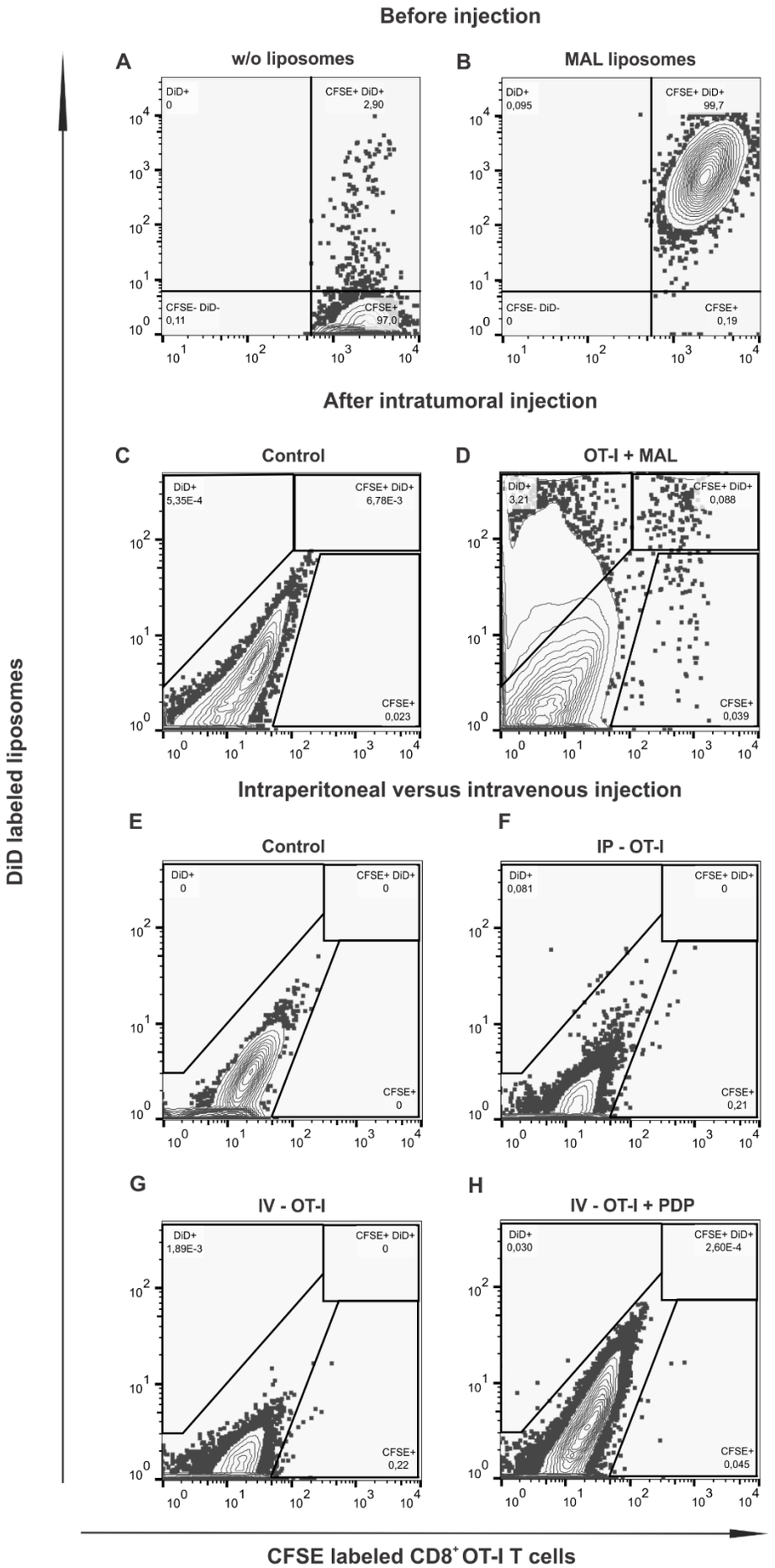

Caption next page

Figure 5. The T cell-mediated delivery of liposomes to MO4 tumors via distinct delivery routes. (A) Density plots representing CFSE-labeled CD8$^+$ OT-I T cells without liposomes and **(B)** cells coupled with DiD-labeled MAL liposomes prior to injection. **(C)** Density plots representing tumor isolated cells of a control mouse and **(D)** a mouse intratumorally injected with MAL liposome-loaded CFSE-labeled OT-I T cells. **(E)** Density plots representing a comparison between mice with MO4 tumors that were injected with PBS as a control, **(F)** intraperitoneally (IP) injected with CFSE-labeled OT-I T cells, **(G)** intravenously (IV) injected with CFSE-labeled OT-I T cells, and **(H)** IV injected with CFSE-labeled OT-I T cells that were loaded with DiD-labeled PDP liposomes.

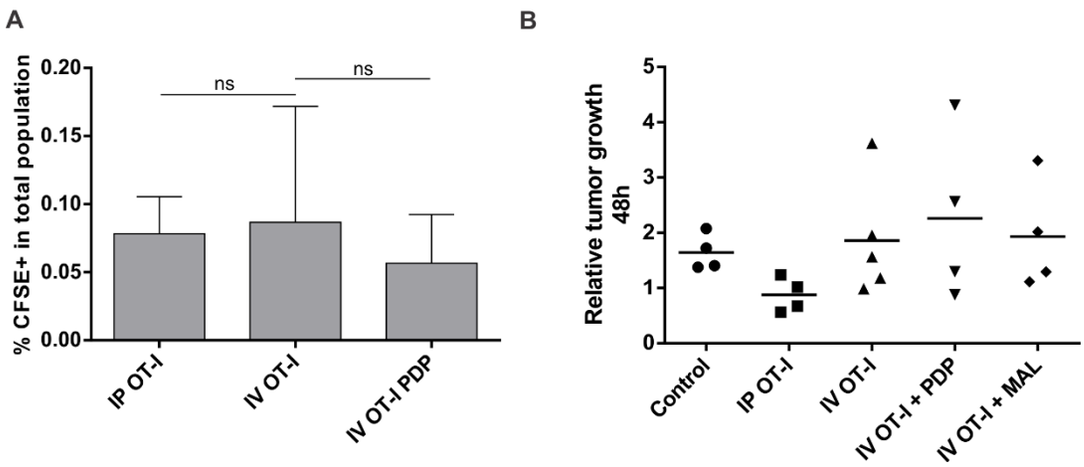

Figure 6. The impact of the delivery route on the tumor infiltration of CD8$^+$ OT-I T cells and the relative tumor growth 48h after transfer. (A) The percentage of CFSE-positive T cells ± SD in the MO4 tumors of mice injected intraperitoneally (IP) versus intravenously (IV) with OT-I T cells, and the IV injection of PDP liposome-loaded OT-I T cells (IP OT-I and IV OT-I PDP: *n* = 4; IV OT-I: *n* = 5; ns = not significant). **(B)** Comparison in relative tumor growth 48h after transfer between mice IP injected with non-loaded OT-I T cells and mice injected IV with non-loaded, PDP liposome-loaded, and MAL liposome-loaded OT-I T cells.

3.5 Coupling of MPLA liposomes to T cells and in vitro evaluation of dendritic cell maturation

Although very low percentages of transferred OT-I T cells infiltrated the tumor, an enhanced tumor killing effect was observed by tumor size measurements. However, an immunosuppressive tumor microenvironment may hinder the therapeutic effects obtained by adoptively transferred T cells. Therefore, we anticipated that by shifting the tumor microenvironment from immunosuppressive to immune-stimulatory, higher therapeutic effects could be obtained. To this end, we incorporated the immune adjuvant monophosphoryl lipid A (MPLA) in the lipid bilayer of the liposomes. First, we evaluated the effect of incorporating MPLA into liposomes on T cell coupling and T cell functionalities. Secondly, we assessed whether the MPLA can induce maturation of dendritic cells (DCs) upon *in vitro* co-culturing with liposome-loaded CD8$^+$ T cells.

3.5.1 Influence of MPLA liposomes on proliferation, viability and cytokine secretion of CD8$^+$ T cells

Figure 7 represents the preliminary effects of coupling MPLA-loaded MAL liposomes (0.6 wt% and 3 wt% MPLA) to CD8$^+$ T cells. As depicted in **Figures 7A-B**, the T cell

proliferation and resulting distribution of DiD-labeled liposomes over the daughter cells, as measured 24h after liposome coupling, was not influenced by the presence of MPLA.

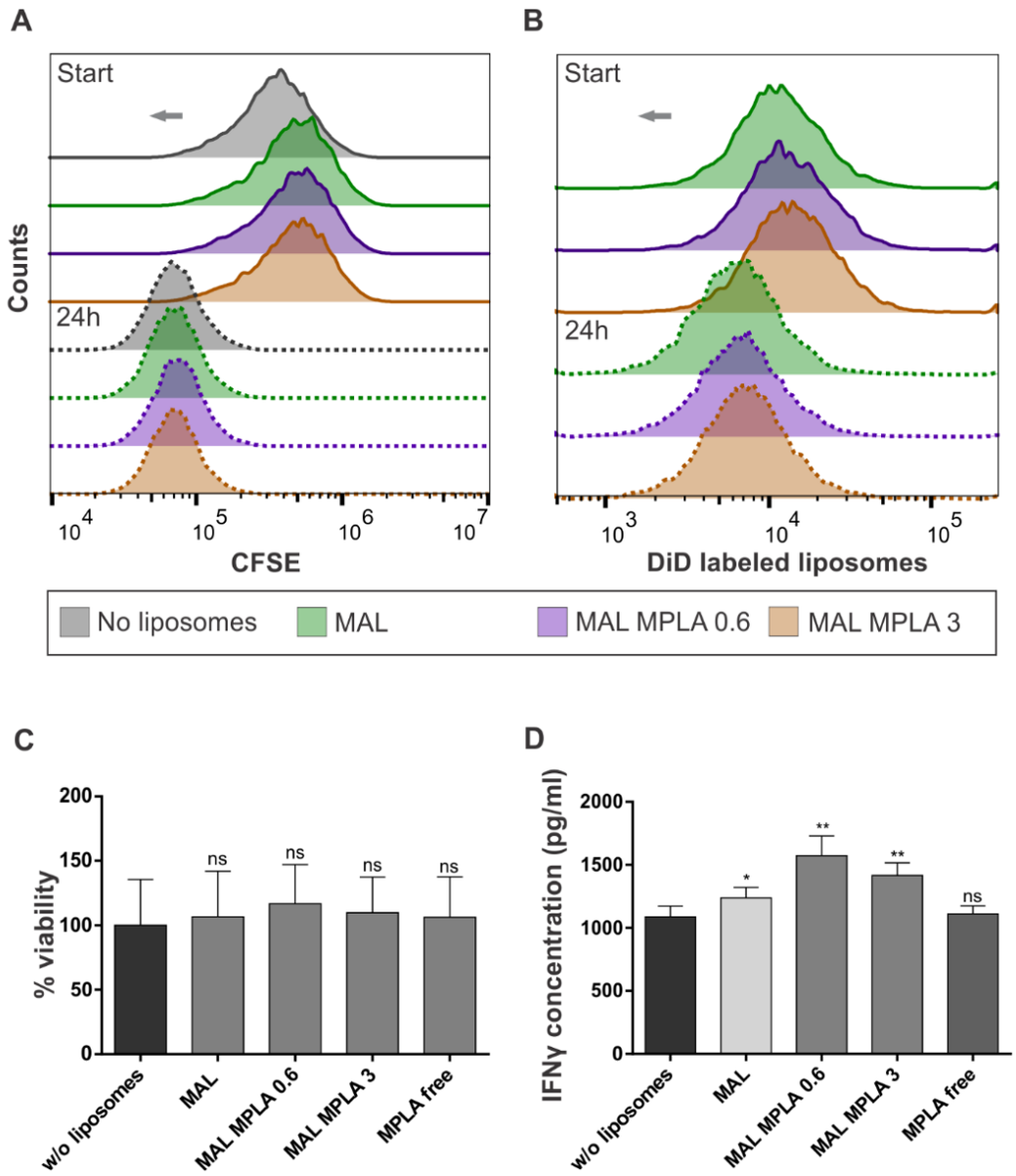

Figure 7. *In vitro* evaluation of proliferation, viability, and IFNγ secretion of CD8⁺ T cells that were coupled with monophosphoryl lipid A (MPLA)-loaded liposomes. CD8⁺ T cells were first labeled with CFSE and incubated with DiD-labeled liposomes (5 mg ml-1 lipids), followed by the incubation over 24h in cell culture medium supplemented with 30 U ml^{-1} rIL-2. Cells without liposomes onto their surface and cells incubated with 0.15 mg ml^{-1} free MPLA were compared with cells anchored with MAL liposomes without MPLA or with 0.6 wt% and 3 wt% MPLA. **(A)** Histograms representing the dilution of CFSE and **(B)** the distribution of the DiD-labeled liposomes over the daughter cells 24h after coupling. **(C)** Percentage cell viability ± SD of the CD8⁺ T cells measured by a CellTiter-Glo® assay 24h after coupling of the liposomes (*n* = 1 experiment with 4 independent samples). **(D)** IFNγ concentration ± SD secreted by CD8⁺ T cells that were coupled with the liposomes during 24h, measured by an ELISA assay (*n* = 1 experiment with 4 independent samples). Statistics represent ns = not significant; * p <0.05; ** p <0.01.

Likewise, T cell viability, as assessed by a CellTiter-Glo® assay, showed no significant differences upon incubation with MPLA or MPLA liposomes (**Figure 7C**). Interestingly, the INFγ cytokine secretion significantly increased upon MPLA-liposome coupling, which was shown to be independent of MPLA (**Figure 7D**).

3.5.2 Maturation of dendritic cells in co-culture with MPLA-containing liposomes loaded onto the surface of $CD8^+$ T cells

In analogy with the study by Van Lint *et al*. that showed the improved survival when tumor-infiltrated DCs were shifted towards a more immunostimulatory phenotype, we focused on determining the effects of MPLA on DCs upon co-culturing with T cells bearing MPLA liposomes on their surface [12]. As a positive control for maturation, the DCs were supplemented with 1 µg ml^{-1} of E. *coli*-derived lipopolysaccharide (LPS), which is a potent initiator of DC maturation. Additionally, DCs incubated with 1 µg ml^{-1} free MPLA were included as a control for maturation by MPLA.

Our preliminary data, as represented in **Figure 8**, showed a marked upregulation of the co-stimulatory receptors CD40 and CD80 on the DC surface as a function of the presence of MPLA. Both free MPLA as MPLA incorporated in liposomes and loaded onto $CD8^+$ T cells were able to induce this effect, with elevated levels when 3 wt% was incorporated versus 0.6 wt%. A distinct higher amount of cells showed augmented CD40/CD80 expression for the 1:1 ratio (T cell:DC) compared with the 1:5 ratio. Further, the coupling via PDP-functionalized liposomes showed a lower percentage of CD40/CD80-positive cells, which cannot be attributed to differences in loading efficiency onto the T cells since for both a similar coupling efficiency was shown (**Figure 9A**).

Next to the upregulation of co-stimulatory receptors when DCs become mature, they also secrete immunostimulatory cytokines such as IL-12. Hence, we measured via an ELISA assay the secretion of IL-12p70, which is the active form of IL-12. The differences in IL-12p70 secretion as depicted in **Figure 9B** had a similar trend as for the maturation markers, which is a confirmation of the latter results. It has been demonstrated in the literature that T cell-anchored liposomes tend to accumulate in the immune synapse upon their interaction with antigen-presenting cells [18]. To verify if this close apposition could result in liposome transfer, we quantified the uptake of fluorescently labeled T cell-coupled liposomes by DCs. Remarkably, we could detect high fluorescent signals in the DC population for the various formulations tested, suggesting effective liposome internalization by DCs. The observed variations in DC fluorescence are indicative of differences in extent of liposome interaction with DCs and are likely correlated with DC maturation as well (**Figure 9C**). Moreover, confocal imaging of co-cultured T cells and DCs demonstrated the internalization of green labeled liposomes by DCs, containing bright fluorescent perinuclear spots (**Figure 9D**).

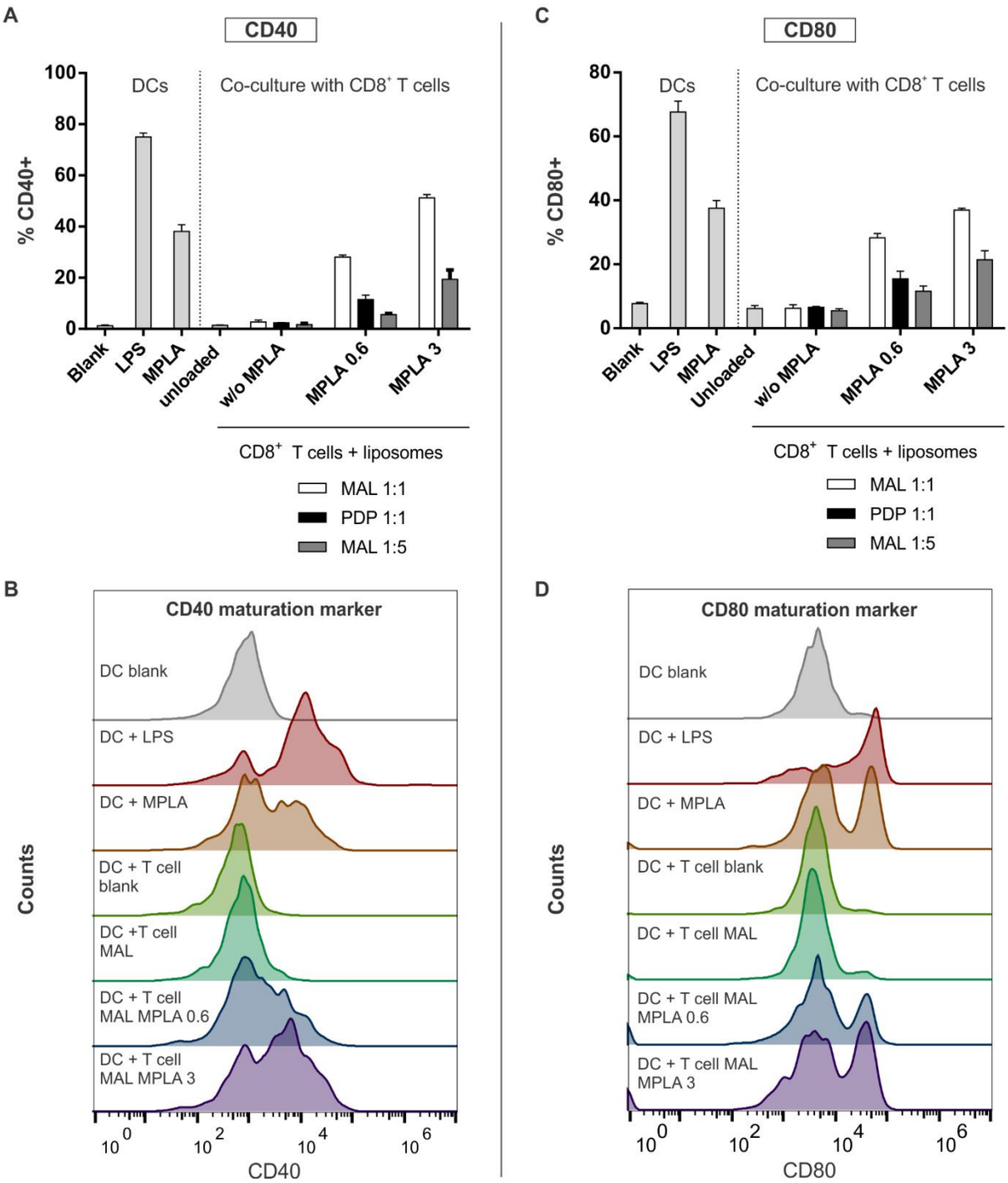

Figure 8. Evaluation of dendritic cell (DC) maturation markers after 24h of co-culturing with monophosphoryl lipid A (MPLA)-containing liposome-loaded CD8⁺ T cells. $CD8^+$ T cells were loaded with PDP- and MAL-functionalized liposomes containing no MPLA, 0.6 wt% MPLA or 3 wt% MPLA. The T cells were co-cultured with DCs during 24h in a 1:1 versus 1:5 ratio of T cells:DCs. Untreated DCs and DCs incubated with 1 µg ml^{-1} of lipopolysaccharide (LPS) or 1 µg ml^{-1} free MPLA were used as negative and positive controls, respectively. **(A)** Graph representing the percentage ± SD of CD40-positive DCs and **(B)** the corresponding histograms. **(C)** Graph representing the percentage ± SD of CD80-positive DCs and **(D)** the corresponding histograms (*n* = 1 experiment with 3 independent samples).

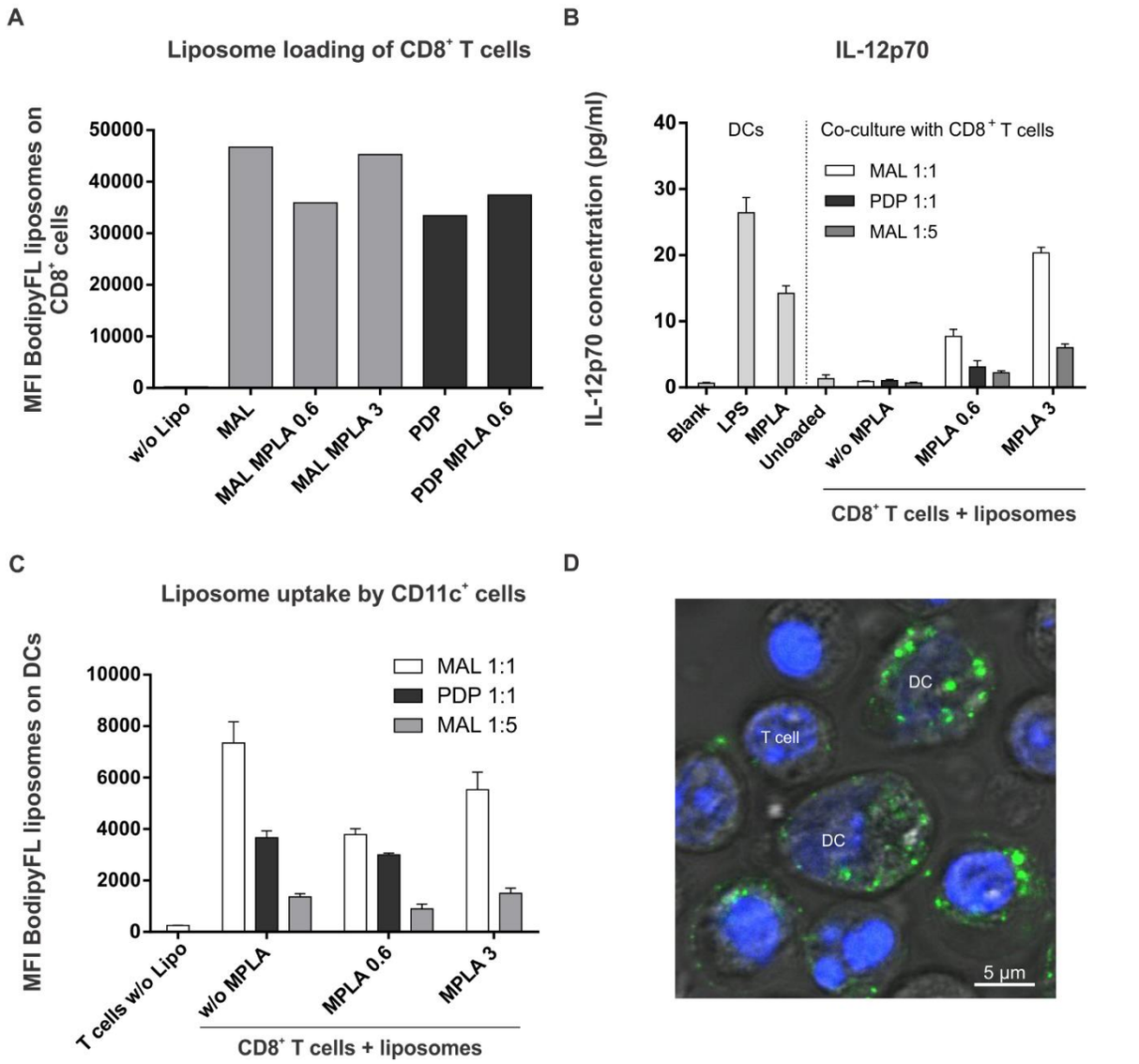

Figure 9. Interaction of monophosphoryl lipid A (MPLA)-loaded liposomes with dendritic cells (DCs) and the subsequent secretion of IL-12p70. (A) Prior to co-culturing with DCs, the $CD8^+$ T cells were loaded with both PDP- and MAL-functionalized liposomes carrying 0.6 wt% or 3 wt% MPLA. The graph represents the mean fluorescence intensity (MFI) of BodipyFL-labeled liposomes per $CD8^+$ T cell (n = 1). **(B)** IL-12p70 concentration ± SD measured by an ELISA assay for DCs that were co-cultured with (MPLA-containing) liposome-loaded T cells for 24h (n = 1 experiment with 3 independent samples). **(C)** Graph representing the mean fluorescence intensity (MFI) per DC ± SD of the BodipyFL-labeled liposomes upon co-culturing with PDP and MAL liposome-loaded T cells (n = 1 experiment with 3 independent samples). **(D)**.Confocal image of a co-culture of DCs and T cells that were previously loaded with BodipyFL-labeled liposomes (green dots). The nuclei of the cells were stained with Hoechst (blue).

3.6 In vivo therapeutic evaluation of T-cell mediated delivery of MPLA-loaded liposomes

As was shown via *in vitro* co-culture experiments, the MPLA-loaded liposomes coupled onto T cells were still able to induce maturation in DCs. However, further *in vivo* evaluation is necessary to prove the therapeutic benefit of this concept in a more complex environment, containing tumor-associated cells as well as a multitude of different immune cells. As a final step in this chapter, we thus aimed to assess whether the incorporation of

MPLA into liposomes that are subsequently coupled to T cells could result in therapeutic benefit in the MO4 tumor model following IT injection.

Mice were inoculated with MO4 tumors as described above for the migration experiments. When tumors reached an average size of 500 mm^3, the mice were IT injected with 1.5 x 10^6 OT-I T cells loaded with PDP- and MAL-functionalized liposomes containing 0.6 wt% MPLA. Mice that were injected with PBS as a control showed rapid tumor growth and had to be sacrificed within two days following treatment. Tumor injection with OT-I T cells with or without (PDP or MAL) liposomes showed little to no therapeutic benefit. Only when mice were treated with T cell-anchored liposomes carrying the MPLA adjuvant, a delay in tumor growth was noticeable, which was most pronounced for the PDP-coupled liposomes. Only for this formulation, a substantial improvement in median survival could be documented in this melanoma tumor model (**Figure 10**).

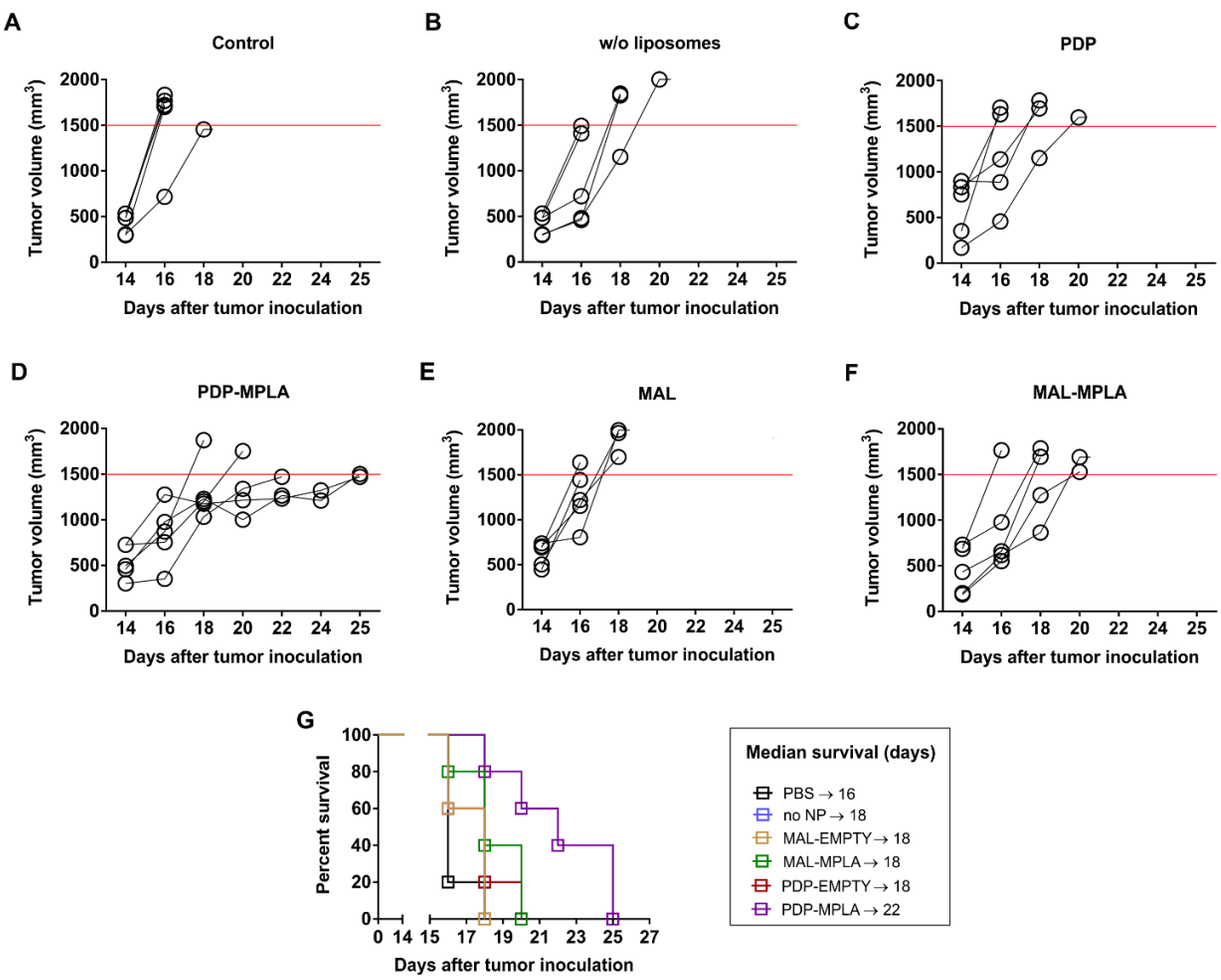

Figure 10. Intratumoral injection of monophosphoryl lipid A (MPLA)-containing liposomes coupled to $CD8^+$ OT-I T cells. 14 days after inoculation of C57BL/6 mice with MO4 tumor cells, the mice were randomized based on tumor volume in 6 treatment groups. The graphs show the tumor growth as a function of time for mice injected with **(A)** PBS as a control, $CD8^+$ OT-I T cells **(B)** without liposomes, with **(C)** PDP-functionalized liposomes, **(D)** MPLA-containing PDP-functionalized liposomes, **(E)** MAL-functionalized liposomes, **(F)** MPLA-containing MAL-functionalized liposomes. **(G)** Representation of the Kaplan-Meier survival curve of the differently treated mice with the median survival data (*n* = 5 mice per treatment group).

4 DISCUSSION

The aim of this study was to investigate whether cytotoxic T cells (CTLs), bearing liposomes on their surface, are able to migrate to the tumor and whether the concomitant delivery of liposome-encapsulated therapeutics improves the therapeutic outcome of adoptive T cell therapy (ACT). Two distinct coupling strategies were simultaneously screened, i.e. using pyridyldithiopropionate (PDP)- and maleimide (MAL)-functionalized lipids, initiating a reversible disulfide bond or a more stable thioether bond, respectively. In analogy with clinical protocols, a lymphodepletion step prior to OT-I transfer was included in the treatment regimen, as it removes suppressive regulatory T cells and cytokine sinks, thus resulting in enhanced anti-tumor responses for ACT [19]. In general, patients are treated with the lymphoablative chemotherapeutics cyclophosphamide and fludarabine or with total body irradiation [20]. Based on the literature, we injected the mice 1 or 2 days before adoptive transfer with a dose of 2 mg cyclophosphamide [17]. Although it was shown by a study of Gattinoni and colleagues that after lymphodepletion through total body irradiation no differences in the infiltration of adoptively transferred T cells could be observed, we clearly showed a substantial increase 24h after transfer in cyclophosphamide pre-treated mice [21].

In literature, both intravenous (IV) and intraperitoneal (IP) injection routes have demonstrated similar accumulation of T cells in the tumor with a comparable effect on tumor growth [22]. In contrast, our data showed a trend for improved control over tumor growth when OT-I T cells were injected IP compared to IV. Unfortunately, both delivery routes were not able to demonstrate concomitant delivery of liposomes in the tumor. Given that the fluorescence intensities of CFSE per cell rapidly decreased over time, it is also conceivable that the fast distribution of the liposome-load over the daughter cells upon proliferation also dilutes the liposome label to undetectable levels. Another hypothesis is the premature release of the liposomes from the T cells before reaching the tumor tissue. Although the PDP-coupled liposomes can possibly be detached in the systemic circulation through disulfide reduction, Irvine and colleagues clearly showed increased levels of MAL-functionalized liposomes in the tumor due to T cell-mediated delivery [23]. In our hands, even 24h following direct intratumoral (IT) injection of MAL-liposome loaded T cells, few T cells with detectable liposome signal could be isolated from the tumor. These data indicate that fast proliferation of the activated T cells indeed limits detection of liposomes in the tumor mass. Interestingly, we could identify a substantial number of CFSE-negative cells in the tumor microenvironment with measurable liposome fluorescence. From these results, we speculate that intercellular liposome transfer can occur upon close contact between the transferred T cells and other cell types in the tumor tissue.

It is key that the modification with liposomes does not negatively affect T cell functions. In agreement with Irvine and colleagues, we demonstrated that the coupling of

liposomes to the T cell surface had no influence on the T cell proliferation. Although these authors also did not observe alterations in cytokine expression levels upon T cell-anchoring of liposomes, our results showed that the secretion of the immunostimulating cytokines IFNγ and TNFα was clearly elevated. The latter observation may contribute to the improved therapeutic effect of liposome-loaded T cells. Indeed, although the presence of liposomes on the T cells surface slightly reduced T cell extravasation into the tumor, possibly through steric hindrance, a significant improvement in tumor growth control was observed, which was most prominent for the MAL-coupled liposomes.

Currently, it has become clear that a single cancer immunotherapy approach in most patients is unlikely to completely eradicate the tumor due to a complex interplay of the tumor microenvironment [24]. For example, ACT can only be successful when T cell effector functions and persistence are not impeded by a tumor growth-supporting microenvironment [25]. This highlights the needs for combination therapy, merging the benefits of distinct anti-cancer treatments. A combination of immunotherapy with chemotherapy holds great potential, not only because tumor cells can effectively be eradicated but also due to the contribution of certain types of chemotherapeutics to induce immunogenic cell death (ICD). This specific cell death mechanism generates endogenous immune adjuvants, which might aid in overcoming the immunosuppressive tumor microenvironment [8, 26]. However, within this study the delivery of chemotherapeutics, as was evaluated for doxorubicin, had an immediate detrimental effect onto the carrier cells, the reason likely being the unstable encapsulation of the compound in the functionalized liposomes (data not shown). The latter observation calls for the use of chemotherapeutics to which carrier T cells are resistant, as shown recently for the active metabolite of the topoisomerase I inhibitor irinotecan [27]. However, the latter study focused on the use of polyclonal T cells that were not able to kill tumor cells and were only used as carriers to deliver the chemotherapeutic cargo to lymphoid tumors.

Besides the tumor cells that can act as mediators of immune suppression, also certain types of immune cells are known to support the tumor growth [28]. For example, upon interaction with immunosuppressive mediators, dendritic cells (DCs) can acquire a suppressive phenotype and stimulate regulatory T cells to counteract CTL responses [29]. Hence, an interesting therapeutic approach is the delivery of therapeutics that can shift the local environment from immunosuppressive to immunostimulatory. To this end, immune adjuvants are very promising. Unfortunately, the systemic administration of several of these adjuvants has shown to induce severe side effects [30, 31]. Therefore, we proposed here the T-cell mediated targeting of adjuvant-loaded liposomes to the tumor.

For this purpose, the immune adjuvant monophosphoryl lipid A (MPLA), a Toll-like receptor 4 (TLR4) agonist, was selected based on studies that showed their role in maturing DCs, leading to the induction of tumor-specific $CD4^+$ and $CD8^+$ T cell responses [32, 33]. In

addition, previous studies showed that MPLA can easily be inserted in the lipid bilayer of liposomes and that the encapsulation in nanocarriers enhances the DC maturation [34-36] (Verbeke *et al.*, manuscript submitted).

Of note, we showed that the incorporation of MPLA into the liposome had no influence on the coupling efficiency or T cell functionalities, including CTL proliferation and IFNγ secretion, which could be expected since $CD8^+$ T cells have low or absent expression of TLR4 on their surface [37]. Importantly, we showed that MPLA liposomes, when loaded onto the T cell plasma membrane, were still able to induce maturation of DCs. The maturation process of DCs to become potent T cell activators is associated with multiple phenotypic changes. We showed here the upregulation of the co-stimulatory receptors CD40 and CD80 and further an increased secretion of the immunostimulatory cytokine IL-12. This cytokine is important for the polarization of T cells to IFNγ-producing T_H1 phenotypes [38].

Based on the literature describing that upon interaction of liposome-loaded T cells with APCs the liposomes tend to accumulate in the synapse, we anticipated that the TLR4 of DCs could be stimulated upon close contact with MPLA-containing liposomes attached to the surface of T cells [18]. Flow cytometry data and confocal imaging revealed that the liposomes were to a significant extent internalized by the DCs, even for the MAL liposomes that are expected to be stably attached to the T cell surface. Although the mechanism behind the transfer of liposomes from T cells to DCs is not yet elucidated, several hypotheses could be formulated. First, when T cells undergo apoptosis, T cell membrane debris with liposomes attached might become available for phagocytosis by DCs. Secondly, it has been shown previously that DCs can internalize fragments of the cell membrane or cytoplasm from other cells upon close contact, through a process called 'nibbling' [39]. Studies have shown that via this nibbling process DCs can internalize antigens from live tumor cells and even B cells [40-42].

Supported by these promising *in vitro* data, we finally aimed to evaluate the therapeutic benefit of the MPLA liposomes *in vivo*, in a mouse model of melanoma. To this end, we opted to first evaluate the activity of our liposome-coupled T cells through IT injection, bypassing several extratumoral barriers, to enable unbiased assessment of the activity of the modified T cells in the complex tumor microenvironment. Interestingly, an enhanced survival was only observed for the mice treated with OT-I cells loaded with MPLA liposomes coupled via a PDP linker. Although *in vitro* data showed a higher maturation of DCs when a MAL linker was used for the T cell coupling, these *in vivo* data suggest the benefit of a reducible coupling system. Future work will be directed to answer the question whether T cell-mediated delivery of immune adjuvants results in clinical benefit with either PDP- or MAL-anchored liposomes, upon systemic injection.

5 CONCLUSION

In this study, we attached liposomes to the surface of CTLs via a reversible (PDP) and stable (MAL) coupling. For both coupling techniques, no negative impact on proliferation or viability of the CTLs could be observed *in vitro*. In addition, it was clearly demonstrated that the coupling induced a higher secretion of the immunostimulatory cytokines IFNγ and TNFα, which might explain the enhanced anti-tumor response of liposome-loaded CTLs observed in a mouse melanoma model. Ultimately, liposomes were loaded with the adjuvant MPLA and coupled to CTLs to improve the immune responses against the tumor. First, we showed the successful maturation of DCs *in vitro* when co-cultured with CTLs that were coupled with MPLA-loaded liposomes. Secondly, an improved survival of mice with melanoma was demonstrated after IT injection of CTLs loaded with MPLA liposomes, from which the anti-tumor effect was most pronounced for the reversible coupling. It remains for future research to evaluate the therapeutic effect of this combinatorial strategy after systemic injection.

ACKNOWLEDGEMENTS

The authors would like to acknowledge Cleo Goyvaerts and Katrijn Broos for their help with the mouse cultures. Koen Raemdonck and Heleen Dewitte are postdoctoral fellows of the Research Foundation-Flanders, Belgium (FWO-Vlaanderen). Laura Wayteck is a doctoral fellow of the Institute for the Promotion of Innovation through Science and Technology in Flanders, Belgium (IWT-Vlaanderen). FWO (Krediet aan Navorsers) and Kom op Tegen Kanker (Beurs Emmanuel van der Schueren) are acknowledged for their financial support.

REFERENCES

1. Anselmo, A.C. & Mitragotri, S. An overview of clinical and commercial impact of drug delivery systems. *J Control Release* **190**, 15-28 (2014).
2. Prabhakar, U. et al. Challenges and key considerations of the enhanced permeability and retention effect for nanomedicine drug delivery in oncology. *Cancer Res* **73**, 2412-7 (2013).
3. Slaney, C.Y., Kershaw, M.H. & Darcy, P.K. Trafficking of T cells into tumors. *Cancer Res* **74**, 7168-74 (2014).
4. von Andrian, U.H. & Mackay, C.R. T-cell function and migration. Two sides of the same coin. *N Engl J Med* **343**, 1020-34 (2000).
5. Butera, D., Cook, K.M., Chiu, J., Wong, J.W. & Hogg, P.J. Control of blood proteins by functional disulfide bonds. *Blood* **123**, 2000-7 (2014).
6. Balkwill, F.R., Capasso, M. & Hagemann, T. The tumor microenvironment at a glance. *J Cell Sci* **125**, 5591-6 (2012).
7. Conde, J., Arnold, C.E., Tian, F.R. & Artzi, N. RNAi nanomaterials targeting immune cells as an anti-tumor therapy: the missing link in cancer treatment? *Materials Today* **19**, 29-43 (2016).
8. Pol, J. et al. Trial Watch: Immunogenic cell death inducers for anticancer chemotherapy. *Oncoimmunology* **4**, e1008866 (2015).
9. Dewitte, H., Verbeke, R., Breckpot, K., De Smedt, S.C. & Lentacker, I. Nanoparticle design to induce tumor immunity and challenge the suppressive tumor microenvironment. *Nano Today* **9**, 743-758 (2014).
10. Badie, B. & Berlin, J.M. The future of CpG immunotherapy in cancer. *Immunotherapy* **5**, 1-3 (2013).
11. Vacchelli, E. et al. Trial watch: FDA-approved Toll-like receptor agonists for cancer therapy. *Oncoimmunology* **1**, 894-907 (2012).
12. Van Lint, S. et al. Intratumoral Delivery of TriMix mRNA Results in T-cell Activation by Cross-Presenting Dendritic Cells. *Cancer Immunol Res* **4**, 146-56 (2016).
13. Hennessy, E.J., Parker, A.E. & O'Neill, L.A. Targeting Toll-like receptors: emerging therapeutics? *Nat Rev Drug Discov* **9**, 293-307 (2010).
14. Baba, J. et al. Depletion of radio-resistant regulatory T cells enhances antitumor immunity during recovery from lymphopenia. *Blood* **120**, 2417-27 (2012).
15. Salem, M.L. et al. Defining the ability of cyclophosphamide preconditioning to enhance the antigen-specific CD8+ T-cell response to peptide vaccination: creation of a beneficial host microenvironment involving type I IFNs and myeloid cells. *J Immunother* **30**, 40-53 (2007).
16. Du Four, S. et al. Axitinib increases the infiltration of immune cells and reduces the suppressive capacity of monocytic MDSCs in an intracranial mouse melanoma model. *Oncoimmunology* **4**, e998107 (2015).
17. Sistigu, A. et al. Immunomodulatory effects of cyclophosphamide and implementations for vaccine design. *Semin Immunopathol* **33**, 369-83 (2011).
18. Stephan, M.T., Stephan, S.B., Bak, P., Chen, J. & Irvine, D.J. Synapse-directed delivery of immunomodulators using T-cell-conjugated nanoparticles. *Biomaterials* **33**, 5776-87 (2012).

19. Klebanoff, C.A., Khong, H.T., Antony, P.A., Palmer, D.C. & Restifo, N.P. Sinks, suppressors and antigen presenters: how lymphodepletion enhances T cell-mediated tumor immunotherapy. *Trends Immunol* **26**, 111-7 (2005).
20. Wayteck, L., Breckpot, K., Demeester, J., De Smedt, S.C. & Raemdonck, K. A personalized view on cancer immunotherapy. *Cancer Lett* **352**, 113-25 (2014).
21. Gattinoni, L. et al. Removal of homeostatic cytokine sinks by lymphodepletion enhances the efficacy of adoptively transferred tumor-specific CD8+ T cells. *J Exp Med* **202**, 907-12 (2005).
22. Petersen, C.C., Petersen, M.S., Agger, R. & Hokland, M.E. Accumulation in tumor tissue of adoptively transferred T cells: A comparison between intravenous and intraperitoneal injection. *J Immunother* **29**, 241-9 (2006).
23. Stephan, M.T., Moon, J.J., Um, S.H., Bershteyn, A. & Irvine, D.J. Therapeutic Cell Engineering Using Surface-Conjugated Synthetic Nanoparticles. *Journal of Immunotherapy* **16**, 1035-41 (2010).
24. Smyth, M.J., Ngiow, S.F., Ribas, A. & Teng, M.W. Combination cancer immunotherapies tailored to the tumour microenvironment. *Nat Rev Clin Oncol* **13**, 143-58 (2016).
25. Schietinger, A. & Greenberg, P.D. Tolerance and exhaustion: defining mechanisms of T cell dysfunction. *Trends Immunol* **35**, 51-60 (2014).
26. Kroemer, G., Galluzzi, L., Kepp, O. & Zitvogel, L. Immunogenic cell death in cancer therapy. *Annu Rev Immunol* **31**, 51-72 (2013).
27. Huang, B. et al. Active targeting of chemotherapy to disseminated tumors using nanoparticle-carrying T cells. *Sci Transl Med* **7**, 291ra94 (2015).
28. Schiavoni, G., Gabriele, L. & Mattei, F. The tumor microenvironment: a pitch for multiple players. *Front Oncol* **3**, 90 (2013).
29. Hargadon, K.M. Tumor-altered dendritic cell function: implications for anti-tumor immunity. *Front Immunol* **4**, 192 (2013).
30. Gunzer, M. et al. Systemic administration of a TLR7 ligand leads to transient immune incompetence due to peripheral-blood leukocyte depletion. *Blood* **106**, 2424-32 (2005).
31. Wingender, G. et al. Systemic application of CpG-rich DNA suppresses adaptive T cell immunity via induction of IDO. *Eur J Immunol* **36**, 12-20 (2006).
32. Chiang, C.L. et al. Oxidation of ovarian epithelial cancer cells by hypochlorous acid enhances immunogenicity and stimulates T cells that recognize autologous primary tumor. *Clin Cancer Res* **14**, 4898-907 (2008).
33. ten Brinke, A. et al. Monophosphoryl lipid A plus IFNgamma maturation of dendritic cells induces antigen-specific CD8+ cytotoxic T cells with high cytolytic potential. *Cancer Immunol Immunother* **59**, 1185-95 (2010).
34. Shariat, S. et al. P5 HER2/neu-derived peptide conjugated to liposomes containing MPL adjuvant as an effective prophylactic vaccine formulation for breast cancer. *Cancer Letters* **355**, 54-60 (2014).
35. Meraz, I.M. et al. Adjuvant cationic liposomes presenting MPL and IL-12 induce cell death, suppress tumor growth, and alter the cellular phenotype of tumors in a murine model of breast cancer. *Mol Pharm* **11**, 3484-91 (2014).
36. Meraz, I.M. et al. Multivalent presentation of MPL by porous silicon microparticles favors T helper 1 polarization enhancing the anti-tumor efficacy of doxorubicin nanoliposomes. *PLoS One* **9**, e94703 (2014).

37. Kabelitz, D. Expression and function of Toll-like receptors in T lymphocytes. *Curr Opin Immunol* **19**, 39-45 (2007).
38. Kaka, A.S., Foster, A.E., Weiss, H.L., Rooney, C.M. & Leen, A.M. Using dendritic cell maturation and IL-12 producing capacity as markers of function: a cautionary tale. *J Immunother* **31**, 359-69 (2008).
39. Harshyne, L.A., Zimmer, M.I., Watkins, S.C. & Barratt-Boyes, S.M. A role for class A scavenger receptor in dendritic cell nibbling from live cells. *J Immunol* **170**, 2302-9 (2003).
40. Dhodapkar, M.V., Dhodapkar, K.M. & Palucka, A.K. Interactions of tumor cells with dendritic cells: balancing immunity and tolerance. *Cell Death Differ* **15**, 39-50 (2008).
41. Palucka, K. & Banchereau, J. Cancer immunotherapy via dendritic cells. *Nat Rev Cancer* **12**, 265-77 (2012).
42. Harvey, B.P. et al. Transfer of antigen from human B cells to dendritic cells. *Mol Immunol* **58**, 56-65 (2014).

4

An enzyme-sensitive linker to reversibly load liposomes onto CD8$^+$ T cells

This chapter contains unpublished data:

Wayteck Laura, Demeester Jo, De Smedt Stefaan, and Raemdonck Koen

ABSTRACT

Cell-mediated delivery of nanoparticles (NPs) to the tumor has been investigated to overcome current NP targeting problems such as low infiltration and poor accumulation of NPs in the tumor tissue. However, the cytosolic delivery of drugs to tumor cells requires the release of drug-loaded NPs from the cell surface. Therefore, a triggered release system based on tumor microenvironmental stimuli such as low pH, high redox potential, and elevated levels of tumor-associated enzymes is of interest. In this study, we exploited enzymes that are known to be upregulated in many cancers as triggers for liposome release. For this purpose, we investigated a novel cleavable peptide construct as a linker between liposomes and $CD8^+$ T cells. We first showed the attachment of the peptide linker to the surface of $CD8^+$ T cells. Next, we demonstrated that the coupling was stable in serum-enriched medium, whereas a substantial amount of liposomes coupled via a reducible disulfide bridge, as investigated in **Chapters 2 and 3**, were released under the same conditions. Although we demonstrated the cleavability of the peptide sequence by specific enzymes when the peptide linker was attached to magnetic beads, only a minor release was observed when this linker was attached to $CD8^+$ T cells. As for trypsin, a highly unspecific protease, the cleavage was maximal, we suggested that steric hindrance at the highly complex cell membrane might be responsible for the low activity of the specific enzymes.

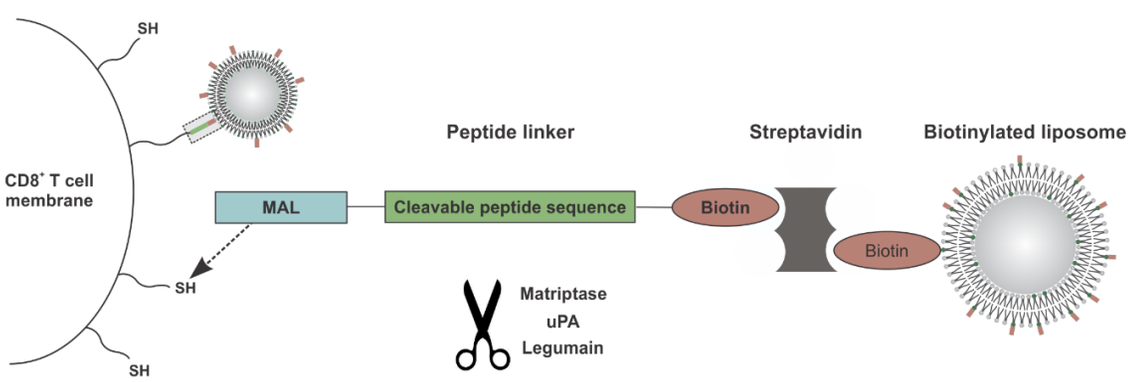

1 INTRODUCTION

Exploiting the tumor-homing ability of cells (*e.g.* stem cells, macrophages, and T cells) for targeted delivery of nanoparticles (NPs) has been shown to improve the infiltration and accumulation of NPs in the tumor tissue [1]. Because several drug compounds (*e.g.* nucleic acids) require intracellular delivery, as they are not able to passively cross cell membranes, triggered release of NPs from the carrier cell surface following extravasation in the tumor is of interest. In **Chapters 2 and 3**, we described PDP-functionalized liposomes that were coupled to $CD8^+$ T cells via a reversible disulfide bond. Although it was demonstrated that these liposomes could be detached again from the T cell surface as a function of glutathione concentration, a significant fraction of liposomes (~40%) remained stably anchored. In addition, such reversible coupling systems may encounter stability problems upon systemic injection, as was shown in the literature that disulfide exchange reaction can occur in the blood [2]. These arguments jointly highlight the need for a coupling system that is stable until the tumor tissue is reached and that is sensitive to a tumor-associated trigger, inducing maximal detachment of the NPs.

In literature, different types of triggers have been described, based on redox potential, pH, enzyme, and temperature [3]. Exploiting these cues for tumor-triggered release requires substantial biochemical differences in the tumor microenvironment compared to normal tissues. However, also external stimuli such as light and ultrasound have been applied to mediate a triggered release of drugs from NPs in the tumor [4, 5]. With regard to internal stimuli, for example, hydrazone bonds that are sensitive to low pH values have been described as linker for the reversible attachment of drug-loaded NPs to the surface of neural stem cells [6]. The interstitial pH in tumors is indeed slightly more acidic (pH 6.5-6.8) compared to other tissues owing to the Warburg effect. However, the limited pH difference also limits the choice of appropriate linkers with sufficient selectivity, typically resulting in slow and inefficient NP release [7]. The differences in redox potential based on the higher levels of extracellular glutathione in the tumor mass compared to normal tissues, were also exploited by us and others as tumor-specific stimuli (**Chapter 2**) [8, 9]. However, based on our study, the disulfide-linked liposomes could not be quantitatively released in the presence of glutathione.

Here, we investigated the use of an enzyme-sensitive peptide linker. Several enzymes are known to be present in the tumor tissue in elevated levels as they play crucial roles in cancer growth, invasion, and metastasis [10]. Linker chemistries sensitive to tumor-associated enzymes, such as matrix metalloproteinases (MMPs) and phospholipases, have been investigated for targeted tumor delivery. For example, a MMP2-sensitive peptide linker was incorporated between a NP and polyethylene glycol (PEG) chain, the latter being essential to safeguard NP stability in the bloodstream and enhance the circulation time of NPs. However, upon extravasation in the tumor, the PEG chain can hinder the uptake of the

NPs by tumor cells. By using a tumor-specific cleavable peptide, it has been shown that the PEG chain can be selectively cleaved in the tumor interstitium, thus enhancing subsequent NP cell internalization [11-13].

Here, we investigated an enzyme-cleavable peptide that was introduced by Desnoyers *et al.* [14]. They selected a peptide linker based on its sensitivity to the proteases matriptase, urokinase-type plasminogen activator (uPA), and legumain, all three enzymes having important roles in tumor invasion and metastasis. Matriptase is a type II transmembrane serine protease that is strictly expressed by epithelial cells and overexpressed in a variety of human carcinomas such as breast, ovarian, lung, cervical, and prostate cancer [15, 16]. uPA is a member of the urokinase plasminogen activator system (uPAS), which is involved in a number of tumor- and metastasis-promoting processes [17]. Moreover, increased tumor levels of uPAS-associated components such as uPA has been shown to be correlated with a poor prognosis [18, 19]. The protease legumain is a lysosomal protease that is expressed in the majority of solid cancers such as breast, colon, ovarian, and prostate cancer [20]. The enzyme is released in the tumor microenvironment and is active in an acidic environment [21]. As for all three enzymes their activity is low in healthy tissues due to the presence of endogenous inhibitors and unfavorable pH conditions, the peptide linker cleavage is restricted to the tumor tissue.

Within this study, we developed a peptide linker that can be used to reversibly attach liposomes to the surface of $CD8^+$ T cells, containing the suggested protease-cleavable peptide sequence. We first assessed the cleavability of the linker by matriptase and uPA via a bead-based assay, followed by the coupling of the linker to the surface of the cells. Importantly, it was investigated whether the peptide linker is stable in serum-enriched medium and can be cleaved from the surface of the cells upon incubation with the enzymes.

2 MATERIALS AND METHODS

2.1 CD8$^+$ T lymphocyte culture

Female C57BL/6 mice were purchased from Harlan Laboratories (Gannat, France) and housed in a specific pathogen free (SPF) facility according to the regulations of the Belgian law and the local Ethical Committee. CD8$^+$ T cells were isolated from the spleen of mice using a negative isolation CD8$^+$ kit (Stem Cell Technologies, Grenoble, France). Cells were activated with anti-CD3/CD28 Dynabeads® (Gibco-Invitrogen, Merelbeke, Belgium) at a density of 2 x 10^6 cells/well and a bead-to-cell ratio of 1:1 in a 24-well plate. The cells were cultured in complete T cell culture medium containing advanced RPMI medium (Gibco-Invitrogen) supplemented with 10% fetal bovine serum (FBS; Hyclone, Thermo Scientific, MA, USA), 2 mM L-glutamine (Gibco-Invitrogen), 1% penicillin/streptomycin (Gibco-Invitrogen). According to the manufacturer's protocol, 30 U ml^{-1} rIL-2 (Miltenyi Biotec, Leiden, The Netherlands) was added to the culture medium. For the experiments described in this study, cells were activated during 5-10 days.

2.2 Preparation of liposomes and characterization

The liposomes were composed of 1,2-dioleoyl-sn-glycero-3-phosphocholine (DOPC), egg phosphatidyl glycerol (egg PG), 18:1 1,2-dioleoyl-sn-glycero-3-phosphoethanolamine-N-[3-(2-pyridyldithio)propionate] (PE-PDP), 1,2-distearoyl-sn-glycero-3-phosphoethanolamine-N-[PDP(polyethylene glycol)-2000] (PE-PEG-PDP), 18:1 1,2-dioleoyl-sn-glycero-3-phosphoethanolamine-N-[4-(p-maleimidophenyl)butyramide] (PE-MAL), and the fluorescent 1,1'-dioctadecyl-3,3,3',3'-tetramethylindodicarbocyanine (DiD). All lipids were purchased from Avanti Polar Lipids (Alabaster, USA) and DiD from Molecular probes (Invitrogen, Merelbeke, Belgium). To create the liposomes, a lipid mixture in chloroform was prepared and pipetted in a round-bottom glass flask, followed by evaporation of the chloroform solvent to form a thin lipid film. The dried lipids were rehydrated in phosphate buffered saline (PBS; Gibco-Invitrogen) at ambient temperature followed by an extrusion of the resultant multilamellar liposomes through a 200 nm polycarbonate filter (Whatman, Diegem, Belgium).

2.3 Evaluation of the enzymatic cleavability of the peptide linker

A mixture of 50 µl peptide linker (200 µg ml^{-1}, Eurogentec, Seraing, Belgium) with 1 µl of EasySep™ Streptavidin RapidSpheres™ (Stem Cell Technologies) was incubated for 10 min at room temperature in a Falcon™ round-bottom polystyrene tube (Corning, Lasne, Belgium). Next, Bodipy® FL-labeled L-cystine (Molecular Probes) was incubated for 45 min at room temperature in 0.5 mg ml^{-1} Tris(2-carboxyethyl)phosphine hydrochloride (TCEP; Sigma-Aldrich, Diegem, Belgium) solution to generate a reduction of the disulfide bond and the subsequent formation of Bodipy® FL-labeled cysteine [22].The reduced cysteine form

was added to the mixture and incubated for 15 min at room temperature. Subsequently, 150 µl PBS supplemented with 1mM ethylenediaminetetraacetic acid (EDTA; Sigma-Aldrich) was added to the mixture and the tube was placed into an EasySep™ Magnet (Stem Cell Technologies). After 1 min, the unbound solution was removed and the magnetic beads were washed two times with 200 µl PBS-EDTA to remove the unbound peptide linker and labeled cysteine. Subsequently, the magnetic beads were incubated for 30 min at 37°C with 100 µl of recombinant human matriptase (1-100 nM) or recombinant human urokinase-type plasminogen activator (uPA; 0.065-6.5 mg ml^{-1}) diluted in PBS-EDTA, and 0.05% trypsin-EDTA (Gibco-Invitrogen). Matriptase and uPA were both purchased from R&D systems (Minneapolis, USA). Next, the tubes were placed in the magnet for 1 min and the unbound solution was transferred to a black 96-well plate for measuring the fluorescence intensity via an EnVision® Multilabel plate reader (Perkin Elmer, Zaventem, Belgium).

2.4 Coupling of PDP- and MAL-functionalized liposomes to $CD8^+$ T cells and incubation in serum-containing media

$CD8^+$ T cells that were activated during 6-15 days were separated from the activation beads and incubated in serum-free advanced RPMI medium with 2 mg ml^{-1} PG, PDP or MAL-functionalized liposomes during 45 min at 37°C. The cells were washed with PBS buffer to remove the unbound liposomes and subsequently incubated with mounting concentrations of FBS (0.5-50% diluted in PBS) for 30 min at 37°C. The cells were washed to remove the released liposomes. The amount of liposomes attached to the $CD8^+$ T cells was quantified via flow cytometry by measuring the DiD fluorescence intensity per cell, using a FACSCalibur™ (BD Pharmingen, Erembodegem, Belgium) and analyzed by BD CellQuest™ and FlowJo (Treestar Inc, Ashland, USA) software.

2.5 Coupling of the peptide linker to $CD8^+$ T cells and measuring stability in serum-containing media

The activated $CD8^+$ T cells were first separated from the activation beads followed by the incubation with mounting concentration of peptide linker, ranging from 2-500 mg ml^{-1} for 30 min at 37°C. The cells were washed two times with PBS buffer supplemented with 0.1% bovine serum albumin (BSA buffer; Sigma-Aldrich), followed by the incubation with 50 µg ml^{-1} Alexa Fluor® 488-labeled streptavidin (Molecular Probes) for 15 min at room temperature. After two washing steps with 0.1% BSA buffer, the coupling of peptide linker to $CD8^+$ T cells was quantified by measuring the Alexa Fluor® 488 fluorescence intensity per cell via flow cytometry. To further evaluate the amount of labeled streptavidin necessary to obtain saturation of the peptide linker, mounting concentrations of labeled streptavidin (50-500 µg ml^{-1}) were added to $CD8^+$ T cells that were first incubated with 20 mg ml^{-1} of peptide linker. To evaluate the stability in serum, the cells were incubated with two different

concentrations of FBS (5 and 50% of FBS in PBS) for 30 min at 37°C, followed by washing the cells with PBS to remove the cleaved peptide linker.

2.6 Evaluation of the enzymatic cleavage when anchored to CD8$^+$ T cells

After incubating CD8$^+$ T cells with the peptide linker (20 µg ml^{-1}) and Alexa Fluor® 488-labeled streptavidin (50 µg ml^{-1}) as described above, the cells were incubated for 30 min at 37°C with mounting concentrations of matriptase (10-100 nM) and uPA (1.3-13 µg ml^{-1}). As a control, cells were incubated with 0.05% trypsin-EDTA for 4 min at 37°C. The cells were washed two times with 0.1% BSA buffer to remove the cleaved peptide linker, followed by the quantification of cleavage using flow cytometry.

2.7 Biotinylation of T cells and visualization by confocal microscopy

Activated CD8$^+$ T cells were incubated for 15 min at room temperature with mounting concentrations of a biotin 3-sulfo-N-hydroxysuccinimide ester sodium salt (Biotin-sulfo-NHS; Sigma-Aldrich), ranging from 0.1 to 100 µM in 0.1% BSA buffer. Cells were washed two times with 0.1% BSA buffer, followed by the incubation with 50 µg ml^{-1} Alexa Fluor® 488-labeled streptavidin for 15 min at room temperature. Cells were washed two times to remove the unbound streptavidin, prior to determining the biotinylation of CD8$^+$ T cells using flow cytometry. Confocal microscopy images of biotinylated CD8$^+$ T cells were acquired using a Nikon C1si confocal laser scanning microscope (Nikon Benelux, Brussels, Belgium) equipped with a Plan Apo VC 60x 1.4 NA oil immersion objective lens (Nikon). The Alexa Fluor® 488 dye was excited with a 488 nm argon-ion laser (CVI Melles Griot, NM, USA).

2.8 Coupling of liposomes to CD8$^+$ T cells via a peptide linker

The activated CD8$^+$ T cells were first biotinylated as described above. To this end, 50 µM of biotin-sulfo-NHS was incubated with the cells. After a washing step with 0.1% BSA buffer, the biotinylated cells were incubated for 15 min at room temperature with 50 mg ml^{-1} streptavidin (from *S.avidinii*, Invitrogen). Before adding the liposomes, the cells were washed to remove unbound streptavidin. The liposomes were prepared as described above and consisted of DOPC, PE-PDP or PE-PEG-PDP, and DiD in a wt% ratio of 87:10:3. The liposomes were first mixed for 15 min at 37°C with the peptide linker, which consisted of a liposome concentration of 0.5 mg ml^{-1} and peptide linker concentration of 0.1 mg ml^{-1}. Next, 50 µl of this liposome solution was added to 5 x 10^5 of (biotinylated) CD8$^+$ T cells and incubated for 15 min at 37°C. The cells were washed two times with 0.1% BSA buffer to remove the unbound liposomes. Subsequently, the cells were incubated with matriptase (100nM) or uPA (13 µg ml^{-1}) for 45 min at 37°C. As a control, cells were incubated with 0.05% trypsin-EDTA for 4 min at 37°C. The cells were washed and the liposome coupling

was quantified by measuring the fluorescence intensity of the DiD label using flow cytometry.

2.9 Statistical analysis

A two-tailed Student's t-test was performed to determine statistical differences between datasets. All statistical analyses were performed using GraphPad Prism 6 software (La Jolla, CA, USA). p-values <0.05 were regarded significant. Statistical significance is indicated as follows: * p <0.05, ** p <0.01, *** p <0.001, **** p <0.0001.

3 RESULTS AND DISCUSSION

To evaluate the reversible coupling of liposomes to the surface of $CD8^+$ T cells via an enzyme-sensitive coupling system, a cleavable peptide linker construct was developed. In **Figure 1**, the enzyme-targeted amino-acid sequence is indicated in bold with on both sides of the sequence glycine/serine-rich flanking sequences (indicated in gray). The sequence of the cleavable peptide within this construct was based on a study by Desnoyers *et al.*, who selected this peptide sequence by a CLiPS library [14]. This library allows determining a peptide sequence that is cleavable by a selected set of proteases. In this case, proteases with well-known upregulation in several cancer types were selected, including matriptase, urokinase-type plasminogen activator (uPA), and legumain. For our purpose, the peptide linker was further optimized to enable attachment with the $CD8^+$ T cell on one side and on the other side with the liposomes. To this end, a maleimide (MAL) and a biotin group were incorporated on opposite sides of the peptide sequence, enabling interaction with T cell exofacial thiol (as described in **Chapter 3**) and biotinylated liposomes, respectively (**Figure 1**).

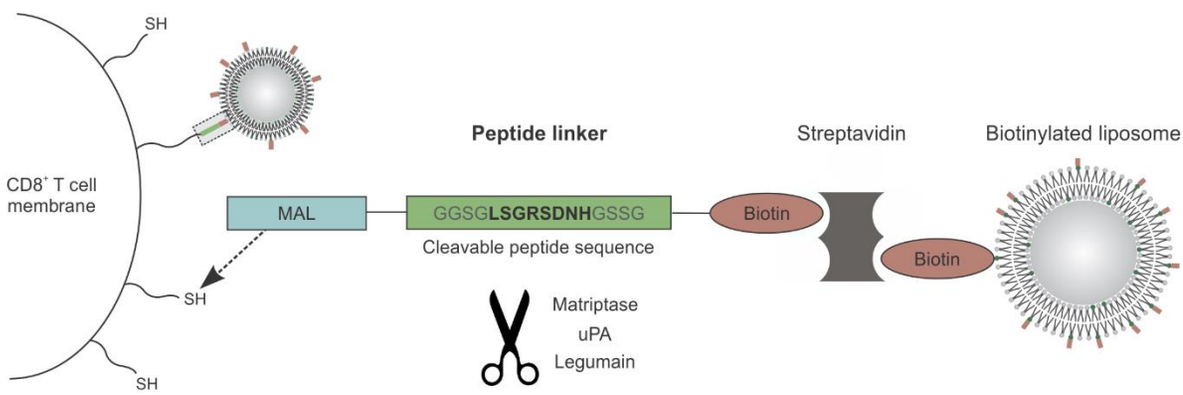

Figure 1. Schematic overview of the peptide linker construct. The peptide linker consists of a maleimide (MAL) group, a cleavable peptide region, and a biotin group. The cleavable peptide contains the specific cleavage sequence as indicated in bold, flanked by glycine/serine-rich short unspecific sequences as indicated in gray. The MAL group can form a stable thioether bond upon interaction with exofacial thiol groups at the $CD8^+$ T cell surface. Subsequently, a streptavidin group is added to attach the peptide linker to the biotinylated liposomes. The peptide linker can specifically be cleaved by three proteases: matriptase, urokinase-type plasminogen activator (uPA), and legumain. G, glycine; S, serine; L, leucine; R, arginine; D, aspartic acid; N, asparagine; H, histidine; SH, thiol.

3.1 Magnetic bead-based assay to assess enzymatic cleavability of the peptide linker

First, it was assessed whether the novel synthesized peptide linker can be cleaved by the suggested enzymes. To this end, the peptide linker was conjugated to streptavidin-functionalized magnetic beads via a biotin-streptavidin interaction, as shown in **Figure 2A**. To quantify the cleavage, the peptide linker-bead construct was incubated with fluorescently-labeled cysteine, which forms a stable thioether bond with the MAL group of

the peptide linker. Matriptase and uPA were selected to evaluate the cleavability of the linker and were added to the construct in mounting concentrations. Subsequently, the beads were placed into a magnet and the medium, containing cleaved material, was transferred to a 96-well plate. The data showed that cleavage by matriptase and uPA increased as a function of their concentration (**Figures 2B-C**). The highest concentration had a similar cleavage as trypsin, which was added as a positive control for the cleavability, as trypsin is a highly unspecific protease [23]. Based on these results, we could conclude that both matriptase and uPA were able to cleave the peptide construct.

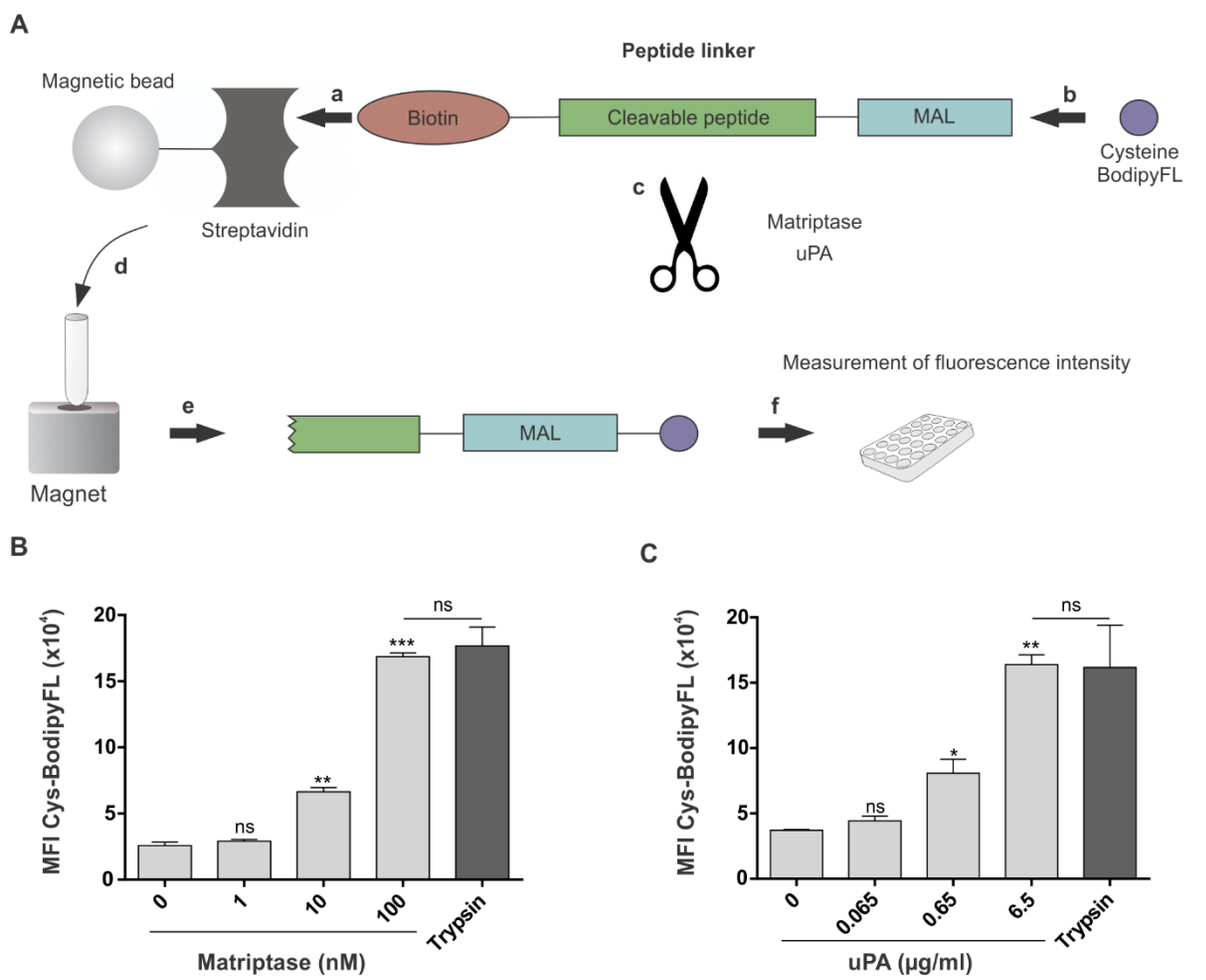

Figure 2. Evaluation of matriptase and urokinase-type plasminogen activator (uPA) enzymatic cleavage of the peptide linker. (A) a The peptide linker that contains a biotin group, the cleavable sequence, and a maleimide (MAL) group can interact with streptavidin on magnetic beads via a biotin-streptavidin interaction. **b** Subsequently, it was incubated with Bodipy® FL cysteine (Cys-BodipyFL) that can bind to the MAL group of the peptide linker. **c** The peptide linker-bead construct was incubated with mounting concentrations of either matriptase or uPA. **d** After incubation with the enzymes, the tube containing the peptide linker-bead construct was placed into a magnet. **e** The medium containing cleaved material was removed to a 96-well plate. **f** The mean fluorescence intensity per sample was measured in a plate reader. **(B)** The peptide linker-bead construct was incubated with mounting concentrations of matriptase, ranging from 10 to 100 nM and **(C)** uPA, ranging from 0.065 to 6.5 µg ml^{-1}. Trypsin was used as a positive control for the cleavability. Graphs are representing the mean fluorescence intensity (MFI) per sample ± SD. Statistics are indicated as ns = not significant; * p <0.05; ** p <0.01; *** p <0.001 (n = 2 independent samples).

3.2 Coupling of the peptide linker to CD8⁺ T cells

In a next step, we evaluated the attachment of this peptide linker to the surface of CD8⁺ T cells. As shown in **Figure 3A**, the coupling between the construct and the cells is based on a MAL group interacting with exofacial thiol groups at the cell surface, which is similar to the anchoring of MAL-functionalized liposomes as described in **Chapter 3**.

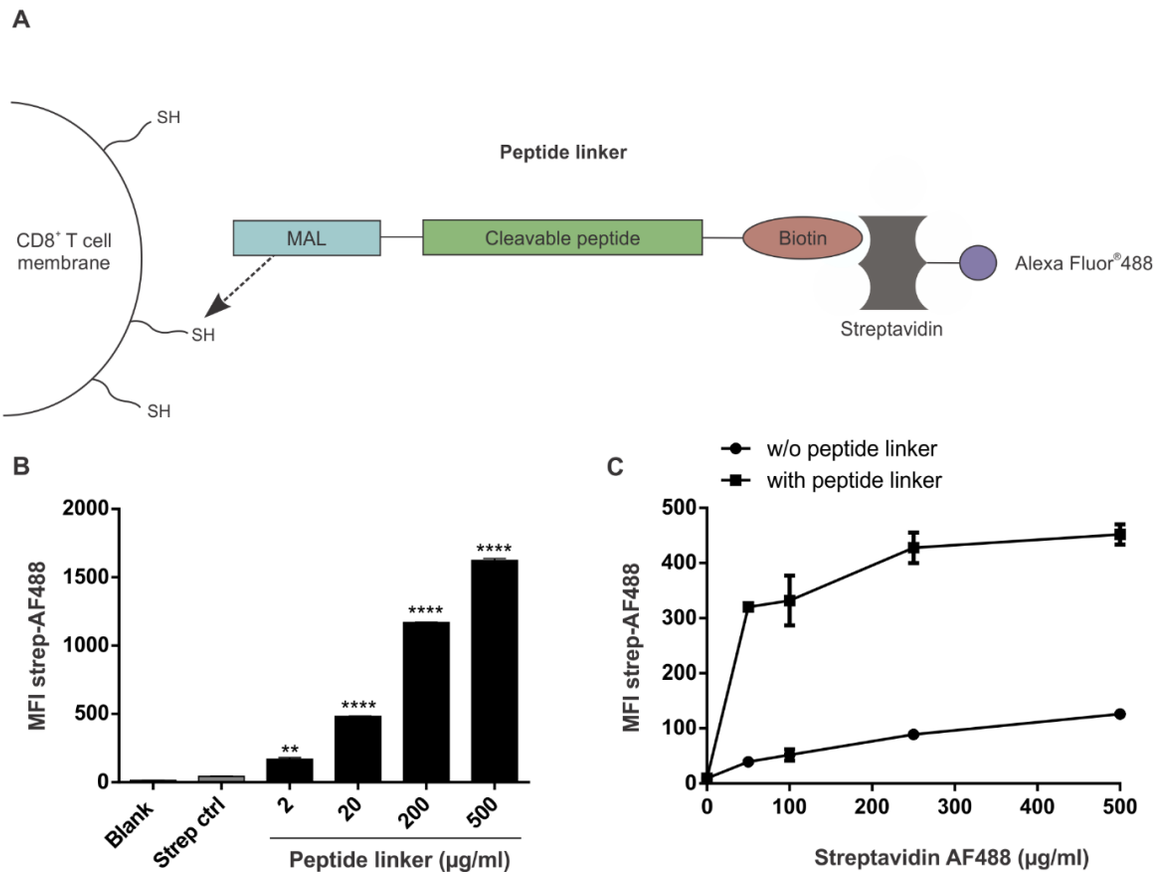

Figure 3. Coupling of a cleavable peptide linker to the surface of CD8⁺ T cells. (A) Schematic overview of the attachment of a cleavable peptide linker to the surface of activated CD8⁺ T cells via a thioether bond between exofacial thiol groups of CD8⁺ T cells and a maleimide (MAL) group incorporated in the peptide linker construct. Subsequently, the cells were incubated with Alexa Fluor® 488-labeled streptavidin to quantify the coupling via flow cytometry. **(B)** Graph representing mean fluorescence intensity (MFI) per cell ± SD of the CD8⁺ T cells incubated with mounting concentrations of peptide linker (2-500 µg ml^{-1}), followed by the incubation with 50 µg ml^{-1} Alexa Fluor® 488-labeled streptavidin (strep-AF488). As a control, cells were incubated with labeled streptavidin without linker (Strep ctrl). **(C)** Graph representing MFI ± SD of cells incubated with 20 µg ml^{-1} peptide linker, followed by the incubation with mounting concentrations of labeled streptavidin (50-500 µg ml^{-1}). As a control, CD8⁺ T cells were incubated with labeled streptavidin without peptide linker. Statistics represent a comparison with the 'Strep ctrl' and are indicated as ns = not significant; ** p <0.01; **** p <0.0001 (n = 2 independent samples).

First, the peptide linker was added to the cells in mounting concentrations, followed by incubation with fluorescently-labeled streptavidin to quantify the binding efficiency (**Figure 3B**). As a negative control, cells were incubated with labeled streptavidin alone. These data show the highly specific interaction of labeled streptavidin with the peptide linker and consequently an efficient attachment of peptide linker to T cells. As for a peptide linker concentration of 20 µg ml^{-1}, all cells were positive for the coupling of a peptide linker, this

concentration was selected for further research (data not shown). In order to quantify the cleavability of this peptide construct from the cell surface by specific enzymes, the peptide linkers need to be saturated with labeled streptavidin. To evaluate this, cells that were pretreated with or without 20 µg ml^{-1} peptide linker were incubated with mounting concentrations of labeled streptavidin (**Figure 3C**). Based on these data, a streptavidin concentration of 250 µg ml^{-1} was selected for further research.

3.3 Stability of the peptide linker in serum and the enzymatic cleavage when anchored to CD8$^+$ T cells

As mentioned in the introduction, the stability of redox-sensitive systems in the systemic circulation cannot be absolutely guaranteed. Therefore, we aimed to investigate the serum stability of PG-, PDP- and MAL-coupled liposomes (**Chapters 2 and 3**) as well as the peptide linker presented in this chapter. First, we compared the stability of aspecifically attached (PG) liposomes with the reversibly attached (PDP) liposomes and stably anchored (MAL) liposomes in fetal bovine serum (FBS) concentrations, ranging from 0.5 to 50% (**Figure 4**). For PG liposomes, an immediate release at 0.5% was observed while PDP and MAL liposomes remained attached. However, mounting the concentration up to 5%, ~40% of the PDP liposomes were detached from the surface. The MAL liposomes only showed a minor release, even when incubated with 50% FBS.

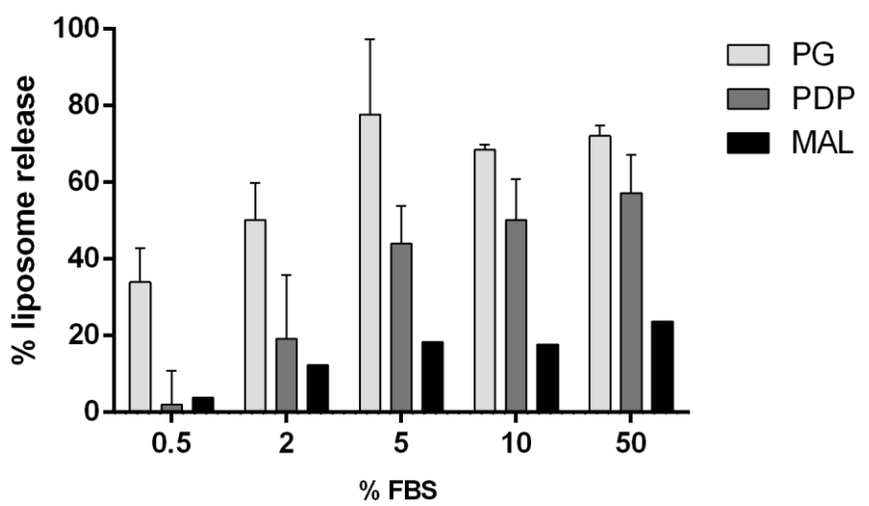

Figure 4. Stability of PDP- and MAL-liposome coupling to CD8$^+$ T cells as a function of the serum concentration. CD8$^+$ T cells were first incubated with 2 mg ml^{-1} PG, PDP or MAL liposomes, followed by the incubation with mounting percentages of fetal bovine serum (FBS) in PBS. The percentage of liposome release was quantified by measuring the mean fluorescence intensity per cell of the DiD-labeled liposomes using flow cytometry. The percentage of released liposomes was quantified by a comparison with cells that were not incubated with FBS. The graph represents the percentage liposome release ± SD (PG: n = 3; PDP: n = 4; MAL: n = 1 with n = number of independent experiments).

Next, we investigated whether the peptide linker performs better in FBS-enriched medium. As represented in **Figure 5A**, the attachment of the peptide linker to $CD8^+$ T cells was stable, even at the highest FBS concentration. Having established the stability of the linker in the systemic circulation, we next aimed to assess the specific cleavability by tumor-associated proteases. Unfortunately, incubating this peptide linker attached to T cells with both matriptase and uPA only resulted in a minor cleavage of less than 20% (**Figure 5B**).

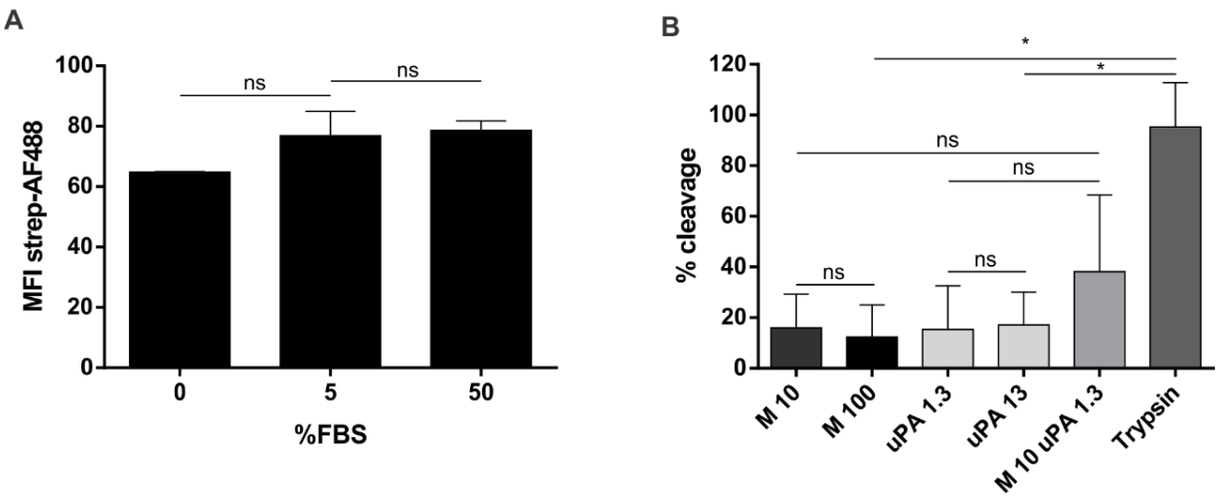

Figure 5. Stability of the peptide linker in serum and cleavage upon incubation with matriptase and urokinase-type plasminogen activator (uPA). $CD8^+$ T cells were first coupled with 20 µg ml^{-1} of the peptide linker, followed by the incubation with 250 µg ml^{-1} Alexa Fluor® 488-labeled streptavidin. **(A)** Graph representing the mean fluorescence intensity (MFI) ± SD of cells subsequently incubated with PBS supplemented with two concentrations of fetal bovine serum (FBS). **(B)** Graph representing the percentage linker cleavage ± SD of cells incubated with different concentrations of matriptase (M; 10-100 nM), uPA (1.3-13 µg ml^{-1}), a combination of both specific enzymes, and 0.05% trypsin. Statistics are indicated as ns = not significant; * p <0.05 (n = 2 independent samples).

Even when combining both enzymes, no significant increase in cleavage could be observed while trypsin, used as a positive control, resulted in almost a complete cleavage of the peptide linker from the cell surface. The fact that trypsin, as a highly unspecific protease, is able to cleave a variety of surface receptors, may suggest that steric hindrance at the cell surface is a major limiting step for the specific enzymes to interact with the peptide linker.

3.4 Evaluation of the reversible coupling of liposomes to $CD8^+$ T cells via an enzyme-sensitive linker

In an attempt to avoid that steric hindrance of the cell membrane impedes the cleavage, we inverted the system, which means that the biotin-streptavidin interaction appears at the cell surface and the interaction with the liposomes occurs via the interaction of the MAL group from the peptide linker with PDP groups incorporated in the liposomes (**Figure 6A**). The reason behind this switch is the hypothesis that streptavidin, with its high molecular weight of 60 kDa, increases the distance between the cleavable peptide and the cell surface, which might reduce the steric hindrance [24].

To enable a biotin-streptavidin interaction at the cell surface, the CD8$^+$ T cells were first biotinylated via incubation with biotin sulfo-*N*-hydroxysuccinimide ester (biotin-sulfo-NHS). Upon interaction of the NHS group with surface amines, the cell surface is decorated with biotin groups. It has been shown previously that biotinylation of cells does not affect their phenotype, viability or homing ability [25]. Additionally, a biotin-streptavidin interaction has already been exploited for the successful conjugation of particles to the surface of mesenchymal stem cells [26].

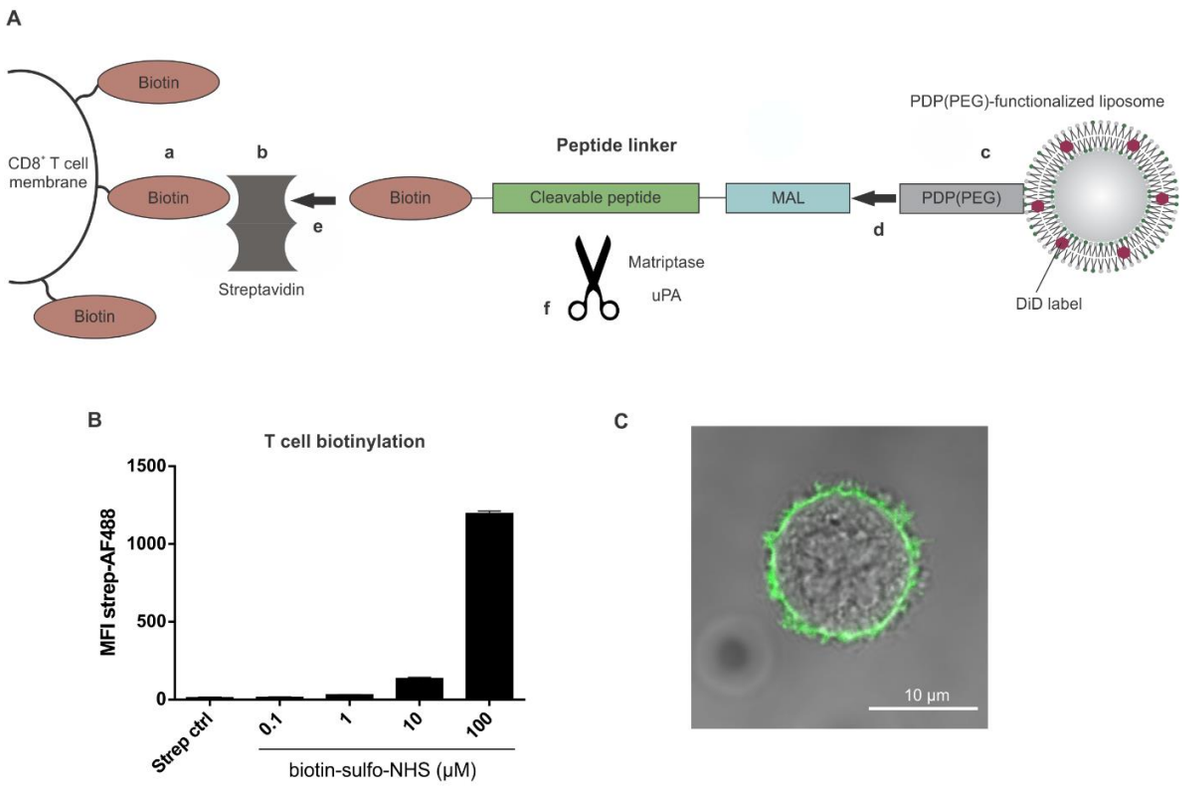

Figure 6. Biotinylation of CD8$^+$ T cells to attach liposomes via a peptide linker. (A) a CD8$^+$ T cells were biotinylated by incubating the cells with 50 µM biotin-sulfo-NHS. **b** After biotinylation, the cells were incubated with 50 mg ml^{-1} streptavidin. **c** DiD-labeled liposomes were prepared containing 10 wt% PE-PDP or PE-PEG-PDP lipids. **d** Next, the liposomes were incubated with the peptide linker to form a stable bond via the maleimide (MAL) group of the peptide linker. **e** The liposome-peptide construct was incubated with CD8$^+$ T cells, which results in the coupling of liposomes to the cell surface via a biotin-streptavidin interaction. **f** The cells were incubated with both matriptase and urokinase-type plasminogen activator (uPA) to initiate the cleavage of the peptide bond. **(B)** Graph representing the mean fluorescence intensity (MFI) ± SD of biotinylated CD8$^+$ T cells by incubating the cells with mounting concentrations of biotin-sulfo-NHS (0.1-100 µM), followed by the incubation with 50 µg ml^{-1} Alexa Fluor® 488-labeled streptavidin. As a control, cells were only incubated with labeled streptavidin (Strep ctrl). **(C)** Confocal image of a CD8$^+$ T cell incubated with 100 µM biotin-sulfo-NHS and 50 µg ml^{-1} Alexa Fluor® 488-labeled streptavidin (Scale bar = 10 µm).

In this study, CD8$^+$ T cells were first biotinylated via incubation with biotin-sulfo-NHS, followed by the incubation with streptavidin (**Figure 6A**). Secondly, DiD-labeled PDP-functionalized liposomes were prepared and incubated with the peptide linker. Finally, the linker-modified liposomes were attached to the T cell surface via a biotin-streptavidin interaction, which has been described in the literature as a very stable bond and resistant to extreme pH, high temperature, and proteolytic enzymes [27, 28]. First, it was verified

whether the surface of $CD8^+$ T cells could easily be biotinylated. As represented in **Figure 6B**, increasing the amount of biotin-sulfo-NHS up to 10 or 100 µM resulted in specific binding of labeled streptavidin. Confocal imaging of the biotinylated T cells revealed the homogenous distribution of the biotin-streptavidin interaction over the cell surface (**Figure 6C**).

Next, we evaluated the coupling of both PEGylated and non-PEGylated PDP-functionalized liposomes. We anticipated that by using a PEG spacer between the liposomes and the peptide linker, steric hindrance due to the attached liposomes might be diminished and subsequently facilitate the interaction of specific enzymes with the cleavable peptide sequence. PDP-functionalized liposomes can interact with a MAL group as previously shown by Geers et al [29]. Unfortunately, it was shown that the coupling was lower for liposomes that were first incubated with the peptide linker compared to the unmodified PDP liposomes, independent of PEGylation (**Figures 7A-B**). This implies that the coupling via this peptide linker construct is less efficient than the disulfide bridges as described in **Chapters 2 and 3**.

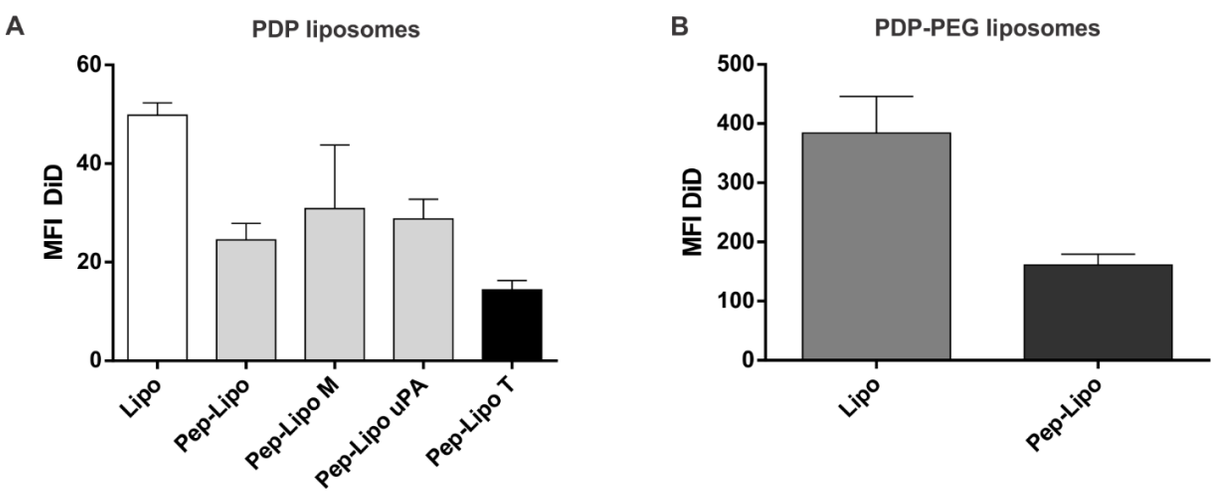

Figure 7. Coupling of liposomes to the surface of $CD8^+$ T cells via an enzyme-sensitive linker. (A) Graphs representing the mean fluorescence intensity (MFI) ± SD of DiD label that was incorporated into the PDP-functionalized liposomes. $CD8^+$ T cells were first biotinylated, followed by the incubation with 50 µg ml^{-1} streptavidin. Next, the liposomes (Lipo) were incubated with or without peptide linker (Pep), followed by the incubation with biotinylated cells. Subsequently, the liposome-loaded cells were incubated with 100 nM matriptase (M), 13 µg ml^{-1} urokinase-type plasminogen activator (uPA) or 0.05% trypsin (T). **(B)** Graphs representing MFI ± SD of DiD that was incorporated together with PE-PEG-PDP lipids in liposomes (Lipo) that were first incubated with (Pep-Lip) or without (Lipo) peptide linker, followed by the incubation with biotinylated $CD8^+$ T cells (*n* = 2 independent samples).

After attachment of PDP liposomes to the T cells via the peptide linker, the cells were incubated with both matriptase and uPA. Unfortunately, no cleavage could be observed as represented in **Figure 7A**. Additionally, as a positive control, cells were treated with trypsin, which resulted in a moderate cleavage of ~40%. In summary, taken together this lower coupling efficiency and no cleavage upon incubation with specific tumor-associated enzymes, we have to conclude that this peptide linker is likely not suitable for this purpose and does not provide benefit over the PDP coupling approach. In the study by Desnoyers *et al.*, the cleavage of a similar peptide linker from an antibody as a prodrug strategy was

very successful for both matriptase and uPA [14]. However, in our strategy, we are confronted with the very complex and highly dynamic nature of the cell membrane, which was shown to be a considerable obstacle for this enzyme-sensitive approach [30].

4 CONCLUSION

For the coupling of liposomes to the surface of $CD8^+$ T cells, it was shown that finding a balance between good stability in serum and optimal triggered release via tumor microenvironmental stimuli is not a simple task. As was shown for the reversible coupling by PDP-functionalized liposomes, the coupling of the PDP linker was reversible upon incubation in glutathione, however not sufficiently stable in serum. In search for a more specific triggered system, we developed a novel linker containing a cleavable peptide. Although cleavability of this linker by specific enzymes such as matriptase and urokinase-type plasminogen activator (uPA) was shown when the linker was attached to magnetic beads and good stability was obtained in serum-containing media, the cleavability when coupled to $CD8^+$ T cells was highly limited. We hypothesized that steric hindrance by the highly complex cell membrane might interfere with the interaction of specific enzymes with the peptide linker. Moreover, as coupling of liposomes via this linker was lower compared to the coupling without linker, we have to conclude that the tested linker is not suitable for this reversible coupling system.

ACKNOWLEDGEMENTS

Laura Wayteck is a doctoral fellow of the Institute for the Promotion of Innovation through Science and Technology in Flanders, Belgium (IWT-Vlaanderen). Koen Raemdonck is a postdoctoral fellow of the Research Foundation-Flanders, Belgium (FWO-Vlaanderen). Koen Raemdonck received additional financial support via a FWO Research Grant (Krediet aan Navorsers).

REFERENCES

1. Durymanov, M.O., Rosenkranz, A.A. & Sobolev, A.S. Current Approaches for Improving Intratumoral Accumulation and Distribution of Nanomedicines. *Theranostics* **5**, 1007-20 (2015).
2. Butera, D., Cook, K.M., Chiu, J., Wong, J.W. & Hogg, P.J. Control of blood proteins by functional disulfide bonds. *Blood* **123**, 2000-7 (2014).
3. Zhu, L. & Torchilin, V.P. Stimulus-responsive nanopreparations for tumor targeting. *Integr Biol (Camb)* **5**, 96-107 (2013).
4. Geers, B. et al. Targeted liposome-loaded microbubbles for cell-specific ultrasound-triggered drug delivery. *Small* **9**, 4027-35 (2013).
5. Viger, M.L. et al. Near-infrared-induced heating of confined water in polymeric particles for efficient payload release. *ACS Nano* **8**, 4815-26 (2014).
6. Mooney, R. et al. Conjugation of pH-responsive nanoparticles to neural stem cells improves intratumoral therapy. *J Control Release* **191**, 82-9 (2014).
7. Ge, Z. & Liu, S. Functional block copolymer assemblies responsive to tumor and intracellular microenvironments for site-specific drug delivery and enhanced imaging performance. *Chem Soc Rev* **42**, 7289-325 (2013).
8. Torchilin, V. Multifunctional and stimuli-sensitive pharmaceutical nanocarriers. *Eur J Pharm Biopharm* **71**, 431-44 (2009).
9. McNeeley, K.M., Karathanasis, E., Annapragada, A.V. & Bellamkonda, R.V. Masking and triggered unmasking of targeting ligands on nanocarriers to improve drug delivery to brain tumors. *Biomaterials* **30**, 3986-95 (2009).
10. Hanahan, D. & Weinberg, R.A. Hallmarks of cancer: the next generation. *Cell* **144**, 646-74 (2011).
11. Zhu, L., Kate, P. & Torchilin, V.P. Matrix metalloprotease 2-responsive multifunctional liposomal nanocarrier for enhanced tumor targeting. *ACS Nano* **6**, 3491-8 (2012).
12. Zhu, L., Wang, T., Perche, F., Taigind, A. & Torchilin, V.P. Enhanced anticancer activity of nanopreparation containing an MMP2-sensitive PEG-drug conjugate and cell-penetrating moiety. *Proc Natl Acad Sci U S A* **110**, 17047-52 (2013).
13. Hatakeyama, H. et al. Systemic delivery of siRNA to tumors using a lipid nanoparticle containing a tumor-specific cleavable PEG-lipid. *Biomaterials* **32**, 4306-16 (2011).
14. Desnoyers, L.R. et al. Tumor-specific activation of an EGFR-targeting probody enhances therapeutic index. *Sci Transl Med* **5**, 207ra144 (2013).
15. List, K., Bugge, T.H. & Szabo, R. Matriptase: potent proteolysis on the cell surface. *Mol Med* **12**, 1-7 (2006).
16. Uhland, K. Matriptase and its putative role in cancer. *Cell Mol Life Sci* **63**, 2968-78 (2006).
17. Ulisse, S., Baldini, E., Sorrenti, S. & D'Armiento, M. The urokinase plasminogen activator system: a target for anti-cancer therapy. *Curr Cancer Drug Targets* **9**, 32-71 (2009).
18. Noh, H., Hong, S. & Huang, S. Role of urokinase receptor in tumor progression and development. *Theranostics* **3**, 487-95 (2013).
19. Duffy, M.J. et al. Urokinase-plasminogen activator, a marker for aggressive breast carcinomas. Preliminary report. *Cancer* **62**, 531-3 (1988).

20. Vandooren, J., Opdenakker, G., Loadman, P.M. & Edwards, D.R. Proteases in cancer drug delivery. *Adv Drug Deliv Rev* **97**, 144-55 (2016).
21. Liu, C., Sun, C.Z., Huang, H.N., Janda, K. & Edgington, T. Overexpression of legumain in tumors is significant for invasion/metastasis and a candidate enzymatic target for prodrug therapy. *Cancer Research* **63**, 2957-2964 (2003).
22. Stephan, M.T., Moon, J.J., Um, S.H., Bershteyn, A. & Irvine, D.J. Therapeutic Cell Engineering Using Surface-Conjugated Synthetic Nanoparticles. *Journal of Immunotherapy* **16**, 1035-41 (2010).
23. Beliveau, F., Desilets, A. & Leduc, R. Probing the substrate specificities of matriptase, matriptase-2, hepsin and DESC1 with internally quenched fluorescent peptides. *Febs Journal* **276**, 2213-2226 (2009).
24. Kobayashi, H. et al. Comparison of the chase effects of avidin, streptavidin, neutravidin, and avidin-ferritin on a radiolabeled biotinylated anti-tumor monoclonal antibody. *Jpn J Cancer Res* **86**, 310-4 (1995).
25. Zhao, W. et al. Cell-surface sensors for real-time probing of cellular environments. *Nat Nanotechnol* **6**, 524-31 (2011).
26. Cheng, H. et al. Nanoparticulate cellular patches for cell-mediated tumoritropic delivery. *ACS Nano* **4**, 625-31 (2010).
27. Holmberg, A. et al. The biotin-streptavidin interaction can be reversibly broken using water at elevated temperatures. *Electrophoresis* **26**, 501-10 (2005).
28. Sano, T., Vajda, S., Reznik, G.O., Smith, C.L. & Cantor, C.R. Molecular engineering of streptavidin. *Ann N Y Acad Sci* **799**, 383-90 (1996).
29. Geers, B. et al. Self-assembled liposome-loaded microbubbles: The missing link for safe and efficient ultrasound triggered drug-delivery. *J Control Release* **152**, 249-56 (2011).
30. McMahon, H.T. & Gallop, J.L. Membrane curvature and mechanisms of dynamic cell membrane remodelling. *Nature* **438**, 590-6 (2005).

5

Delivery of small interfering RNA to cytotoxic T cells via vapor nanobubble photoporation

This chapter was submitted as:

Wayteck Laura[a], Xiong Ranhua[a,b], Braeckmans Kevin[a,b], De Smedt Stefaan[a], and Raemdonck Koen[a], Delivery of small interfering RNA to cytotoxic T cells via vapor nanobubble photoporation.

[a]Laboratory for General Biochemistry and Physical Pharmacy, Department of Pharmaceutical Sciences, Ghent University, Ottergemsesteenweg 460, 9000 Ghent, Belgium

[b]Center for Nano-and Biophotonics, Ghent University, Ottergemsesteenweg 460, 9000 Ghent, Belgium

ABSTRACT

The success of cancer immunotherapy through the adoptive transfer of cytotoxic T lymphocytes (CTLs) is highly dependent on the potency of the elicited anti-tumor responses generated by the transferred cells, which can be hindered by a variety of upregulated immunosuppressive pathways. Downregulation of these pathways in the T cells via RNA interference (RNAi) could significantly boost their capacity to infiltrate tumors, proliferate, persist and eradicate tumor cells, thus leading to a durable anti-tumor response. Unfortunately, it is well known that primary T cells are hard-to-transfect and conventional non-viral transfection agents are generally ineffective. Viral transduction and electroporation are more efficient but their use is restricted by high cost, safety issues, and cytotoxicity. Photoporation has recently gained interest as a gentle alternative physical approach to deliver membrane-impermeable macromolecules into cells. By attaching gold nanoparticles (AuNPs) to the cell surface followed by pulsed laser illumination, transient membrane pores can be generated that allow the diffusion of macromolecules directly into the cell cytosol. Here, we evaluated this technique for the non-toxic and effective delivery of siRNA and subsequent silencing of target genes in activated CTLs. We compared photoporation with nucleofection, the current standard physical technique for T cell transfection, and demonstrated a significantly reduced cytotoxicity and improved loading efficiency for the photoporation technique.

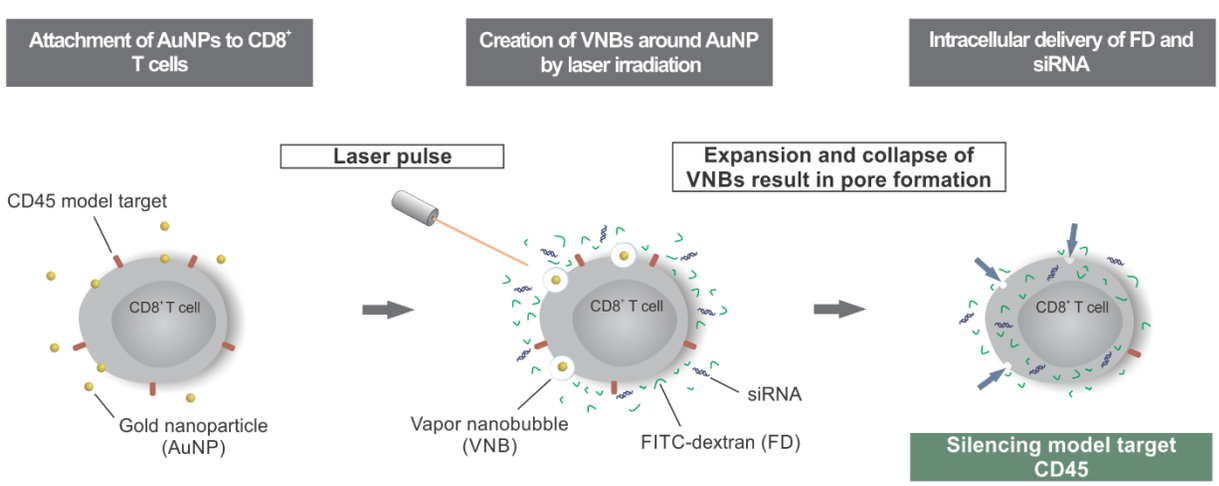

1 INTRODUCTION

As introduced in **Chapter 1**, adoptive T cell therapy (ACT) has emerged as a powerful approach to cure advanced cancers [1]. Although ACT already showed impressive clinical outcomes for specific types of cancer, *e.g.* melanoma, the number of patients that do not respond to the therapy remains high [2]. Indeed, many cancers have adopted a variety of strategies to escape immune surveillance, thus limiting the efficacy of ACT. Suppressive interactions between cytotoxic T cells (CTLs) and other cells within the tumor microenvironment are in part regulated by inhibitory immune checkpoint receptors present on the CTL surface, such as the cytotoxic T lymphocyte-associated antigen 4 (CTLA-4) and programmed cell death 1 (PD-1) [3]. Their blockage by monoclonal antibodies has shown durable clinical responses in a variety of tumors within the past years, underscoring the importance of such immunosuppressive signals on the clinical outcome of ACT [4-6]. However, the use of monoclonal antibodies is restricted to the inhibition of extracellular targets. Recent research elucidated various alternate immune-regulatory pathways that are active in the CTL cytoplasm and contribute to the impaired T cell-mediated anti-tumor response [7, 8]. Consequently, it is of outstanding interest to investigate to what extent inhibition of these intracellular pathways could further improve the efficacy of ACT [9].

RNA interference (RNAi) is a powerful tool that enables sequence-specific downregulation of gene expression using synthetic small interfering RNA (siRNA) molecules [10, 11]. Key to successful gene silencing is the efficient delivery of siRNAs to the cytosol of the target cells [12]. Although viral gene transfer results in acceptable transduction efficiency of T lymphocytes, the use of viral vectors is labor-intensive, expensive and associated with important safety concerns [13, 14]. On the other hand, primary T cells have been shown to be particularly hard-to-transfect via conventional non-viral transfection methods, such as lipid-and polymer-based nanoparticles [15-18]. Although few studies have shown significant silencing by siRNA-loaded nanoparticles in both $CD4^+$ and $CD8^+$ T lymphocytes, the majority of particles struggles with low endocytic uptake as well as the inefficient endosomal escape of siRNA molecules, factors that all contribute to their limited success so far [19-22]. Therefore, physical techniques such as electroporation might be favorable as they allow delivery of macromolecular drugs across the cell membrane directly into the cytosol [23]. Although it enables higher transfection efficiencies compared to nanoparticle-based delivery methods, cytotoxicity issues are a major limiting factor [18]. Hence, there is a need for practicable transfection methodologies to enable non-toxic and efficient siRNA delivery to primary T cells.

Within this study, we propose photoporation as an alternative physical technique to transfect primary CTLs with siRNA and this with significantly reduced cytotoxicity [24]. This approach transiently permeabilizes the plasma membrane by focusing nanosecond laser pulses onto cells with gold nanoparticles (AuNPs) attached to the cell surface. The property

of surface plasmon resonance allows AuNPs to efficiently absorb light and regulate the transfer of light energy in thermal energy. Short laser pulses of sufficiently high intensity cause a rapid increase in temperature of the irradiated AuNPs, causing the evaporation of water in their direct vicinity, resulting in the formation of vapor nanobubbles (VNBs) [25]. Within nanoseconds, the VNBs expand and collapse, thereby inducing local membrane damage by high-pressure shockwaves, forming reversible pores in the cell membrane through which surrounding macromolecules can directly enter into the cell's cytoplasm [26, 27]. The delivery of macromolecules such as siRNA to adherent tumor cell lines by this technique was recently successfully demonstrated by our research group, achieving efficient target gene knockdown with negligible cytotoxicity [28]. However, the value of photoporation for siRNA delivery to hard-to-transfect (primary) suspension cells such as CTLs remains to be explored.

Here, we report on the potential of VNB photoporation to silence target genes in CTLs. First, we assessed the optimal number of AuNPs per cell for safe and effective delivery of model macromolecules (10 kDa dextran) as well as siRNA in isolated murine $CD8^+$ T cells. In addition, we compared photoporation with nucleofection, which currently is the standard non-viral method for transfecting primary T lymphocytes. Although photoporation and nucleofection resulted in a comparable knockdown in the surviving cells, due to cell viability issues with the nucleofection technique, a higher amount of transfected cells is effectively achieved with photoporation. These results show the potential of VNB photoporation as a novel physical technique to efficiently and safely deliver distinct membrane-impermeable macromolecules to primary suspension cells for both therapeutic and diagnostic purposes.

2 MATERIALS AND METHODS

2.1 CD8$^+$ T lymphocyte culture

Female C57BL/6 mice were purchased from Harlan Laboratories (Gannat, France) and housed in a specific pathogen free (SPF) facility according to the regulations of the Belgian law and the local Ethical Committee. CD8$^+$ T cells were isolated from the spleen of mice using a negative isolation CD8$^+$ kit (Stem Cell Technologies, Grenoble, France). Cells were activated with anti-CD3/CD28 Dynabeads® (Gibco-Invitrogen, Merelbeke, Belgium) at a density of 2 x 10^6 cells/well and a bead-to-cell ratio of 1:1 in a 24-well plate. The cells were cultured in complete T cell culture medium containing advanced RPMI medium (Gibco-Invitrogen) supplemented with 10% fetal bovine serum (FBS; Hyclone, Thermo Scientific, MA, USA), 2 mM L-glutamine (Gibco-Invitrogen), 1% penicillin/streptomycin (Gibco-Invitrogen). According to the manufacturer's protocol, 30 U ml^{-1} rIL-2 (Miltenyi Biotec, Leiden, The Netherlands) was added to the culture medium. For the experiments described in this study, cells were activated during 6-8 days.

2.2 Determining the number of gold nanoparticles per cell

CD8$^+$ T cells were activated during 7 days and 2.4 x 10^5 cells were incubated with 1:70 and 1:350 dilutions of the stock concentration (8.2 x 10^{11} particles/ml) of 70 nm cationic gold nanoparticles (AuNPs, #CU11-70-P30-50, Nanopartz, Loveland, CO, USA). The AuNPs were diluted in T cell culture medium for incubation with the cells during 30 min or 1h at 37°C. The AuNPs had a zeta potential of 30 mV as measured by a Zetasizer Nano ZS (Malvern, UK) equipped with Dispersion Technology Software (DTS). Subsequently, the cells were washed with T cell culture medium to remove the unbound AuNPs. 4 x 10^4 cells were transferred to a glass-bottom 96-well plate for imaging. Confocal laser scanning microscopy (C1si, Nikon Benelux, Brussels, Belgium) in reflection mode with a 60× water immersion lens (Plan Apo 60x, NA 1.2, Nikon) was used to image AuNP adsorbed to the cell membrane. Microscopy images were analyzed in ImageJ (National Institutes of Health) to determine the number of AuNPs per cell.

2.3 Generation of vapor nanobubbles to deliver macromolecules to CD8$^+$ T cells

CD8$^+$ T cells were first incubated with AuNPs at varying concentrations for 30 min at 37°C in T cell culture medium, followed by a washing step with advanced RPMI medium to remove unbound AuNPs. Subsequently, the cells were resuspended in advanced RPMI medium supplemented with either 2 mg ml^{-1} FITC-labeled dextrans of 10 kDa alone (FD; Sigma-Aldrich, Bornem, Belgium) or combined with 5 µM Cy5-fluorescently labeled small interfering RNA (siRNA; Eurogentec, Seraing, Belgium). The cells were transferred to a 96-well plate to perform laser treatment. A homemade setup, including an optical system and electric timing system, was used to generate the vapor nanobubbles (VNBs) [28]. A pulsed

laser (~7 ns) tuned at a wavelength of 561 nm (OpoletteTM HE 355 LD, OPOTEK Inc., Faraday Ave, CA, USA) was used for illumination of AuNPs to generate VNBs. The laser beam was fixed at ~150 µm and the laser intensity was adjusted to 160 µJ. After laser treatment, the cells were washed with T cell culture medium. The amount of cells that were photoporated with FD was quantified by flow cytometry using a FACSCalibur™ (BD Pharmingen, Erembodegem, Belgium) or a CytoFLEX (Beckman Coulter, Suarlée Belgium) and analyzed by FlowJo (Treestar Inc, Ashland, USA) software.

2.4 Confocal microscopy

Laser treatment was performed as described above, followed by the incubation of the cells in 2 µM Calcein red-orange AM (Molecular Probes, Merelbeke, Belgium) for 30 min at room temperature. Prior to confocal imaging, the cells were washed with T cell culture medium and transferred to a glass-bottom 96-well plate. Confocal microscopy images were acquired using a Nikon C1si confocal laser scanning microscope equipped with a 10x objective lens (Plan Apo, NA 0.45, Nikon). The Calcein red-orange AM dye and FITC label were excited with a 561 nm diode laser and a 488 nm argon-ion laser, respectively (both purchased from CVI Melles Griot, NM, USA).

2.5 Viability assay

Activated $CD8^+$ T cells were first incubated with different concentrations of AuNPs, ranging from 1.6 to 12 x 10^9 AuNPs/ml (1:500 to 1:70 dilution of the stock AuNP concentration). Photoporation of the CTLs was performed as described previously, followed by a washing step with T cell culture medium to remove the free FD. Finally, the cells were resuspended in T cell culture medium supplemented with 30 U ml^{-1} rIL-2 and 5 x 10^4 cells/100 µl/well were transferred to an opaque 96-well plate. After 24h of incubation, the cells were treated with a CellTiter-Glo® luminescent Cell Viability Assay (Promega, Leiden, The Netherlands), according to the manufacturer's instructions. In brief, the cells were first incubated for 30 min at room temperature, followed by the addition of 100 µl of the CellTiter-Glo® reagent. After 10 min incubation, the luminescence signal was recorded by a GloMax™ 96 Luminometer (Promega).

2.6 Gene silencing via vapor nanobubble-mediated photoporation

For silencing experiments, the activated $CD8^+$ T cells were photoporated in the presence of siRNA molecules. Twenty-one nucleotide siRNA duplexes that were targeted against tyrosine phosphatase receptor type C (CD45) or used as a control were purchased from Eurogentec. The 5'-ends of the antisense strands were phosphorylated and both sense and anti-sense strands had a UU-overhang at the 3'-end. siRNA targeting the CD45 gene (siCD45) had the following sequence: sense strand = 5'-GAA-GAAUGC-UCA-CAG-AUA-A-3'; antisense strand = 5'-UUA-UCU-GUG-AGCAUU-CUU-C-3'. The control duplex, (siCTRL)

had the following sequence: sense strand = 5'-UGC-GCU-ACG-AUC-GACGAU-G-3'; antisense strand = 5'-CAU-CGU-CGA-UCG-UAG-CGC-A-3'. The $CD8^+$ T cells were photoporated as previously described with different concentrations of siRNA, ranging from 0.2 µM to 5 µM together with 2 mg ml^{-1} FITC-dextran (FD) dissolved in advanced RPMI. After laser treatment, the cells were washed with T cell culture medium and resuspended in this medium supplemented with 30 U ml^{-1} rIL-2. The cells were transferred to a U-bottom 96-well plate (Falcon, BD Biosciences, Erembodegem, Belgium) at a concentration of 0.5-1 x 10^5 cells/200 µl/well. After 24h, 48h or 72h of incubation, the cells were washed with phosphate buffered saline (PBS; Gibco-Invitrogen) supplemented with 5% FBS. Subsequently, the cells were incubated for 30 min at room temperature with PerCP-Cy™5.5 fluorescently-labeled CD45 antibody (BD Pharmingen) in PBS supplemented with 5% FBS. After washing the cells, the amount of transfected cells was determined by the FITC signal and silencing of the CD45 receptor was quantified using flow cytometry.

2.7 Nucleofection

$CD8^+$ T cells were stimulated for 7 days with anti-CD3/CD28 Dynabeads® as previously described. The cells were nucleofected with FD and siRNA using the Amaxa® Mouse T Cell Nucleofector™ kit (Lonza, Cologne, Germany) and a Nucleofector™ 2b device (Lonza), according to the manufacturer's protocol. In brief, 1 x 10^6 $CD8^+$ T cells were resuspended in T cell Nucleofector® solution supplemented with a final concentration of 2 mg ml^{-1} FD and the indicated concentration of siRNA. The cell suspension was transferred to a cuvette and transfected in the Nucleofector™ device using program X-01, followed by the dilution in 500 µl prewarmed Amaxa® T cell culture medium, supplemented with 30 U ml^{-1} rIL-2. Subsequently, the cells were transferred to a 12-well plate containing 1.5 ml prewarmed culture medium and were cultivated at 37°C and 5% CO_2 for 48h. For the viability assay, the cells were also diluted in prewarmed Amaxa® T cell culture medium supplemented with 30 U ml^{-1} rIL-2, followed by transferring 1 x 10^5 cells to an opaque 96-well plate for 24h of incubation. A CellTiter-Glo® viability assay was performed as previously described.

2.8 Statistical analysis

A two-tailed Student's t-test was performed to determine statistical differences between datasets. All statistical analyses were performed using GraphPad Prism 6 software (La Jolla, CA, USA). p-values <0.05 were regarded significant. Statistical significance is indicated as follows: * p <0.05, ** p <0.01, *** p <0.001, **** p <0.0001.

3 RESULTS

3.1 Intracellular delivery of macromolecules to cytotoxic T lymphocytes via photoporation

To investigate whether vapor nanobubble (VNB) photoporation can be applied to transfect cytotoxic T cells (CTLs) with macromolecules, gold nanoparticles (AuNPs) were first attached to the surface of activated $CD8^+$ T cells. A schematic presentation of the photoporation procedure is shown in **Figure 1A**.

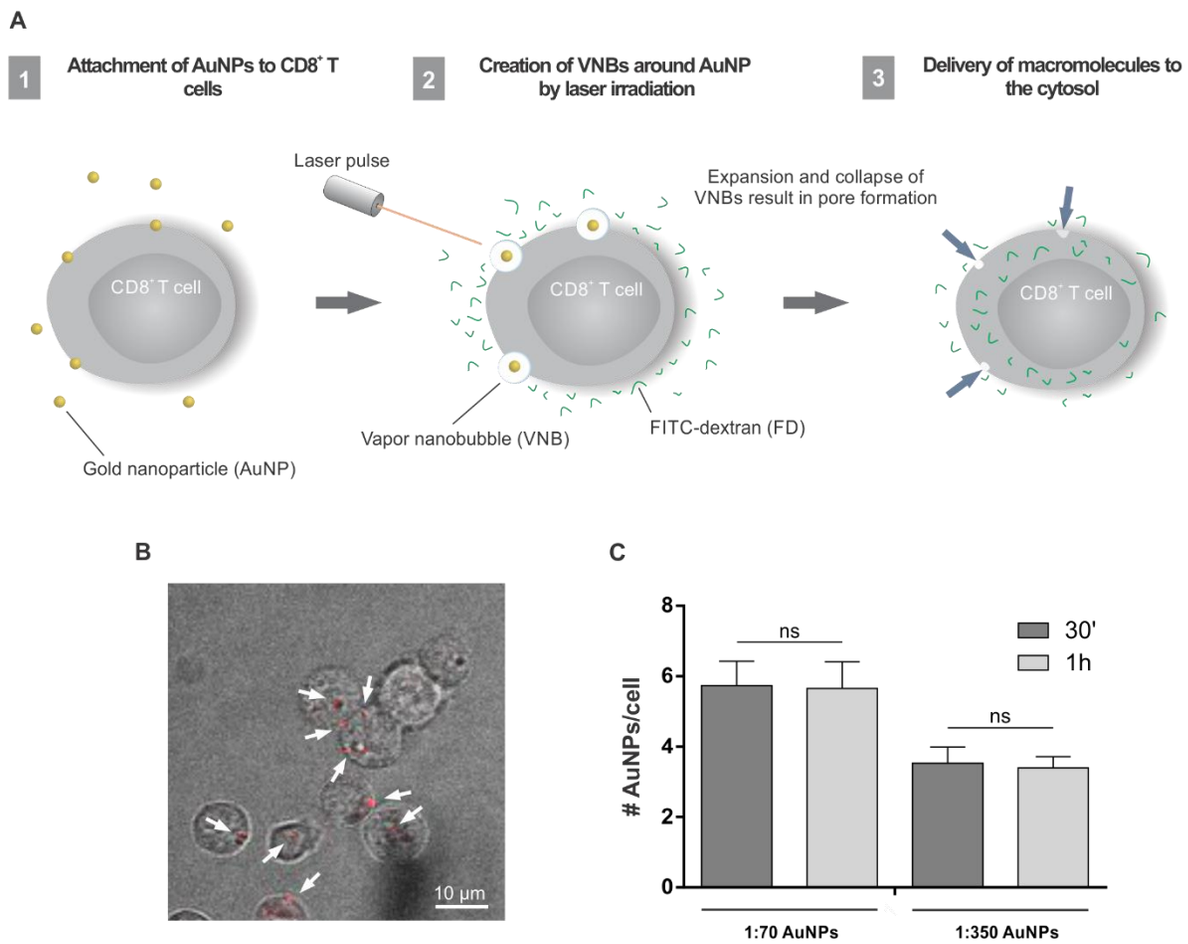

Figure 1. Vapor nanobubble-mediated photoporation of cytotoxic T lymphocytes (CTLs) via the attachment of gold nanoparticles (AuNPs) to the cell membrane. (A) Schematic overview of the photoporation of CTLs by first incubating the cells with AuNPs that adsorb to the cell surface, followed by a nanosecond laser pulse that creates vapor nanobubbles (VNBs) around the cell-attached AuNPs. The collapse of the VNBs forms pores in the cell membrane through which extracellular macromolecules such as fluorescently labeled 10 kDa dextrans can enter the cells. **(B)** The number of AuNPs attached to the CTLs was determined by confocal reflection microscopy (red dots indicated with arrows) and subsequent image processing, in which both the number of AuNPs and the number of cells were counted. **(C)** Representation of the number of AuNPs per CTL ± SD (n = 5 images; ~65 cells/image) of cells incubated with two different concentration of AuNPs (1:70 versus 1:350) for 30 min and 1h (ns = not significant).

3.1.1 Determining the number of gold nanoparticles per CD8⁺ T cell

Cationic AuNPs of 70 nm were used to allow electrostatic adsorption to the negatively charged cell membrane. To optimize the number of cell-attached AuNPs, the cells were incubated with varying concentrations of AuNPs, ranging from 1.6 to 12 x 10^9 AuNPs/ml. The AuNP concentrations in the graphs are represented as dilutions of the stock concentration of AuNPs (8.2 x 10^{11} AuNPs/ml). Following a washing step to remove unbound particles, the number of attached AuNPs per cell could be determined by confocal microscopy and subsequent image processing, exploiting the excellent light scattering properties of the AuNPs (**Figure 1B**). Cells incubated with 12 x 10^9/ml (1:70) versus 2.3 x 10^9/ml (1:350) AuNPs had an average of 6 versus 3 AuNPs per cell, respectively (**Figure 1C**). Increasing the incubation time from 30 min to 1h did not result in higher attachment.

3.1.2 Determining the photoporation efficiency and cytotoxicity

For photoporation, after removing the unbound AuNPs, CTLs were incubated with 10 kDa FITC-labeled dextran (FD) as a model macromolecule. Next, the CTL-attached AuNPs were illuminated by a single 7 ns laser pulse (0.9 J/cm²) for VNB generation, hence creating small transient pores in the cell membrane through which FD can diffuse into the cytoplasm [28]. For increasing AuNP concentrations, we found an increasing percentage of cells with a detectable FD signal. Up to 80% FD-positive cells were obtained for the highest AuNP concentration tested (**Figure 2A**). As a control, cells devoid of AuNPs were treated with a laser pulse ('laser control') leading to a low percentage of FD-positive cells (~10%) compared to untreated CTLs. In parallel, a CellTiter-Glo® assay was performed to assess cytotoxicity of the treatment, measured after 24h (**Figure 2B**). The cytotoxicity clearly increased with increasing AuNP concentration. At a concentration of 1:350, an acceptable 70% cell viability was obtained, for which 55% of the cells were FD-positive. Confocal microscopy of CTLs photoporated in the presence of FD and incubated with the live cell imaging dye Calcein red/orange AM confirmed the intracellular FD delivery and survival of the cells (**Figures 2C-E**). Considering both delivery efficiency and toxicity, we thus selected the 1:350 dilution for further investigation.

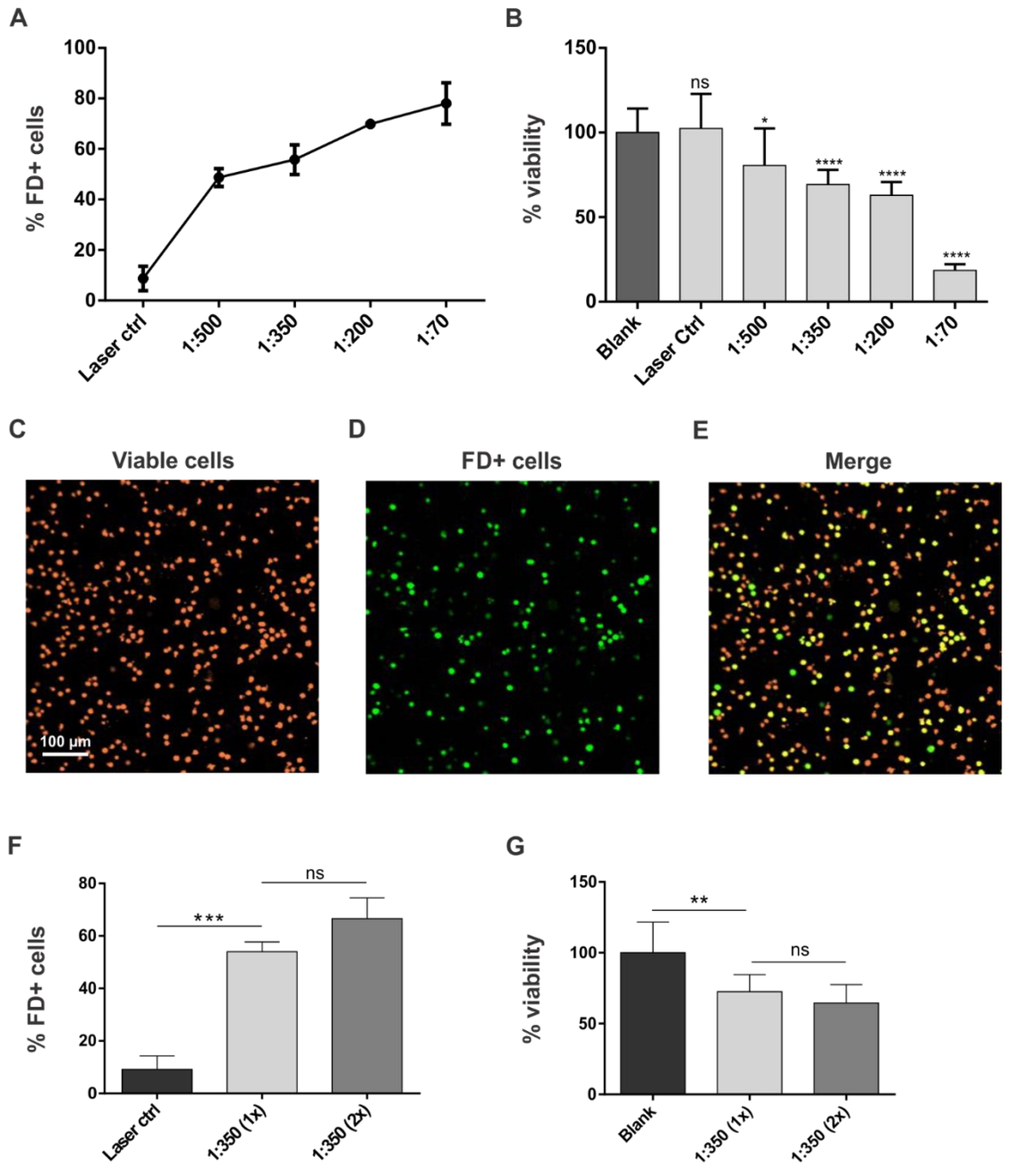

Figure 2. Cytosolic delivery of model macromolecules to cytotoxic T cells (CTLs) via photoporation. (A) CTLs were incubated with four different concentrations of gold nanoparticles (AuNPs) ranging from 1:500 - 1:70 dilution of the AuNP stock concentration (8.2 x 10^{11} AuNPs/ml), followed by a nanosecond laser pulse in the presence of 2 mg ml^{-1} 10 kDa FITC-dextran (FD). As a control, cells without AuNPs received similar treatment (Laser ctrl). The graph represents the number of FD positive cells ± SD (*n* = 3) that was measured by flow cytometry. **(B)** The percentage cell viability ± SD was determined as a function of AuNP concentration (*n* = 3). Cells without any treatment (blank) or treated with laser alone (withouth AuNPs; Laser ctrl) are shown as control. All samples treated with laser were compared to the blank sample. **(C)** Confocal microscopy images of CTLs first incubated with 1:350 dilution of the AuNP stock concentration, followed by the incubation with the Calcein red-orange AM dye to stain living cells after **(D)** photoporation in the presence of 2 mg ml^{-1} FD. **(E)** Merged confocal image of orange and green fluorescence channels, showing both viable and FD-positive cells (yellow). **(F)** CTLs were treated two times with a laser pulse for the selected 1:350 AuNP dilution. The graph represents the number of FD-positive cells ± SD (*n* = 3) compared to cells treated with one time laser pulse but without AuNPs (Laser ctrl). **(G)** Percentage cell viability ± SD as a function of multiple laser treatments compared to blank cells (*n* = 3). Statistics are indicated as ns = not significant; * p <0.05; ** p <0.01; *** p <0.001; **** p <0.0001.

Another way to improve transfection efficiency instead of increasing AuNP concentration is to repeat the photoporation procedure a second or third time. Although subjecting T cells to two consecutive photoporation treatments did not result in a significant increase in FD delivery, a clear trend to an additional 10-15% of FD-positive cells was observed in all experiments (**Figure 2F**). Importantly, this second laser treatment did not result in a significant additional cytotoxicity as shown in **Figure 2G**. A third laser treatment was shown to equally increase the number of positive cells with another 10% (**Figure 3**). Of note, as AuNPs likely melt and break up in smaller fragments after being heated by the first laser pulse, every additional laser treatment requires an additional incubation with AuNPs, which is rather time-consuming [28, 29]. Therefore, we selected the protocol with two consecutive laser treatments using a 1:350 dilution of AuNPs for all further experiments.

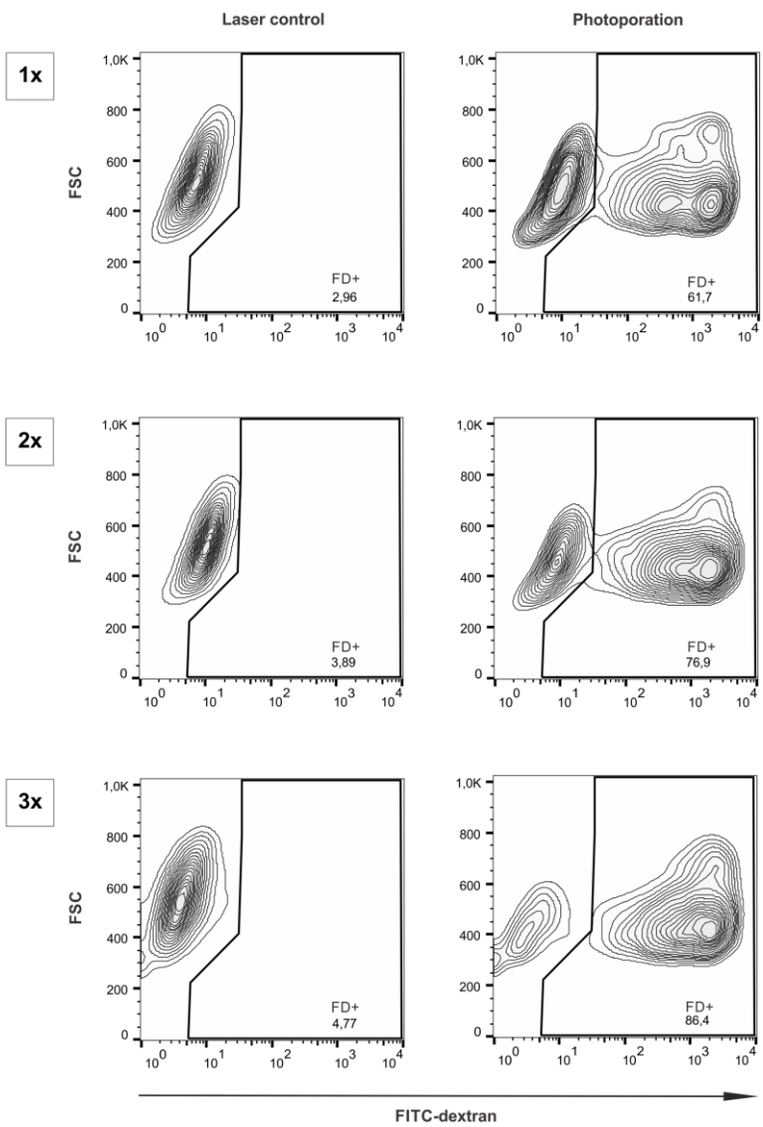

Figure 3. Cytosolic delivery of FITC-dextran (FD) to cytotoxic T cells (CTLs) as a function of number of laser treatments. CTLs were incubated 1, 2 or 3 times with a 1:350 dilution of gold nanoparticles (AuNPs - stock concentration 8.2 x 10^{11} AuNPs/ml), each time followed by a single laser pulse in the presence of 10 mg ml^{-1} FD. As a control, cells without AuNPs were similarly treated in the presence of FD (Laser ctrl). (FSC = Forward scatter)

3.2 Evaluation of siRNA delivery and gene silencing in cytotoxic T lymphocytes via photoporation

Having optimized the photoporation protocol on activated CTLs using FD as a model macromolecule, we next sought to investigate its suitability toward siRNA delivery and gene silencing. To this end, the protein tyrosine phosphate receptor type C (CD45) was selected as model target. The receptor is expressed by all hematopoietic cells and was already widely used as model target molecule in several immune cell types [22, 30]. We evaluated gene knockdown on the protein level by antibody staining using flow cytometry. To quantify the fraction of photoporated cells, FD was co-delivered with the siRNA. To validate whether FD can indeed be used as a marker for siRNA delivery, we performed a photoporation experiment with fluorescently labeled siRNA. The extent of cellular delivery of Cy5-labeled siRNA and FD via photoporation of CTLs is positively correlated, as is represented in **Figure 4**. Moreover, it was shown that the presence of FD had no influence on the delivery efficiency of siRNA. These results confirm that FD can be used as marker for successful siRNA delivery by photoporation.

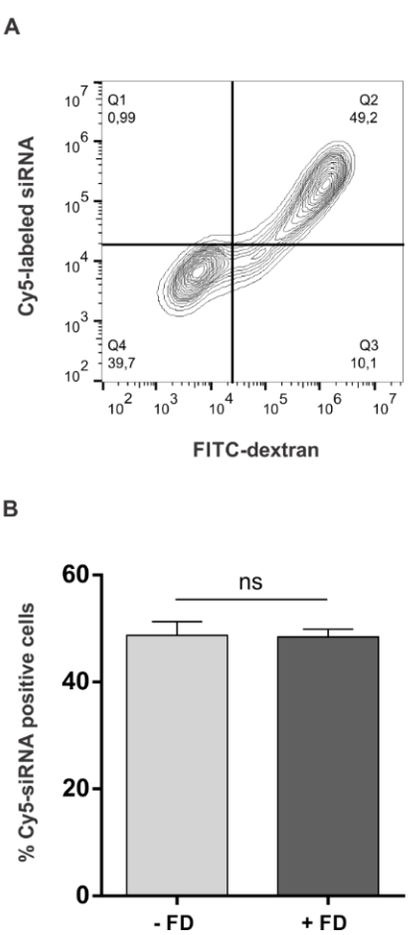

Figure 4. Co-delivery of FITC-dextran (FD) and fluorescently-labeled siRNA to cytotoxic T cells (CTLs). (A) CTLs were incubated with a 1:350 dilution of gold nanoparticles (AuNPs) prior to laser treatment in the presence of Cy5-labeled siRNA. Flow cytometry plot representing the delivery of FD versus Cy5-labeled siRNA. **(B)** Percentage of siRNA positive cells ± SD (*n* = 1 experiment with 2 independent samples; ns = not significant) with or without the co-delivery of FD.

As represented in **Figure 5A**, a broad distribution on the amount of FD delivered per CTL was observed. Since the delivery of FD and siRNA are positively correlated, also a higher silencing could be expected for the cells showing a higher FD signal. To evaluate this, CTLs were incubated with 2 mg ml^{-1} FD and either 1 µM siRNA against CD45 (siCD45) or control siRNA (siCTRL). Following photoporation, we divided the FD-positive cells in a FD+ and FD++ population. The FD+ population comprises the total FD-positive population while FD++ represents 35% of the total FD-positive population (**Figure 5A**). For both populations the percentage of knockdown was obtained by normalizing the CD45 expression of siCD45 treated cells to the expression levels of cells photoporated in the presence of siCTRL. As expected, silencing was absent for the FD-negative population, while for the FD++ population a trend toward higher silencing compared to FD+ was observed (**Figures 5B-C**). The highest silencing was observed 48h after laser treatment reaching ~40 and ~60% reduction of CD45 protein expression for FD+ and FD++ cells, respectively (**Figures 5D-E**). Further increasing the concentration of siRNA to 5 µM did not show a significant increase in silencing (measured after 48h), which is in agreement with previous reports showing that applying more siRNA does not result in higher knockdown efficiency but rather in a prolonged silencing effect (**Figures 5F-G**) [31]. Moreover, also a five-fold reduction of the siRNA concentration did not significantly lower CD45 silencing, which suggests that at this concentration already maximal silencing was obtained.

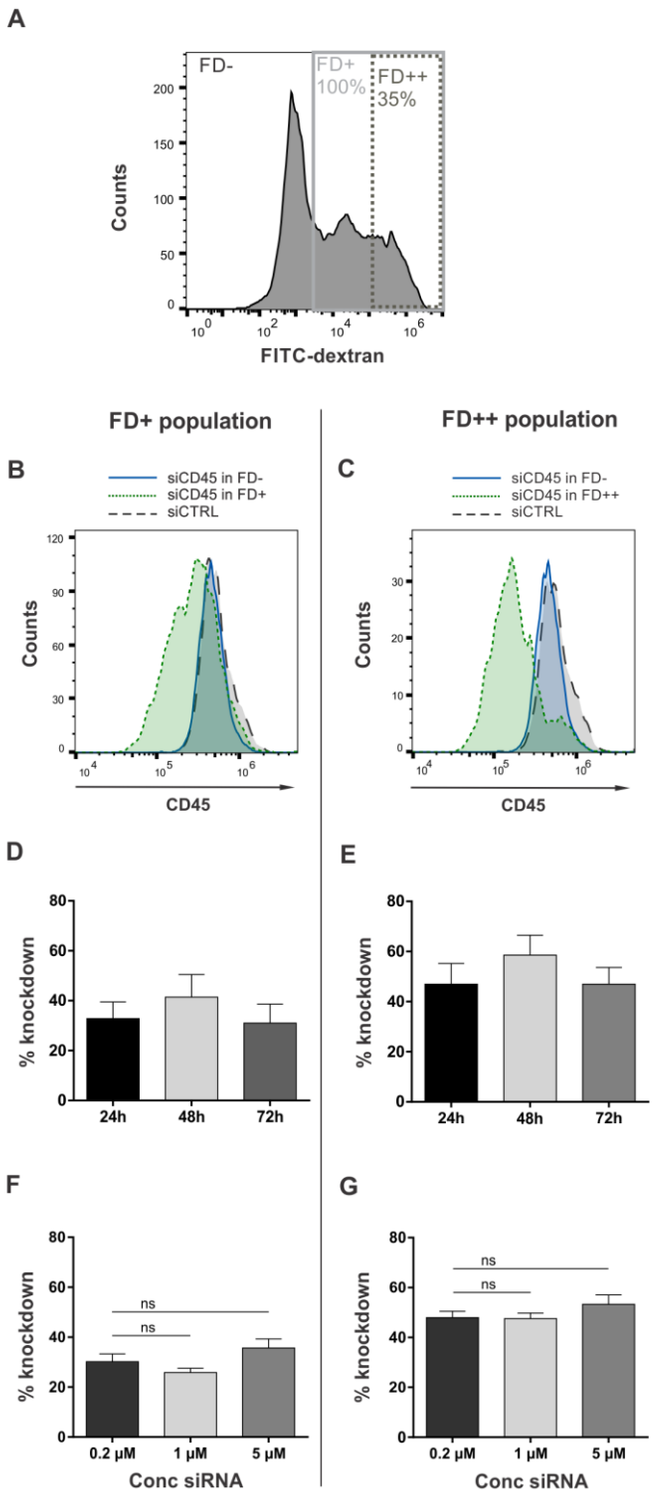

Figure 5. Gene silencing in cytotoxic T cells (CTLs) by the delivery of siRNA via vapor nanobubble (VNB)-mediated photoporation. CTLs were incubated with a 1:350 dilution of the gold nanoparticles (AuNPs) followed by laser treatment in the presence of 1 µM siRNA and 2 mg ml^{-1} FITC-dextran (FD). CTLs were either incubated with siRNA against CD45 (siCD45) or with control siRNA (siCTRL). **(A)** Histogram representing the delivery of FD to the CTLs 24h after delivery, combined with gating of cells showing total FD-positive (FD+, light gray solid line) and high FD-positive signal (top 35% of the positive cells, FD++,dark gray dotted line). **(B)** Histograms representing the expression of CD45 after 48h of incubation for samples treated with 1 µM siCD45 versus siCTRL for the FD-, FD+ and **(C)** FD++ population. **(D)** Percentage CD45 knockdown ± SD (*n* = 3) in the FD+ population and **(E)** FD++ population as a function of post-photoporation incubation time. **(F)** Percentage CD45 knockdown ± SD (*n* = 2; ns = not significant) as a function of the siRNA concentration, ranging from 0.2 to 5 µM for FD+ and **(G)** FD++ cells.

3.3 Comparing siRNA delivery efficiency and cell viability via vapor nanobubble-mediated photoporation with nucleofection

The Nucleofector™ technology is an electroporation-based technique marketed by Lonza (Amaxa®) for the delivery of plasmids and siRNA in target cells, including hard-to-transfect cells. Also this technique utilizes the temporary creation of small pores in the cell membrane by electrical pulses to allow the delivery of nucleic acid therapeutics directly in the cell cytoplasm. As nucleofection is currently the most commonly used technique for siRNA delivery to primary T cells, we chose to compare VNB photoporation with this technique [18]. For this purpose, an optimized Nucleofector™ protocol, as suggested by the manufacturer for the transfection of primary T cells, was used. Corroborating earlier reports in the literature, in our hands the nucleofection of primary T cells likewise resulted in high levels of cell death. After 24h, only 17% of the treated cells survived the nucleofection protocol versus 70% for the optimized photoporation approach (**Figure 6A**). However, within this small fraction of surviving cells, 95% was FD-positive compared with 65% FD-positive cells for photoporation. From these data, we can conclude that for nucleofection the gain of viable FD-positive cells is 16% versus 45.5% for photoporation. Additionally, when cells were treated with 1 µM siRNA, a comparable knockdown of CD45 protein levels was observed for both techniques (**Figure 6B**). As shown in **Figure 6C**, similar to results obtained via photoporation, CD45 knockdown efficiency was not significantly altered when applying different siRNA concentrations (0.2 to 5 µM).

Moreover, the extent of delivery greatly differed between both techniques, as demonstrated for FD. Although a more homogenous distribution of the delivered FD cargo was observed for nucleofection, the majority of FD-positive cells showed markedly higher fluorescence intensities when treated by photoporation (**Figure 6D**).

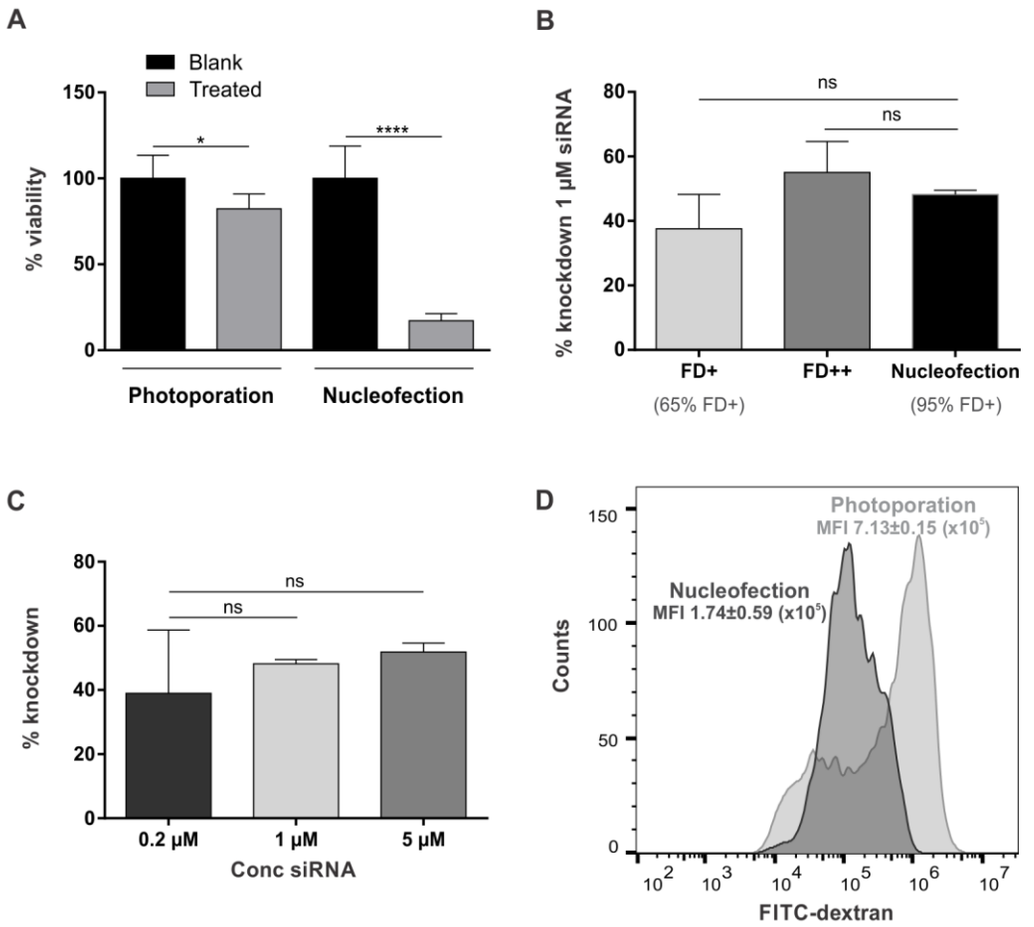

Figure 6. Cell viability and gene silencing in cytotoxic T lymphocytes (CTLs) by photoporation versus nucleofection. CTLs were nucleofected according to the manufacturer's protocol in the presence of siRNA and 2 mg ml^{-1} FITC-dextran (FD). **(A)** Percentage CTL viability ± SD (n = 3) as a function of the technique for the delivery of 2 mg ml^{-1} FD compared to blank CTLs. CTLs that were transfected by photoporation were treated two consecutive times with nanosecond laser pulses. (**B)** Percentage knockdown ± SD (photoporation n = 4; nucleofection n = 2; ns = not significant) of cells treated by photoporation (65% FD-positive cells) versus nucleofection (95% FD-positive cells) with 1 µM siRNA. Photoporated CTLs were divided in two populations represented as FD+ (100% FD-positive cells) and FD++ (top 35% of FD-positive cells). **(C)** Percentage knockdown ± SD (n = 2; ns = not significant) of cells nucleofected with different concentrations of siRNA, ranging from 0.2 to 5 µM. **(D)** Histograms of the FD-positive cells comparing the fluorescence intensity of the delivered FD by photoporation versus nucleofection, immediately after treatment. Statistics are indicated as ns = not significant; * p <0.05; **** p <0.0001.

4 DISCUSSION

The goal of this study was to investigate whether target genes in cytotoxic T cells (CTLs) can be silenced by delivering small interfering RNA (siRNA) molecules via vapor nanobubble (VNB)-mediated photoporation. Because photoporation is mediated by plasmonic gold nanoparticles (AuNPs), we first investigated the attachment of positively charged AuNPs to the anionic CTL surface. In general, the endocytic uptake of nanoparticles in T cells is impaired, which implies that the majority of the particles remains attached to the surface without internalization [32, 33]. In this work, we aim to exploit this feature to selectively permeabilize the cell membrane. The number of adsorbed AuNPs per cell could be quantified from confocal images obtained in reflection mode. As expected, increasing the AuNP concentration resulted in more attached AuNPs. However, an average of 6 AuNPs per CTL already resulted in high toxicity. This toxicity can be explained by the formation of multiple pores per T cell, thus compromising the integrity of the cell membrane beyond repair. Therefore, a AuNP concentration corresponding to ~3 AuNPs per cell was selected as it showed the most optimal balance between delivery efficiency and viability. These results are in line with a previous study showing that only a few or even single particles per cell may result in efficient cellular delivery [34]. In addition, we showed that repeating the photoporation procedure a second time enhanced the transfection efficiency up to 65% while not substantially increasing the toxicity.

The delivery of siRNA resulted in 40-60% silencing of the CD45 gene, which was used as a model target. Compared to the Nucleofector™ technology, which is the standard method to deliver siRNA to CTLs, photoporation at the optimized conditions of 70% cell viability yields a lower percentage of transfected cells albeit with a markedly higher average macromolecular dose per cell and significantly reduced cytotoxicity. This improved delivery by photoporation could become very important to maintain sufficiently high drug concentrations per cell when CTLs proliferate and divide their cytosolic content over the daughter cells. The low toxicity can in part be explained by the relatively small pores (<1 µm) generated by the photoporation technique together with their rapid repair that takes only a few tens of seconds [35]. Although the AuNPs reach a high temperature for the formation of VNBs, it was already demonstrated by us and others that this does not induce heat transfer to the surrounding medium as virtually all heat energy is converted to mechanical energy, also contributing to the reduced toxicity [28, 36]. Moreover, the size of the generated vapor nanobubbles and hence the extent of membrane damage can be further tuned by optimizing laser properties such as intensity and pulse duration, as was shown for T cells previously [37].

Photoporation typically generates a broad distribution on the amount of macromolecules delivered per cell, which can likely be explained by the variation in the number of AuNPs per cell. Upon activation, the $CD8^+$ T cells will considerably expand. As

was previously shown by our group, the number of nanoparticles that can be attached per T cell is highly dependent on the activation status and the resultant size of the $CD8^+$ T cells [33]. For adoptive T cell transfer, $CD8^+$ T cells need to be activated to exert their tumor-migratory and cytotoxic function. Additionally, it has been shown that activated T cells are more amenable for transfection than their resting counterparts [38, 39].

In general, nucleofection showed a higher percentage of transfected cells compared to photoporation. However, when considering the severe cell toxicity after 24h for nucleofection, it can be concluded that almost three times more CTLs can be generated with a comparable knockdown via the photoporation technique. Non-viral siRNA-loaded nanoparticles typically achieve lower transfection efficiencies in primary T lymphocytes, yet they are likely more suitable for *in vivo* use compared to physical methods such as photoporation and electroporation [22, 40]. We envision the use of photoporation during the *ex vivo* treatment of T lymphocytes in the context of adoptive T cell therapy (ACT), in which T cells are isolated from a patient and modulated *ex vivo* before reinfusion. Recent research showed that in many patients the success of ACT is still blunted by numerous factors that inhibit the activity of the CTLs, causing tumor escape [41]. Manipulating the immune escape mechanisms by immune checkpoint inhibitors such as CTLA-4 and PD-1 antibodies has shown clinical success but the application of antibodies remains restricted to extracellular targets [42]. Exciting is the current elucidation of new intracellular targets in CTLs that upon silencing promote a more effective anti-tumor response, i.e. increase the tumor infiltration, T cell proliferation, and release of immune-stimulating cytokines [43, 44]. To this end, the delivery of siRNA targeting this suppressive intracellular circuitry via the photoporation technique may further boost the anti-tumor activity of the transferred T cells in the immunosuppressive tumor microenvironment, which will be the subject of future research.

The focus of this work was to test the photoporation technique on CTLs in the context of ACT. Of note, preliminary data indicate that photoporation might be of value to transfect other types of immune cells as well, as we observed similar delivery efficiencies for both $CD8^+$ and $CD8^-$ splenocytes, including $CD4^+$ T cells and B cells (**Figure 7**). Furthermore, the photoporation technique can be extended to the delivery of other types of membrane-impermeable macromolecules for both therapeutic and diagnostic use.

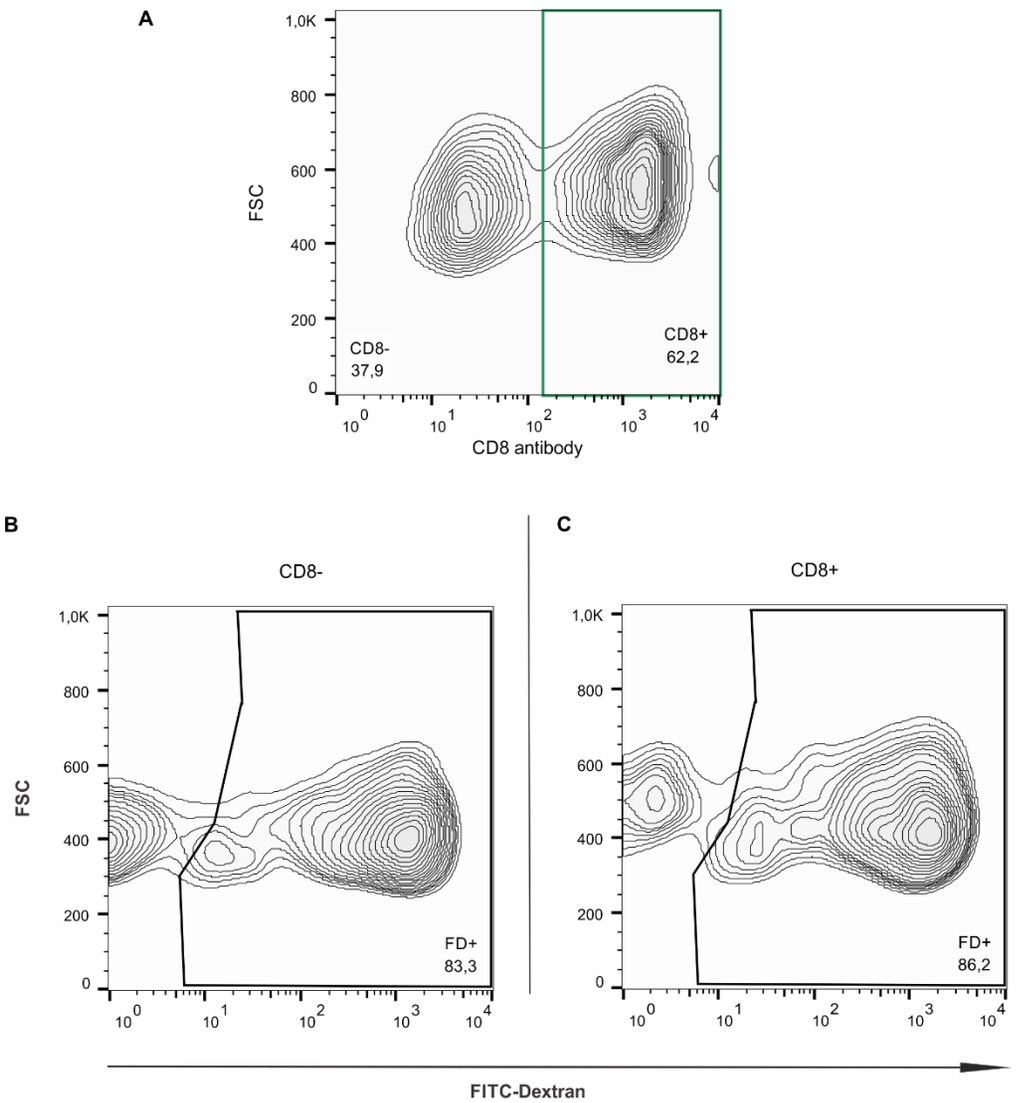

Figure 7. Cytosolic delivery of FITC-dextran (FD) to splenocytes. Splenocytes were activated during 9 days and incubated with 1:350 dilution of gold nanoparticles (AuNPs - stock concentration 8.2 x 10^{11} AuNPs/ml) followed by two consecutive laser treatments in the presence of 10 mg ml^{-1} FD. After laser treatment, the cells were washed and stained with anti-CD8 antibodies in PBS supplemented with 5% FBS. **(A)** Flow cytometry plot representing the CD8 negative versus positive cells in the total splenocyte population. **(B)** Plot representing the percentage FD-positive cells in the $CD8^-$ population versus **(C)** $CD8^+$ population.

5 CONCLUSION

We proposed a novel technique for the efficient delivery of siRNA molecules to CTLs by VNB-mediated photoporation. To this end, we optimized the amount of AuNPs and number of laser treatments to obtain high delivery efficiency in combination with low toxicity. We further showed the co-delivery of fluorescently labeled dextrans with siRNA molecules, resulting in the silencing of the CD45 model protein. A comparison of photoporation with nucleofection, the latter being the standard non-viral method to deliver siRNA to CTLs, showed a three-fold higher number of efficiently transfected and viable T cells for photoporation, mainly as a result of the high cell toxicity with the Nucleofector™ technology.

ACKNOWLEDGEMENTS

Laura Wayteck is a doctoral fellow of the Institute for the Promotion of Innovation through Science and Technology in Flanders, Belgium (IWT-Vlaanderen). Kom op Tegen Kanker is acknowledged for their financial support (Beurs Emmanuel van der Schueren). Koen Raemdonck is a postdoctoral fellow of the Research Foundation-Flanders, Belgium (FWO-Vlaanderen). Koen Raemdonck received additional financial support via a FWO Research Grant (Krediet aan Navorsers). The authors would like to thank Katrien De Mulder and Dorien Clarisse (Ghent University Hospital) for their help with the use of the Nucleofector™ 2b device.

REFERENCES

1. Feldman, S.A., Assadipour, Y., Kriley, I., Goff, S.L. & Rosenberg, S.A. Adoptive Cell Therapy--Tumor-Infiltrating Lymphocytes, T-Cell Receptors, and Chimeric Antigen Receptors. *Semin Oncol* **42**, 626-39 (2015).
2. Tang, H., Qiao, J. & Fu, Y.X. Immunotherapy and tumor microenvironment. *Cancer Lett* **370**, 85-90 (2016).
3. Pardoll, D.M. The blockade of immune checkpoints in cancer immunotherapy. *Nat Rev Cancer* **12**, 252-64 (2012).
4. Zamarin, D. & Postow, M.A. Immune checkpoint modulation: rational design of combination strategies. *Pharmacol Ther* **150**, 23-32 (2015).
5. Hodi, F.S. et al. Improved survival with ipilimumab in patients with metastatic melanoma. *N Engl J Med* **363**, 711-23 (2010).
6. Brahmer, J.R. et al. Safety and activity of anti-PD-L1 antibody in patients with advanced cancer. *N Engl J Med* **366**, 2455-65 (2012).
7. Zhou, P. et al. In vivo discovery of immunotherapy targets in the tumour microenvironment. *Nature* **506**, 52-7 (2014).
8. Waugh, K.A., Leach, S.M. & Slansky, J.E. Targeting Transcriptional Regulators of CD8+ T Cell Dysfunction to Boost Anti-Tumor Immunity. *Vaccines (Basel)* **3**, 771-802 (2015).
9. Sakib Hossain, D.M., Duttagupta, P. & Kortylewski, M. The aptamer-siRNA conjugates: reprogramming T cells for cancer therapy. *Ther Deliv* **6**, 1-4 (2015).
10. de Fougerolles, A., Vornlocher, H.P., Maraganore, J. & Lieberman, J. Interfering with disease: a progress report on siRNA-based therapeutics. *Nat Rev Drug Discov* **6**, 443-53 (2007).
11. Wittrup, A. & Lieberman, J. Knocking down disease: a progress report on siRNA therapeutics. *Nat Rev Genet* **16**, 543-52 (2015).
12. Wittrup, A. et al. Visualizing lipid-formulated siRNA release from endosomes and target gene knockdown. *Nat Biotechnol* **33**, 870-6 (2015).
13. June, C.H., Blazar, B.R. & Riley, J.L. Engineering lymphocyte subsets: tools, trials and tribulations. *Nat Rev Immunol* **9**, 704-16 (2009).
14. Yin, H. et al. Non-viral vectors for gene-based therapy. *Nat Rev Genet* **15**, 541-55 (2014).
15. Van Tendeloo, V.F. et al. High-level transgene expression in primary human T lymphocytes and adult bone marrow CD34+ cells via electroporation-mediated gene delivery. *Gene Ther* **7**, 1431-7 (2000).
16. Goffinet, C. & Keppler, O.T. Efficient nonviral gene delivery into primary lymphocytes from rats and mice. *FASEB J* **20**, 500-2 (2006).
17. Cron, R.Q., Schubert, L.A., Lewis, D.B. & Hughes, C.C. Consistent transient transfection of DNA into non-transformed human and murine T-lymphocytes. *J Immunol Methods* **205**, 145-50 (1997).
18. Freeley, M. & Long, A. Advances in siRNA delivery to T-cells: potential clinical applications for inflammatory disease, cancer and infection. *Biochem J* **455**, 133-47 (2013).
19. Gilleron, J. et al. Image-based analysis of lipid nanoparticle-mediated siRNA delivery, intracellular trafficking and endosomal escape. *Nat Biotechnol* **31**, 638-46 (2013).
20. Sharei, A. et al. Ex vivo cytosolic delivery of functional macromolecules to immune cells. *PLoS One* **10**, e0118803 (2015).

21. Li, S.Y. et al. Restoring anti-tumor functions of T cells via nanoparticle-mediated immune checkpoint modulation. *J Control Release* **231**, 17-28 (2016).
22. Ramishetti, S. et al. Systemic Gene Silencing in Primary T Lymphocytes Using Targeted Lipid Nanoparticles. *ACS Nano* **9**, 6706-16 (2015).
23. Lakshmanan, S. et al. Physical energy for drug delivery; poration, concentration and activation. *Adv Drug Deliv Rev* **71**, 98-114 (2014).
24. Kalies, S. et al. Enhancement of extracellular molecule uptake in plasmonic laser perforation. *J Biophotonics* **7**, 474-82 (2014).
25. Hu, M. et al. Gold nanostructures: engineering their plasmonic properties for biomedical applications. *Chem Soc Rev* **35**, 1084-94 (2006).
26. Lukianova-Hleb, E. et al. Plasmonic nanobubbles as transient vapor nanobubbles generated around plasmonic nanoparticles. *ACS Nano* **4**, 2109-23 (2010).
27. Lapotko, D. Plasmonic nanoparticle-generated photothermal bubbles and their biomedical applications. *Nanomedicine (Lond)* **4**, 813-45 (2009).
28. Xiong, R. et al. Comparison of gold nanoparticle mediated photoporation: vapor nanobubbles outperform direct heating for delivering macromolecules in live cells. *ACS Nano* **8**, 6288-96 (2014).
29. Yao, C., Qu, X., Zhang, Z., Huttmann, G. & Rahmanzadeh, R. Influence of laser parameters on nanoparticle-induced membrane permeabilization. *J Biomed Opt* **14**, 054034 (2009).
30. De Backer, L. et al. Hybrid pulmonary surfactant-coated nanogels mediate efficient in vivo delivery of siRNA to murine alveolar macrophages. *J Control Release* **217**, 53-63 (2015).
31. Mantei, A. et al. siRNA stabilization prolongs gene knockdown in primary T lymphocytes. *Eur J Immunol* **38**, 2616-25 (2008).
32. Stephan, M.T., Moon, J.J., Um, S.H., Bershteyn, A. & Irvine, D.J. Therapeutic cell engineering with surface-conjugated synthetic nanoparticles. *Nat Med* **16**, 1035-41 (2010).
33. Wayteck, L. et al. Hitchhiking nanoparticles: Reversible coupling of lipid-based nanoparticles to cytotoxic T lymphocytes. *Biomaterials* **77**, 243-54 (2016).
34. Heinemann, D. et al. Gold nanoparticle mediated laser transfection for efficient siRNA mediated gene knock down. *PLoS One* **8**, e58604 (2013).
35. Yamane, D. et al. Electrical impedance monitoring of photothermal porated mammalian cells. *J Lab Autom* **19**, 50-9 (2014).
36. Lapotko, D. Plasmonic nanobubbles as tunable cellular probes for cancer theranostics. *Cancers (Basel)* **3**, 802-40 (2011).
37. Lukianova-Hleb, E.Y., Wagner, D.S., Brenner, M.K. & Lapotko, D.O. Cell-specific transmembrane injection of molecular cargo with gold nanoparticle-generated transient plasmonic nanobubbles. *Biomaterials* **33**, 5441-50 (2012).
38. Gust, T.C. et al. RNA interference-mediated gene silencing in murine T cells: in vitro and in vivo validation of proinflammatory target genes. *Cell Commun Signal* **6**, 3 (2008).
39. McManus, M.T. et al. Small interfering RNA-mediated gene silencing in T lymphocytes. *J Immunol* **169**, 5754-60 (2002).
40. Peer, D. Induction of therapeutic gene silencing in leukocyte-implicated diseases by targeted and stabilized nanoparticles: a mini-review. *J Control Release* **148**, 63-8 (2010).
41. Crespo, J., Sun, H., Welling, T.H., Tian, Z. & Zou, W. T cell anergy, exhaustion, senescence, and stemness in the tumor microenvironment. *Curr Opin Immunol* **25**, 214-21 (2013).

42. Shin, D.S. & Ribas, A. The evolution of checkpoint blockade as a cancer therapy: what's here, what's next? *Curr Opin Immunol* **33**, 23-35 (2015).
43. Hinterleitner, R. et al. Adoptive transfer of siRNA Cblb-silenced CD8+ T lymphocytes augments tumor vaccine efficacy in a B16 melanoma model. *PLoS One* **7**, e44295 (2012).
44. Palmer, D.C. et al. Cish actively silences TCR signaling in CD8+ T cells to maintain tumor tolerance. *J Exp Med* **212**, 2095-113 (2015).

6

Broader international context, relevance and future perspectives

Within this study, we showed how the interplay of nanomedicines with adoptive T cell therapy has potential to enhance anti-cancer responses. We proposed strategies to improve cancer immunotherapy by combining adoptive T cell therapy with the concomitant delivery of nanomedicines to the tumor and described a novel technique exploiting gold nanoparticles to deliver small interfering RNA (siRNA) molecules to primary cytotoxic T cells (CTLs), aiming to make them more effective. In this chapter, the broader context of this project will be sketched by discussing the recent progress in the field of cancer immunotherapy and nanomedicines, the challenges that currently limit the successes of both therapies, and how the concepts outlined in this thesis could help to overcome these important issues.

In recent years, **cancer immunotherapeutics**, in particular the monoclonal antibodies for checkpoint blockade, have become part of the standard therapies for cancer [1]. Compared to conventional chemotherapeutics, immunotherapy has advantages in terms of reducing off-target side effects and inducing an anti-tumor memory that may protect patients from relapse. Moreover, besides eradicating primary tumor, also metastases are a target for the generated immune responses. Since the regulatory approval of the checkpoint inhibitor ipilimumab (anti-CTLA-4; marketed as Yervoy®) in 2011, cancer immunotherapy has become the fastest-growing area in pharmaceutical industry [2]. Moreover, Science magazine selected cancer immunotherapy as the breakthrough of the year in 2013 [3]. Nowadays, it becomes increasingly clear that for cancers not treatable via surgery or radiotherapy, the current standard of care, consisting of chemotherapy and targeted therapies will be challenged by immunotherapy and that the latter one has the potential to become the backbone of cancer therapy in the future.

Successful clinical data of the administration of tumor-infiltrating lymphocytes (TILs) to patients with metastatic melanoma who were refractory to the standard therapies, paved the way for the use of **adoptive T cell therapy** (ACT) in a broader range of tumors by engineering T cells to express a novel, tumor-specific T-cell receptor (TCR) or chimeric antigen receptor (CAR). Recently, studies have demonstrated the impressive efficacy of CAR therapies targeting CD19 in patients with acute lymphoblastic leukemia [4]. The high number of clinical trials registered for CAR T cell therapy clearly illustrates its increasing popularity (~130 studies worldwide from which 12 in Europe; clinicaltrials.gov).

In spite of the impressive clinical results of CAR in blood cancers, it is important to consider which specific **T cell subsets** have the highest potential in ACT to further improve the therapeutic outcome in solid tumors [5]. Currently, most of the clinical protocols involve the stimulation of unselected T cells with CD3/CD28 beads in the presence of IL-2, which is also the protocol that was followed in this thesis [6]. However, in the future, the pre-selection of superior subsets of T cells will become increasingly important in clinical research [7].

Less-differentiated T cells were shown to have a higher proliferative capacity and better persistence, which resulted in the eradication of large established tumors and the induction of long-term immunity [7, 8]. The selection of less-differentiated cells such as memory T cells (T memory stem cells, central memory T cells) can provide greater therapeutic potential of ACT, as recently demonstrated by Riddell and coworkers [9]. Moreover, the expansion of T cells in the presence of IL-7, IL-15 and IL-21 has been demonstrated to favor a T cell memory phenotype with increased survival and anti-tumor activity, which might outperform the incubation with IL-2 [10]. Moreover, in this study we mainly focused on the use of $CD8^+$ T cells, whereas the role of $CD4^+$ T cells may not be underestimated. Several studies have illustrated that $CD4^+$ T cells help to improve the therapeutic outcome and support the development of $CD8^+$ T cell memory functions [11, 12]. As was shown in this study, $CD4^+$ T cells can be equally loaded with liposomes as $CD8^+$ T cells, which supports the idea to combine both cell types for further research.

A second important feature is the upregulation of T cell inhibitory receptors or immune checkpoints such as cytotoxic T lymphocyte-associated antigen 4 (CTLA-4) and programmed cell death 1 (PD-1) on activated T cells [13, 14]. Interactions of tumor cells or antigen-presenting cells with these immune checkpoints can promote the exhaustion of T cells [15]. **Exhausted or dysfunctional T cells** lose their capacity to proliferate, to produce immunostimulatory cytokines, and to exert cytolytic activity [14]. Consequently, the combination of T cell therapy with checkpoint inhibitors has demonstrated to enhance the therapeutic effect in preclinical studies [16, 17]. Moreover, the recent elucidation of several intracellular pathways involved in the dysfunctional status of the T cells has triggered research towards therapeutics that target these pathways [18]. As monoclonal antibodies can only target cell surface receptors, other mechanisms such as **RNA interference** (RNAi) are of interest. Indeed, several *in vivo* studies have illustrated the enhanced infiltration of T cells, the increased survival rates and improved memory functions after downregulating intracellular pathways via siRNA [19, 20]. For the delivery of such siRNAs, it is important to keep in mind that for ACT, cells are isolated from a patient to expand them, which allows the application of *ex vivo* transfection techniques. However, innovative approaches are still required, as the use of conventional *ex vivo* transfection methods, i.e. viral vectors and electroporation/nucleofection, are limited due to high production costs, safety issues and loss in viability. To this end, we proposed a novel strategy based on **vapor nanobubble-mediated photoporation** for the *ex vivo* delivery of siRNA, directly to the cytosol of the T cells. As a proof-of-concept, we showed the silencing of a model target while significantly improving the amount of viable transfected cells compared to nucleofection. To further investigate the potential of this strategy, future research needs to elaborate on this concept by using specific siRNA sequences that silence suppressive pathways to boost the survival, proliferative capacity and effector functions of T cells before adoptive transfer.

Besides making the T cells more effective, interfering with the **immunosuppressive tumor microenvironment** may also enhance clinical success. Nowadays, the tumor microenvironment is one of the major challenges in the development of cancer immunotherapies. It can impede the infiltration of anti-tumor T cells while a lack of immunostimulatory cytokines and the upregulation of various immunosuppressive pathways inhibit T cell stimulation and persistence. Besides immune checkpoints, other important mediators in the tumor microenvironment were shown to contribute to the dysfunction of T cells, such as the presence of tumor-promoting cytokines (*e.g.* IL-10, TGFβ) and the interaction with several immunosuppressive cells (*e.g*. regulatory T cells (T_{regs}), myeloid-derived suppressor cells (MDSCs), and tumor-associated macrophages (TAMs)) [21]. Therefore, the identification and therapeutic targeting of these immunosuppressive players in the tumor microenvironment gained a lot of interest in recent years.

It is clear that the success of a selected immunotherapy is influenced by a multitude of different mediators in the tumor microenvironment. Nowadays, it becomes more clear that combining different immunotherapies, interfering concomitantly with multiple immune mediators, entails synergistic effects [22, 23]. The best-studied combination is the administration of ipilimumab (anti-CTLA-4) together with nivolumab (anti-PD-1), which showed improved clinical outcome and will soon find its way to the clinic [24, 25]. Although monoclonal antibodies show good clinical responses, the unbalancing of the immune system can also generate severe side effects, referred to as immune-related adverse events (IRAEs). Because this is a new type of side effects in the clinic, it will be important to educate oncologists how to recognize and handle these side effects [26].

Despite good clinical responses of immune checkpoints, this approach requires a T cell-infiltrated tumor with the presence of high amounts of TILs that can eradicate all tumor cells. Unfortunately, it has been demonstrated that the amount of TILs is often very low and that the tumor tissue is very heterogeneous, which explains why several tumor cells escape from T cell-mediated killing and induce relapse [27, 28]. Hence, this encourages researchers to further investigate in combination strategies with other types of immunotherapies. In **Figure 1**, the mechanisms of action associated with different types of anti-cancer therapeutics are illustrated.

Within our study, we investigated the combination of ACT with the concomitant delivery of the **immune adjuvant** monophosphoryl lipid A (MPLA) to the tumor. We anticipated a tumor killing effect by the adoptively transferred CTLs accompanied by an enhanced activity of tumor-infiltrated dendritic cells (DCs) via MPLA. It has been shown previously that tumor-infiltrated DCs may have an immunosuppressive role, which counteract the CTL responses [29]. The Toll-like receptor 4 (TLR4) agonist MPLA may shift the phenotype of DCs in the tumor microenvironment from immunosuppressive to tumor-

suppressive. A recent study has demonstrated the potential of boosting DCs in the tumor microenvironment by the delivery of adjuvant mRNA, inducing the reactivation of suppressed tumor-infiltrating T cells and the activation of new CTLs in the lymph nodes [30]. *In vitro*, we showed the maturation of DCs when incubated with T cells loaded with MPLA liposomes, which induced the production of IL-12, an immunostimulatory cytokine. Moreover, intratumoral injection of tumor-specific MPLA-loaded T cells resulted in improved survival of tumor-bearing mice. However, further research is needed to investigate whether the therapeutic outcome is also improved after systemic injection, which is the final goal of this combined strategy. We selected MPLA in our study based on its amphiphilic properties, which enables its incorporation in liposomes, and its activity at the cell surface, circumventing the need for cellular internalization. However, it should be considered that MPLA is possibly not the most optimal immune adjuvant to manipulate the tumor microenvironment. Indeed, in recent years much controversy has arisen concerning the immunostimulatory function of TLR4 agonists. Several studies have illustrated that TLR4 agonists can induce anti-cancer responses while a few other studies have now demonstrated the opposite effect, *i.e.* the promotion of tumor growth [31, 32]. It was suggested that the pro- or anti-cancer effects might depend on the environmental conditions in the tumor [32]. In addition to TLR4 agonists, other adjuvants stimulating TLR 7/8 and TLR9 were shown to have great potential in stimulating DCs and could be of value to modulate the tumor microenvironment [31]. Importantly, although we anticipated that the stable T cell coupling of MPLA liposomes would induce DC maturation via close interaction with TLR4 receptors at the DC surface, our results showed an extensive internalization of liposomes by DCs, *e.g.* via the hypothesized 'nibbling' process. From this observation, it is clear that also other types of adjuvants (*e.g.* CpG, poly(I:C)) that require the cytosolic delivery can be of interest for targeted delivery to the tumor.

In addition, combining ACT with the delivery of **immunostimulatory cytokines** as described by Irvine and colleagues to support the activity of the transferred T cells can be extended by the delivery of cytokines that have an immune-stimulating effect on the tumor microenvironment [33]. For example, it has been investigated whether T cells can be engineered to produce IL-12, which can shift multiple cell types within the tumor microenvironment from pro-oncogenic to tumor-suppressive [34]. However, in most studies, viral vectors are used to perform this genetic engineering, which increases concerns about safety and cost. For this purpose, the delivery of IL-12 via NPs could be a valuable alternative. As IL-12 was already shown to be easily entrapped within liposomes, the coupling of IL-12 loaded liposomes to T cells for adoptive transfer might be a novel interesting approach [35].

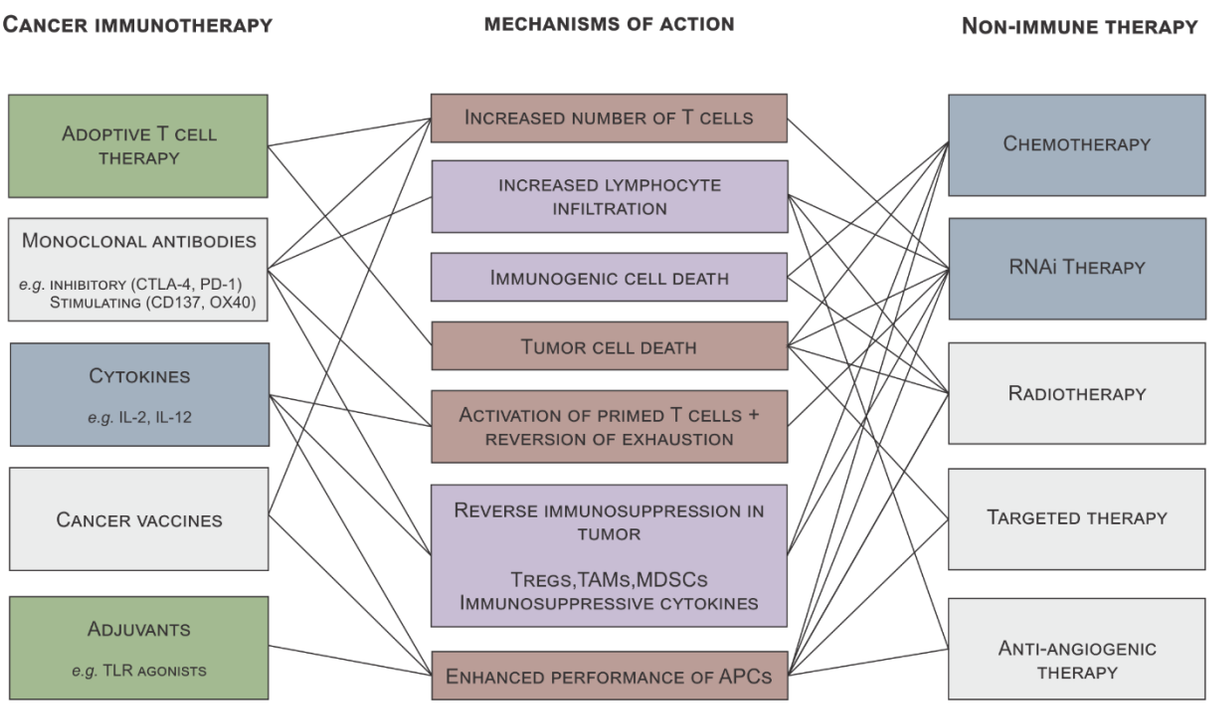

Figure 1. Mechanisms of action of different anti-cancer therapies. This figure was adapted from Ref. [23] and adjusted based on our own research. Cancer immunotherapies can be combined with either other type of immunotherapy or standard non-immune therapy, of which the latter one is now mainly used in the clinic, with the exception of RNA interference (RNAi). RNAi is already clinically investigated, however, not yet approved or available on the market. The types of immunotherapies that were evaluated within this work are indicated in green and their mechanisms of action in red. The therapeutic strategies that are suggested here as interesting therapies to combine with our concept are indicated in blue albeit that further development and investigation such as loading the nanoparticles with cytokines, chemotherapeutics, and RNAi, are needed. By combining these strategies, also other mechanisms of action (indicated in purple) can be exploited, leading to a synergistic outcome.

Besides combining different immunotherapeutics, **Figure 1** also indicates that combinations with standard anti-cancer therapies may act on distinct (immune) mechanisms of action, entailing synergistic effects. For example, combining immunotherapy with **chemotherapeutics** seems very interesting as it was recently observed that the induction of immunogenic cell death by specific types of chemotherapeutics may contribute to anti-cancer immune responses [36]. In particular, when tumor cells are destroyed in an immunogenic way, they release tumor antigens as well as factors to attract and activate antigen-presenting cells [37]. Therefore, in contrast to the detrimental impact of chemotherapeutics such as doxorubicin (DOX) on the immune system, the identification of DOX as an inducer of immunogenic cell death provided a rationale for its synergistic application with immunotherapy. Of course, DOX, as well as other chemotherapeutics, have the disadvantage of off-target toxicity, when administered systemically. To overcome this, chemotherapeutics are packaged in NPs (*e.g.* Doxil®/Caelyx®) to reduce side effects, increase circulation time, and enhance accumulation in the tumor tissue based on the enhanced permeation and retention (EPR) effect [38]. However, the general problem with EPR-mediated passive tumor-targeted delivery of nanomedicines is the heterogeneity of the EPR effect leading to low or even absent nanomedicine extravasation in tumors showing

limited EPR. This issue can be addressed by cell-mediated delivery of NPs containing chemotherapeutics, as proposed in this work. Following the successful anchoring of liposomes to the surface of CTLs, we evaluated the incorporation of DOX into these liposomes for T cell-mediated delivery. Unfortunately, we were not able to develop a sufficiently stable liposomal carrier that could avoid premature drug release and prevent toxicity to the T cell carriers (data not shown). To this end, it is important to further investigate the development of either a NP that can prevent premature drug release or selecting a chemotherapeutic for which T cells are resistant to therapeutic doses [39].

Also nucleic acid therapeutics, like siRNA, require the formulation into NPs prior to *in vivo* administration. NP encapsulation can protect them from degradation by nucleases and can help to overcome the cell membrane barrier for intracellular delivery. The delivery of siRNA to tumor cells, targeting genes involved in cell cycle arrest, cell apoptosis, and proliferation, has already been shown to induce tumor regression [40]. Besides targeting tumor cells, also certain types of immune cells such as regulatory DCs, MDSCs, and TAMs could be potential targets, as these cells were shown to promote tumor outgrowth. Hence, the downregulation of immunosuppressive pathways via siRNA in these cells can be an important therapeutic approach for future research. An example of a target that was already shown to induce a potent anti-tumor effect when downregulated is signal transducer and activator of transcription 3 (STAT3) in DCs [41]. Moreover, a combination of RNAi with immunostimulatory agents such as TLR agonists is suggested to even further enhance the anti-tumor response [42]. In analogy with NPs loaded with low molecular weight chemotherapeutics, siRNA loaded NPs face the same delivery challenges *in vivo*. To improve the accumulation of siRNA-loaded NPs in the tumor, we demonstrated in **Chapter 2** that lipid-coated nanogels could be loaded with siRNA molecules and coupled to $CD8^+$ T cells. Importantly, to allow intracellular delivery of siRNA to the abovementioned target cells, the NPs need to be released again from the carrier T cells in the tumor. To this end, we investigated a redox-sensitive coupling system enabling triggered release of liposomes from the T cell surface upon incubation with the reducing agent glutathione. However, optimal coupling stability in serum-enriched medium via this redox-sensitive linker could not be guaranteed. Therefore, we also evaluated the coupling via an enzyme-sensitive linker. Although stability problems in serum-enriched medium were solved, the enzyme-triggered release was very low, indicating the complexity of maintaining specific enzymatic activity on the highly dynamic cell membrane. To address the issue of stability, a more stable thioether bond proved to avoid premature NP release after systemic injection as shown by a rather limited release of liposomes upon contact with serum. Although the mechanism remains elusive, the ability of DCs to internalize nanoparticles that are stably attached to the T cell surface might be useful for the delivery of siRNA as well. However, it remains to be investigated what the most suitable coupling strategy is for *in vivo* delivery of NPs to the tumor, which subsequently influences the choice of therapeutic that can be delivered.

As explained here, a multitude of different combinations can lead to synergistic effects. However, the increasing number of (immuno)therapeutics, inter-patient variability in immune responses, and the tumor heterogeneity augment the need for **predictive biomarkers** to identify patients that may benefit from a selected therapeutic strategy and allow physicians to direct patients to the most suitable therapies [23, 43]. This personalized strategy may offer advantages in terms of reducing side effects and costs for patients that might not show therapeutic response. The implementation of a personalized approach in cancer immunotherapy can be further extended to the rational selection of suitable **tumor antigens** as targets in cancer vaccination and ACT with TCR/CAR engineered T cells. Self-antigens can be used in a broad range of patients, although their clinical use is severely hampered by off-target toxicity and immune tolerance, as previously observed in clinical trials [44, 45]. Therefore, the identification of tumor-specific antigens or neoantigens as targets for these therapies will become increasingly important. Decreasing costs of next-generation sequencing platforms will make this identification in a patient-specific manner more feasible in the future [46, 47]. Moreover, considering the heterogeneity within the primary tumor on the one hand and between metastases on the other hand, together with the well-known phenomenon of antigen loss in cancer cells under pressure of an antigen-specific immune response, will require targeting of different neoantigens within a single treatment by ACT [27, 48, 49].

Both the use of biomarkers and the search for patient-specific neoantigens highlight the need for a personalized treatment, which is in contrast with the paradigm of pharmaceutical companies to produce "off-the-shelf" therapeutics. However, the past few years have witnessed the emergence of several new biotechnology companies that focus on the **commercialization of ACT** [50, 51]. In coming years, ACT has great potential to play a major role in the treatment of cancer patients, which addresses the need for its commercialization [52]. The current issues related to this are how to manufacture cell therapies in a cost-effective way and how to provide safe and sterile products while maintaining adherence to the Good Manufacturing Practices (GMP) guidelines. Of note, based on lessons learned from the production of the cellular product sipuleucel-T, the therapeutic efficacy needs to be high enough to justify the cost and complexity of the production. Therefore, pharmaceutical companies are currently investigating the automation of T cell manipulations in closed systems with the aim to reduce cost and the risk for contamination, while further improving the scalability of the manufacturing process. However, it depends on the therapeutic success of ACT whether commercialization in the future will be successful or not. Therefore, clinical trials proving the induction of long-term remissions in a high number of patients will be highly recommended. Furthermore, novel approaches, such as the use of allogeneic T cells, were proposed to lower the cost and to consequently augment the success rate. This allogeneic T cell approach consists of the isolation of T cells from healthy donors and the genetic engineering of the cells to replace

the endogenous TCR by a CAR or tumor-targeted TCR [50]. Although the allogeneic T cell concept for ACT aims to create again "off-the-shelf" products to reduce costs, the previously described benefit of targeting tumor-specific antigens further supports a personalized approach. In general, it is all about finding a balance between the personalization of the treatment to enhance the efficacy on the one hand and the use of off-the-shelf therapeutics to reduce costs on the other hand.

Besides commercialization, the development of personalized immunotherapeutics and cell-based therapies for cancer may give rise to a number of additional **regulatory challenges**. In these therapies, not all of the general guidelines in current drug development can be applied. For example, assessment of the stability and shelf life of autologous cell-based products cannot be established for every batch due to the 'on-demand' production and short time until administration. Regulatory agencies that control the pre-market testing and marketing approval are currently working to define optimal guidelines for the manufacturing of these cellular products [52, 53].

In summary, nowadays cancer immunotherapy is a hot topic, which is justified because of its superior effectiveness in patients refractory to conventional therapies. Unfortunately, still a major set of issues are crossing its path to ultimate success, for example the presence of exhausted T cells, the immunosuppressive tumor microenvironment, and tumor heterogeneity. Combining different types of cancer immunotherapies or the combination with other anti-cancer therapies may tackle these limitations. Several of these therapeutics benefit from the encapsulation in nanocarriers to protect them from degradation, modify their pharmacokinetics and/or enhance the intracellular delivery. However, targeting of these NPs to the tumor is still a major bottleneck in the field of anti-cancer nanomedicine. In this work, we have explored the possibility to utilize the tumor-migratory capacity of adoptively transferred T cells to deliver nanomedicines to the tumor, in order to develop a synergistic anti-tumor therapy. As highlighted in this chapter, our experimental data clearly show the potential of such a combination strategy as well as highlight a number of hurdles that need to be addressed in future research to translate such therapies from the laboratory to the patient.

REFERENCES

1. Lee, L., Gupta, M. & Sahasranaman, S. Immune Checkpoint inhibitors: An introduction to the next-generation cancer immunotherapy. *J Clin Pharmacol* **56**, 157-69 (2016).
2. Hoos, A. Development of immuno-oncology drugs - from CTLA4 to PD1 to the next generations. *Nat Rev Drug Discov* **15**, 235-47 (2016).
3. Couzin-Frankel, J. Breakthrough of the year 2013. Cancer immunotherapy. *Science* **342**, 1432-3 (2013).
4. Maude, S.L., Teachey, D.T., Porter, D.L. & Grupp, S.A. CD19-targeted chimeric antigen receptor T-cell therapy for acute lymphoblastic leukemia. *Blood* **125**, 4017-23 (2015).
5. Klebanoff, C.A., Gattinoni, L. & Restifo, N.P. Sorting through subsets: which T-cell populations mediate highly effective adoptive immunotherapy? *J Immunother* **35**, 651-60 (2012).
6. Klebanoff, C.A. et al. Memory T cell-driven differentiation of naive cells impairs adoptive immunotherapy. *J Clin Invest* **126**, 318-34 (2016).
7. Busch, D.H., Frassle, S.P., Sommermeyer, D., Buchholz, V.R. & Riddell, S.R. Role of memory T cell subsets for adoptive immunotherapy. *Semin Immunol* **28**, 28-34 (2016).
8. Restifo, N.P., Dudley, M.E. & Rosenberg, S.A. Adoptive immunotherapy for cancer: harnessing the T cell response. *Nat Rev Immunol* **12**, 269-81 (2012).
9. Chakradhar, S. Prime pick: Researchers get selective about T cells for cancer therapy. *Nat Med* **22**, 456-458 (2016).
10. Golubovskaya, V. & Wu, L. Different Subsets of T Cells, Memory, Effector Functions, and CAR-T Immunotherapy. *Cancers (Basel)* **8**, 36 (2016).
11. Sommermeyer, D. et al. Chimeric antigen receptor-modified T cells derived from defined CD8(+) and CD4(+) subsets confer superior antitumor reactivity in vivo. *Leukemia* **30**, 492-500 (2016).
12. Shedlock, D.J. & Shen, H. Requirement for CD4 T cell help in generating functional CD8 T cell memory. *Science* **300**, 337-9 (2003).
13. Day, C.L. et al. PD-1 expression on HIV-specific T cells is associated with T-cell exhaustion and disease progression. *Nature* **443**, 350-4 (2006).
14. Zarour, H.M. Reversing T-cell Dysfunction and Exhaustion in Cancer. *Clin Cancer Res* **22**, 1856-64 (2016).
15. Minn, A.J. & Wherry, E.J. Combination Cancer Therapies with Immune Checkpoint Blockade: Convergence on Interferon Signaling. *Cell* **165**, 272-5 (2016).
16. Morales-Kastresana, A., Labiano, S., Quetglas, J.I. & Melero, I. Better performance of CARs deprived of the PD-1 brake. *Clin Cancer Res* **19**, 5546-8 (2013).
17. John, L.B. et al. Anti-PD-1 antibody therapy potently enhances the eradication of established tumors by gene-modified T cells. *Clin Cancer Res* **19**, 5636-46 (2013).
18. Zhou, P. et al. In vivo discovery of immunotherapy targets in the tumour microenvironment. *Nature* **506**, 52-7 (2014).
19. Hinterleitner, R. et al. Adoptive transfer of siRNA Cblb-silenced CD8+ T lymphocytes augments tumor vaccine efficacy in a B16 melanoma model. *PLoS One* **7**, e44295 (2012).
20. Berezhnoy, A., Castro, I., Levay, A., Malek, T.R. & Gilboa, E. Aptamer-targeted inhibition of mTOR in T cells enhances antitumor immunity. *J Clin Invest* **124**, 188-97 (2014).

21. Beavis, P.A. et al. Reprogramming the tumor microenvironment to enhance adoptive cellular therapy. *Semin Immunol* **28**, 64-72 (2016).
22. Smyth, M.J., Ngiow, S.F., Ribas, A. & Teng, M.W. Combination cancer immunotherapies tailored to the tumour microenvironment. *Nat Rev Clin Oncol* **13**, 143-58 (2016).
23. Melero, I. et al. Evolving synergistic combinations of targeted immunotherapies to combat cancer. *Nat Rev Cancer* **15**, 457-72 (2015).
24. Larkin, J. et al. Combined Nivolumab and Ipilimumab or Monotherapy in Untreated Melanoma. *N Engl J Med* **373**, 23-34 (2015).
25. Wolchok, J.D. et al. Nivolumab plus ipilimumab in advanced melanoma. *N Engl J Med* **369**, 122-33 (2013).
26. Michot, J.M. et al. Immune-related adverse events with immune checkpoint blockade: a comprehensive review. *Eur J Cancer* **54**, 139-48 (2016).
27. Jensen, S.M. et al. Increased frequency of suppressive regulatory T cells and T cell-mediated antigen loss results in murine melanoma recurrence. *J Immunol* **189**, 767-76 (2012).
28. Gajewski, T.F. The Next Hurdle in Cancer Immunotherapy: Overcoming the Non-T-Cell-Inflamed Tumor Microenvironment. *Semin Oncol* **42**, 663-71 (2015).
29. Hargadon, K.M. Tumor-altered dendritic cell function: implications for anti-tumor immunity. *Front Immunol* **4**, 192 (2013).
30. Van Lint, S. et al. Intratumoral Delivery of TriMix mRNA Results in T-cell Activation by Cross-Presenting Dendritic Cells. *Cancer Immunol Res* **4**, 146-56 (2016).
31. Pradere, J.P., Dapito, D.H. & Schwabe, R.F. The Yin and Yang of Toll-like receptors in cancer. *Oncogene* **33**, 3485-95 (2014).
32. Awasthi, S. Toll-like receptor-4 modulation for cancer immunotherapy. *Front Immunol* **5**, 328 (2014).
33. Stephan, M.T., Moon, J.J., Um, S.H., Bershteyn, A. & Irvine, D.J. Therapeutic Cell Engineering Using Surface-Conjugated Synthetic Nanoparticles. *Journal of Immunotherapy* **16**, 1035-41 (2010).
34. Chinnasamy, D. et al. Local delivery of interleukin-12 using T cells targeting VEGF receptor-2 eradicates multiple vascularized tumors in mice. *Clin Cancer Res* **18**, 1672-83 (2012).
35. Simpson-Abelson, M.R. et al. IL-12 delivered intratumorally by multilamellar liposomes reactivates memory T cells in human tumor microenvironments. *Clin Immunol* **132**, 71-82 (2009).
36. Pol, J. et al. Trial Watch: Immunogenic cell death inducers for anticancer chemotherapy. *Oncoimmunology* **4**, e1008866 (2015).
37. Kroemer, G., Galluzzi, L., Kepp, O. & Zitvogel, L. Immunogenic cell death in cancer therapy. *Annu Rev Immunol* **31**, 51-72 (2013).
38. Barenholz, Y. Doxil(R)--the first FDA-approved nano-drug: lessons learned. *J Control Release* **160**, 117-34 (2012).
39. Huang, B. et al. Active targeting of chemotherapy to disseminated tumors using nanoparticle-carrying T cells. *Sci Transl Med* **7**, 291ra94 (2015).
40. Zuckerman, J.E. & Davis, M.E. Clinical experiences with systemically administered siRNA-based therapeutics in cancer. *Nat Rev Drug Discov* **14**, 843-56 (2015).

41. Luo, Z. et al. Nanovaccine loaded with poly I:C and STAT3 siRNA robustly elicits anti-tumor immune responses through modulating tumor-associated dendritic cells in vivo. *Biomaterials* **38**, 50-60 (2015).
42. Conde, J., Arnold, C.E., Tian, F.R. & Artzi, N. RNAi nanomaterials targeting immune cells as an anti-tumor therapy: the missing link in cancer treatment? *Materials Today* **19**, 29-43 (2016).
43. Whiteside, T.L., Demaria, S., Rodriguez-Ruiz, M.E., Zarour, H.M. & Melero, I. Emerging Opportunities and Challenges in Cancer Immunotherapy. *Clin Cancer Res* **22**, 1845-55 (2016).
44. Johnson, L.A. et al. Gene therapy with human and mouse T-cell receptors mediates cancer regression and targets normal tissues expressing cognate antigen. *Blood* **114**, 535-46 (2009).
45. Morgan, R.A. et al. Cancer regression and neurological toxicity following anti-MAGE-A3 TCR gene therapy. *J Immunother* **36**, 133-51 (2013).
46. Castle, J.C. et al. Exploiting the mutanome for tumor vaccination. *Cancer Res* **72**, 1081-91 (2012).
47. Gerlinger, M. et al. Intratumor heterogeneity and branched evolution revealed by multiregion sequencing. *N Engl J Med* **366**, 883-92 (2012).
48. DuPage, M., Mazumdar, C., Schmidt, L.M., Cheung, A.F. & Jacks, T. Expression of tumour-specific antigens underlies cancer immunoediting. *Nature* **482**, 405-9 (2012).
49. Klebanoff, C.A., Rosenberg, S.A. & Restifo, N.P. Prospects for gene-engineered T cell immunotherapy for solid cancers. *Nat Med* **22**, 26-36 (2016).
50. June, C.H., Riddell, S.R. & Schumacher, T.N. Adoptive cellular therapy: a race to the finish line. *Sci Transl Med* **7**, 280ps7 (2015).
51. Walker, A. & Johnson, R. Commercialization of cellular immunotherapies for cancer. *Biochem Soc Trans* **44**, 329-32 (2016).
52. Kaiser, A.D. et al. Towards a commercial process for the manufacture of genetically modified T cells for therapy. *Cancer Gene Ther* **22**, 72-8 (2015).
53. Vatsan, R.S. et al. Regulation of immunotherapeutic products for cancer and FDA's role in product development and clinical evaluation. *J Immunother Cancer* **1**, 5 (2013).

Summary and conclusions

Cancer remains one of the most devastating diseases worldwide, with every year 14 million new cases and 8 million cancer-related deaths. Over the past few years, the search for new anti-cancer approaches has increased tremendously. Nowadays, conventional cancer therapies consist of surgery, radiotherapy, and chemotherapy. These methods, however, hold a potential risk for relapse, metastasis, and systemic toxicity. To reduce the risk of systemic toxicities, researchers have developed strategies to encapsulate chemotherapeutics in nanocarriers, aiming to improve the specific delivery of therapeutics to the tumor. Despite the success of anti-cancer nanomedicines in (pre)clinical trials, the number of commercially available therapeutics remains remarkably low. One of the main causes is their low targeting capacity and limited infiltration into the tumor after systemic injection. Therefore, this project aimed to investigate the cell-mediated delivery of nanomedicines to the tumor. For this purpose, cytotoxic T cells (CTLs) were selected as transport vehicles based on their spontaneous migration to the tumor and their potential to specifically kill tumor cells. In addition, we evaluated the delivery of small interfering RNA (siRNA) molecules to the cytosol of CTLs via a vapor nanobubble-mediated photoporation technique, aiming to improve T cell effector functions against the tumor.

Chapter 1 provided a general overview of the two major research fields that were combined in this work; cancer nanomedicines and cancer immunotherapy. We provided a brief overview of the different types of nanocarriers and encapsulated therapeutics that are currently investigated for the treatment of cancer. One of the major drawbacks in the delivery of nanomedicines to the tumor is their limited infiltration and accumulation in the tumor tissue. Therefore, cell-mediated drug delivery via tumoritropic cells can be an interesting alternative. In this strategy, tumoritropic cells, such as mesenchymal stem cells, monocytes, macrophages, and T lymphocytes, are loaded with nanoparticles (NPs) to evade the various barriers NPs normally encounter on their way to the tumor. We described the different cell types and various coupling techniques that can be used in this cell-mediated drug delivery. In a second part, a summary is provided of the different types of cancer immunotherapies that are currently in (pre)clinical trials or on the market, including cancer vaccination, adoptive T cell therapy (ACT), immunostimulatory cytokines, checkpoint inhibitors, and immune adjuvants. In addition, this section highlighted the advantages of combining immunotherapy with non-immune therapies such as chemotherapy and RNA interference. In a final part, we described *in vivo* and *ex vivo* transfection methods for the genetic modification of T cells to express tumor-specific T cell receptors and to enhance their tumor infiltration, survival, and cytolytic effect. In addition, we focused on different techniques for the delivery of siRNA to T lymphocytes, including NP-mediated delivery, electroporation/nucleofection, and CellSqueeze microfluidics.

Chapter 2 described the development of a novel reversible coupling strategy to attach lipid-based NPs to the surface of both activated and non-activated $CD8^+$ T cells. The incorporation of high amounts of pyridyldithiopropionate (PDP)-functionalized lipids (up to 50 wt%) was shown to drastically improve the coupling efficiency. Importantly, the coupling of liposomes did not affect their *in vitro* proliferation and cytolytic activity. The release of liposomes from the surface by a tumor-related trigger offers advantages for the delivery of membrane-impermeable macromolecular drugs that require cytosolic delivery, for example siRNA. Triggered release of the liposomes that were attached to the cells via a disulfide bond can be obtained via the incubation with a reducing agent. Based on the literature that has described the presence of elevated levels of glutathione in the extracellular tumor microenvironment, glutathione was selected as trigger to evaluate the NP release. For both activated and non-activated T cells, up to 50-60% of the anchored liposomes were shown to detach from the surface. Notably, the liposomes did not tend to aggregate upon release, which is important for their subsequent uptake in tumor cells. As a proof-of-concept, siRNA molecules were encapsulated in a lipid-polymer nanocomposite, which efficiently encapsulated siRNA in the nanogel core and allowed coupling to $CD8^+$ T cells via the PDP-functionalized lipid shell. In addition, we demonstrated that the lipid shell improved the stability of siRNA in the nanoformulation when incubated with human serum. In addition to the coupling of NPs to $CD8^+$ T cells, $CD4^+$ T cells were shown to attach liposomes in similar amounts, which might be of interest for future research as $CD4^+$ T cells have been described in the literature to augment the proliferation, survival and efficacy of $CD8^+$ T cells.

As the final aim of this research was to exploit the CTL's capacity to deliver drug-loaded NPs to the tumor, **Chapter 3** examined the *in vivo* migration of NP-loaded CTLs to the tumor. Therefore, we used a melanoma mouse model and investigated the tumor infiltration of CTLs as a function of their NP-load. The reversible coupling was extended by a stable coupling strategy based on the incorporation of maleimide (MAL)-functionalized lipids in the liposome composition. Although the data revealed a lower infiltration of liposome-loaded CTLs in the tumor 48h after transfer, we could not observe a negative impact of the NP-load on the anti-tumor responses of the T cells. On the contrary, when loaded with NPs, the CTLs showed an enhanced control over the tumor growth. The *in vitro* observation that T cells loaded with PDP- and MAL-functionalized liposomes secreted significantly higher levels of interferon gamma (IFNγ) and tumor necrosis factor alpha (TNFα) might contribute to this enhanced anti-tumor effect. In a next step, the liposomes were loaded with monophosphoryl lipid A (MPLA), an immune adjuvant from which it has been shown in the literature to boost the immune system against cancer. First, it was demonstrated that MPLA incorporated in PDP and MAL liposomes had no influence on the T cell proliferation, viability, and coupling efficiency. In addition, these data also showed an increased secretion of IFNγ when T cells were loaded with liposomes. Moreover, this increased secretion could be uniquely attributed to the NP coupling because free MPLA did

not induce this effect. A co-culture of dendritic cells (DCs) and T cells loaded with MPLA liposomes demonstrated the upregulation of the co-stimulatory molecules CD40 and CD80 and an increased secretion of the immunostimulatory cytokine IL-12, which all indicated successful maturation of DCs. In a final step, intratumoral delivery of T cells showed improved survival of mice injected with T cells coupled with MPLA liposomes via a reversible coupling. Future research will be needed to investigate the therapeutic benefit after systemic injection.

Considering the observation that a reversible coupling by a disulfide linker encountered stability problems in serum-enriched medium and that half of the liposomes remained attached to the surface after triggered release, we searched for a more specific cleavable system. Therefore, in **Chapter 4,** we investigated the coupling of liposomes via an enzyme-sensitive coupling system in which the liposomes were attached to the T cells via a cleavable peptide linker. The peptide sequence is cleavable by the specific proteases matriptase, urokinase-type plasminogen activator (uPA), and legumain, from which elevated levels are present in several tumor types. In this chapter, we showed successful coupling of the peptide linker construct to the CTL surface with optimal stability in serum-enriched medium. Although the cleavability of the construct was demonstrated when attached to magnetic beads, when coupled onto T cells, only a small fraction was cleaved from the surface by matriptase or uPA. Because incubation with the aspecific protease trypsin illustrated high cleavage of the construct from the T cells, we hypothesized that steric hindrance by the highly complex cell surface might contribute to the low specific cleavage.

Besides the ability of CTLs to transport nanomedicines to the tumor, they also have the intrinsic capacity to kill tumor cells. However, a variety of immunosuppressive pathways can inhibit their anti-tumor responses. Downregulation of these pathways via siRNA is of interest to improve the therapeutic outcome of ACT. As T cells are hard-to-transfect cells, the conventional lipid/polymer-based NPs and nucleofection have been shown to induce a low transfection efficiency and high toxicity, respectively. Therefore, in **Chapter 5** we proposed vapor nanobubble-mediated photoporation as an alternative approach. We demonstrated the delivery of siRNA molecules to the cytosol of T cells, leading to knockdown of the model target CD45. Compared to nucleofection, a similar silencing was obtained and the viability was drastically improved, resulting in three times more silenced T cells with the photoporation technique.

In **Chapter 6**, we summarized the current challenges in the field of cancer immunotherapy. We highlighted the possibility to combine different therapeutic strategies, in particular nanomedicines, with cancer immunotherapy, to overcome the immunosuppressive tumor microenvironment and to elicit more potent anti-cancer immune responses in patients.

CONCLUSIONS

We demonstrated the potential of combining nanomedicines with cancer immunotherapy, in particular ACT, for the treatment of cancer. We were the first to show the reversible coupling of lipid-based NPs to the surface of CTLs for tumor-targeted delivery of membrane-impermeable macromolecules such as siRNA. Further, preliminary *in vitro* and *in vivo* data illustrated promising results for the combination of CTLs with NPs that were loaded with immune adjuvants. Besides the use of CTLs as carriers for the delivery of drug-loaded NPs to the tumor, they also have the ability to kill tumor cells, which has already been extensively exploited in ACT. However, a variety of immunosuppressive mediators, especially in the tumor microenvironment, was shown to hinder the T cell anti-tumor responses. To tackle this important challenge, we developed a technique based on vapor-nanobubble photoporation for the efficient delivery of siRNA molecules to CTLs, inducing silencing of target genes. Consequently, the knockdown of important immunosuppressive pathways can give T cells more power to eradicate tumors.

Samenvatting en conclusies

Kanker is één van de meest verwoestende ziektes van deze tijd, met wereldwijd per jaar ongeveer 14 miljoen nieuwe gevallen en 8 miljoen overlijdens als gevolg van de ziekte. Het is dan ook niet verwonderlijk dat wetenschappelijk onderzoek naar nieuwe therapeutische mogelijkheden om kanker te bestrijden hoogtij viert. Behandeling van kanker kan via chirurgische resectie, radiotherapie en/of het gebruik van chemotherapeutica. Het risico op remissie, metastase en systemische toxiciteit blijft echter groot. Nanoscopische dragers bieden mogelijkheden om het anti-kanker geneesmiddel selectiever naar het tumorweefsel te begeleiden. Hierbij bestaat de mogelijkheid om de dosis aan kankerbestrijdend geneesmiddel te verhogen ter hoogte van de tumor, terwijl systemische bijwerkingen gereduceerd worden. Ondanks de beloftevolle (pre-)klinische resultaten, blijft het aanbod aan commerciële kankerbestrijdende nanotherapeutica beperkt. Eén van de belangrijkste oorzaken is het te weinig gericht afleveren van de partikels in de tumor na intraveneuze toediening. Daarom werd in dit project onderzocht of de aflevering van nanopartikels (NP's) in de tumor verhoogd kan worden door middel van cel-gemedieerde aflevering. Hierbij werden cytotoxische T-cellen (CTL's) verkozen als drager omwille van hun spontane migratie naar de tumor en hun potentieel om heel gericht kankercellen af te doden. Verder werd ook 'fotoporatie' onderzocht als techniek voor de aflevering van *small interfering RNA* (siRNA) in het cytosol van de CTL's met als doel de T-cel responsen in de tumor te verhogen door het onderdrukken van welbepaalde *pathways*.

Hoofdstuk 1 geeft een overzicht van de twee grote onderzoeksvelden die in deze thesis gecombineerd werden, namelijk kanker nanomedicijnen en kanker immunotherapie. Dit hoofdstuk beschrijft kort de verschillende types nanodragers en de geneesmiddelen die op dit moment onderzocht worden voor het behandelen van kanker. Op dit ogenblik zijn slechts een beperkt aantal van deze geneesmiddelen op de markt. De oorzaak van dit beperkt aantal succesvolle nanomedicijnen kan toegeschreven worden aan de lage infiltratie en accumulatie in de tumor na systemische toediening. Cel-gemedieerde aflevering werd reeds onderzocht om de aflevering van deze NP's in de tumor te verhogen. Verschillende types van tumoritrope cellen zoals mesenchymale stamcellen, monocyten, macrofagen en T-lymfocyten werden daartoe beladen met NP's via verschillende koppelingsstrategieën. Een tweede deel van deze introductie bevat een overzicht van de verschillende immunotherapieën die momenteel in (pre-)klinische studies onderzocht worden of die reeds commercieel beschikbaar zijn. Deze therapieën omvatten kanker vaccinatie, adoptieve T-cel therapie (ACT) en de behandeling met immuun-stimulerende cytokines, imuunadjuvantia of de zogenaamde *checkpoint* inhibitoren. Daarnaast werd in dit hoofdstuk ook de combinatie van immunotherapie met andere niet-immuun-gerelateerde therapieën, zoals chemotherapie en *RNA interference,* aangehaald. Ten slotte werden verschillende *in*

vivo en *ex vivo* methoden besproken voor het transfecteren en het genetisch modificeren van T-cellen met als doel specifieke T-cel receptoren tot expressie te laten brengen en verder ook om hun infiltratie, overleving en cytotoxische functies te verbeteren. Daarnaast werden er ook verschillende methodes opgesomd die zorgen voor de aflevering van siRNA in het cytosol van T-cellen, zoals NP's, electroporatie, nucleofectie en *CellSqueeze* microfluidica.

In **Hoofdstuk 2** werd de ontwikkeling van een nieuw reversibel koppelingssysteem beschreven voor het beladen van zowel geactiveerde als niet-geactiveerde $CD8^+$ T-cellen met lipide NP's. De koppeling werd sterk verhoogd wanneer een grote hoeveelheid van een pyridyldithiopropionaat (PDP)-gefunctionaliseerd lipide (tot 50 gewichtsprocent) werd geïncorporeerd in de liposoom compositie. Een belangrijke observatie was dat de proliferatie en het cytolytisch effect van de T-cellen niet verstoord werd door de belading met liposomen. Het loskoppelen van deze liposomen op basis van een trigger in de tumor omgeving kan gunstig zijn voor het afleveren van membraan-impermeabele macromoleculaire geneesmiddelen zoals siRNA. Aangezien de liposomen gekoppeld werden op de T-cellen via een disulfide binding kan door middel van een reducerende molecule deze binding verbroken worden. Op basis van literatuur waarin reeds beschreven werd dat de tumor omgeving een reducerend milieu is door de aanwezigheid van verhoogde hoeveelheden glutathion, werd deze laatste geselecteerd als trigger voor de vrijstelling van de liposomen. Voor zowel de geactiveerde als niet-geactiveerde cellen werd een vrijstelling van 50 tot 60% van de gekoppelde liposomen bekomen. Er werd aangetoond dat deze liposomen na loskoppeling niet geaggregeerd waren, wat van belang is voor hun verdere opname in targetcellen. Om dit '*proof-of-concept*' verder uit te bouwen, werden siRNA moleculen geïncorporeerd in een hybride nanoformulatie. Hierbij werden de siRNA moleculen verpakt in een nanogel matrix en omhuld door lipiden die een membraan vormden rond de nanogel kern. Door de incorporatie van PDP-gefunctionaliseerde lipiden in dit membraan werd een goede aanhechting van de siRNA-beladen NP's waargenomen. Verder werd ook aangetoond dat deze lipide omhulling bescherming bood tegen het vrijstellen van siRNA moleculen uit de formulatie wanneer deze geïncubeerd werd in serum. Naast de koppeling van NP's aan $CD8^+$ T-cellen, werd aangetoond dat ook $CD4^+$ T-cellen gelijkaardige hoeveelheden aan partikels kunnen dragen. Aangezien onderzoek heeft aangetoond dat $CD4^+$ T-cellen ook naar de tumor migreren en de proliferatie, overleving en anti-tumor effecten van $CD8^+$ T-cellen kunnen verhogen, zijn deze ook interessant om in de toekomst verder te onderzoeken voor de cel-gemedieerde aflevering van NP's.

Het ultieme doel van deze studie is om CTL's te gebruiken als dragers van NP's naar de tumor. Daarom werd in **Hoofdstuk 3** de *in vivo* migratie en de infiltratie van NP-beladen, geactiveerde $CD8^+$ T-cellen onderzocht in een muis melanoom model. Naast de reeds besproken reversibele koppeling, werd hier ook een stabiele koppeling onderzocht. Voor het vormen van een stabiele koppeling werden er aan de liposoom samenstelling, in plaats

van PDP-gefunctionaliseerde lipiden, maleimide (MAL)-gefunctionaliseerde lipiden toegevoegd. Ondanks de observatie dat na 48 uur een kleinere hoeveelheid aan NP-beladen CTL's de tumor bereikte in vergelijking met de niet-beladen cellen, werd geen negatieve invloed waargenomen van deze belading op het therapeutisch effect. In tegendeel, er werd zelfs een verminderde tumorgroei vastgesteld in de muizen die geïnjecteerd werden met de NP-beladen CTL's. De observatie dat CTL's, beladen met PDP en MAL liposomen, *in vitro* een verhoogde productie van interferon gamma (IFNγ) en tumor necrose factor alfa (TNFα) vertoonden, zou kunnen verklaren waarom een verhoogde anti-kanker immuunrespons *in vivo* werd waargenomen. In een volgende stap werden de liposomen beladen met het immuun adjuvans monofosforyl lipide A (MPLA), waarvan in literatuur reeds werd aangetoond dat deze het immuunsysteem kan *boosten* tegen kanker. Eerst werd er aangetoond dat het MPLA, wanneer verpakt in de PDP en MAL liposomen en gekoppeld op de T-cellen, geen invloed had op de T-cel proliferatie of viabiliteit en verder ook de koppeling zelf niet beïnvloedde. Daarnaast werd aangetoond dat de verhoogde productie aan IFNγ enkel afkomstig was van de NP's en niet van het MPLA, aangezien vrij MPLA geen invloed vertoonde op de IFNγ secretie. Vervolgens werden dendritische cellen (DC's) en T-cellen, die beladen werden met MPLA-liposomen, samen gecultiveerd. Er werd een toegenomen expressie van de co-stimulerende receptoren CD40 en CD80 en een verhoogde secretie van het immuun-stimulerende cytokine IL-12 waargenomen, wat een succesvolle inductie van de maturatie van DC's aantoonde. Ten slotte werd *in vivo* een verbeterde overleving waargenomen bij muizen die intratumoraal geïnjecteerd werden met MPLA-beladen T-cellen, en dit in het bijzonder voor het reversibele koppelingssysteem. Verder onderzoek is noodzakelijk om het therapeutisch potentieel van deze strategie na systemische injectie te evalueren.

Op basis van de observatie dat 50% van de liposomen vastgehecht blijven aan de T-cellen na een specifieke trigger en dat deze reversibele koppelingsstrategie mogelijkerwijs gehinderd kan worden door het vroegtijdig vrijstellen van de liposomen in serum, werd er gezocht naar een meer specifiek reversibel koppelingssysteem. Daarom werd in **Hoofdstuk 4** de koppeling op basis van een splitsbare peptidebinding onderzocht. De gebruikte peptidesequentie kan gesplitst worden op basis van drie specifieke proteasen, namelijk matriptase, urokinase-type plasminogeen activator (uPA) en legumine, waarvan verhoogde concentraties aanwezig zijn in een groot aantal tumoren. Eerst werd aangetoond dat de koppeling van het peptideconstruct aan de CTL's stabiel was wanneer het geïncubeerd werd in serum-bevattend medium. Ondanks de observatie dat het peptide gesplitst werd door matriptase en uPA wanneer het gekoppeld was op magnetische *beads*, werd slechts een kleine vrijstelling waargenomen wanneer het gekoppeld was op het oppervlak van de CTL's. Aangezien na incubatie met het aspecifieke protease trypsine een hoge vrijstelling van het construct werd gemeten, werd verondersteld dat voornamelijk

sterische hinder ter hoogte van het complexe celmembraan verantwoordelijk was voor de lage activiteit van de specifieke proteasen.

Naast het gebruik van CTL's als dragers van NP's, hebben deze ook de capaciteit om tumorcellen af te doden. Helaas bevat het tumorweefsel een grote variëteit aan onderdrukkende moleculen en cellen die de anti-tumor responsen van T-cellen kunnen inhiberen. Het onderdrukken van deze immunosuppressieve *pathways* in de T-cellen op basis van siRNA zou een verhoogd therapeutisch effect kunnen opleveren. Aangezien T-cellen moeilijk te transfecteren zijn en omdat de conventionele strategieën voor het afleveren van siRNA zoals NP-gemedieerde aflevering en nucleofectie vaak tekortschieten, werd in **Hoofdstuk 5** een alternatieve strategie voorgesteld op basis van *vapor nanobubble*-gemedieerde fotoporatie. Via deze techniek werd de efficiënte aflevering van siRNA molecule aangetoond, wat vervolgens resulteerde in de onderdrukking van de geselecteerde CD45 receptor. Wanneer deze strategie vergeleken werd met de standaard niet-virale methode om T-cellen te transfecteren, namelijk nucleofectie, werd een vergelijkbare onderdrukking waargenomen. Aangezien nucleofectie een veel hogere cellulaire toxiciteit vertoonde dan fotoporatie, werden er op basis van deze laatste techniek tot drie keer meer getransfecteerde cellen bekomen.

Ten slotte werd in **Hoofdstuk 6** een samenvatting gegeven van de huidige uitdagingen in het onderzoek naar kanker immunotherapieën. Hierbij werd vooral aandacht besteed aan hoe verschillende therapieën, nanomedicijnen in het bijzonder, gecombineerd kunnen worden met kanker immunotherapie om op deze manier de immunosuppressieve tumoromgeving te overwinnen en betere immuunresponsen op te leveren.

CONCLUSIES

In deze studie werd aangetoond dat het combineren van nanomedicijnen met immuuntherapie veelbelovend is voor het behandelen van kanker. Voor het eerst werd een reversibele koppeling van lipide NP's op het oppervlak van CTL's aangetoond met als doel membraan-impermeabele macromoleculen zoals siRNA specifiek in de tumor af te leveren. Verder werd er via preliminair *in vitro* en *in vivo* onderzoek vastgesteld dat CTL's beladen met immuun adjuvantia een veelbelovende strategie is om anti-kanker immuunresponsen te verhogen. Naast de tumoritrope functie van CTL's voor het afleveren van anti-kanker geneesmiddelen in de tumor, hebben deze ook de capaciteit om tumorcellen zelf af te doden, zoals reeds uitgebreid onderzocht werd in ACT. Daarbij dient wel rekening gehouden te worden met de aanwezigheid van welbepaalde immuuninhiberende moleculen en cellen in de tumoromgeving die deze T-cel immuunresponsen kunnen onderdrukken. Om de T-cellen hier tegen te wapenen, werd in de context van ACT een techniek ontwikkeld om siRNA-moleculen efficiënt en veilig af te leveren in T-cellen, alvorens ze bij de patiënt te

injecteren. Via siRNA kunnen namelijk imuuninhiberende *pathways* in de CTL's onderdrukt worden, wat tot krachtigere anti-kanker immuunresponsen zou kunnen leiden.

Curriculum Vitae

PERSONALIA

Name	Wayteck
First name	Laura
Nationality	Belgian
Place of birth	Aalst
Date of birth	07/11/1988
Private address	Galglaan 27, 9000 Ghent, Belgium
Telephone	+32 (0)473 51 85 79
Professional address	Laboratory of General Biochemistry and Physical Pharmacy, Faculty of Pharmaceutical Sciences, Ghent University Ottergemsesteenweg 460 9000 Ghent, Belgium
Telephone / Fax	+32 (0)9 264 83 60 / +32 (0)9 264 81 89
Email	Laura.Wayteck@UGent.be laura_wayteck@hotmail.com
Websites	https://www.biofys.ugent.be https://www.researchgate.net/profile/Laura_Wayteck

EDUCATION

June 2011	Master in Drug Development – Pharmaceutical Sciences with great distinction Ghent University, Ghent, Belgium Master thesis: "Effects of endocytosis inhibitors on transfection mediated by polyplexes and lipoplexes carrying mRNA", under supervision of Dr. Joanna Rejman and the promotorship of Prof. dr. Kevin Braeckmans Laboratory of General Biochemistry and Physical Pharmacy, Ghent University, Belgium
June 2005	High school degree (Science & Mathematics) Sint-Jozefsinstituut, Geraardsbergen, Belgium

INTERNATIONAL PEER REVIEWED PUBLICATIONS

Wayteck L., Breckpot K., Demeester J., De Smedt S.C., Raemdonck K., A personalized view on cancer immunotherapy. *Cancer Letters*, 352 (2014) 113-125. (DOI: 10.1016/j.canlet.2013.09.016). (**IF 2013 = 5.621**)

Wayteck L., Dewitte H., De Backer L., Breckpot K., Demeester J., De Smedt S.C.*, Raemdonck K.*, Hitchhiking nanoparticles: reversible coupling of lipid-based nanoparticles to cytotoxic T lymphocytes. *Biomaterials*, 77 (2016) 243-254.
(DOI: 10.1016/j.biomaterials.2015.11.016). (**IF 2013 = 8.557**)

*Both authors contributed equally to this work

Wayteck L., Xiong R., Braeckmans K., De Smedt S.C., Raemdonck K., Delivery of small interfering RNA to cytotoxic T cells via vapor nanobubble photoporation. **Submitted**

Verbeke R., Dewitte H., **Wayteck L.**, Breckpot K., De Smedt S.C.*, Lentacker I.*, Messenger RNA DOTAP-Cholesterol lipoplexes containing TLR agonists allow single step antigen-loading and maturation of dendritic cells in the presence of serum. **Submitted**

*Both authors contributed equally to this work

CONFERENCE PROCEEDINGS

Wayteck L., De Smedt S.C., Raemdonck K., Evaluation of small interfering RNA delivery by nanoparticle-loaded tumoritropic cells. Human Gene Therapy, 23 (2012) A71-A71. (**IF 2013 = 3.623**)

Raemdonck K., De Backer L., **Wayteck L.**, Stremersch S., Braeckmans K., Demeester J., De Smedt S.C., Bio-inspired approaches for siRNA delivery. Human Gene Therapy, 25 (2014) A75-A75. **(IF 2013 = 3.623)**

NATIONAL & INTERNATIONAL CONFERENCES WITH ORAL PRESENTATION

Wayteck L., De Smedt S.C., Raemdonck K., Evaluation of small interfering RNA delivery by nanoparticle-loaded tumoritropic cells. *16th Forum of Pharmaceutical Science*, Blankenberge (Belgium), May 7-8 2012

Wayteck L., De Smedt S.C., Raemdonck K., Hitchhiking nanoparticles: reversible coupling to tumor-specific T cells for targeted cancer drug delivery. *Meeting of the Belgian-Dutch Biopharmaceutical Society*, Ghent, December 18th 2013

Wayteck L., De Smedt S.C., Raemdonck K., Hitchhiking nanoparticles: reversible coupling to tumor-specific T cells for targeted cancer drug delivery. *Oncopoint*, Ghent, February 6th 2014 (Storm session)

Wayteck L., Dewitte H., Breckpot K., Demeester J., De Smedt S.C., Raemdonck K., Hitchhiking nanoparticles: Reversible coupling to tumor-specific T cells for targeted cancer drug delivery. *BioNanoMed 2015*, Graz, Austria, April 8-10 2015

Wayteck L., Dewitte H., Breckpot K., Demeester J., De Smedt S.C., Raemdonck K., Cytotoxic T cells as transport vehicles for tumor-targeted delivery of nanomedicines. *Crossing biological barriers – Advances in Nanocarrier Design for Targeted Drug Delivery*, Dresden, Germany, November 9-11 2015

NATIONAL & INTERNATIONAL CONFERENCES WITH POSTER PRESENTATION

Wayteck L., De Smedt S.C., Raemdonck K., Evaluation of small interfering RNA delivery by nanoparticle-loaded tumoritropic cells. *European Society of Gene and Cell Therapy Collaborative congress*, Versailles, France, October 25-29 2012

Wayteck L., De Smedt S.C., Raemdonck K., Evaluation of small interfering RNA delivery by nanoparticle-loaded tumoritropic cells. *Meeting of the Belgian-Dutch Biopharmaceutical Society*, Utrecht, The Netherlands, November 9th 2012

Wayteck L., De Smedt S.C., Raemdonck K., Evaluation of small interfering RNA delivery by nanoparticle-coated tumoritropic cells. *11th Annual Meeting CIMT*, Mainz, Germany, May 14-16 2013

Wayteck L., De Smedt S.C., Raemdonck K., Evaluation of small interfering RNA delivery by nanoparticle-coated tumoritropic cells. *Knowledge for growth*, Ghent (Belgium), May 30th 2013

Wayteck L., De Smedt S.C., Raemdonck K., Hitchhiking nanoparticles: reversible coupling to tumor-specific T cells for targeted cancer drug delivery. *The 13th edition of the European Symposium on Controlled Drug Delivery*, Egmond aan Zee, The Netherlands, April 16 – 18 2014

Wayteck L., De Smedt S.C., Raemdonck K., Hitchhiking nanoparticles for targeted cancer drug delivery. *Knowledge for growth*, Ghent, May 8th 2014

Wayteck L., Dewitte H., Breckpot K., Demeester J., De Smedt S.C., Raemdonck K., Cytotoxic T cells as transport vehicles for nanoparticle delivery to the tumor. *Meeting of the Belgian-Dutch Biopharmaceutical Society*, Utrecht, The Netherlands, December 12th 2014

Wayteck L., Dewitte H., Breckpot K., Demeester J., De Smedt S.C., Raemdonck K., Cytotoxic T cells as transport vehicles for nanoparticle delivery to the tumor. *Meeting of the Belgian-Dutch Biopharmaceutical Society*, Leuven, Belgium, November 23th 2015

TEACHING ACTIVITIES

2012-2015	Lab instructor for the Pharmaceutical Bachelor Proof (FaBaP).
2012-2015	Supervisor of:
	Claudia Schuder, Erasmus internship (Pharmaceutical Sciences, Universität Regensburg). Evaluation of the coupling of nanoparticles to RF33.70 cells. (2012-2013)
	Nele Dendauw, Master dissertation (Pharmaceutical Sciences, Ugent). Folate-functionalized nanoparticles for cell-mediated tumoritropic delivery of small interfering RNA. (2012-2013)
	Mónica Sofia Nobre Antão, Erasmus internship (Bioengineering, Universidade Do Porto). Reversible coupling of nanoparticles to the activated $CD8^+$ T cell surface. (2013-2014)
	Jana Ongenaet, Master dissertation (Pharmaceutical Sciences, Ugent). Cytotoxische T cellen als transportmiddel voor een tumor-gerichte toediening van nanomedicijnen. (2014-2015)
2011-2015	Selected problem solving based education (PGO) session on DNA within the course of Biochemistry and Biophysics by Prof. dr. apr. Jo Demeester and Prof. dr. apr. Katrien Remaut

SCIENTIFIC COURSES

2012-2013	Laboratory Animal Science I & II (by Prof. Katleen Hermans) at Ghent University
February 2013	Particle Characterization. Belgian Particle, Colloid and Interface Society
September 2013	Applied Flow Cytometry Course (Joint organization by UGent, UA and VUB)

Acknowledgements

Dankwoord

Toen ik 18 jaar geleden mijn grootmoeder verloor aan de gevolgen van kanker, heb ik gezegd dat één van m'n dromen voor de toekomst was om kanker uit de wereld te helpen. Een grote droom uiteraard en we zijn er nog steeds niet maar de progressie die er de afgelopen jaren geboekt werd, is alleen maar veelbelovend. En hoe klein mijn bijdrage ook is tot dit grote onderzoeksveld, ik ben een heleboel mensen heel erg dankbaar dat ik de vooruitgang van dichtbij heb mogen volgen en het onderzoek zelf heb mogen beleven. Daarom wil ik graag een aantal mensen bedanken die me tijdens deze toch wel bijna 5 jaar-durende doctoraatsperiode hebben geholpen en gesteund.

Eerst en vooral wil ik mijn beide promotoren van dit werk bedanken. **Stefaan,** jouw deur staat altijd open voor iedereen. Ik wil jou heel graag bedanken voor de wetenschappelijke input, voor de kans die ik gekregen heb om dit doctoraat in zo'n leuk labo met fantastische sfeer te kunnen afwerken en voor de hulp ondertussen bij de zoektocht naar een nieuwe job.

Koen, ik bewonder jouw ongelofelijke geheugen! Zoveel doctoraatsstudenten te begeleiden met heel verschillende onderwerpen en jij slaagt erin om alle literatuur bij te houden en steeds opnieuw massaal veel nieuwe ideeën te verzamelen. Ik kan alleen maar heel enthousiast zijn over onze samenwerking. Als het onderzoek even moeilijk liep, kon ik steeds op jou rekenen om samen te zoeken naar oplossingen of om andere strategieën te bedenken. 's Avonds snel nog wat wetenschappelijke twitter-berichten doorsturen of even informeren hoe het experiment de voorbije dag verlopen was….wat er op wijst dat jij steeds heel betrokken was bij dit onderzoek. Het verbeteren van het vele schrijfwerk deed je steeds tot in de puntjes met heel veel oog voor detail, iets wat ik heel hard kon appreciëren! Ik wil jou uiteraard nog een heel mooie carrière toewensen.

Jo, **Kevin** en **Katrien**, graag wil ik ook jullie bedanken om samen met Stefaan een heel succesvol onderzoekslabo te creëren met veel mogelijkheid tot wetenschappelijk overleg, de kans om ook regelmatig een conferentie bij te wonen en steeds bereikbaar te zijn voor vragen.

Als er twee mensen zijn waar je altijd op kan rekenen dan zijn het zeker en vast Bart en Ine L. Wat zouden wij doen zonder **Bart**…. Ontelbare keren stond ik aan jouw bureau met zovele vragen en nooit was iets jou teveel. Altijd bereid om te luisteren naar de kleine

frustraties over experimenten, om te helpen bij vanalles en nog wat en ervoor te zorgen dat praktisch alles op wieltjes loopt. Ik ben ook heel blij dat ondertussen **Hilde** er is bijgekomen zodat het vele werk toch wat kan verdeeld worden en jullie zien er een fantastisch team uit! **Ine L.**, jij bent echt een voorbeeld van hoe je op een efficiënte wijze een academische carrière kan combineren met het gezinsleven en het daarbij op beide vlakken fantastisch goed te doen! Hoedje af!

Office-ladies **Lynn**, **Heleen** en **Joke**, wat was het door jullie altijd zo gezellig bij ons op het bureau. Jullie hebben me zo hard geholpen tijdens dit doctoraat. Heel erg bedankt voor zowel de motiverende babbels, want die waren op het einde van dit doctoraat van onschatbare waarde en voor de gesprekken over van alles en nog wat…ook vooral niet wetenschappelijk ☺. Wat ga ik jullie zo hard missen… Ik denk niet dat ik m'n bureau ooit nog zal mogen delen met zo'n drie fantastische madammen!

Lynn, waar moet ik beginnen…Ik ga starten met te zeggen dat ik jou ongelofelijk hard ga missen. Ik was zo blij als het nieuws er vorig jaar kwam dat ik toch geen afscheid van jou moest nemen en dat je er toch nog zou bij zijn wanneer ik de laatste fase van het doctoraat zou doormaken. Je bent in deze doctoraatsperiode een echte vriendin geworden voor mij, iemand waarmee ik alles gedeeld heb de voorbije jaren, van mooie tot verdrietige momenten, alsook succes- en stress-momentjes. Het zal raar doen om nu niet meer elke dag te weten hoe Sam het op school doet of te weten wat de plannen voor het weekend zijn of om gewoonweg ons hart eens te kunnen luchten. En nee, Berlare, of binnenkort Lebbeke is helemaal niet zo ver. Ik kijk al zo hard uit naar de geboorte van het kindje! En je mag er zeker van zijn, het zal niet lang duren of ik daar zal staan, op babybezoek.

Heleen, ondertussen hebben we ook zoveel mooie herinneringen samen zoals, DC-T cel experimenten plannen, een Moulin Rouge love medley zingen in Versailles en nog wat verder zingen op de hotelkamer samen met Ine DC, samen behangpapier verwijderen, samen voorbereiden voor een 80's feestje en terug naar huis gaan zonder te weten hoe dat feestje nu eigenlijk geëindigd was, samen knutselwerkjes maken voor Lynn, met 'glowing hair'-gel onszelf versieren voor een feestje… Gedurende m'n hele doctoraat was jij m'n grote voorbeeld. Zelfs na heel lang nadenken vind ik nog steeds niet één iets waar je niet goed in bent… Ik heb zoveel van jou geleerd! Bij de start tot het einde van m'n doctoraat kon ik steeds op jou rekenen. Je hebt een gigantische kennis over zoveel verschillende zaken en je bent eindeloos efficiënt in alles wat je doet. Jij hebt alles om een heel mooie carrière uit te bouwen, ga ervoor!

Joke, wat ben jij een zotte doos ☺ en wat ga jij gemist worden als je ooit het labo verlaat. Altijd konden wij op jou rekenen voor het ineensteken van filmpjes, zelfs tot in de late uurtjes, voor het uitlenen van verkleedkledij, want ik kan niet direct iets bedenken wat jij niet hebt liggen thuis en voor het op gang trekken van feestjes en deze ook tot in de late

uurtjes door te trekken. Ook op het bureau en in de fitness hebben we heel wat leuke babbels gehad. Je bent er altijd voor het geven van goede raad, het motiveren met geruststellende woorden en het vertellen van een mopje hier en daar. In het begin van je doctoraat was het wat zoeken, maar nu heb je samen met Karen helemaal je draai gevonden. Jullie zijn een super team en dat oog-labo is een feit!

Sangram, you are a very friendly, warm, and optimistic person! We were so lucky that you joined us in the office. I wish you all the best in India with the new research experience and I wish you lots of luck for your personal life. You were always there to help or to motivate me in periods when the experiments failed. I am happy that I learned a lot about the Indian culture and I hope that I can come to visit you one day.

Karen, we kunnen er niet omheen, met jou erbij is het nooit stil aan de eettafel. Jij bent een echte sfeermaker! Ik bewonder jouw eindeloze enthousiasme, doorzettingsvermogen en het talent om mensen te motiveren. Hoe kan ik jou ooit bedanken voor de zovele fantastische en soms zelfs hypnotiserende massages. Ook als het even wat moeilijk ging, was jij er om te babbelen, te troosten, te zoeken naar oplossingen. Eén ding wil ik jou nog meegeven, twijfel vooral niet aan jezelf! Je bent super goed bezig! Hopelijk blijven we ook nog heel lang een badminton DREAMTEAM!

Ine DC, de voorbije 10 jaar hebben wij hetzelfde parcours afgelegd, samen studeren, samen thesissen, samen starten aan het doctoraat, net niet samen naar Seattle…helaas... Het deed de afgelopen maanden wel heel raar dat jij er niet meer was op het labo. Wie gaat er mij nu nog 'kaasgunstig' verklaren? ;-)

Freya, wij hebben een tijd lang samen heel wat uurtjes doorgebracht in het cel labo. Samen met Ine DC hadden we elk ons eigen plaatsje veroverd in de LAF-kasten, waar het ongelofelijk gezellig was om samen te experimenteren. Samen hebben we heel wat concertjes gedaan, van het geweldige concert van Macklemore tot het melodieuze optreden van Ibeyi. Ik wil jou heel veel succes wensen met de laatste fase van het doctoraat!

Rita, I was so sad when you had to leave our lab for the first time, because we had such a nice time with you in our office. Fortunately, you came back! So we could do some fitness together, watch soccer games, organize dinner, visit Dresden by night while having a nice talk…and hopefully we can still plan many things more before you leave again to write your thesis in Portugal.

George, ik ga dit in het Nederlands schrijven voor jou aangezien jij onze taal op zo korte tijd hebt geleerd en ik dat zo hard bewonder. Ik heb heel veel van jou bijgeleerd over de situatie in Israël tijdens één van onze avonden op congres in Dresden, waardoor ik nu nog meer dan ooit begrijp waarom jij jouw toekomst hier in Europa ziet. Daarom duim ik

voor jou mee voor een leuke job in België na je doctoraat, want ik weet dat je zo graag hier wil blijven.

Lieve **Lotte**, ik bewonder jouw doorzettingsvermogen want de 'swept field' maakt het jou niet makkelijk. Ik duim zo hard met jou mee dat die problemen allemaal snel achter de rug zullen zijn en dat je gewoon kan verder experimenteren.

Eline, jou heb ik pas echt leren kennen tijdens het fitnessen samen. Ik hoop jullie in de toekomst nog steeds te vergezellen tijdens het harde zwoegen met de gewichtjes heffen, het trampoline springen, de buikspieroefeningen en natuurlijk jouw favoriete onderdeel…het planken ;-). Jij bent een heel spontane, toffe madam en daarnaast ook nog eens een heel harde werker, dat wordt ongetwijfeld een topdoctoraat!

Koen, samen zijn wij ons doctoraat gestart en nu nemen we ook zo goed als samen afscheid van het labo. Ik ben ervan overtuigd dat we beide de fantastische sfeer in het labo zullen missen, want er zijn de afgelopen 4 jaar toch heel wat leuke momenten geweest, zoals een avondje doorbrengen in de Riderz, een beetje schuren in de Oude Vismijn, een interessant overleg over wat wij structureel zouden veranderen ;-) en nog zoveel meer.

Stephan, je bent er ook bijna mee klaar! Nog even aftellen en het doctoraat is binnen. Je hebt er heel hard voor gewerkt, dus ik tel samen met jou af tot het einde en ook tot een heel belangrijk moment, het papa worden!

Reintje, je bent me er eintje! Jouw uitspraken zijn geniaal. Ik heb jou leren kennen als een heel empathisch persoon. Altijd heel even vragen hoe alles loopt met de experimenten, of het wel lukt met het schrijven en een schouderklopje onderweg naar het bureau van Heleen. En ik moet toegeven dat het verhaal van het borsthaar toch een openbaring was en dat ik me dit nog heel lang zal herinneren ☺.

Elisa, it was never boring with you in the microscopy room as you entertained us with your beautiful voice. **Ranhua**, you were definitely the one who gave me the nickname 'Lola' in the lab ☺. **Pieterjan**, het is altijd heel leuk babbelen met jou. Je bent een heel intelligente persoon met zoveel maturiteit. **Silke**, zelfde als voor Joke, wat ben jij een zotte doos, maar wel eentje met het hart op de tong. Ik hoop dat we elkaar nog vaak zullen terug zien op de badminton. Topping **TOON**, carTOON, badminTOON, ik ben al benieuwd wat er nog zal volgen…Jij bent echt een ongelofelijke aanwinst voor het labo, altijd bereid om te helpen met de microscopen, altijd into een gezellige babbel met een biertje of een spelletje badminton. Wat je ook doet, je gaat er altijd voor! **Jing**, you are a very smart, sweet and warm person. I really enjoyed our badminton games together. **Heyang**, thank you so much for your kind message on my desk before my internal defense. You are a sweet person and hopefully we can still meet to eat some Chinese dinner together…but maybe not the chicken legs ;). **Molood**, you are still at the beginning of your PhD, so I wish you all the best with

the coming experiments. **Jelter**, helaas heb ik de afgelopen weken niet veel tijd gehad om samen met jou te experimenteren of jou beter te leren kennen. Wat ik ondertussen wel weet is dat jij het T cel-project fantastisch zal verder zetten. Je hebt al heel wat ervaring en je bent heel gemotiveerd, daarom wil ik jou een heel mooie doctoraatsperiode toewensen met heel veel succesvolle resultaten!

Katharine en **Ilse**, jullie rol om alles draaiende te houden in het labo is helemaal niet te onderschatten! Steeds bereid tot het oplossen van administratieve problemen, want we moeten daar eerlijk in zijn, wij hebben daar helaas weinig kaas van gegeten.

Thomas, jij was voor mij altijd een vaste waarde in het labo. Steeds bereid om te helpen, steeds aanwezig op een feestje of bereid om mee te filmen of ideeën te bedenken voor de doctoraatsfilmpjes. Daarom deed het ook heel raar toen jij er niet meer was. Ik moet jou toch nog voor een aantal zaken bedanken. Eerst en vooral voor het opleggen van m'n ketting toen ik daar zelf niet zo goed meer in staat toe was, voor het wijzen van de weg van de Sioux naar de Charlatan, gelukkig was dat net om te hoek en om er op m'n verjaardag in de Oude Vismijn een topfeestje van te maken. **Katrientje**, ook al ben je ondertussen al even weg uit het labo, toch horen wij elkaar nog heel regelmatig. Je bent heel hulpvaardig en we konden altijd op jou rekenen, voor een leuke photoshop, voor hulp als de confocale microscoop even niet wou werken en voor een lesje hoe-werk-ik-met-mijn-reflexcamera. **Broes**, ook al ben ik mijn doctoraat begonnen toen jij net het labo verliet, toch hebben wij elkaar goed leren kennen door jouw aanwezigheid op de vele labo-activiteiten. Leuk dat je na al die jaren nog steeds zo verbonden bent met het labo! **Oliwia**, I still remember our very pleasant drive to the Biopharmacy day a couple of years ago in The Netherlands with sing along songs all drive long!

Joanna, we had a very good collaboration during my master thesis through which I got very interested in doing research. Because of your motivating words I started this PhD adventure. You convinced me that I would be a good researcher and that I should think about starting a PhD. For this, I would really like to thank you.

Karine, ook jou wil ik heel graag bedanken voor de heel leuke en vlotte samenwerking. Het was altijd heel fijn om naar Brussel te komen voor de in vivo experimenten. Niets is jou te veel, altijd bereid om te helpen. Ook al lukte het allemaal niet van de eerste keer, jij bekeek alles positief, een ingesteldheid waar ik nog heel veel aan zal terug denken. Ik wens jou het allerbeste voor de toekomst met heel veel succesvol onderzoekswerk in de strijd voor een wereld zonder kanker!

I would also like to thank my four thesis students **Claudia, Nele, Mónica,** and **Jana** for the nice collaboration. We did a lot of experiments together and you were all very motivated to do a very good thesis.

Sara, je bent ongelofelijk hard bedankt voor het ontwerpen van de cover van m'n doctoraat. Ik was zo blij dat jij het zag zitten om jou hier mee bezig te houden tijdens jouw zwangerschapsverlof en ik ben heel erg blij met het resultaat!

Ook al mijn lieve **vrienden** die er steeds waren om even voor wat afleiding te zorgen en om een aanmoedigingssmsje te sturen voor de belangrijke momenten tijdens het doctoraat, wil ik graag bedanken. Jullie hebben er geen idee van hoeveel deugd dit steeds deed.

Mijn familie is ook in deze doctoraatsperiode heel belangrijk geweest. Eerst en vooral wil ik m'n **grootouders** bedanken die me steeds gesteund hebben tijdens m'n studies en ook tijdens dit doctoraat. Jullie waren steeds geïnteresseerd hoe het verliep met de studies en dan tijdens de laatste jaren ook met het onderzoek. Helaas heeft m'n peter dit doctoraatseinde niet meer mogen meemaken, maar ik ben zeker dat hij heel trots zou geweest zijn.

Mama en papa, wat heb ik geluk met zo'n fantastische ouders. Elke keer kijk ik er naar uit om een weekendje in Galmaarden door te brengen! Jullie zijn er altijd voor mij en hebben me steeds heel hard gesteund. Ik ben soms wel eens een stresskonijntje, dus ik maakte het jullie tijdens m'n examens aan de unief en ook tijdens de voorbereidingen van m'n IWT niet makkelijk. Maar door jullie aanmoedigingen heb ik ook dit doctoraat tot een goed einde kunnen brengen. **Mama**, wij waren altijd samen op stap als een onafscheidelijk duo! Ik heb zo een mooie kindertijd en studententijd gehad. Voor en na school was je er steeds om te luisteren naar al m'n verhalen, me sterk te maken tegen de onrechtvaardigheid in de wereld en me te steunen door dik en dun. **Papa**, zoals ze wel vaker zeggen lijken we als twee druppels water op elkaar, maar toch denk ik dat jouw werkijver nooit te evenaren valt. Af en toe is het dan wel eens goed om tegen elkaar te zeggen dat het ook wel iets rustiger aan mag ☺.

En als laatste…allerliefste **Karac**…ik ken je nog maar anderhalf jaar, maar ik kan me niet voorstellen wat ik zou doen zonder jou. Door jou heb ik deze laatste periode van dit doctoraat overleefd. Ik heb het jou niet makkelijk gemaakt met onder andere het vele gezaag over het schrijven, de stress voor de interne verdediging, de bijna slapeloze nachten door gepieker over het doctoraat. Maar jij wist hoe me kalm te krijgen, me te motiveren om er toch nog heel even voor te gaan en er steeds te zijn als het even wat moeilijker ging. Wij zijn de afgelopen maanden heel wat samen aan het werk geweest in de weekends en op vakantiedagen, jij met de thesis en de examens en ik met het doctoraat. Maar nu zijn we er allebei klaar mee dus tijd om samen heel wat leuke dingen te plannen!

Laura